AGRONOMIA COLOMBIANA

Doi: 10.15446/agron.colomb

VOLUME XL, No. 3 SEPTEMBER-DECEMBER 2022 ISSN 0120-9965

Centro Editorial
Facultad de Ciencias Agrarias
Sede Bogotá

UNIVERSIDAD NACIONAL DE COLOMBIA

AGRONOMIA COLOMBIANA

VOLUME XL | No. 3 | SEPTEMBER-DECEMBER 2022 | ISSN (print): 0120-9965 / ISSN (online): 2357-3732

PUBLICATION OF A SCIENTIFIC-TECHNICAL NATURE BY THE FACULTY OF AGRICULTURAL SCIENCES OF THE UNIVERSIDAD NACIONAL DE COLOMBIA, BOGOTA

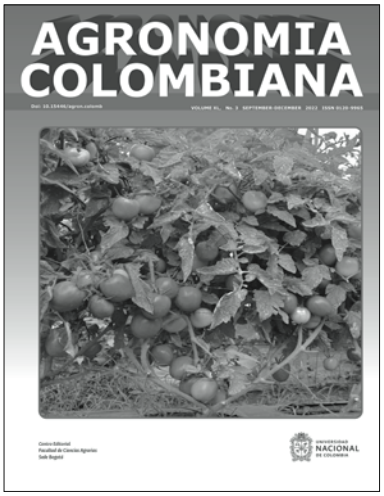

Our cover:

Agronomic evaluation of chonto tomato (*Solanum lycopersicum* Mill.) lines of determinate growth

Article on pages 336-343

Publication registered at the Ministerio de Gobierno Resolution No. 00862 of March 24, 1983

Information, correspondence, subscription and exchange:

Revista Agronomía Colombiana
Faculty of Agricultural Sciences,
Universidad Nacional de Colombia

P.O. Box 14490, Bogota-Colombia

Phone: (571) 316 5355 / 316 5000 ext. 10265

Fax: 316 5176

E-mail: agrocol_fabog@unal.edu.co

Electronic version available at:

http://www.revistas.unal.edu.co/index.php/agrocol

http://www.scielo.org.co/scielo.php?script=sci_serial&pid=0120-9965

ISSN: 2357-3732 (Online)

Published: Triannual
Number of copies: 20

Editorial assistance
Juan Carlos Anduckia Ávila
Zulma Catherine Cardenal Rubio
Álvaro Arley García Gómez
Luz Mery Grass Bernal
Stanislav Magnitskiy

Translators and English proofreaders
Thomas Defler
Paul Priolet

Electronic Design and Development
Isabel Sandoval Montoya

Agronomía Colombiana is a technical-scientific publication classified by Colciencias in category B of the Índice Nacional de Publicaciones Seriadas y Científicas y Tecnológicas (Publindex) (Colombia). The journal is indexed in the Scientific Electronic Library Online (SciELO) and Scopus, and is ranked Q4 in the Scimago Journal Rank (SJR). Internationally, the journal is referenced in Redalyc, Latindex, AGRIS (FAO), ResearchGate, Family Farming Knowledge Platform (*Plataforma de Conocimientos sobre Agricultura Familiar*), and integrated in CABI Full Text and the following databases of CAB-ABSTRACTS: Agricultural Engineering Abstracts, Agroforestry Abstracts, Crop Physiology Abstracts, Field Crop Abstracts, Grasslands and Forage Abstracts, Horticultural Science Abstracts, Irrigation and Drainage Abstracts, Maize Abstracts, Nematological Abstracts, Ornamental Horticulture, Plant Breeding Abstracts, Plant Growth Regulator Abstracts, Postharvest News and Information, Potato Abstracts, Review of Agricultural Entomology, Review of Aromatic and Medicinal Plants, Review of Plant Pathology, Rice Abstracts, Seed Abstracts, Soils and Fertilizers, Sugar Industry Abstracts, Weed Abstracts y World Agricultural Economics and Rural Sociology Abstracts.

The authors of the articles submitted to the journal Agronomía Colombiana must be aware of and avoid scientific misconduct related to: scientific fraud in all or part of the data of the study and data falsification and manipulation; dishonesty due to fictitious authorship or gifting or exchange of co-authorship, duplicate publications, partial or complete, in different journals and self-plagiarism by reusing portions of previous writings; citation omission, citation copying without consultation and excessive self-citation, among others.

AGRONOMIA COLOMBIANA

VOLUME XL | No. 3 | SEPTEMBER-DECEMBER 2022 | ISSN (print): 0120-9965 / ISSN (online): 2357-3732

TABLE OF CONTENTS

The editorial team of *Agronomía Colombiana* informs its readers that the journal stops publishing in print from volume 40 issue 3 of 2022 (September-December) and will continue to be published, distributed, and delivered exclusively in digital format with ISSN 0120-9965.

This decision has the approval of the Editorial Committee of the Faculty of Agricultural Sciences and the endorsement of the Faculty Council recorded in official letter dated August 8, 2022.

Sincerely,

El equipo editorial de *Agronomía Colombiana* informa a sus lectores que a partir del volumen 40 No. 3 de 2022 (septiembre-diciembre), la revista suspende la impresión en papel y se publicará, distribuirá y entregará exclusivamente en formato digital con ISSN de enlace 0120-9965.

La decisión cuenta la aprobación del Comité Editorial de la Facultad de Ciencias Agrarias, y con el aval del Consejo de la Facultad, consignado en el oficio del 08 de agosto de 2022.

Atentamente,

MAURICIO PARRA QUIJANO
Editor-in-Chief / Editor en Jefe (e)
Revista Agronomía Colombiana

Intellectual property on the design of genetically modified tobacco containing a *phaC* gene for peroxisomal biosynthesis of polyhydroxyalkanoates

Propiedad intelectual sobre el diseño de tabaco genéticamente modificado que contiene un gen *phaC* para la biosíntesis peroxisomal de polihidroxialcanoatos

Diana Daniela Portela[1*], Fabián Villamil-Bolaños[1], Felipe Sarmiento[1], Alejandro Chaparro-Giraldo[1 †], and Silvio Alejandro López-Pazos[2]

ABSTRACT

Genetically modified (GM) plants producing polyhydroxyalkanoates (PHA) are protected by patents. This study analyzes the status of patents covering PHA-producing GM plants, focusing on the production of GM tobacco expressing the *phaC* gene of *Aeromonas caviae* for PHA synthesis. Thirty patent applications for PHAs producing GM plants were identified. Patent applications covering the design of GM tobacco expressing the *A. caviae phaC* gene for biosynthesis of PHAs in peroxisomes were found from our searches; five safeguard the rights on the *A. caviae phaC* gene, and three protect the transit peptide. In addition, 96 records related to *Nicotiana tabacum* breeder's rights were identified, with 22 varieties still protected.

Key words: patent, R-3 hydroxycarboxylic acid monomers, *Aeromonas caviae* PHA synthase, *Nicotiana tabacum,* plant breeder's rights.

RESUMEN

Las plantas modificadas genéticamente (GM) productoras de polihidroxialcanoatos (PHA) son protegidas por patentes. Este estudio analiza el estado de las patentes que protegen las plantas GM productoras de PHA, centrándose en la producción de tabaco GM que expresa el gen *phaC* de *Aeromonas caviae* para la síntesis de PHA. Se identificaron 30 solicitudes de patentes para plantas GM productoras de PHAs. De las solicitudes de patentes vigentes que cubren el diseño de tabaco GM que expresa el gen *phaC* de *A. caviae* para la biosíntesis de PHAs en peroxisomas, cinco patentes cubren el gen *phaC* de *A. caviae y* tres patentes cubren el péptido de tránsito. Además, se identificaron 96 registros relacionados con los títulos de obtentor de *Nicotiana tabacum* dentro de los cuales 22 variedades aún se encuentran protegidas.

Palabras clave: patente, monómeros del ácido hidroxicarboxílico R-3, PHA sintasa de *Aeromonas caviae*, *Nicotiana tabacum*, derechos de fitomejorador.

Introduction

Polyhydroxyalkanoates (PHAs) have been used to replace synthetic petroleum-derived plastics that are environmentally recalcitrant and polluting (Muneer *et al*., 2020). Advances in biotechnology related to synthetic biology and systems biology can provide efficient strategies to produce PHAs in other organisms, such as genetically modified (GM) plants, by introducing the genes encoding for enzymes involved in the biosynthesis of PHAs in cytosol, plastids, mitochondria, or peroxisomes (Lössl *et al*., 2003; Anderson *et al*., 2011; Bohmert-Tatarev *et al*., 2011). Polyhydroxybutyrate (PHB) is the most common type of PHA (Stouten *et al*., 2019), which is synthesized from acetyl-CoA by the bacterium *Cupriavidus necator* involving three enzymes: (i) β-ketothiolase (*phaA* gene) catalyzes the condensation of two molecules of acetyl-CoA to acetoacetyl-CoA; (ii) acetoacetyl-CoA reductase (*phaB* gene) catalyzes the reduction of acetocatyl-CoA to (R)-3-hydroxybutyryl-CoA; (iii) PHA synthase (*phaC* gene) catalyzes the polymerization of (R)-3-hydroxybutyryl-CoA monomers (Gupta *et al*., 2021).

Acetyl CoA is produced in numerous metabolic pathways in plants. In general, the metabolic pathway of glycolysis occurs in the cytosol; once pyruvate has been produced it is oxidized by pyruvate dehydrogenase into acetyl-CoA to enter the citric acid cycle. The acetyl-CoA can be used by the β-ketothiolase present in the cytosol to carry out the first metabolic reaction that produces PHB. Insertion of *phaB* and *phaC* genes into the plant genome is required to complete the synthesis of PHB in the cytosol (Jeon *et al*.,

Received for publication: April 25, 2022. Accepted for publication: September 2, 2022 Doi: 10.15446/agron.colomb.v40n3.102306

[1] Grupo de Ingeniería Genética de Plantas, Departamento de Biología, Universidad Nacional de Colombia, Bogotá (Colombia).
[2] Facultad de Ciencias, Universidad Antonio Nariño, Bogotá (Colombia).
[†] Died shortly after concluding this study.
[*] Corresponding author: didporteladu@unal.edu.co

2014). The production of acetyl-CoA in plastids is obtained through *de novo* biosynthesis of fatty acids, and the synthesis of PHB in this organelle can be carried out through the insertion of the three PHA related bacterial genes (Bohmert-Tatarev *et al*., 2011). Plant peroxisomes produce 3-hydroxyacyl-CoA intermediates through β-oxidation of fatty acids that can be used as precursors in the synthesis of PHAs; therefore, the biosynthesis of peroxisomal PHB can be obtained by inserting a *phaC* gene into the nuclear genome and targeting the enzyme to peroxisomes with a transit peptide (Arai *et al*., 2002; Tilbrook *et al*., 2014). PHA synthase from *C. necator* produces PHB from acetyl-CoA in the cytosol and plastids, while PHA synthases from *Aeromonas caviae* (*phaC*$_{A.c}$ gene) and *Pseudomonas aeruginosa* (*phaC1* gene) produce PHB (cytosol, plastids and peroxisomes) and different PHAs using 3-hydroxyacyl-CoA intermediates (Jeon *et al*., 2014; Jia *et al*., 2016).

The development of commercial PHA-producing GM plant lines must take into consideration elements such as transformation vectors, genes, regulatory regions, proteins, strains, plant genotypes, and plant transformation protocols. These elements may be protected by intellectual property rights (IPR): patents, plant variety certificates, confidentiality agreements, and material transfer agreements (Carroll, 2016). However, legal aspects related to patents can circumvent IPR and prompt the development of PHA-producing GM plants. Patents expire due to nonpayment of maintenance or the completion of the protection period, leaving the invention in the public domain where the authorization of its original owners is no longer required for its use. Likewise, patents have national jurisdiction, meaning they are only valid in the countries where they were requested and granted (Wolf, 2008; Heikkilä & Lorenz, 2018).

The development of a GM plant line for commercial purposes requires a related IPR analysis to verify if the elements involved are protected and, if so, the term and the countries in which its development, application, and commercialization do not infringe the rights of third parties. The number of patents protecting this technology can increase the costs associated with development due to the payment of royalties or licenses (Alandete-Saez *et al*., 2015).

Nicotiana tabacum is one of the most used plants for genetic transformation. Its plasticity, susceptibility to transformation mediated by *Agrobacterium tumefaciens*, and ability to generate biomass places GM tobacco as a potential green factory for the production of proteins for medical or industrial use (Buyel & Fisher, 2012; Ibrahim *et al*., 2019; McNulty *et al*., 2021; Fearon *et al*., 2022).

This study analyzes the IPRs status through patents on PHA-producing GM plants worldwide, focusing on the design of a GM tobacco line that expresses the *phaC*$_{A.c}$ gene from *A. caviae* for the synthesis of PHAs in peroxisomes in order to identify patent-free elements for the development of a GM tobacco event producing agrobiogeneric PHB.

Materials and methods

A search in public access patent databases was performed in order to identify: (i) patents that protect the development of GM PHA-producing plants in the world, and (ii) patents that protect elements used in the design of a GM tobacco line that expresses the *phaC*$_{A.c}$ gene. The Lens (https://www.lens.org), Espacenet (https://worldwide.espacenet.com/), and Google Patent (https://patents.google.com/) databases were used. In addition, patents requested through the Patent Cooperation Treaty (PCT), directed by the World Intellectual Property Organization (WIPO), were also considered.

PCT allows the applicants to simultaneously request protection of their invention in signatory countries with a single application. Applicants have 30 months to request a patent in the desired regional office (Barreto *et al*., 2020). The search terms used to identify the appropriate Classification Symbols of the international patent code (IPC) were: "Genetic term", "Genetic engineering", "Mutants or genetically engineered organisms", "Mutations or genetic engineering" and "New plants per se". Patent priority dates, current maintenance status, application through the PCT, and jurisdictions were established. An analysis of the trend of patent requests over time was performed.

The patent status of the elements used in the development of the GM line that expresses the *phaC*$_{A.c}$ gene was done with the IPC terms mentioned above and the following keywords: "*phaA* gene", "*phaB* gene", " *phaC*$_{A.c}$ gene", "*PHAC* synthase from *Aeromonas caviae*", "CaMV35S promoter", "CaMV35 promoter enhancer", "T-Nos terminator", "Target in malate synthase signal", "Transgenic producer of polyhydroxyalkanoates", "Production of polyhydroxyalkanoates in tobacco", "Polyhydroxyalkanoates", and "PHA Copolymer". The collected patent application data consisted of patent application families (patent documents requested in several countries that protect the same invention). It included their legal status, priority date, geographic coverage, and claims. The search was conducted from April 2019 until December 2021. All data were processed with R software.

Results and discussion

Patent families and patent applications related to the development of PHA-producing GM plants were explored in worldwide databases (from 1991 until 2010). Twenty-three patent families were assigned through PCT, and six patents requested at a national patent office were identified. The United States of America (US) has the highest number of applications, followed by Australia and some countries of the European Union (EU) (Fig. 1).

Eighteen patent families expired from 2012 to 2020. Patents in these families were granted in the US, Australia, the EU, Brazil, Mexico, Japan, India, and China. Eight patent families expired between 2004 and 2018 because annual maintenance payment was not recorded. Four patent families remain valid and will expire between 2022 and 2030; these patents were granted through the PCT in the US, Brazil, and Australia. GM seeds covered by patents limit the use of this technology because profitability is generated for crops cultivated in large areas.

PHA synthesis in the cytosol, plastids, and peroxisomes of GM plants has been generated from intermediary substrates of metabolic pathways such as glycolysis, fatty acid synthesis, and fatty acid degradation. The identified patents protect the development of GM plants that produce PHAs in the cytosol, plastids, and peroxisomes. Strategies to improve PHA synthesis in these subcellular compartments are WO1992019747, WO1993002187, WO1994012014, WO2004006657, US8487159, and WO2011034945. These protect GM plants such as *Arabidopsis thaliana*, cotton, switchgrass, sugarcane, and oil crops, which produce between 1.6% and 7% of PHB per unit of dry cell weight in the cytosol by insertion of *phaA*, *phaB*, and *phaC* genes from *C. necator*, *Pseudomonas oleovorans*, and *Zoogloea ramigera*, respectively. Patent application WO2012037324 covers the development of GM turf and poplar in which the carbon flux in the Calvin-Benson cycle was increased by the insertion of genes coding for sedoheptulose 1,7-bisphosphatase, fructose 1,6-bisphosphatase, transketolase, or aldolase to improve PHB production (Tab. 1).

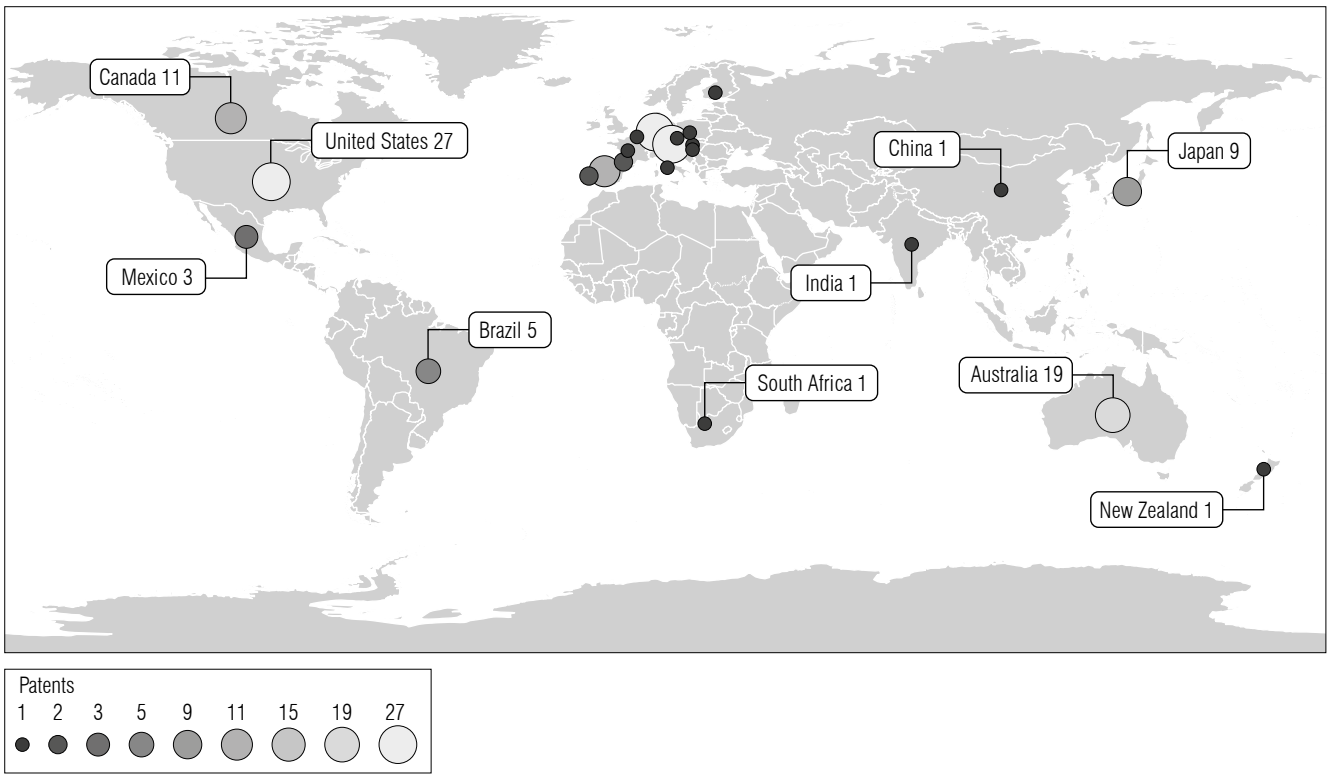

FIGURE 1. Numbers of patents related to PHA-producing GM plants.

TABLE 1. Patents related to the development of PHA-producing GM plants.

Patent title	Priority application	Application by PCT	Owner	Country	Application date
Production of polyhydroxyalkanoates in plants	GB9108756	WO1992019747	Metabolix Inc.	US, Germany, Australia, Spain, Canada, UK, Denmark, Austria	23/04/1991
Transgenic plants producing polyhydroxyalkanoates	US73224391	WO1993002187	Michigan State University	US, Canada, Mexico, Brazil, Italy, The Netherlands, Norway, Japan, India, Australia, Germany, New Zealand, France, Belgium, Poland, Portugal, Hungary, Finland, Slovakia, Czech Republic, Austria, Spain	18/07/1991
Transgenic cotton plants producing heterologous bioplastic compounds	US98052192	WO1994012014	Agracetus	Australia, US, Canada	20/11/1992
Production of polyhydroxyalkanoate in plants	GB9302286	WO1994011519	Zeneca Ltd, Philip Anthony Fentem	UK, Australia	04/11/1992
Processes for producing polyhydroxybutyrate and related polyhydroxyalkanoates in the plastids of higher plants	US10819393 US25435794	WO199505472	Michigan State University	US, Austria, Germany, Spain, China, Japan	16/08/1993
Methods for isolating polyhydroxyalkanoates from plants	US54884095	WO1997015681	Metabolix Inc.	Australia, US, Germany, Spain, Austria, Japan	25/10/1995
DNA sequence employed in the production of polyhydroxyalkanoates	AU70057696	WO1998006854	Metabolix Inc.	US, Germany, Japan, Australia, EU	12/08/1996
Polyhydroxyalkanoates of narrow molecular weight distribution prepared in transgenic plants	US61487796 US62803996 US67338896 US91220597 US44040099	None	Metabolix Inc., Monsanto	US	12/03/1996
Use of DNA encoding plastid pyruvate dehydrogenase and branched chain oxoacid dehydrogenase components to enhance polyhydroxyalkanoate biosynthesis in plants	US5129197 US5525597 US7654498	WO1999000505	University of Missouri	US, Australia	29/06/1997
Biological systems for synthesis of polyhydroxyalkanoate polymers containing 4-hydroxyacids	US5937397	WO1999014313	Metabolix	US, Austria, Germany, Canada, Australia, Japan	19/09/1997
Biosynthesis of medium chain length polyhydroxyalkanoates	US9800083	WO1999035278	Monsanto, Poirier Yves, Mittendorf Volker	Australia, EU, US	04/01/1998
Polyhydroxyalkanoate synthesis in plants	US5260798	None	University of Minnesota	US	30/03/1998
Modified *Pseudomonas oleovorans PhaC*1 nucleic acids encoding bispecific polyhydroxyalkanoate polymerase	US5260798	None	University of Minnesota	US	30/03/1998
Polyhydroxyalkanoate biopolymer compositions	US8639698 US31656599 US48834800	WO1990061624	Metabolix Inc., Cheiljedang Corporation Research Center LLC	Canada, Australia, US, Mexico, Germany, Austria, Japan	21/05/1998
Modification of metabolism of fatty acids in plants	US7710798	WO1999045122	Metabolix Inc.	Canada, Mexico, Australia, Japan, US	05/03/1998
Methods of optimizing substrate pools and biosynthesis of poly (3-hydroxybutyrate-co-3-hydroxyvalerate in bacteria and plants	US59422660	None	Monsanto	US	13/10/1999

Continued on the next page

Patent title	Priority application	Application by PCT	Owner	Country	Application date
Transgenic systems for synthesis of poly(3-hydroxybutyrate-co-3-hydroxyhexanoate	US 23587599	WO2000043523	Metabolix Inc.	US, Germany, Austria, Canada, Australia, Japan	21/01/1999
Multigene expression vector for the biosynthesis of products via multienzyme biological pathways	US12301599	WO2000052183	Monsanto	US, EU, Australia	04/03/1999
Production of polyhydroxyalkanoates in plants	US15680799 US0026963 US8928102 US48771806	None	DuPont	US	28/09/1999
Method for producing polyhydroxyalkanoates in recombinant organisms	US12441799	WO200055328	Laval University, CA Ministry for Agriculture & Food	US, Canada, Austria, Germany, Portugal, Denmark, Spain	14/03/1999
Production of polyhydroxyalkanoates in plants	US15680799	WO2001023596	Pioneer Hi-Bred, DuPont	Australia, US	28/09/1999
Methods for transformation of plants, transformed plants and processes for preparation of polyesters	JP22583999	None	Riken	US, Germany	08//08/2000
Production of medium chain length polyhydroxyalkanoates from fatty acid biosynthetic pathways	US24953500	WO2002040690	Metabolix Inc.	US, Germany, Spain, Canada, Japan, Australia, Austria	16/11/2000
Transgenic plants used as a bioreactor system	US39486902	WO2004006657	Sugar Research Australia Limited, Bureau of Sugar Experiment Stations, The University of Queensland	US, Australia, Brazil, South Africa	10/07/2002
Production of polyhydroxybutyrate in switchgrass	US4843608 US43142809	None	Metabolix Inc.	US	27/04/2008
Polyhydroxyalkanoate synthesis in the plant peroxisomes	AU2008906035	WO2010057271	Sugar Industry Innovation Pty LTD, The University of Queensland, Brumbley Stevens	Australia	20/11/2008
Stable, fertile, high polyhydroxyalkanoate producing plants and methods of producing them	US15780909	WO2010102217	Metabolix Inc.	US, EU, Canada, Australia, Brazil, Germany, Spain, Austria	04/03/2009
Generation of high polyhydroxybutyrate producing oil seed crops	US24252209	WO2011034945	Metabolix Inc., Donald Danforth Plant Science Center, Patterson Nii, Tang Jihong, Cahoon Edgar, Jaworski Jan G, Peoples Oliver P, Snell Kristi D	US, EU, Australia, Canada, Brazil	14/09/2009
Increasing carbon flow for polyhydroxybutyrate production in biomass crops	US38314210	WO2012037324	Metabolix Inc.	US, Brazil	14/09/2010

Continued on the next page

Patent title	Priority application	Application by PCT	Owner	Country	Application date
Patents that protect plant vector, *phaC* gene and transit peptide					
pCAMBIA2301 plant vector	US90892807	None	CAMBIA	US	29/03/2007
phaC gene from *A. caviae*	US9685398	WO2000011188	Metabolix Inc.	Canada, Australia, EU, Korea, Mexico, Germany, US	17/08/1998
	US23587599	WO2000043523	Metabolix Inc.	Australia, Canada, Japan, Germany, EU, Spain, US	21/01/1999
	US49275606	None	Kaneka Corp.	US	25/07/2006
	US26016409	WO2011060048	Massachusetts Institute of Technology	Canada, Australia, Korea, Spain, China, Japan, US	10/11/2009
	JP2014067674	WO2015146195	Kaneka Corp.	Germany, EU, Japan, US	27/03/2014
Transit peptide ARL	US9800083	WO1999035278	Monsanto, Poirier Yves, Mittendorf Volker	Australia, EU	04/01/1998
	US23587599	WO2000043523	Metabolix Inc.	Canada, Australia, US, EU, Spain, Japan	21/01/2003
	AU2008906035	WO2010057271	Sugar Industry Innovation Pty LTD, The University of Queensland, Brumbley Stevens	Australia	20/11/2008

Patent applications WO1990061624 and US6228623 cover a method to produce polyhydroxypropionate, PHB, poly(3-hydroxypropionate-co-5-hydroxyvalerate) copolymers poly(3-hydroxypropionate-co-3-hydroxyvalerate), poly(3-hydroxybutyrate-co-4-hydroxyvalerate), poly(4-hydroxybutyrate-co-3-hydroxyhexanoate) and poly(3-hydroxybutyrate-co-4-hydroxybutyrate-co-3-hexanoate) in the cytosol of GM plants and in bacteria (Tab. 1).

Patent application WO1999000505 protects a genomic fragment and a method to enhance levels of substrates needed to generate the copolymers 3-hydroxybutyrate (3HB) and 3-hydroxyvalerate (3HV) through the insertion of *phaA*, *phaB*, *phaC* genes and encoding enzymes involved in the biosynthesis of the aspartate family amino acids and threonine deaminase.

Patent applications WO199505472, WO2010102217, and US6620601, protect a methodology to produce up to 10% PHB per unit of dry cell weight in *A. thaliana* and *N. tabacum* plastids by insertion of *phaA*, *phaB,* and *phaC* genes fused to a transit peptide to direct polymer biosynthesis in plastids. Granted patent WO200202040690 describes a GM plant expressing transgenes encoding the enzymes 3-hydroxyacyl ACP thioesterase and PHA synthase to produce PHA from fatty acids in plant plastids. Granted patent WO1992019747 describes a GM *Brassica* plant that produces PHAs when the genome contains genes encoding enzymes for the PHA biosynthetic pathway in the cytosol or plastids (Tab. 1).

Patent applications WO2001023596, WO1999035278, WO2000043523, and WO2010057271 cover a method to produce 1-2% dry weight of PHA polymers and copolymers in *A. thaliana* and sugarcane peroxisomes through the insertion of genes encoding 3-ketoacyl-CoA reductase or 2-enoyl-CoA hydratase and acetyl transferase attached to a transit peptide to direct peroxisome biosynthesis. These enzymes are derived from *A. caviae*, *C. necator, P. putida,* and *Klebsiella aerogenes* (Tab. 1). Patent WO1994011519 protects a PHB production system in oil seed crops transformed with a gene that mediates PHA biosynthesis fused to a switch gene induced by a chemical substrate that allows the synthesis of PHB in the cytosol or glyoxysomes of the seeds. Patent applications WO1998006854 and WO1999045122 request the protection of a methodology to modify the biosynthesis of fatty acids and produce polymers in plants by insertion of genes encoding the enoyl-CoA hydratase and epimerase from *P. putida* FaoAB involved in PHA biosynthesis, directing the enzymes towards the peroxisomes or plastids.

A patent family analysis on the production of PHAs in GM plants was performed to identify if these documents indicate the countries where the applicants seek technology protection. Demand for patents on PHA production in GM plants is highest in countries of North America followed by countries from Oceania (Fig. 2).

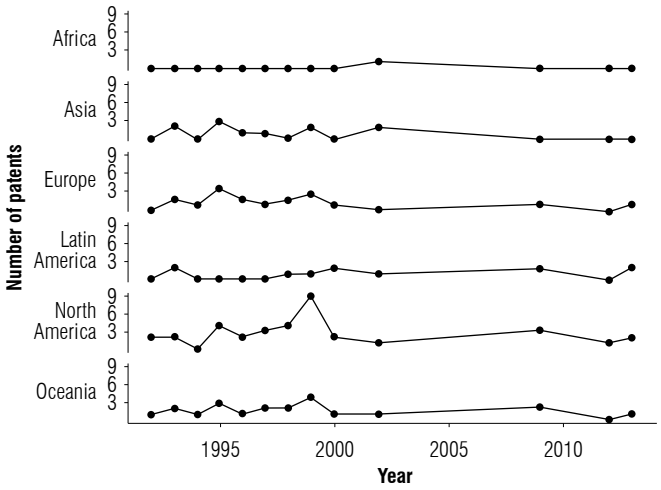

FIGURE 2. Trends on patents of PHA producing GM plants.

Trends indicate an average of 1.52 patent applications per year; the highest demand for patent applications was in 1999 in North America, Oceania, Europe, and Asia, while in Latin America the highest number of patents was registered in 1998 and 2009 (Fig. 2). This information shows a transition of patent demand since 1992, the year in which the first patent applications were registered. The number of patents related to this technology grew from 1995 to 1999; no applications were found between 2003 and 2007. The period from 2000 to 2010 shows a decrease in the rate of new advances. These data reveal that this technology could be classified as emerging in Latin America and as declining in North America, Oceania, and Europe.

The reduction in patent requests since 2000 may be because the technology still has not obtained enough yields in the production of biopolymers, and efforts have focused on microbial fermentation as demonstrated by Kosseva and Rusbandi (2018) improving the availability of substrates with a high carbon source and optimal growth conditions. Dobrogojski *et al*. (2018) suggest that it is necessary to increase the efficiency in the accumulation of PHAs in plants by optimizing the tissue conditions where PHAs are stored.

The technological areas related to PHA-producing GM plants patents are clustered in the groups: "human needs" and "chemicals and metallurgy" assigned by the IPC with A and C codes, respectively. The subclasses are plant reproduction by tissue culture techniques (A01H), biotechnology and genetic engineering (C12N), fermentation or enzymes using processes to synthesize a desired chemical compound (C12P), cracking hydrocarbon oils, production of liquid hydrocarbon mixtures (C10G), fuels not otherwise provided for (C10L), macromolecular compounds obtained from reactions not involving unsaturated carbon to carbon bonds (C08G) peptides (C07K) and sugar/nucleic acid/nucleosides (C07H). Applications across the IPC database is concentrated in the areas of biotechnology and genetic engineering (88.23%) followed by fermentation (35.29%), new plants (33.33%), and, in lesser percentage, peptides (9.8%), etc. (Fig. 3). Patent search in the IPC database not only facilitated the recovery of documents in the previously mentioned areas, but documents in other less common areas such as the composition of the epoxy resin or cracking hydrocarbon oils were also retrieved. Given that the IPC identifies each of the components that make up the technology, this system is useful for patent examiners and inventors to find documents that help identify the state of the technique.

Forward citation analyses are relevant to determine the progress of scientific knowledge related to the patented activity and to identify the relationship between science and technology for industrial development (Verbeek *et al*., 2003). An analysis of citations on the identification of PHA-producing GM plants patents across 1992-2013 found that old patents are cited more than recent ones, from 1992 to 1993. WO1994012014 was cited 45 times; between 1994 to 1995, WO1992019747 was mentioned 67 times; between 1996 and 1997, US6228623 was cited 88 times; between 2009 and 2010, WO2010102217 was mentioned 29 times; from 2012 to 2013, patent WO2012037324 was cited three times, and patent WO2011034945 was cited twice. The number of forward citations is an indicator of technological, social, and economic value of patents (Harhoff *et al*., 2002). In this case, patents such as WO1992019747 and US6103956 represent a benchmark of innovation. Patent WO1992019747 was requested by the company Metabolix Inc. in the US,

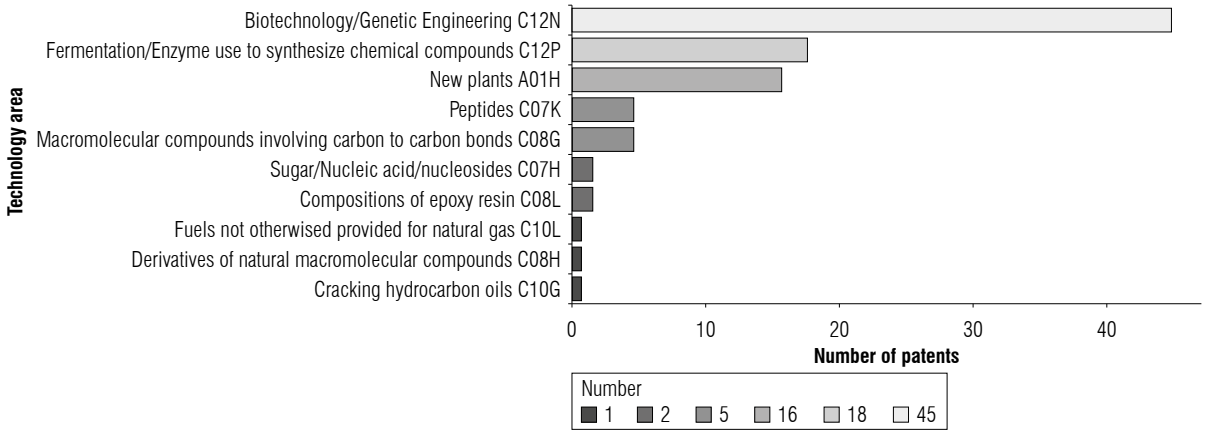

FIGURE 3. Technological areas of PHA-producing GM plant patents.

Australia, United Kingdom, and EU and had its highest peak of citations between 1998 and 2001. Patent US6228623 was requested by Metabolix Inc. and Bayer/Monsanto; its highest peak of citations was between 2010 and 2013. On the other hand, the low number of citations of recent patents, such as WO2012037324 and WO2011034945, is, probably, because, as of 2013, the technology has not shown a major advance in new applications (Tab. 1).

A freedom to operate (FTO) analysis was carried out for the development of GM tobacco events expressing *phaC* gene from *A. caviae* with the lowest possible patent load. Patent claims identification was done for the relevant elements involved in the making of a GM tobacco with the desired trait. It identified elements that composed this biotechnological product (vectors, transformation methods or genes) and analyzed the claims of the patents. Similarly, countries where requests and grants of a patent were made were determined as well as the patent status (Nagori & Mathur, 2009; Hincapié Rojas & Chaparro-Giraldo, 2014). These reports show limitations in the claims of the patents which may favor the development of new free patent products or facilitate the negotiation of licenses with the owners. Relevant patents were divided into five sections: *A. tumefaciens* strain and transformation method, promoters and transcription terminator, cloning vector, $phaC_{A.C}$ gene, and transit peptide.

A tissue culture protocol and a genetic transformation method must be established initially to obtain a GM tobacco line. Transformation mediated by *A. tumefaciens* strain LBA4404 is accomplished using leaf fragments as explants that generate new seedlings by direct organogenesis. Four patent families protect *A. tumefaciens* strain LBA440 as a method to transform dicotyledonous and monocotyledonous plants in a stable or transitory manner. Patent WO2004082368 protects this strain as an optimized method of genetic transformation based on *A. tumefaciens*-mediated transformation of *Brassica juncea* and was granted in Australia, the US and the EU; this patent will expire in 2023. Patent WO2013149726 protects a transient leaf transformation process using strain LBA4404; it was registered in Brazil and the US and was granted in Argentina, Australia, Canada, China, Mexico, Japan, and the EU. This patent will expire in 2032. Patent WO2010078445 covers a method of plant cell transformation and regeneration mediated by auxotrophic strains of *A. tumefaciens* (LBA4404, EHA101, C58, EHA105, AGL1, or GV3101) carrying a mutation in the *thyA* gene, a condition that prevents their growth in culture media lacking thymidine. This patent was requested in Australia and Canada and was granted in the US and China. Although it is valid until 2028, according to the information retrieved in the Lens database, no maintenance payment has been recorded since 2016. Therefore, it expired in February 2017. Patent WO2012016222 covers *A. tumefaciens* strains with genes that enhance transformation and are located in plasmids capable of replicating independently of the *Agrobacterium* chromosome. This patent was requested in Colombia, South Africa and Brazil and was granted in Australia, China, the EU, Mexico, the US, and Russia; it is valid until 2030. Patent W02010078445 is related to the transformation method, covering a process to produce a GM plant through systemic infection with an auxotrophic strain of *A. tumefaciens* LBA4404. This patent expired in 2017. Patent WO2004038023 covers an improved method of plant transformation with *A. tumefaciens* through a time interval between the preparation, inoculation, and co-culture stage. This patent was requested in Mexico, the EU, Canada and was granted in Australia, the US and Russia; it

is valid until 2022. Patent application WO2012098119 was granted to the Philip Morris Company in Brazil, China, Japan, the EU, the US, and Russia. This patent protects a transformation method to transiently express recombinant proteins through pressure infiltration of empty leaves of *N. tabacum* with *A. tumefaciens*. This patent will expire in 2031.

For the transcription of the *phaC* gene inserted into the plant genome, a 35S promoter from the cauliflower mosaic virus (35S CaMV) and the nopaline synthase terminator from *A. tumefaciens* (T-nos) is used. According to the information retrieved from the databases, one patent family protecting the CaMV 35S promoter was identified. Granted patent US5352605A protects the 35S CaMV promoter and the 19S CaMV promoter as part of expression constructs and plant transformation vectors in dicotyledonous plants using chimeric constructs. These patents expired in 2003; therefore, this promoter is already in the public domain. Likewise, there is a version with a duplicated 35S CaMV promoter that has an enhanced overexpression of the gene. Patent application US5164316 protects a transcription start sequence formed by tandem sequences of the 35S CaMV promoter and covers its use in plant genetic transformation. This patent expired in 2007. The terminator sequence of the T-nos expression construct is associated with patent US5034322, which protects chimeric genes containing the nopaline synthase promoter (*A. tumefaciens*) and a 3'-untranslated region of the nopaline synthase gene as well as the terminator sequence. This patent expired in 2003.

A group of vectors suitable for plant transformation is pCAMBIA plasmids. The Center for the Application of Molecular Biology to International Agriculture (CAMBIA) is a nonprofit research center in the field of botanical biotechnology that focuses on reforming the open science innovation system and intellectual property. pCAMBIA vectors are binary because they have an origin of replication in *Escherichia coli* and *A. tumefaciens* and contain the T-DNA region that houses the gene of interest to be transferred to the plant. CAMBIA has generated an open-source license in which the use of these vectors does not generate a royalty payment for institutions with research, academic, or nonprofit purposes, as well as for developing countries (CAMBIA, 2022). The expression constructs containing the coding region of the region of the $phaC_{A.C}$ gene from *A. caviae* assembled with the 35S CaMV promoter and the T-nos terminator are assembled into a vector of the family pCAMBIA; therefore, patents associated with pCAMBIA vectors were searched. Patent US20090075358 was granted in the US. Under this patent, two families of vectors are protected; the first covers vectors containing at least one functional origin of replication for non-rhizobial species and a T-DNA border sequence linked to the sequence of interest; the second family covers the vectors that contain a functional origin of replication in at least one non-rhizobial species and harbor *virA*, *virG*, *virJ* operons, and a mutant *virG*. This vector is incorporated into a bacterial host chromosome. This patent protects their use in the transformation of plants by *A. tumefaciens*. The patent expires in 2027 (Tab.1).

The $phaC_{A.c}$ is associated with five patent families and one patent application; patent application WO200011188 covers recombinant strains of microorganisms with the genes involved in PHA biosynthesis, where the gene encoding for PHA synthase was derived from *A. caviae*. This patent expired in 2018 (Tab.1). Patent WO2000043523 protects a method to produce PHA-producing GM organisms through the insertion of a PHA synthase gene from *A. caviae*, *Comamonas testosteroni*, and *Thiocapsa pfennigii,* among others. This patent was granted in Australia, Canada, the EU, and Japan. The payment of the maintenance fee was not made in 2016, according to the search done in the Lens database, and it lost its validity on January 17, 2017 (Tab.1). Patent WO2011060048, accepted through the PCT, protects a recombinant *C. necator*, which harbors the $phaC_{A.c}$ *gene from A. caviae to produce* poly(hydroxybutyrate-co-hydroxyhexanoate) copolymer; this patent is valid until 2033 in China, Japan, South Korea, Australia, the US, and the EU (Tab.1). Patent WO2015146195, granted in the EU, the US, Australia, and Japan, covers a method for the improvement of PHA copolymer synthesis using a microorganism with a gene encoding for a PHA synthase of *Aeromonas* sp. and a gene encoding for a different PHA synthase to produce two or more PHAs with different melting points; this patent will expire in 2035 (Tab.1). Patent US7384766, granted in the US, protects a transgenic microbial strain which contains a gene encoding PHA synthase from *A. caviae* to produce a PHA copolymer constituted by monomer units from 3-hydroxybutyric acid, 3-hydroxyhexanoic acid, 3-hydroxyheptanoic acid; this patent is valid until 2028 (Tab.1).

Studies conducted to produce biopolymers in tobacco, directing their biosynthesis towards chloroplasts at the nuclear level, have produced plants with chlorosis and delayed development (Lössl *et al*., 2003; Matsumoto *et al*., 2011). In other species, such as *Arabidopsis* and sugarcane, where the synthesis of biopolymers is targeted towards peroxisomes, no deleterious effects were observed in the plants (Matsumoto *et al*., 2006; Anderson *et al*., 2011; Tilbrook *et al*., 2011). An Ala-Arg-Leu (ARL) transit peptide is

attached at the C-terminal end of the expression construct containing the coding sequence of the $phaC_{A.c}$ gene from *A. caviae* to direct the enzyme PHA synthase towards peroxisomes (Tilbrook *et al*., 2014) (Tab.1). The transit peptide ARL is associated with three patent families assigned in Australia, Canada, Japan, the EU, and the US (WO1999035278, WO2000043523, and WO2010057271). These patents cover the expression of a PHA synthase and its targeting to plant peroxisomes by tripeptides Ala-Arg-Met, Ser-Arg-Met, Ser-Lys-Leu, Ala-Arg-Leu, Ser-Arg-Leu, Pro-Ser-Ile or Pro-Arg-Met, and the production of PHB in sugarcane peroxisomes by targeting *phaA*, *phaB,* and *phaC* gene products using a Arg-Ala-Val-Ala-Arg-Leu (RAVARL) signal sequence or any similar functional fragment. Patent WO1999035278 lost its validity in 2018, while patents WO2000043523 and WO2010057271 are valid until 2023 and 2028, respectively (Tab.1).

Plant breeder's rights (PBR) is a *sui generis* IPR resource used to protect varieties developed by genetic improvement, and the person who obtains these new varieties is called a breeder (UPOV, 2022). The granting of PBR entitles the holder to ownership of that variety and any person wishing to commercialize it must be authorized by the holder (breeder). This authorization is generally granted in the form of a license agreement. A variety can be protected by PBR if it meets all the following criteria: novelty, distinction, uniformity, and stability; it must also be given an appropriate denomination. The PBR is valid for 25 years from the grant date in the case of fruit trees, forest trees and vines and for 20 years in other species. Its validity is jurisdictional and is in force in the country where it was granted; however, if it is requested through intergovernmental organizations, the right is valid in all member states of the organization (ICA, 2017). The intergovernmental organization, the International Union for the Protection of New Varieties of Plants (UPOV), promotes an effective system of plant variety protection; its database (Pluto) contains plant breeder's titles requested in UPOV member countries for different plant species. UPOV members are eligible for the breeder's exemption, which allows all breeders to use protected varieties for further breeding activities (UPOV, 2013). PBR registrations for *N. tabacum* were identified in the Pluto database in the US, Canada, Mexico, Argentina, Colombia, the EU, Russia, South Korea, and China. The US and Bulgaria were the countries with the most PBR registrations for this species from 1950 to 2022. Ninety-six varieties were identified; protection is still in force for 22 of them. Some of the varieties that are in force are: KF109 (South Korea), KB111LC (South Korea), Wan6513 (China), Guang Yang (China), Vector 21-41 (Canada), Speight 22 (US), AOB176 (US), MB47 (Argentina), and MB411 (Argentina).

Once the patents expire, it is possible to develop generic seeds with the technology without prior authorization from the owner (Jefferson *et al*., 2015). The use of the technology without the need to pay for a license or royalties reduces costs of production and development and, increases access to technology for small-scale farmers or developing countries.

Where an agbiogeneric crop is generated, the developer of that GM crop must face the challenges of opening up a commercial authorization, especially those related to discordant harmonization between procedures because the regulations issued by the countries vary widely, not only in quantity but also in the level of aspect (Jefferson *et al*., 2015). GM crop regulation varies depending on whether the events belong to first, second or third generation. First GM generation events have traits such as herbicide tolerance and insect resistance, second GM generation crops have traits related to food and feed quality while third generation GM events comprise recombinant proteins or industrial products (*e.g*., pharmaceutics or biodegradable polymers) (Spök *et al*., 2008). The Cartagena Protocol on Biosafety (Law 740 of 2002 in Colombia) contains specific regulations on GM organisms. In essence, it is a normative body that dictates policies and suggested actions for the different dimensions of intended use, whether these are to be exported or imported or cultivated for food or feed (Turnbull *et al*., 2021). First and second generation GM crops projected for feed usually require substantial equivalence studies, a comparison of a GM product and its conventional counterpart, including an agronomic performance assessment and tests to determine any adverse effect on environment or human health (allergenicity and toxicity) (McHughen, 2016; National Academies of Sciences Engineering and Medicine, 2016). For third generation GM events, in addition to agronomic, environmental, and human health biosafety requirements, an environmental commercial release plan must be provided to ensure that there will be no contamination of seeds used for human or animal consumption (Spök *et al*., 2008).

In some countries, regulations are centered around GM crops for food and animal feed, while in other countries, the focus is more on importation of GM products for human consumption. In the US, the GM crops are regulated by different agencies (USDA APHIS, 2022). In contrast, Canadian regulations for GM crops are based on novel traits, so they

may also be described as having a new trait rather than as a GM crop in itself, with methods not taken into account (CFIA, 2020). The Council of the European Union passes regulations, usually focusing on the GM products imported to their own countries rather than cultivation (Eriksson *et al*., 2020). In the case of Latin America, there are efforts to achieve a harmonized regulatory framework by crops and products, with a case-by case examination for those countries where use and cultivation is allowed, including Brazil, Argentina, Colombia, Costa Rica, Honduras, Paraguay, and Uruguay (Benítez *et al*., 2020).

A global data package containing the tests and evaluations performed by the holder of the expired patent is a relevant step in a series of conditions designed for the commercial approval of an agbiogeneric by the authorities in the countries where GM events can be marketed for cultivation (Rüdelsheim *et al*., 2018). When a GM event is deregulated in the US, it can be freely marketed without the need for new approval requests unless new traits are introduced or there are changes to the GM event (USDA-APHIS). In the European Union, China and South Korea among others, authorizations for an approval extension must be requested by providing updated information and periodical reports (Rüdelsheim *et al*., 2018). If a GM event is no longer protected and the original inventor or patent holder no longer has an updated approval for a specific country, an agbiogeneric cannot be commercialized in that country, given that the original developer holds the rights to the regulatory data and the regulatory offices considers them confidential. An alternative would be for the agbiogeneric developer to reach an agreement involving a license (Rüdelsheim *et al*., 2018). The other option is to initiate a regulatory process with own data by tests specific to regions where the commercial approval is planned. It is also important to note that if an agbiogeneric represents a new GM event, the developer must provide information about insertion location and effects on agronomic traits. A common cost-cutting measure is to negotiate management agreements to access and use general information valid for several events (transgene source, nucleotide sequence, protein, genetic trait, allergenicity, toxicity) (Rüdelsheim *et al*., 2018).

Conclusions

The patent analysis related to PHA-producing GM plants shows that, for some countries (*e.g.*, the US or Australia), development has not continued with the same intensity. This technology in Latin America is just launching. Of the six patent applications for PHA-producing GM plants, only four are in force: WO2004006657 expires in 2022, WO2010102217 and WO2010057271 expires in 2029, and WO2012037324 expires in 2032. Upon expiration, the protected invention becomes public; a generic manufacturer can develop the PHA-producing GM tobacco agbiogeneric, such as drought-tolerant GM corn or glyphosate-tolerant GM soybean (Zanga *et al*., 2015; Rojas Arias *et al*., 2017). Up to the date of this study, there is no patent that includes PHA-producing GM tobacco using the *A. caviae phaC* gene for in the peroxisome synthesis.

Acknowledgments

This study was funded by the Colombian Ministry of Science, Technology, and Innovation (code 123380763011, contract 802-2018) and Banco de la República de Colombia (project 4552). DDPD is grateful to the Colombian Huila department and the Colombian Ministry of Science, Technology, and Innovation for her Ph.D. fellowship (contract 677-2015).

Conflict of interest statement

The authors declare that there is no conflict of interests regarding the publication of this article.

Author's contributions

DDPD: Conceptualization, data analysis, analysis, research, writing of original draft and editing. FVB: Formal analysis, research. FSS: Research, resources, formal analysis. ACG: Conceptualization, resources. SALP: Conceptualization, data analysis, analysis, research, writing of original draft, and editing. All authors reviewed the final version of the manuscript.

Literature cited

Alandete-Saez, M., Chi Ham, C., Graff, G., Boettiger, S., & Bennet, A. B. (2016). Intellectual property in agricultural biotechnology: Strategies for open access. In N. Stewart (Ed.), *Plant biotechnology and genetics: Principles, techniques, and applications* (pp. 347–363). John Wiley & Sons.

Anderson, D. J., Gnanasambandam, A., Mills, E., O'Shea, M. G., Nielsen, L. K., & Brumbley, S. M. (2011). Synthesis of short-chain-length/medium-chain length polyhydroxy alkanoate-(PHA) copolymers of peroxisomes in transgenic sugarcane. *Tropical Plant Biology*, *4*, 170–184. https://doi.org/10.1007/s12042-011-9080-7

Arai, Y., Nakashita, H., Suzuki, Y., Kobayashi, Y., Shimizu, T., Yasuda, M., & Yamaguchi, I. (2002). Synthesis of a novel class of polyhydroxyalkanoates in *Arabidopsis* peroxisomes, and their use in monitoring short-chain-length intermediates of β-oxidation. *Plant & Cell Physiology*, *43*(5), 555–562. https://doi.org/10.1093/pcp/pcf068

Barreto González, A., Lamus Becerra, M., Acuña Porras, A., Asprilla, A., Ramírez Orozco, M., & Smith, G. (2020). *Manual sobre el*

tratado de cooperación de patentes (PCT). (SIC, Ed.). https://www.sic.gov.co/sites/default/files/files/Publicaciones/Cartilla%20Manual%20PCT%20FInal.pdf

Benítez Candia, N., Fernández Ríos, D. R., & Vicién, C. (2020). Paraguay's path toward the simplification of procedures in the approval of GE crops. *Frontiers in Bioengineering and Biotechnology, 8*, Article 1023. https://doi.org/10.3389/fbioe.2020.01023

Bohmert-Tatarev, K., McAvoy, S., Daughtry, S., Peoples, O. P., & Snell, K. D. (2011). High levels of bioplastic are produced in fertile transplastomic tobacco plants engineered with a synthetic operon for the production of polyhydroxybutyrate. *Plant Physiology*, *155*(4), 1690–1708. https://doi.org/10.1104/pp.110.169581

Buyel, J. F., & Fischer, R. (2012). Predictive models for transient protein expression in tobacco (*Nicotiana tabacum* L.) can optimize process time, yield, and downstream costs. *Biotechnology and Bioengineering*, *109*(10), 2575–2588. https://doi.org/10.1002/bit.24523

CAMBIA. (2022, February 12). *Legacy pCAMBIA vectors.* https://cambia.org/welcome-to-cambialabs/cambialabs-projects/cambialabs-projects-legacy-pcambia-vectors-pcambia-legacy-vectors-1

Carroll, M. J. (2016). The importance of regulatory data protection or exclusive use and other forms of intellectual property rights in the crop protection industry. *Pest Management Science*, *72*(9), 1631–1637. https://doi.org/10.1002/ps.4316

CFIA. (2022, September 01). *Plant with novel traits*. https://www.inspection.gc.ca/plant-varieties/plants-with-novel-traits/eng/1300137887237/1300137939635

Dobrogojski, J., Spychalski, M., Luciński, R., & Borek, S. (2018). Transgenic plants as a source of polyhydroxyalkanoates. *Acta Physiologiae Plantarum*, *40*, Article 162. https://doi.org/10.1007/s11738-018-2742-4

Eriksson, D., Custers, R., Björnberg, K. E., Hansson, S. O., Purnhagen, K., Qaim, M., Romeis, J., Schiemann, J., Schleissing, S., Tosun, J., & Visser, R. G. (2020). Options to reform the European Union legislation on GMOs: scope and definitions. *Trends in Biotechnology, 38*, 231–234. https://doi.org/10.1016/j.tibtech.2019.12.002

Fearon, S. H., Dennis, S. J., Hitzeroth, I. I., Rybicki, E. P., & Meyers, A. E. (2022). Plant expression systems as an economical alternative for the production of iELISA coating antigen AHSV VP7. *New Biotechnology, 68*, 48–56. https://doi.org/10.1016/j.nbt.2022.01.009

Gupta, J., Rathour, R., Maheshwari, N., & Thakur, I. S. (2021). Integrated analysis of whole genome sequencing and life cycle assessment for polyhydroxyalkanoates production by *Cupriavidus* sp ISTL7. *Bioresource Technology*, *337*, Article 125418. https://doi.org/10.1016/j.biortech.2021.125418

Harhoff, D., Scherer, F. M., & Voepel, K. (2002). Citations, family size, opposition and the value of patent rights. *Research Policy*, *32*(8), 1343–1363. https://doi.org/10.1016/S0048-7333(02)00124-5

Heikkilä, J., & Lorenz, A. (2018). Need for speed? Exploring the relative importance of patents and utility models among German firms. *Economics of Innovation and New Technology*, *27*(1), 80–105. https://doi.org/10.1080/10438599.2017.1310794

Hincapié Rojas, V. P., & Chaparro-Giraldo, A. (2014). Estudio de libertad de operación para una línea genéticamente modificada de papa (*Solanum tuberosum* L.). *Revista Colombiana de Biotecnología*, *16*(1), 119–128. https://doi.org/10.15446/rev.colomb.biote.v16n1.44260

Ibrahim, A., Odon, V., & Kormelink, R. (2019). Plant viruses in plant molecular pharming: toward the use of enveloped viruses. *Frontiers in Plant Science, 10*, Article 803. https://doi.org/10.3389/fpls.2019.00803

ICA. (2017). *Legislación sobre protección a los derechos de obtentores de variedades vegetales* (4th ed.). Produmedios. https://www.ica.gov.co/getattachment/ICAComunica/Infografias/cartilla_legislacion_obtentores.pdf.aspx?lang=es-CO

Jefferson, D. J., Graff, G. D., Chi-Ham, C. L., & Bennet, A. B. (2015). The emergence of agbiogenerics. *Nature Biotechnology*, *33*(8), 819–823. https://doi.org/10.1038/nbt.3306

Jeon, J.-M., Brigham, C. J., Kim, Y.-H., Kim, H.-J., Yi, D.-H., Kim, H., Rha, C., Sinskey, A. J., Yang, Y.-H. (2014). Biosynthesis of poly(3-hydroxybutyrate-co-3-hydroxyhexanoate) (P(HB-co-HHx)) from butyrate using engineered *Ralstonia eutropha*. *Applied Microbiology and Biotechnology*, *98*, 5461–5469. https://doi.org/10.1007/s00253-014-5617-7

Jia, K., Cao, R., Hua, D. H., & Li, P. (2016). Study of class I and class III polyhydroxyalkanoate (PHA) synthases with substrates containing a modified side chain. *Biomacromolecules*, *17*(4), 1477–1485. https://doi.org/10.1021/acs.biomac.6b00082

Kosseva, M. R., & Rusbandi, E. (2018). Trends in the biomanufacture of polyhydroxyalkanoates with focus on downstream processing. *International Journal of Biological Macromolecules*, *107*(Part A), 762–778. https://doi.org/10.1016/j.ijbiomac.2017.09.054

Lössl, A., Eibl, C., Harloff, H.-J., Jung, C., & Koop, U.-H. (2003). Polyester synthesis in transplastomic tobacco (*Nicotiana tabacum* L.): significant contents of polyhydroxybutyrate are associated with growth reduction. *Plant Cell Reports, 21*, 891–899. https://doi.org/10.1007/s00299-003-0610-0

Matsumoto, K., Arai, Y., Nagao, R., Murata, T., Takase, K., Nakashita, H., Taguchi, S., Shimada, H., & Doi, Y. (2006). Synthesis of short-chain-length/medium-chain-length polyhydroxyalkanoate (PHA) copolymers in peroxisome of the transgenic *Arabidopsis thaliana* harboring the PHA synthase gene from *Pseudomonas* sp. 61-3. *Journal of Polymers and the Environment*, *14*, 369–374. https://doi.org/10.1007/s10924-006-0035-2

Matsumoto, K., Morimoto, K., Gohda, A., Shimada, H., & Taguchi, S. (2011). Improved polyhydroxybutyrate (PHB) production in transgenic tobacco by enhancing translation efficiency of bacterial PHB biosynthetic genes. *Journal of Bioscience and Bioengineering*, *111*(4), 485–488. https://doi.org/10.1016/j.jbiosc.2010.11.020

McHughen, A. (2016). A critical assessment of regulatory triggers for products of biotechnology: Product vs. process. *GM Crops & Food, 7*, 125–158. https://doi.org/10.1080/21645698.2016.1228516

McNulty, M. J., Xiong, Y., Yates, K., Karuppanan, K., Hilzinger, J. M., Berliner, A. J., Delzio, J., Arkin, A. P., Lane, N. E., Somen, N., & McDonald, K. A. (2021). Molecular pharming to support human life on the moon, Mars, and beyond. *Critical Reviews in Biotechnology, 41*(6), 849–864. https://doi.org/10.1080/07388551.2021.1888070

Muneer, F., Rasul, I., Azeem, F., Siddique, M. H., Zubair, M., & Nadeem, H. (2020). Microbial polyhydroxyalkanoates (PHAs): efficient replacement of synthetic polymers. *Journal of Polymers and the Environment*, *28*, 2301–2323. https://doi.org/10.1007/s10924-020-01772-1

Nagori, B. P., & Mathur, V. (2009). Basics of writing patent non-infringement and freedom-to-operate opinions. *Journal of Intellectual Property Rights*, *14(*1), 7–13.

National Academies of Sciences Engineering and Medicine. (2016). *Genetically engineered crops: Experiences and prospects.* National Academies Press. https://doi.org/10.17226/23395

Rojas Arias, C., Palacio, J. L., Chaparro-Giraldo, A., & López-Pazos, S. A. (2017). Patents and genetically modified soybean for glyphosate resistance. *World Patent Information*, *48*, 47–51. https://doi.org/10.1016/j.wpi.2017.01.002

Rüdelsheim, P., Dumont, P., Freyssinet, G., Pertry, I., & Heijde, M. (2018). Off-patent transgenic events: Challenges and opportunities for new actors and markets in agriculture. *Frontiers in Bioengineering and Biotechnology, 6*, Article 71. https://doi.org/10.3389/fbioe.2018.00071

Spök, A., Twyman, R. M., Fischer, R., Ma, J. K., & Sparrow, P. A. (2008). Evolution of a regulatory framework for pharmaceuticals derived from genetically modified plants. *Trends in Biotechnol*ogy, *26*(9), 506–517. https://doi.org/10.1016/j.tibtech.2008.05.007

Stouten, G. R., Hogendoorn, C., Douwenga, S., Kilias, E. S., Muyzer, G., & Kleerebezem, R. (2019). Temperature as competitive strategy determining factor in pulse-fed aerobic bioreactors. *The ISME Journal*, *13*(12), 3112–3125. https://doi.org/10.1038/s41396-019-0495-8

Tilbrook, K., Gebbie, L., Schenk, P. M., Poirier, Y., & Brumbley, S. M. (2011). Peroxisomal polyhydroxyalkanoate biosynthesis is a promising strategy for bioplastic production in high biomass crops. *Plant Biotechnology Journal*, *9*(9), 958–969. https://doi.org/10.1111/j.1467-7652.2011.00600.x

Tilbrook, K., Poirier, Y., Gebbie, L., Schenk, P. M., McQualter, R. B., & Brumbley, S. M. (2014). Reduced peroxisomal citrate synthase activity increases substrate availability for polyhydroxyalkanoate biosynthesis in plant peroxisomes. *Plant Biotechnology Journal*, *12*(8), 1044–1052. https://doi.org/10.1111/pbi.12211

Turnbull, C., Lillemo, M., & Hvoslef-Eide, T. A. (2021). Global regulation of genetically modified crops amid the gene edited crop boom–A review. *Frontiers in Plant Science, 12*, Article 630396. https://doi.org/10.3389/fpls.2021.630396

Unión Internacional para la Protección de las Obtenciones Vegetales - UPOV. (2022, March 1). Notas explicativas sobre la definición de obtentor con arreglo al acta de 1991 del convenio de la UPOV. https://www.upov.int/edocs/expndocs/es/upov_exn_brd.pdf

USDA APHIS. (2022, March 1). Petitions for determination of non-regulated status. https://www.aphis.usda.gov/aphis/ourfocus/biotechnology/permits-notifications-petitions/petitions/petition-status

Verbeek, A., Debackere, K., & Luwel, M. (2003). Science cited in patents: A geographic "flow" analysis of bibliographic citation patterns in patents. *Scientometrics*, *58*(2), 241–263. https://doi.org/10.1023/A:1026232526034

Wolf, T. E. (2008). Freedom-to-operate patent searching: my six basis rules. *Searcher-the Magazine for Database Professionals*, *16*(5), 34–39.

Zanga, D., Capell, T., Zhu, C., Christou, P., & Thangaraj, H. (2015). Freedom-to-operate analysis of a transgenic multivitamin corn variety. *Plant Biotechnology Journal, 14*(5), 1225–1240. https://doi.org/10.1111/pbi.12488

Agronomic evaluation of chonto tomato (*Solanum lycopersicum* Mill.) lines of determinate growth

Evaluación agronómica de líneas de tomate chonto (*Solanum lycopersicum* Mill.) de crecimiento determinado

Alexis Josué Vallecillo Godoy[1]*, Sanín Ortiz Grisales[1], Franco Alirio Vallejo Cabrera[1], Myrian Del Carmen Salazar Villareal[1], Dilmer Gabriel Guerra Guzmán[1], and Fredy Antonio Salazar Villareal[2]

ABSTRACT

The aim of this study was to evaluate the results of the agronomic performance of five chonto tomato lines of determinate growth in Valle del Cauca, Colombia, with plants of indeterminate growth Unapal Maravilla as control. In the field, a randomized complete block design was used for four evaluations, with four replicates and five plants as an experimental unit, respectively. The final plant height for all the lines, except Unapal Maravilla, was evaluated between 90 and 100 d with no statistical differences (P<0.05) between treatments. The lines of determinate growth expressed no differences (P<0.05) with Unapal Maravilla for the number of clusters per plant and the number of fruits per cluster. At the same time, they surpassed Unapal Maravilla in fruit weight at 117 g/fruit (lines JV9, JV7, and JV12), and final yield was greater than 4 kg/plant. The lines of determinate growth at physiological maturity were similar to Unapal Maravilla in the uniform final color of fruits (cherry red), fruit shape round in equatorial diameter and slightly elongated in polar diameter, and number of locules (bicavitary); they expressed inferiority for total fruit solids between 3.5 and 3.6° Brix vs. 4.32° Brix to the control (P<0.05). The final height for the lines of determinate growth ranged between 97.7 and 109.0 cm, respectively, while the Unapal Maravilla plants had more than 200 cm in height.

Key words: crop performance, fruit quality, genotype, plant breeding.

RESUMEN

El objetivo de este estudio fue evaluar el comportamiento agronómico de cinco líneas de tomate chonto de crecimiento determinado en el Valle del Cauca, Colombia. Se usaron cinco líneas de crecimiento determinado y un testigo de crecimiento indeterminado Unapal Maravilla. En campo, se usó un diseño de bloques completamente aleatorizados, con cuatro repeticiones y cinco plantas como unidad experimental respectivamente para las cuatro evaluaciones. La altura final de las plantas, para todas las líneas, excepto Unapal Maravilla, se evaluó entre 90 y 100 d sin diferencias estadísticas (P<0.05) entre tratamientos. Las líneas de crecimiento determinado no expresaron diferencias (P<0.05) con Unapal Maravilla para número de racimos por planta y número de frutos por racimo, mientras que el rendimiento fue superior a Unapal Maravilla en: peso del fruto, mayor a 117 g/fruto (líneas JV9, JV7 y JV12) y rendimiento final mayor a 4 kg/planta. Las líneas de crecimiento determinado en madurez fisiológica fueron similares a Unapal Maravilla en color final uniforme (rojo cereza), formato del fruto redondo en el diámetro ecuatorial y ligeramente elongado en el diámetro polar, y número de lóculos (bicavitarios); y expresaron inferioridad para sólidos totales en fruto entre 3.5 y 3.6 °Brix vs. 4.32 °Brix respecto al testigo (P<0.05). La altura final para las líneas de crecimiento determinado fluctuó entre 97.7 y 109.0 cm respectivamente, mientras que las plantas Unapal Maravilla tuvieron más de 200 cm de altura.

Palabras clave: desempeño de cultivo, calidad del fruto, genotipo, fitomejoramiento.

Introduction

The tomato (*Solanum lycopersicum* Mill.) is the most cultivated vegetable in the world, associated with the increasing demand for fresh and processed consumption (Maham *et al*., 2020; Rawat *et al*., 2020) as well as with its contribution to the socioeconomic welfare of horticulture and agribusiness worldwide (Tabe & Molua, 2017; Stilwell, 2020).

In Colombia, during 2020, 8,787 ha were cultivated and harvested, with 656,647 t ha^{-1} (FAOSTAT, 2020) produced in the departments of Cundinamarca, Norte de Santander, Valle del Cauca, Boyacá, Huila, Antioquia, Risaralda, and Caldas (Perilla *et al*., 2011).

However, in Colombia, the production of this vegetable is restrained by the limited release of new varieties with

Received for publication: July 6, 2022. Accepted for publication: November 5, 2022 Doi: 10.15446/agron.colomb.v40n3.103518

[1] Universidad Nacional de Colombia, Palmira, Valle del Cauca (Colombia).
[2] Genetic Improvement Area, Sugarcane Research Center of Colombia-Cenicaña, Cali (Colombia).
* Corresponding author: avallecillog@unal.edu.co

greater adaptability, causing significant pre-harvest losses due to pests and diseases (Burbano & Vallejo, 2017). Other problems are the high production costs attributed to the type of growth habit; in this case, those of indeterminate habit (most used by farmers) involve arduous pruning, trellising, and greater consumption of materials and inputs (Piotto & Perreira, 2012).

To minimize the cost of production and environmental damage by excess use of pesticides and improve productivity, chonto tomato cultivars are needed for their specific growth habit (small and compact plant without a tutor system). This facilitates lower production costs (Sun *et al*., 2019; Casavian *et al*., 2021). This topic has been the subject of study of the Vegetable Breeding and Seed Production Program (PMGPSH, for its acronym in Spanish) at the Universidad Nacional de Colombia. This basic research has been conducted for more than six years, generating chonto tomato lines with a determinate growth habit from backcrossing between the Brazilian cultivar IPA 4 donor of the SP (*Self Pruning*) gene and the Colombian cultivar (recurrent progenitor) UNAPAL-Maravilla.

Research is needed to obtain new cultivars of determinate growth, with the objective of making better use of the natural resources used by farmers to achieve sustainability and profitability of crops.

Materials and methods

Plant material and location

Five lines of determinate growth chonto tomato (DGCT) (Fig. 1) generated by the Vegetable Program of theUniversidad Nacional de Colombia were used. As a control, indeterminate growth Chonto tomato cultivar Unapal Maravilla (IGCT) was used. Four field trials were conducted in the experiment, three of them at the experimental station Mario Gonzales Aranda (GMGA) farm in 2018 and 2019. This farm is located in Palmira, Valle del Cauca, Colombia, at an altitude of 998 m a.s.l. The mean temperature is 23°C, monthly rainfall is 60 mm, and average relative humidity is 80%. The experimental area's soil was classified as low organic matter, with a slightly acidic pH (5-6) and a low cation exchange capacity.

The fourth test was carried out in Candelaria, Valle del Cauca, Colombia, at the Experimental Station of the Universidad Nacional de Colombia, Palmira campus. It is located at an altitude of 980 m a.s.l., with a monthly rainfall of 26 mm, a mean temperature of 24°C, and a relative humidity of 76%. The experimental area's soil has low contents of organic matter (1.48 g 100 g^{-1}), a neutral pH of 6.8, and a high cation exchange capacity (27.1 cmol kg^{-1}).

Experimental conditions

All plants were transplanted 22 d after planting. Ten vigorous seedlings of each line were taken to the field. Unapal-Maravilla was used as a control in the experiment, and each genotype was placed in a furrow. The field layout was 1.50 and 0.50 m between rows and plants. Drip irrigation hoses were placed at a distance of 20 cm per dripper; individual tutors were used for each plant, and plastic thread was used to hold them. Fieldwork, such as fertilization and plant protection, was done based on the recommendation of the Vegetable Breeding Program of the Universidad Nacional de Colombia (Estrada *et al*., 2004).

Variables evaluated

The descriptors for tomato of the International Plant Genetic Resources Institute (IPGRI) (1996), now called Bioversity International, and the evaluation criteria suggested by Burbano and Vallejo (2017) were used. Phenology variables were: days to flowering initiation (DFI), days to harvest (DH), duration to harvest (HD), crop cycle (CC); yield component variables were: number of clusters per plant (NCPP), number of fruits per cluster (NFPC), number of fruits per plant (NFPP), fruit weight (FW) (g/fruit), yield per plant (YPP) (kg/plant); morphological variables were: final plant height (FPH) (cm), fruit color (FC), sphericity index (SI), polar fruit diameter (PD) (cm), equatorial fruit diameter (ED) (cm), number of locules per fruit (NL), pericarp thickness (PT), and contents of total soluble solids (TSS).

Statistical analysis

A randomized complete block design was used with four replicates, five DGCT lines in the test, and IGCT line as a control. One furrow per line was used, with ten plants per furrow and five central plants as experimental unit.

For the different variables, descriptive statistics, analysis of variance (ANOVA), and test of difference of means between lines (Tukey test at 5%) were performed using SAS v. 9.4 (Statistical Analysis System Institute, Cary, NC, USA).

FIGURE 1. Genotypes generated by the Vegetable Program of the Universidad Nacional de Colombia, Palmira (Colombia).

Results and discussion

The combined analysis of variance for the phenological variables (Tab. 1) showed highly significant differences ($P<0.01$) for the source of variation genotypes in the variables DFI, DH, CC, FPH, YPP, FW, NFPP, TSS, NL, PD, ED, and PT. These results indicated a heterogeneity between the genotypes for these characteristics, with differences in the values of the evaluated variables. No significant differences were found for NCPP, NFPC, and FC, suggesting that there are no genetic differences between the genotypes evaluated for these traits.

TABLE 1. Combined analysis of variance with its mean squares and significance for the variables under study between determinate growth chonto tomato (DGCT) lines and the indeterminate growth chonto tomato (IGCT) cultivar Unapal-Maravilla.

Variables	Source of variation					CV (%)	Mean
	Genotype(G)	Environment(E)	Rep(E)	GXE	Error		
	DF	5	3	11	15	55		
DFI	11.0**	52.9**	2.5**	2.6**	0.91	6.13	15
DH	128.3**	668.1**	10.4*	18.2**	5.16	3.37	67
HD	8.2ns	796.6**	15.2*	25.5**	7.2	10.69	25
CC	109.9**	1562.5**	7.9ns	27.3**	6.8	2.84	91
FPH	32240.6	1280.4	103.9	159.9	111.2	8.54	123.4
NCPP	0.35ns	139.97**	3.59ns	2.4ns	3.2	12.58	12.5
NFPC	0.06ns	0.21ns	0.2ns	0.15ns	0.12	9.41	3.6
NFPP	306.52**	1000.92ns	21.51ns	52.23ns	33.45	15.44	37.5
FW	157.72ns	829.75**	41.14ns	77.74*	41.83	5.64	114.66
YPP	6.65**	19.91**	0.3ns	0.48ns	0.39	15.56	4.03
TSS	0.69**	0.55**	0.02ns	0.03ns	0.06	6.63	3.69
NL	0.49**	0.08**	0.01ns	0.04**	0.01	4.8	2
PD	2.48**	1.96**	1.39ns	1.39ns	1.33	17.48	6.6
ED	0.1**	0.12**	0.03ns	0.03ns	0.02	2.58	5.62
PT	2.21**	3.02**	0.05ns	0.11ns	0.07	3.48	7.56
FC	0.07ns	0.04*	0.11**	0.03ns	0.03	2.1	6.8

Rep: replicate; DF: degrees of freedom; *significant (5% probability), **highly significant (1% probability), ns = not significant, DFI: days to flowering initiation; DH: days to harvest; HD: duration to harvest; CC: crop cycle; FPH: final plant height (cm); YPP: yield per plant (kg/plant); FW: fruit weight (g/fruit); NCPP: number of clusters per plant; NFPC: number of fruits per cluster; NFPP: number of fruits per plant; TSS: total soluble solids (°Brix); NL: locule number; PD: polar diameter (cm): ED: equatorial diameter (cm); PT: pericarp thickness (mm); FC: fruit color.

Days to flowering initiation (DFI)

All lines, except EB-L14, initiated flowering in a shorter time, between 14 and 15 d, with respect to the control. The JV6 line initiated flowering at 14 d, the earliest among the genotypes evaluated. These data coincide with the 16, 14, and 18 d in DGCT for days to flowering initiation in Kumar *et al*. (2016) and Burbano and Vallejo (2017) and contrasts with the 25 and 36 d for flowering initiation in DGCT in Sherpa *et al*. (2014) and the 44.4, and 34.7 reported by Raj *et al*. (2018) for DGCT. Genotypes that present a reduction in the DFI have less production time, a feature that is desirable in tomato breeding programs.

Days to harvest (DH)

For the variable "days to harvest", the lines DGCT were similar (P<0.05) with a period of approximately 65 d, earlier than the control, with a value of 73 d. This finding matches with Mahebub *et al*. (2021), who reported a DH of 67.7 d in determinate-growth tomato. However, Burbano and Vallejo (2017) working with the same DGCT lines of this study found DH greater than 70 d.

Duration to harvest (HD)

The average HD expressed no significant differences (P<0.05) between the lines and control, with an HD between 24 and 26 d. Some studies show that, in the case of indeterminate tomato, the HD corresponds to a period of 37 d, while for determinate tomato, it corresponds to 16 and 27 d (Moya *et al*., 2003).

Crop cycle (CC)

For IGCT, all activity was suspended just as the DGCT lines finished production and aged, which meant equal DH for the lines and DGCT (Tab. 2). This may seem incorrect, as IGCT remains in production for up to 150 d. The DGCT lines presented a lower productive cycle compared to the control, with a duration of 96 d; the EB-L14 line had the lowest cycle with a mean of 89.6 d, the other lines had a longer growth cycle, between 90.2 and 91.5 d (Tab. 2). Burbano and Vallejo (2017) report a much shorter productive cycle for determinate growth accessions with duration up to 87 to 88 d and for indeterminate type a period of 111 d.

Obtaining short cycle genotypes is of great interest in breeding programs, since it allows a reduction of the plant exposure in the field and adverse environmental situations such as drought stress and diseases (Nascimento *et al*., 2020). In addition, the amount of chemical fertilizer applications is reduced, which is beneficial in ecological and economic terms, since fewer inputs are required (Burbano & Vallejo, 2017).

Final plant height (FPH)

Overall, the DGCT lines expressed the expected height, with a 50% difference from IGCT (P<0.05), ranging between 97.7 and 109.0 cm for JV6 and EB-L14, respectively (Tab. 2). These results agree with Muhammad *et al.* (2019) who report DGCT accessions of no more than 1 m until reaching height and initiating senescence. In the same sense and in contrast to the present study data, Kumar *et al.* (2016) evaluated 40 DGCT genotypes and reported a final plant height ranging between 52.1 and 184.5 cm.

According to the above data, determinate growth lines of tomato presented the desired height, which implies a reduction in production costs from less labor, less use of materials and inputs, and less pruning (Piotto & Peres, 2012). In addition, determinate-growth tomatoes are ideal in the open field because sympodial shoots quickly differentiate into flowers that result in rapid and uniform fruit maturity (Jiang *et al.*, 2013). This rapid and uniform maturity of the fruits allows for the mechanized harvest in tomatoes in open field, ideal for the industry (Silva *et al.*, 2017). Therefore, a new alternative is available that could be adopted by Colombian farmers in the Cauca Valley region in the future.

TABLE 2. Comparison of means for phenological variables and final plant height of determinate growth chonto tomato (DGCT) lines and the indeterminate growth chonto tomato (IGCT) cultivar Unapal-Maravilla.

Genotypes	DFI	DH	HD	CC	FPH
JV6	15.0c	66.2b	24.7a	90.7b	97.7b
JV9	14.7c	65.8b	24.98a	90.2b	102.9b
JV7	15.2bc	67.0b	24.0a	91.8b	108.6b
EB-L14	16.1ab	66.3b	25.7a	89.6b	109.0b
JV12	15.1bc	65.8b	258a	90.8b	102.8b
UNAPAL-Maravilla	16.9a	73.0a	26.0a	96.5a	219.4a
Mean	15.5	67.4	25.1	91.5	123.4
LSD	1.0	2.4	2.9	2.80	11.3

In the column, values with the same letter are equal (P<0.05) LSD = least significant differences. DFI = days to flowering initiation (d); DH = days to harvest (d); HD = duration to harvest (d); CC = crop cycle (d); FPH = final plant height (cm).

Number of clusters per plant (NCPP) and number of fruits per cluster (NFPC)

The NCPP and NFPC variables were not significantly different (P<0.05) between the lines and the control (Tab. 3). The NCPP presented a mean of 14.2 in the plants. The NFPC values were above 3.5; these results are similar to those reported by Kumar *et al.* (2016), who evaluated 40 genotypes of determinate and semi-determinate habit and found a mean of 3.8 NFPC for determinate and semi-determinate genotypes. This coincides with the data reported by Sinha *et al.* (2020) in 14 genotypes of indeterminate growth tomato where NFPC was between 3.6 and 3.8.

Number of fruits per plant (NFPP)

No statistical differences (P<0.05) were observed among the lines for the variable of number of fruits per plant NFPP. The determinate growth lines presented a mean surpassing the commercial control. Line JV6 produced the highest number of fruits per plant with 49.4; for the other lines, the NFPP was similar, between 37.7 and 39.0 fruits per plant. The control produced 29.6 fruits per plant, being the genotype with the lowest number of fruits. Elsadek *et al.* (2022) reported values of 36.5 fruits per plant in tomato with indeterminate habit; other studies conducted by Martínez-Solís *et al.* (2005) in indeterminate tomato ball type obtained values ranging from 17.7 to 29.3. These results are similar to those found in Unapal Maravilla for this study.

On the other hand, Kouam *et al.* (2018) evaluated two hybrids of determinate growth (Roma Savana and Roma Rossol), obtaining values of 22 to 24 fruits per plant, respectively. These results were lower than those observed in this study.

Fruit weight (FW)

For the FW variable, no statistical differences (P<0.05) were found between the lines and the control, where lines JV9, JV7, and JV12 obtained the heaviest fruits with values greater than 117 g/fruit while lines EB-L14 and JV6 presented the lowest weight fruits with values of 112.05 and 113.04 g/fruit, respectively. When comparing the lines with the control, all plants were superior, with fruits with weights of 110 g/fruit. However, these results were superior to those reported by Burbano and Vallejo (2017), where the determinate growth lines failed to overcome the control Unapal Maravilla with a weight of 104.5 g/fruit. The values found in the lines are similar to those observed by Shamil *et al.* (2017), who reported weight of 118.33 g/ fruit in determinate growth varieties. The data found for the Unapal-Maravilla control were similar to those reported by Malia *et al.* (2015) on indeterminate grown tomatoes (Santa Clara) with a FW of 110.2 g/fruit.

Yield per plant (YPP)

The determinate growth lines presented a superior performance to the Unapal Maravilla control with yields between 4.1 and 4.3 kg/plant, while the control produced a yield of 3.35 kg/plant. In addition, among the lines, the yield was statistically similar. These results are not similar to those reported by Burbano and Vallejo (2017) who found a yield of 4.6 kg/plant in the variety Unapal Maravilla, which

was superior to the determinate growth line. These results agree with Maciel *et al*. (2016), who reported a yield of 3.83 kg/plant in tomato hybrids of indeterminate growth. These results show that there are promising tomato lines for the yield characteristic which is of great importance for breeding programs. These lines could be registered as a new variety or provide farmers with basic seed for them to carry out their own breeding program.

TABLE 3. Comparison of means for yield components between determinate growth chonto tomato (DGCT) lines and the indeterminate growth chonto tomato (IGCT) cultivar Unapal-Maravilla.

Genotypes	NCPP	NFPC	NFPP	FW	YPP
JV6	14.1a	3.5a	41. 4a	112.05ab	4.65a
JV9	14.5a	3.6a	39.0a	117.45a	4.58a
JV7	14.2a	3.58a	39.7a	117.51a	4.67a
EB-L14	13.9a	3.72a	38.7a	113.04ab	4.38a
JV12	14.2a	3.6a	37.7a	117.59a	4.44a
UNAPAL-Maravilla	14.2a	3.5a	29.6b	110.34b	3,29b
Mean	14.2	3.6	37.7	114.76	4.33
LSD	1.93	0.36	6.24	6.97	0.67

In the column, values with the same letter are equal ($P<0.05$), LSD = least significant differences. NCPP = number of clusters per plant; NFPC = number of fruits per cluster; NFPP = number of fruits per plant; FW = fruit weight (g/fruit^{-}); YPP = yield per plant (kg/plant).

Number of locules per fruit (NL)

In general, the DGCT lines expressed a manifest bilocular behavior, with no differences among them ($P<0.05$). At the same time, the IGCT control showed a decided tendency towards a trilocular fruit structure (Tab. 4). These results are in agreement with Eklund *et al*. (2005), who found an NL with a mean of 2.5 and 2.2 in DGCT type Santa Cruz and Santa Clara, respectively. Bilocular fruits are desired at the market since they are more stable for postharvest handling. In any case, the DGCT control showed similar results in full agreement with Sherpa *et al*. (2014), who evaluated 18 DGCT genotypes and found NL between 3.1 and 4.3. This agrees with what was expressed in this study by the Unapal Maravilla cultivar.

Sphericity index (SI)

All of the DGCT lines expressed an SI between 1.16 and 1.28 (slightly elongated), without statistical differences among them ($P<0.05$). In contrast, the Unapal Maravilla cultivar (IGCT) expressed an SI=1.06 (Tab. 4). Vasiform or fleshy berry shaped fruits, such as fresh Chonto tomatoes, probably, have a higher acceptance if they have an appearance close to sphericity. This depends on the non-percentage ratio between the polar diameter (PD) and the equatorial diameter (ED) of the fruits; this ratio generates an index of sphericity (SI) such that, if SI ≥ 1, then the fruit is elongated; if SI = 0, the fruit is spherical and, finally if SI ≤1, the fruit is a flat (Niño *et al.,* 2019). In general, SI has a direct impact on consumer preference (Niño *et al*., 2019; Waiba *et al*., 2021); the commercial Unapal Maravilla cultivar and the lines of determinate growth could be considered as desirable genotypes because they present a format according to the demands of the Colombian market, which prefers fruits with a Chonto type format, either rounded or elongated rounded.

The JV7 line had the highest PD with a mean of 7.26 cm and an SI of 1.28, while the other lines presented statistically similar means with values between 6.59 and 6.64 cm. In addition, all the lines surpassed the Unapal Maravilla control for this variable, which obtained a mean of 5.91. The JV6 line and the control were the genotypes with the lowest ED, with values of 5.50 cm and 5.54 cm, respectively; the other genotypes had a mean between 5.59 cm and 5.71 cm.

These results coincide with those reported by Santos *et al*. (2011), who reported values of 6.0 to 7.25 cm for fruit PD and 5.57 cm for fruit ED in IGCT. Other studies (Srivastav *et al.,* 2022) reported values in DGCT below 5.2 and 4.0 cm for PD and ED, respectively.

Pericarp thickness (PT)

The lines under study were superior to the control in pericarp thickness (PT) and statistically equal to each other ($P<0.05$), with values between 7.66 and 7.80 mm. The results obtained were lower than those found by Trento *et al*. (2021), who worked with five tomato cultivars of determinate growth and obtained pericarp thickness averages between 7.2 mm and 10.4 mm. However, there is no pattern as Sherpa *et al*. (2014) found PD for DGCT between 4.13 to 6.89 mm, lower than those reported in this study. In any case, Chonto tomato fruits with a greater pericarp thickness are desirable because they provide a longer shelf life and better withstand transport; in addition, they contribute more weight to the yield and influence fruit size, an important consideration for both fresh and industrial tomato consumption (Waiba *et al*., 2021).

Fruit color (FC)

All genotypes presented a mean above 6.7, corresponding to the Chonto red color from stages 5 and 6. In this sense, tomatoes in the categories above are considered desirable organoleptic quality by the consumer, who appreciates the color of the fruits and the significant contribution of lycopene, vitamin C, and carotenoids (Siueia Júnior *et al*., 2020).

Total soluble solids content (TSS)

For all DGCT lines in the trial, TSS values were significantly equal ($P<0.05$) with values between 3.54 and 3.62 °Brix; with evident superiority of the IGCT cultivar Unapal Marvilla, with 4.32 °Brix (Tab. 4). TSS content is one of the most important characteristics in the processing industry (Salim *et al*., 2020); quality is associated with soluble sugars (flavor and sweetness), which is correlated with the degree of maturity and vitamin C (Huang & Chen, 2018; Siueia *et al*., 2020). Total soluble solids are affected by the type of growth habit, where tomatoes with determinate growth tend to have a lower amount of soluble solids in the fruits compared to those with indeterminate growth, as shown in the data found in this research, because the latter have a greater number of leaves in relation to the number of fruits, which generates a greater capacity of the fruits to extract photoassimilates (Vicente *et al*., 2015), 4.3 and 5.5 for IGCT.

TABLE 4. Comparison of means for morphological variables and soluble solids of determinate growth chonto tomato (DGCT) lines and the indeterminate growth chonto tomato (IGCT) cultivar Unapal-Maravilla.

Genotypes	NL	PD	ED	SI	PT	FC	TSS
JV6	2.2b	6.40ab	5.5c	1.21a	7.80a	6.7a	3.62b
JV9	2.2b	6.61ab	5.7a	1.16ab	7.56a	6.8a	3.63b
JV7	2.3b	7.26a	5.7b	1.28a	7.82a	6.8a	3.48b
EB-L14	2.2b	6.59ab	5.6b	1.18a	7.76a	6.8a	3.54b
JV12	2.3b	6.63ab	5.6b	1.18a	7.66a	6.8a	3.56b
UNAPAL-M	2.7a	5.91b	5.5c	1.06b	6.78b	6.9a	4.32a
Mean	2.3	6.6	5.6	1.7	7.56	6.8	3.69
LSD	0.12	1.24	0.15	0.10	0.28	0.19	0.4

Values in the column with the same literal are equal ($P<0.05$), LSD = least significant differences. NL: locule number; PD: polar diameter (cm); ED: equatorial diameter (cm); SI: Sphericity index; PT: pericarp thickness (mm); FC: fruit color; TSS: total soluble solids (°Brix).

Conclusions

The Chonto tomato lines of determinate growth showed a statistically similar agronomic performance among the lines, which would allow the producers to receive basic seed of all the lines. Growers can be part of the continuation of the breeding process, which can be participative or a pool of the five lines of determinate growth habit, to obtain a new cultivar for the Colombian farmers.

Conflict of interest statement

The authors declare that there is no conflict of interests regarding the publication of this article.

Author's contributions

AJVG, FAVC, SOG, and MCSV designed the experiments, AJVG, MCSV, and DGGG carried out the field and laboratory experiments, FASV and DGGG contributed to the data analysis, AJVG, FAVC, and SOG wrote the article. All authors reviewed the final version of the manuscript.

Literature cited

Burbano, E., & Vallejo, F. A. (2017). Producción de líneas de tomate "chonto", *Solanum lycopersicum* Mill., con expresión del gen *sp* responsable del crecimiento determinado. *Revista Colombiana de Ciencias Hortícolas*. *11*(1), 63–71. https://doi.org/10.17584/rcch.2017v11i1.5786

Eklund, C. R. B., Caetano, L. C. S., Shimoya, A., Ferreira, J. M., & Gomes, J. M. R. (2005). Desempenho de genótipos de tomateiro sob cultivo protegido. *Horticultura Brasileira*. *23*(4), 1015–1017. https://doi.org/10.1590/S0102-05362005000400031

Elsadek, W., Elshinawy, M., Elminiawy, S. E., & Ayoub, F. (2022). Evaluation of some indeterminate exotic genotypes of tomato. *Arab Universities Journal of Agricultural Sciences*, *30*(1), 117–127. https://doi.org/10.21608/AJS.2022.105853.1436

Estrada, E. I., García, M. A., Baena, D., Gutierrez, A., Cardozo, C. I., Sánchez, M. S., & Vallejo, F. A. 2004. *Cultivo de tomate: Variedad UNAPAL Maravilla* (2nd ed.). Universidad Nacional de Colombia Sede Palmira. https://repositorio.unal.edu.co/bitstream/handle/unal/51973/9588095204.PDF?sequence=1&isAllowed=y

FAOSTAT. (2020, June 15). Production crops. https://www.fao.org/faostat/en/#data/QCL

Huang, Y., Lu, R., & Chen, K. (2018). Assessment of tomato soluble solids content and pH by spatially-resolved and conventional Vis/NIR spectroscopy. *Journal of Food Engineering*, *236, 19*–28. https://doi.org/10.1016/j.jfoodeng.2018.05.008

IPGRI. (1996*). Descriptors for tomato (Lycopersicon spp.).* International Plant Genetic Resources Institute. https://cgspace.cgiar.org/bitstream/handle/10568/73041/Descriptors_Tomato_286.pdf?sequence=1&isAllowed=y

Jiang, K., Liberatore, K. L., Park, S. J., Alvarez, J. P., & Lippman, Z. B. (2013). Tomato yield heterosis is triggered by a dosage sensitivity of the florigen pathway that fine-tunes shoot architecture. *PLoS Genetics*, *9*(12), Article e1004043. https://doi.org/10.1371/journal.pgen.1004043

Kouam, E. B., Dongmo, J. R., & Djeugap, J. F. (2018). Exploring morphological variation in tomato (*Solanum lycopersicum*): A combined study of disease resistance, genetic divergence and association of characters. *Agricultura Tropica et Subtropica*, *51*(2), 71–82. https://doi.org/10.2478/ats-2018-0008

Kumar, P. A., Reddy, K. R., Reddy, R. V. S. K., Pandravada, S. R., & Saidaiah, P. (2016). Per se performance of dual-purpose tomato genotypes for growth, yield and quality attributes. *Plant Archives*, *16*(2), 695–699.

Maciel, G. M., Fernandes, M. A., Melo, O. D., & Oliveira, C. S. (2016). Potencial agronômico de híbridos de minitomate com hábito de crescimento determinado e indeterminado. *Horticultura Brasileira*, *34*(1), 144–148. https://doi.org/10.1590/S0102-053620160000100022

Maham, S. G., Rahimi, A., Subramanian, S., & Smith, D. L. (2020). The environmental impacts of organic greenhouse tomato production based on the nitrogen-fixing plant (*Azolla*). *Journal of Cleaner Production*, *245*, Article 118679. https://doi.org/10.1016/j.jclepro.2019.118679

Mahebub, P. A., Babu, M. R., & Sasikala, K. (2021). Studies on genetic variability in tomato (*Solanum lycopersicum* L.) for growth, yield and quality traits. *The Pharma Innovation Journal*, *10*(10), 1741–1743.

Malia, H. A., Ecole, C. C., Melo, W. F., & Resende, F. V. (2015). Avaliação agronómica de variedades de tomate. In L. L. Haber, C. C. Ecole, W. Bowen, & F. V. Resende (Eds.), *Horticultura em Moçambique: caracteristicas, tecnologias de produção e de pós-colheita* (pp. 194–198). https://ainfo.cnptia.embrapa.br/digital/bitstream/item/137011/1/Horticultura-em-Mocambique-PDF-Cap-18.pdf

Martínez-Solís, J., Peña-Lomelí, A., Rodríguez-Pérez, J. E., Villanueva-Verduzco, C., Sahagún-Castellanos, J., & Peña-Ortega, M. G. (2005). Comportamiento productivo en híbridos de jitomate y sus respectivas poblaciones F2. *Revista Chapingo Serie Horticultura, 11*(2), 299–307.

Muhammad, I., Muhammad, S. K., Syed, S. S., Ali, Z., Ali, Z., Tawab, S., & Muhammad, N. (2019). Assessment of different tomato genotypes for yield and morphological attributes. *Pure and Applied Biology*, *8*(1), 295–303. https://doi.org/10.19045/bspab.2018.700188

Nascimento, M. V., Ávila, M. C. R., de Abreu-Tarazi, M. F., Nogueira, A. P. O., Campos, L. F. C., & dos Reis Nascimento, A. (2020). Identification of promising tomato breeding lines with determinate growth by selection index. *Advances in Horticultural Science*, *34*(3), 337–347.

Niño, W. D., Jiménez, F. R., & Jiménez, A. F. (2019). Algorithms to estimation of size and shape tomato using Artificial Vision Techniques.*Proceedings of the 17th LACCEI International Multi-Conference for Engineering, Education and Technology*. https://doi.org/10.18687/LACCEI2019.1.1.5

Perilla, A., Rodríguez, L. F., & Bermúdez, L. T. (2011). Estudio técnico-económico del sistema de producción de tomate bajo invernadero en Guateque, Sutatenza y Tenza (Boyacá). *Revista Colombiana de Ciencias Hortícolas*, *5*(2), 279–294. https://doi.org/10.17584/rcch.2011v5i2.1269

Piotto, F. A., & Pereira, L. E. (2012). Base genética do hábito de crescimento e florescimento em tomateiro e sua importância na agricultura. *Ciência Rural*, *42*(11),1941–1946. https://doi.org/10.1590/S0103-84782012001100006

Raj, T., Bhardwaj, M. L., Pal, S., Kumari, S., & Dogra, R. K. (2018). Performance of tomato (*Solanum lycopersicum* L.) hybrids for yield and its contributing traits under mid-hill conditions of Himachal Pradesh. *International Journal of Bio-resource and Stress Management*, *9*(2), 282–286. https://doi.org/10.23910/IJBSM/2018.9.2.1862

Rawat, M., Singh, D., & Kathayat, K. (2020). Studies on genetic parameters for yield and yield attributing traits in tomato (*Solanum lycopersicum* L.). *Pharmacognosy and Phytochemistry, 9*(3), 1439–1442

Salim, M. M. R. R., Rashid, M. H., Hossain, M. M., & Zakaria, M. (2020). Morphological characterization of tomato (*Solanum lycopersicum* L.) genotypes. *Journal of the Saudi Society of Agricultural Sciences*, *19*(3), 233–240. https://doi.org/10.1016/j.jssas.2018.11.001

Santos, F. F. B., Ribeiro, A., Siqueira, W. J., & Melo, A. M. (2011). Desempenho agronômico de híbridos F1 de tomate de mesa. *Horticultura Brasileira*, *29*(3), 304–310. https://doi.org/10.1590/S0102-05362011000300008

Shamil, A., Abebe, G., & Wakjira, G. (2017). Study on performance evaluation of tomato (*Lycopersicon esculentum* Mill.) varieties under off-season condition at Teppi, Southwestern part of Ethiopia. *Greener Journal of Agricultural Sciences*, *7*(5), 120–125.

Sherpa, P., Pandiarana, N., Shende, V. D., Seth, T., Mukherjee, S., & Chattopadhyay, A. (2014). Estimation of genetic parameters and identification of selection indices in exotic tomato genotypes. *Electronic Journal of Plant Breeding, 5*(3), 552–562.

Silva, W. B., Vicente, M. H., Robledo, J. M., Reartes, D. S., Ferrari, R. C., Bianchetti, R., & Zsögön, A. (2018). SELF-PRUNING acts synergistically with DIAGEOTROPICA to guide auxin responses and proper growth form. *Plant Physiology*, *176*(4), 2904–2916. https://doi.org/10.1104/pp.18.00038

Sinha, A., Singh, P.; Bhardwaj, A., & Kumar, R. (2020). Evaluation of tomato (*Solanum lycopersicum* L.) genotypes for morphological, qualitative and biochemical traits for protected cultivation. *Current Journal of Applied Science and Technology*, *39*(2), 105–111. https://doi.org/10.9734/CJAST/2020/v39i230503

Siueia Júnior, M., Silva, M. L. S., Trevizam, A. R., Faquin, V., & Silva, D. F. (2020). Postharvest quality of tomato as affected by nitrogen and sulfur interaction. *Acta Agronomica*, *69*(2), 130–135. https://doi.org/10.15446/acag.v69n2.73691

Srivastav, P., Yadav, S., Ali, R., Kumar, R., & Singh, H. (2022). Study of heritability and genetic advance in the different genotypes and trails of tomato in sub-tropical condition. *The Pharma Journal*, *11*(6), 507–510.

Stilwell, M. (2020). *The 2020 processed tomato yearbook*. http://www.tomatonews.com/pdf/yearbook/2020/files/assets/ common/downloads/TOMATO%20NEWS%202020%20YEARBOOK.pdf

Sun, X., Shu J., Ali, M., Mohamed, A., Deng, X., Zhi, X., Bai, J., Cui, Y., Lu, X., Du, Y., Wang, X., Huang, Z., Guo, Y., Liu, L., & Li, J. (2019). Identification and characterization of EI (Elongated Internode) gene in tomato (*Solanum lycopersicum*). *International Journal of Molecular Sciences*, *20*(9), Article 2204. https://doi.org/10.3390/ijms20092204

Tabe-Ojong, M. P., & Molua, E. L. (2017). Technical efficiency of smallholder tomato production in semi-urban farms in Cameroon: A stochastic frontier production approach. *Journal of Management and Sustainability, 7*(4), 27–35. https://doi.org/10.5539/jms.v7n4p27

Trento, D. A., Antunes, D. T., Fernandes Júnior, F., Zanuzo, M. R., Dallacort, R., & Seabra Júnior, S. (2021). Desempenho de cultivares de tomate italiano de crescimento determinado em cultivo protegido sob altas temperaturas. *Nativa, 9*(4), 359–356. https://doi.org/10.31413/nativa.v9i4.10945

Vicente, M. H., Zsögön, A., Sá, A. F. L., Ribeiro, R. V., & Peres, L. E. P. (2015). Semi-determinate growth habit adjusts the vegetative-to-reproductive balance and increases productivity and water-use efficiency in tomato (*Solanum lycopersicum*). *Journal of Plant Physiology, 117*, 11–19. https://doi.org/10.1016/j.jplph.2015.01.003

Waiba, K. M., Sharma, P., Kumar, K. I., & Chauhan, S. (2021). Studies of genetic variability of tomato (*Solanum lycopersicum* L.) hybrids under protected environment. *International Journal of Bio-resource and Stress Management*, *12*(4), 264–270. https://doi.org/10.23910/1.2021.2211

Fitting growth curves of coffee plants in the nursery stage of growth: A functional approach

Ajuste de curvas de crecimiento de plantas de café durante la etapa de crecimiento de almácigo: Un enfoque funcional

Andrés Felipe León-Burgos[1, 5], Carlos Ramírez[2], José Raúl Rendón Sáenz[1], Luis Carlos Imbachi-Quinchua[3], Carlos Andrés Unigarro-Muñoz[4], and Helber Enrique Balaguera-López[5*]

ABSTRACT

The growth patterns of coffee plants are determined by interactions between genetic, physiological, and climate factors. The objective of this study was to evaluate the growth patterns of coffee plants in the nursery under the climatic conditions of Chinchiná, Caldas, Colombia, during the first semester of 2019. Measurements were carried out in the Cenicafé 1 variety during six months. Growth parameters such as leaf area, number of leaves, height, stem diameter, and length of the main root were evaluated every 15 d after transplanting (DAT) in 20 plants and the average of absolute growth (Ĝ) rate of each growth variable were calculated. For the total leaf area, total number of leaves, and stem height, a sigmoidal-type growth curve was adjusted, while the growth curve was linear for the stem diameter ($R^2 = 0.97$) and main root length ($R^2 = 0.95$). Average values were obtained for 520 cm^2 for total leaf area, with an Ĝ of 3.31 cm^2 d^{-1}, 11 for total leaves (Ĝ 0.055 leaves d^{-1}), 30.23 cm for height (Ĝ 0.155 cm d^{-1}), 4.87 mm for stem diameter (Ĝ 0.199 mm d^{-1}), and 28.80 cm for main root length (Ĝ 0.087 cm d^{-1}) at 180 DAT. These results suggest that growth curves could be a useful tool for describing the growth patterns of coffee seedlings during the nursery stage of growth.

Key words: *Coffea arabica* L., nonlinear regression, goodness of fit, leaf area, absolute growth rate.

RESUMEN

Los patrones de crecimiento de las plantas de café están determinados por las interacciones entre los factores genéticos, fisiológicos y climáticos. El objetivo de este estudio fue evaluar los patrones de crecimiento de las plantas de café en etapa de almácigo bajo condiciones climáticas de Chinchiná, Caldas, Colombia, durante el primer semestre de 2019. Las mediciones se realizaron en plantas de la variedad Cenicafé 1 durante seis meses. Se evaluaron los parámetros de crecimiento como área foliar, número de hojas, altura, diámetro del tallo y longitud de la raíz principal, cada 15 d después del trasplante (DDT) de 20 plantas y se calculó la tasa promedio de crecimiento absoluto (Ĝ) de cada variable de crecimiento. Para el área foliar total, número total de hojas y altura del tallo, se ajustó una curva de crecimiento tipo sigmoidal, mientras que fue lineal para el diámetro del tallo ($R^2 = 0.97$) y longitud de la raíz principal ($R^2 = 0.95$). Se obtuvieron valores promedio a los 180 DDT de 520 cm^2 de área foliar total con Ĝ 3.31 cm^2 d^{-1}, 11 hojas totales (Ĝ 0.055 hojas d^{-1}), 30.23 cm de altura (Ĝ 0.155 cm d^{-1}), 4.87 mm para diámetro del tallo (Ĝ 0.199 mm d^{-1}) y 28.80 cm para longitud de la raíz principal (Ĝ 0.087 cm d^{-1}). Estos resultados sugieren que las curvas de crecimiento pueden ser una herramienta útil para describir los patrones de crecimiento de las plantas de café durante la etapa de almácigo.

Palabras clave: *Coffea arabica* L., regresión no lineal, criterios de ajuste, área foliar, tasa absoluta de crecimiento.

Introduction

Coffee (*Coffea arabica* L.) is one of the most important tropical crops worldwide, with Colombia ranked third in production with 13,4 million bags of green beans (60 kg) and 884 thousand ha (Nab & Maslin, 2020; Ceballos-Sierra & Dall' Erba, 2021; FNC, 2021). The growth of coffee plants is a process regulated by interactions between genetics, physiological processes, and climatic conditions, with implications for agronomic management and crop success (Paine *et al*., 2012; Liu *et al*., 2018; Rakocevic & Matsunaga, 2018). Factors such as solar radiation, temperature, water availability in soil, and humidity in atmosphere are key climatic conditions that influence the growth and development of the plants (DaMatta, 2007; Bote & Vos, 2017; Jaramillo, 2018; León-Burgos *et al*., 2022). Growth patterns

Received for publication: May 12, 2022. Accepted for publication: July 28, 2022 Doi: 10.15446/agron.colomb.v40n3.101333

[1] Department of Fitotecnia, Centro Nacional de Investigaciones del Café Cenicafé, Manizales (Colombia).
[2] Department of Genetic Breeding, Centro Nacional de Investigaciones del Café Cenicafé, Manizales (Colombia).
[3] Department of Biometry, Centro Nacional de Investigaciones del Café Cenicafé, Manizales (Colombia).
[4] Department of Plant Physiology, Centro Nacional de Investigaciones del Café Cenicafé, Manizales (Colombia).
[5] Departamento de Agronomía, Facultad de Ciencias Agrarias, Universidad Nacional de Colombia, Bogotá (Colombia).
* Corresponding author: hebalagueral@unal.edu.co

in each phenological stage could serve as an important tool for planning agronomic practices such as planting density, spatial arrangements, application of fertilizers and liming, controls of pests, diseases and weeds, and management of the crop pruning systems (Arcila, 2007; Rendón, 2020). This is necessary to ensure adequate growth and development of plants in the field and, thus, a high production potential.

Plants in the nursery constitute an early phase of growth in coffee crops that lasts from four to six months, with implications in the growth and development of plants in the field and production cycle (Arcila, 2007; Moraes *et al*., 2010, Castillo & Andrade, 2021). Shoot growth at this phase takes place in the meristematic zones located in the apical and lateral buds of the main stem (Arcila *et al*., 2002). The purpose of the coffee nursery stage is to select plants with appropriate growth characteristics, such as the number of leaves, height and leaf area, so that, when established in the field, they can adapt to the climate and soil conditions to avoid damages to their physiological performance that can cause plant death (Jaramillo, 2018; Castillo & Andrade, 2021). Furthermore, at the initial stages of projection in perennial crops life cycles, it is necessary to ensure good quality of the plant material from the point of view of crop health, so that, in the production cycle, it would express the highest production (Arcila, 2007; Gaitán *et al*., 2011). Therefore, the nursery stage of growth is a determining step for planning crop management and production projection in Colombian coffee cultivation (Rendón, 2020).

Growth curves are widely used in agriculture to simulate plant growth patterns as a function of time under particular climatic conditions (Poorter & Garnier, 1996; Paine *et al*., 2012; Liu *et al*., 2018; Bakhshandeh *et al*., 2020). Analyses have been developed with functions or mathematical models through linear or nonlinear regressions that are adjusted according to statistical criteria. These criteria define the degree of prediction of the changes and behavior in the magnitudes of growth, based on data measured in plants, called a functional approach (Kaufmann, 1981; Hunt *et al*., 2002; Liu *et al*., 2018). This technique is mainly used to evaluate the temporal variation of plant growth dynamics at phenological stages of interest, since only a few individuals are measured but with many replicates throughout the time, particularly during rapid changes in growth (Hunt, 1979; Paine *et al*., 2012). Therefore, these methods can be used to describe changes in the magnitude of growth and to define selection criteria that may ensure good quality and growth of the plants coming from nursery stage.

Currently the coffee variety "Cenicafé 1" makes up approximately 80% of the cultivable area for coffee in Colombia (FNC, 2021). There is little information on the growth patterns and selection criteria for classifying good growth performance of the plants during the nursery stage. In this research we considered the following objectives: i) evaluation of the fit of mathematical functions that could simulate the growth from a functional approach and ii) description of the growth patterns of coffee plants during the nursery stage under the climatic conditions of Chinchiná-Caldas, located in the central coffee zone of Colombia. Mathematical functions were studied to describe plant growth patterns as a function of time using five growth measures: total leaf area (cm^2), number of leaves, stem height (cm), stem diameter (mm), and length of main root (cm). With the adjusted mathematical functions and growth patterns, it is possible to predict the growth magnitude and to define selection criteria for coffee plants under nursery conditions.

Materials and methods

Study area and growth conditions

The plant material was the coffee Cenicafé 1 variety, established on the Plan alto Farm of the National Coffee Research Center-Cenicafé (04°59'34.9'' N, 75°35'50.5'' W), located at km 4 of the old Manizales-Chinchiná road (Caldas, Colombia), at an altitude of 1,332 m a.s.l. This material is a variety made up by eight progenies, resistant to coffee rust (*Hemileia vastatrix*) and coffee berry disease (CBD) (*Colletotrichum kahawae*) (Maldonado & Ángel-Giraldo, 2020). During the study period between January and July, 2019, the nursery was established in the area with following average climatic conditions: temperature of 21.8°C (maximum: 28.5°C and minimum: 17.4°C), relative air humidity of 82%, with an accumulated rainfall of 1,419 mm and 782 h of sunlight (Meteorological Stations of the National Federation of Coffee Growers of Colombia, Agroclima, 2019).

The plants (*chapolas*, in Spanish) were transplanted from seed germinators 75 d after sowing the seeds; at the moment of transplant the plants were at the BBCH10 phenological stage, when the cotyledonary leaves were fully expanded. Subsequently, the plants were established in a nursery with a 50% shade net in 17 × 23 cm plastic bags (Arcila, 2007). The substrate consisted of a mixture of disinfected (solarized) soil with decomposed coffee pulp at a 3:1 ratio (v/v). For the fertilization of the plants, 2 g of diammonium phosphate (DAP, 18-46-0) were applied at two and four months after transplant according to the recommendations of Sadeghian (2014). Agronomic practices reported by Gaitán *et al*. (2011) as the regulation of excess shade,

waterlogging avoidance, and applications of cyproconazole (0.7 cc L^{-1}) were carried out to manage brown eye spot disease (*Cercospora coffeicola* Berkeley & Curtis); and destructive monthly samples were performed for the monitoring of the pest known as mealybug (Pseudococcidae).

Measurements and data collection

To evaluate the growth behavior of coffee plants during their nursery stage, 400 plants were established. At 30 d after transplanting (DAT), when the first pair of leaves was developed, 20 plants were randomly selected as a sampling unit. This selection was sampled every 15 d until 180 DAT. In each sampling, the following growth measurements were recorded: total leaf area (cm^2), total number of leaves, stem height (cm), stem diameter (mm), and main root length (cm). The leaf area was determined by measuring the leaf blade length, and width on the central part of the leaf blade of each leaf using a ruler without including the petiole. The data were then incorporated into Equation 1, proposed by Unigarro-Muñoz *et al*. (2015):

$$LAE = 0.99927 \times (L \times (-0.14757 + 0.60986*W)) \quad (1)$$

where *LAE* is the estimate of the leaf area in cm^2, *L* is leaf length in cm, and *W* is leaf width in cm.

The total number of leaves was determined with direct counts on the plants; height was measured from the base to the apex of the stem with a ruler; and the diameter was measured with a Vernier digital caliper (500-196-30B, Mitutoyo, Brazil) from the basal part of the stem. For the length of the main root, destructive sampling was done, measuring length from the base to the apex of this organ.

For each growth measurement, the absolute growth rate ($\hat{G}$) was estimated with Equation 2, proposed by Hunt (1990):

$$\hat{G} = \frac{V2 - V1}{t2 - t1} \quad (2)$$

where $\hat{G}$ is the average absolute growth rate, *V1* (cm^2, cm, or mm) is the value of the growth variable for time *t1* (d), and *V2* is the value of the growth variable for time *t2* (d).

Data analysis

To describe the behavior of growth measurements over time, four mathematical functions, described in Table 1, were evaluated using linear and nonlinear regressions. For the adjustment and selection of each mathematical function, the following statistical criteria were used: coefficient of determination R^2, widely used for the adjustment of models or functions; adjusted coefficient of determination - adj R^2, a criterion with greater precision adjusted according to the degrees of freedom. The mean square error (MSE), a criterion that measures the degree of error that a model or function can simulate. The standard error of the estimates (SEE) that refers to the normal deviation of the residuals. Finally, the Akaike (AIC) and Bayesian-Schwarz (BIC) information criteria, measuring the accuracy and complexity of the model as well as the relationship between its bias and variance and the significance of the parameters of each equation according to the t-student test at 5% significance (Torres *et al*., 2012; Voorend *et al*.,2014; Liu *et al*., 2018). Subsequently, the relationship between the observed values for each growth measure and the estimated values for each adjusted and selected mathematical function was determined with a simple linear regression analysis to verify that the regression coefficient was statistically equal according to the 1% t-test.

TABLE 1. Studied functions for the fit of growth curves of coffee plants.

Mathematical functions	Function	Parameters
Linear	$Y = y0 + a \times x$	y0 a
Quadratic	$Y = y0 + a \times x + b \times x^2$	y0 a b
Sigmoidal	$Y = \frac{a}{1 + exp\left(-\left(\frac{x - x0}{b}\right)\right)}$	a x0 b
Exponential	$Y = a \times (1 - exp(-b \times x))$	a b

All analyses were performed with the software R, version 3.6.0 with statistical package stats and nls2 (R Development Core Team, 2019; Grothendieck, 2022).

Results and discussion

Fitting of growth curves of coffee plants

In general, average values of 496.13 cm^2 ± 3.64 (mean ± standard error (SE)) for total leaf area (TLA), 12.0 ± 0.40 for total number of leaves (TNL), 30.01 cm ± 1.30 for stem height (HS), 4.91 ± 0.26 mm for stem diameter (DS) and 29.09 ± 0.83 cm for length of the main root (LMR) were recorded in the coffee plants at 180 DAT, considered a suitable age for establishment in field conditions. The linear, quadratic, sigmoidal, and exponential functions used to simulate the growth patterns of the coffee plants during the nursery stage varied in the behavior of the growth measurements. The TLA, TNL and HS were fitted to a sigmoidal growth, and for the DS and LMR, a linear type was used (Fig. 1). Similar trends in the growth of coffee plants during this stage have been reported by Silveira *et al*. (2014) and

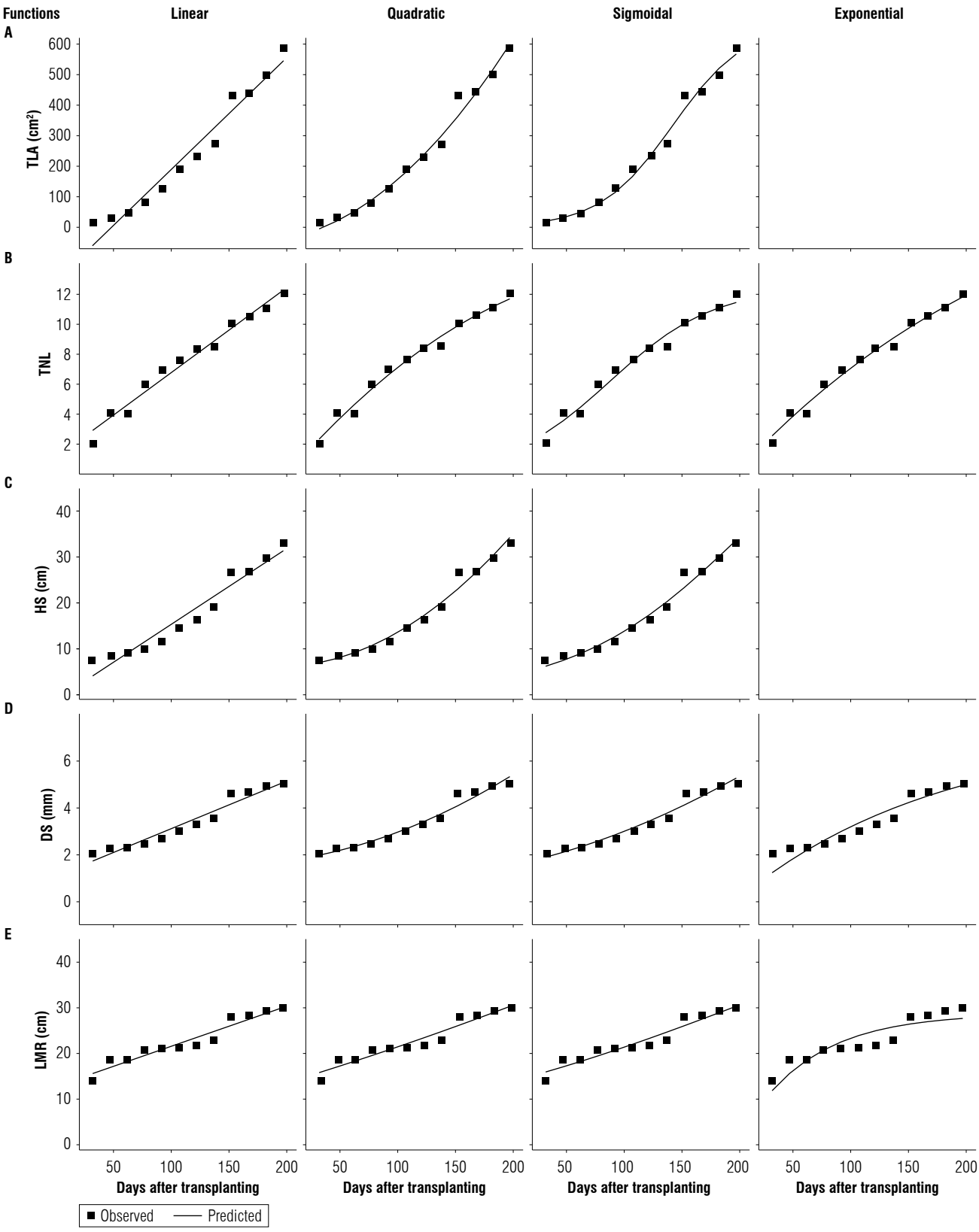

FIGURE 1. Growth curves of coffee seedlings at the nursery stage for each studied mathematical function. A) total leaf area (TLA), B) total number of leaves (TNL), C) height of the stem (HS), D) diameter of the stem (DS), E) length of the main root (LMR). Each point represents the mean (n=20).

Encalada *et al*. (2016). The opposite occurred in studies by Neiva *et al*. (2019) and Castillo and Andrade (2021) that describe quadratic behaviors in the growth of coffee plants during the nursery stage with contrasting results given the particular climatic conditions of the study areas.

Sigmoidal growth for the total leaf area, total leaf number and height described a growth pattern where the size of these variables increased along with the speed (Hunt, 1979; Kaufmann, 1981). However, the behavior of these growth variables was divided into two phases, a slow phase that started from 0 to 60 DAT, with average values between 19.91 to 49.13 cm^2 for TLA, 3 to 4 leaves and 6.21 until 8.95 cm for HS, and an accelerated phase (75 to 180 DAT) with values of 75.61 to 520.00 cm^2 for TLA, 6 until 12 leaves and between 10.68 to 30.16 cm for HS. DS and LMR increase lineal according to DAT. Average values of 3.23 mm for DS and 22.23 cm for LMR were reported throughout the study (Fig. 1).

Once the mathematical functions were defined for each growth variable evaluated in the coffee plants, the significance of each parameter estimated by the functions was compared. In general, all parameters of the functions for TLA (sigmoidal), TNL (sigmoidal), HS (sigmoidal), DS (linear), and LMR (linear) showed significant differences (P<0.05) from the other mathematical functions. Therefore, the selected functions were representative of each growth measurement evaluated in this study (Tab. 2).

The statistical criteria selected to evaluate the adjustment and selection of the mathematical functions have been used to simulate, adjust, and predict plant growth (Torres *et al*., 2012; Voorend *et al*., 2014; Liu *et al*., 2018). To interpret the selection of each function, the adjustment criteria (R^2 and R^2-adjusted) must be close to 1; and the selection criteria MSE, SEE, AIC and BIC must be the lowest values recorded by each function or model (Torres *et al*., 2012; Liu *et al*., 2018). The sigmoidal function of the TLA registered adjustment values with R^2 0.99 and R^2-adjusted 0.98, along with the selection criteria MSE (694.88), SEE (26.36), AIC (117.12), and BIC (119.06). These were lower than values recorded in the linear and quadratic function, except for the exponential one, where it was not possible to adjust the total leaf area data because of the non-convergence of the function (Tab. 3). Therefore, this adjustment can simulate the growth of TLA in coffee plants during the nursery stage, this same adjustment mathematical function with R^2 values between 0.96 and 0.99 has been reported by Schmildt *et al*. (2014) and Unigarro-Muñoz *et al*. (2015).

The sigmoidal function of TNL and HS were selected and adjusted to represent the most appropriate values both fit (R^2 = 0.97) and selection (MSE= 0.42, SEE= 0.65) to describe the behavior of these growth measurements according to DAT. This growth pattern both TNL and HS in coffee plants were reported by the Arcila and Chaves (1995) and Silveira *et al*. (2014). For the HS measurement, it is not possible to adjust the exponential function because of the non-convergence of this function with the data measured in the plants (Tab. 3). The opposite occurred for the DS (R^2= 0.97, MSE= 0.07, and SEE= 0.27) and LMR (R^2= 0.95, MSE= 2.46, and SEE= 1.56). The values of the statistical criteria evaluated were adjusted to the linear function. However, for the HS and DS, the values of both the adjustment and selection criteria were similar to the quadratic function

TABLE 2. Estimates of parameters for the fitted mathematical functions of the coffee plant growth.

Functions	Y0	X0	A	b
		TLA (cm^2)		
Linear	-176.7118	-	3.6599*	-
Quadratic	-38.8708	-	0.6331ns	0.0132^{ns}
Sigmoidal	-	141.9468*	666.3588*	31.5924*
Exponential	-	-	-	-
		TNL		
Linear	1.0890^{ns}	-	0.0564*	-
Quadratic	-0.3687^{ns}	-	0.0884*	-0.0001^{ns}
Sigmoidal	-	88.1591*	12.3858*	44.6322*
Exponential	-		22.7510*	0.0037*
		HS (cm)		
Linear	-1.1801^{ns}	-	0.1654*	-
Quadratic	6.1252*	-	0.005^{ns}	0.007*
Sigmoidal	-	203.9372*	70.8206*	73.456*
Exponential	-	-	-	-
		DS (mm)		
Linear	1.0646*	-	0.0203*	-
Quadratic	1.6960*	-	0.0065^{ns}	0.00006^{ns}
Sigmoidal	-	260.5549^{ns}	14.099^{ns}	122.0635*
Exponential	-		7.3769*	0.0056*
		LMR (cm)		
Linear	12.8724*	-	0.0875*	-
Quadratic	13.3904*	-	0.0761^{ns}	0.00004^{ns}
Sigmoidal	-	207.0409^{ns}	62.6259^{ns}	163.7977^{ns}
Exponential	-	-	28.7558*	0.0168*

* Significance according to t-student test (P<0.05). ^{ns} No significance.

TLA: total leaf area; TNL: total number of leaves; HS: height of the stem; DS: diameter of the stem; LMR: Length of the main root.

TABLE 3. Goodness-of-fit criteria for the studied mathematical functions.

Functions	R^2	Adjusted R^2	MSE	SEE	AIC	BIC
TLA (cm^2)						
Linear	0.97	0.95	1954.47	44.20	128.8012	130.2559
Quadratic	0.99	0.97	860.14	29.32	119.6875	121.6271
Sigmoidal	0.99	0.98	694.88	26.36	117.129	119.0686
Exponential	-	-	-	-	-	-
TNL						
Linear	0.97	0.94	0.55	0.74	30.77351	32.22823
Quadratic	0.98	0.95	0.46	0.68	29.50542	31.44504
Sigmoidal	0.97	0.95	0.42	0.65	27.72089	29.17561
Exponential	0.97	0.94	0.56	0.75	31.74271	33.68234
HS (cm)						
Linear	0.97	0.94	5.08	2.25	57.3758	58.83502
Quadratic	0.99	0.97	1.96	1.40	46.69788	48.63751
Sigmoidal	0.99	0.97	2.00	1.41	46.93079	48.87041
Exponential	-	-	-	-	-	-
DS (mm)						
Linear	0.97	0.94	0.07	0.27	6.904349	8.359069
Quadratic	0.98	0.95	0.05	0.23	4.155049	6.094676
Sigmoidal	0.98	0.95	0.05	0.24	4.578776	6.518402
Exponential	0.93	0.86	0.17	0.41	16.86562	18.32034
LMR (cm)						
Linear	0.95	0.90	2.46	1.56	48.67703	50.12545
Quadratic	0.95	0.88	2.71	1.64	50.58916	52.52879
Sigmoidal	0.95	0.88	2.73	1.65	50.66634	52.60597
Exponential	0.88	0.75	5.94	2.43	59.248	60.70272

TLA = total leaf area; TNL = total number of leaves; HS = height of the stem; DS = diameter of the stem; LMR = Length of the main root.

(Tab. 3). However, the adjustment of the function was made based on the significance of the parameters of the functions (Tab. 2). The results of the growth behavior of the DS measurements were similar to those reported by Criollo *et al*. (2019) in coffee plants grown in the municipality of La Unión (Nariño, Colombia) as well as in the study by Souza *et al*. (2016). Similar descriptions were also recorded in the growth of LMR in coffee plants (Silveira *et al*., 2014).

The results of the fitted growth curves reported in this study may be used to hold the recommendations of the agronomic management of the coffee plants during the nursery stage of growth. These particularly include the fertilization, pest, disease, and weed controls focused during the 60 DAT to guarantee suitable conditions before the start of accelerated growth, where the growth of coffee plants are increased (Rendón, 2020; Sadeghian & Ospina-Penagos, 2021).

Description of the growth of coffee plants at nursery stage

The growth curves simulated with the adjusted mathematical functions correctly described the growth behavior of coffee plants under nursery conditions. In this way, a coffee plant at the 180 DAT, according to the adjusted functions, registered average values of 520 cm^2 for TLA, 11.0 for TNL, 30.23 cm for HS, 4.87 mm for DS, and LMR of 28.80 cm. These results of growth variables as TLA (240 to 438 cm^2), TNL (10 leaves) and HS (14 until 21 cm) have been reported for *C. arabica* cvs. Caturra and Castillo Tambo plants during the nursery stage that were established with 50% shading net under climate conditions from Cuba and Colombia (Encalada *et al*., 2016; Castillo and Andrade, 2021). In this way, the growth variables evaluated were confirmed as adequate criteria for the selection of plant material with good growth performance for establishment under field conditions. They were associated with physiological

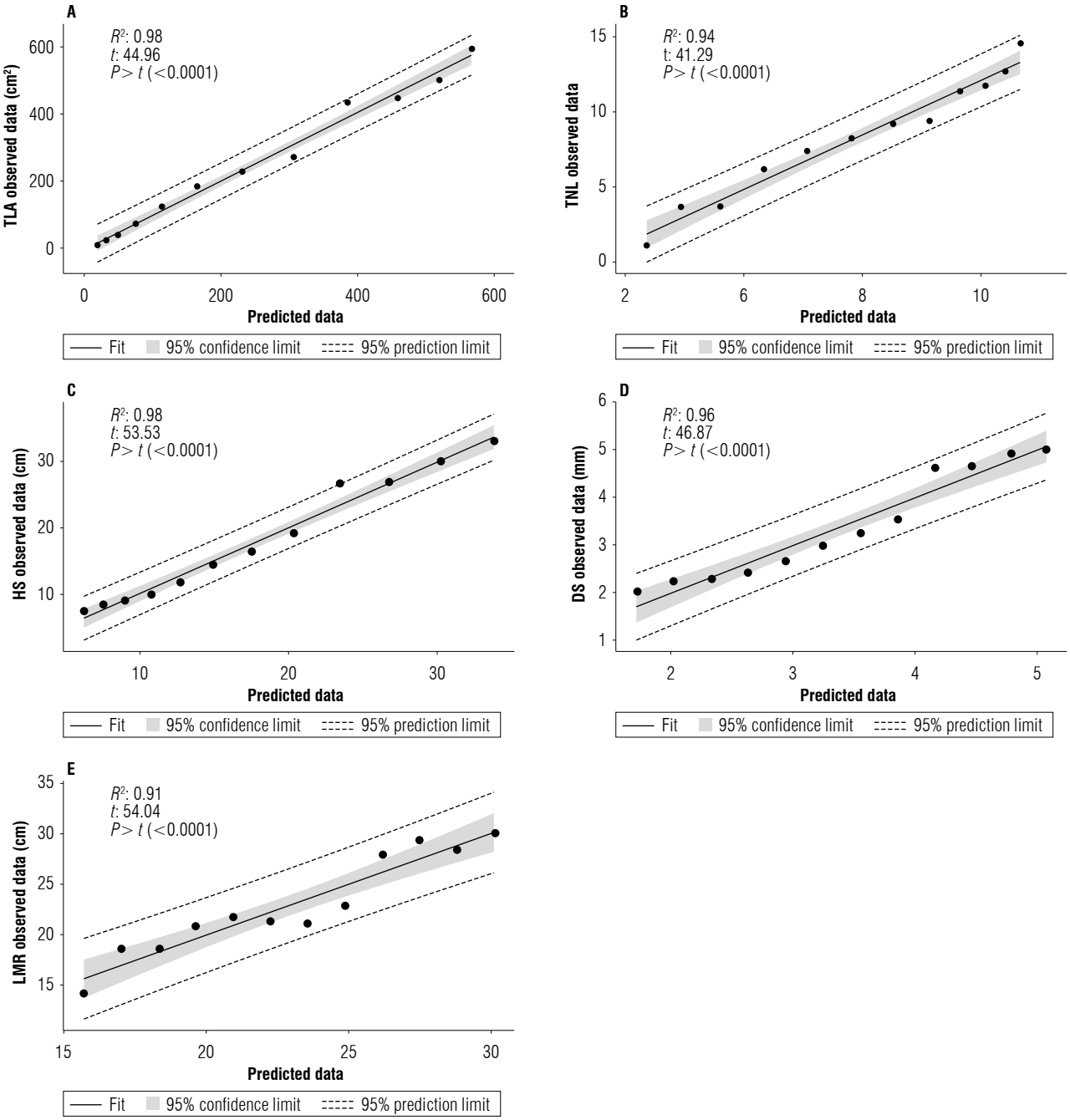

FIGURE 2. Relationships between data predicted by each fitted mathematical function and observed data for growth measurements of coffee plants. A) total leaf area (TLA), B) total number of leaves (TNL), C) height of the stem (HS), D) diameter of the stem (DS), and E) length of the main root (LMR).

processes, such as water and nutrient uptake and carbon metabolism in the plants. However, the dry mass also was a measure that allows us to understand the growth of the plants under particular climate conditions (Tatagiba *et al*., 2010; Rodríguez-López *et al*., 2014; Maradiaga *et al*., 2017).

The regression coefficient was significantly different from zero, based on the 1% t-test, obtaining R^2 values between 0.91 to 0.98 (Fig. 2). These results showed that the functions do not overestimate or underestimate the estimated data for each growth measurement evaluated in this study (Unigarro-Muñoz *et al*., 2015). Therefore, the TLA, TNL, HS, DS, and LMR of coffee plants under the climatic conditions of this study can be simulated and predicted with these functions.

The average absolute growth rate $\hat{G}$, used to analyze the growth of coffee plants is shown in Figure 3 for each growth

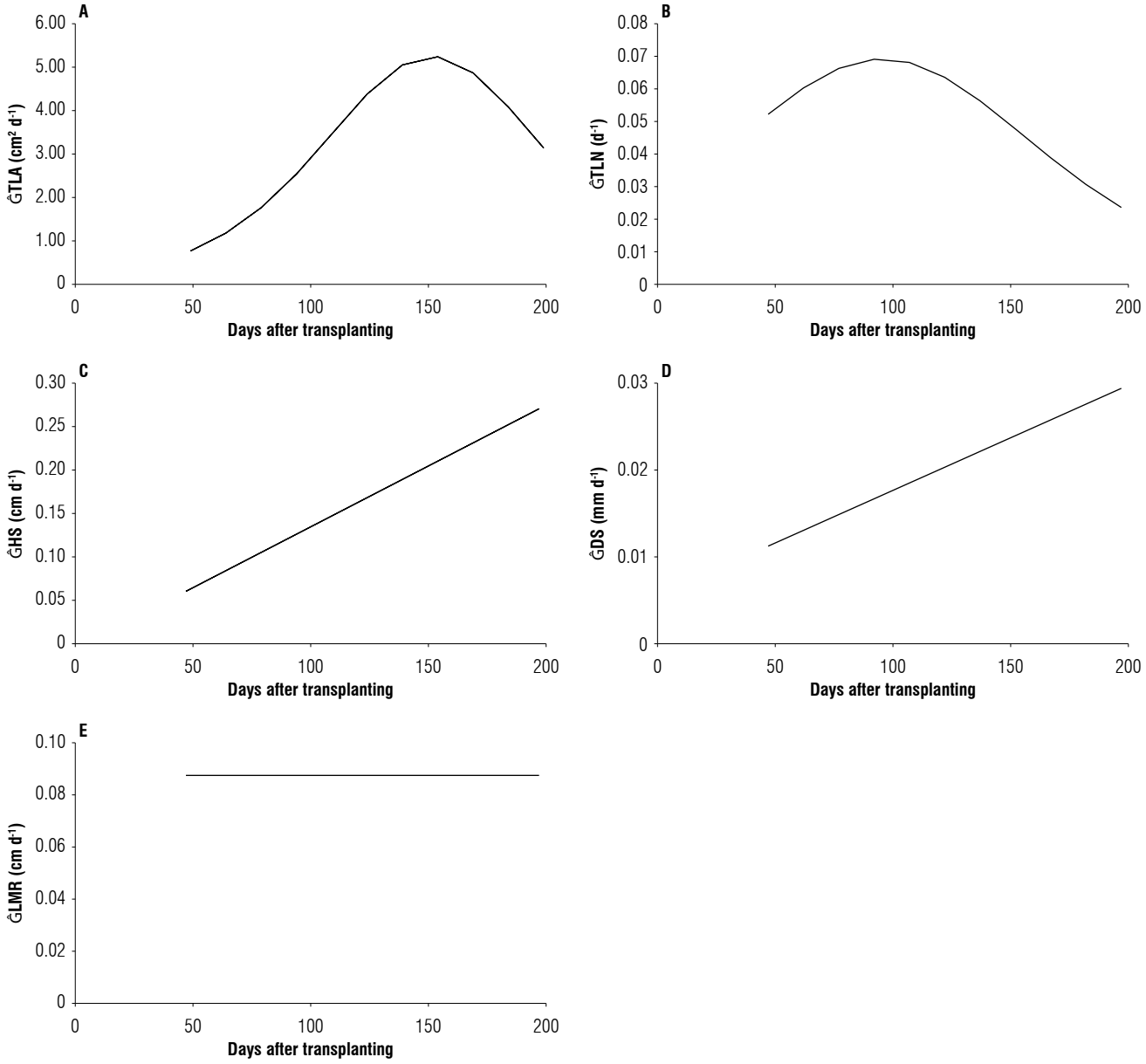

FIGURE 3. Mean absolute growth rate (Ĝ) of coffee seedlings. A) mean absolute growth rate for the total leaf area (ĜTLA); B) mean absolute growth rate for the total leaf number (ĜTNL); C) mean absolute growth rate for the stem height (ĜHS); D) mean absolute growth rate for the diameter of the stem (ĜDS), and E) mean absolute growth rate for the length of the main root (ĜLMR).

measurement evaluated in this study. The average absolute growth rate of total leaf area (ĜTLA) throughout the study was 3.31 $cm^2\ d^{-1}$, with representative increases in size (4.90 $cm^2\ d^{-1}$) after 120 to 150 DAT, showing a decrease from 160 DAT (4.47 $cm^2\ d^{-1}$). The opposite occurred with the average absolute growth rate of the total number of leaves (ĜTNL), since its representative increases were from 30 to 90 DAT (between 0.052 and 0.069 leaves d^{-1}) with average values throughout the study of 0.055 leaves d^{-1}. The average absolute growth rates of height (ĜHS) and stem diameter (ĜDS) increased proportionally during the study, from 0.060 to 0.25 cm d^{-1} for ĜHS and between 0.011 and 0.030 mm d^{-1} for ĜDS. While, for the average growth rate of the main root length-ĜLMR there was no increase over time, reporting average values throughout the study of 0.087 cm d^{-1} (Fig. 3). These trends on the increase of Ĝ from 150 DAT, particularly on the ĜTLA (5 $cm^2\ d^{-1}$) have been reported by Encalada *et al*. (2016) in coffee cultivar Caturra plants established in a nursery stage with 50% shading net under climate conditions of Cuba.

Conclusions

In general, the fitted sigmoidal growth curves for TLA, TNL and HS, and linear for the DS and LMR reported in this study, adequately describe the growth of coffee plants of the variety Cenicafé 1 in the nursery stage. The statistical criteria guaranteed a highest degree of fit and selection of each mathematical functions for simulating the growth measures evaluated in the coffee plants. Finally, the estimate of the growth parameters reported at 180 DAT with mathematical functions may be selection criteria to ensure adequate plant material for establishment under field conditions.

Acknowledgments

The authors would like to thank the Federación Nacional de Cafeteros de Colombia (FNC) and Centro Nacional de Investigaciones de Café (Cenicafé) for funding this study and Ninibeth Sarmiento for help with the climatic data.

Conflict of interest statement

The authors declare that there is no conflict of interests regarding the publication of this article.

Author's contributions

AFLB, CR, JRRS, LIQ and CU developed and designed the methodology. AFLB, CR and JRRS performed the field experiment. AFLB, LIQ and CU contributed to the data analysis and result description. AFLB and HBL wrote the draft. All authors reviewed and approved the manuscript.

Literature cited

Arcila, P. J. (2007). Crecimiento y desarrollo de la planta de café. In J. Arcila Pulgarín, F. Farfán, A. M. Moreno, L. F. Salazar, & E. Hincapié (Eds.), *Sistemas de producción de café de Colombia* (pp. 22–60). Cenicafé. http://hdl.handle.net/10778/720

Arcila, P. J., Buhr, L., Bleiholder, H., Hack, H., Meier, U., & Wicke, H. (2002). Application of the extended BBCH scale for the description of the growth stages of coffee (*Coffea* spp.). *Annals of Applied Biology*, *141*(1), 19–27. https://doi.org/10.1111/j.1744-7348.2002.tb00191.x

Arcila, P. J., & Chaves C. B. (2005). Desarrollo foliar del cafeto en tres densidades de siembra. *Cenicafé, 46(*1), 5–20.

Bakhshandeh, E., Pirdashti, H., Vahabinia, F., & Gholamhossieni, M. (2020). Quantification of the effect of environmental factors on seed germination and seedling growth of Eruca (*Eruca sativa*) using mathematical models. *Journal of Plant Growth Regulation*, *39*(1), 190–204. https://doi.org/10.1007/s00344-019-09974-1

Bote, A. D., & Vos, J. (2017). Tree management and environmental conditions affect coffee (*Coffea arabica* L.) bean quality. *NJAS - Wageningen Journal of Life Sciences*, *83*, 39–46. https://doi.org/10.1016/j.njas.2017.09.002

Castillo, J. Á., & Andrade, D. (2021). Coffee (*Coffea arabica* L, var. Castillo) seedling growth in Nariño, Colombia. *Revista de Ciencias Agrícolas*, *38*(1), 62–74. https://doi.org/10.22267/rcia.213801.145

Ceballos-Sierra, F., & Dall'Erba, S. (2021). The effect of climate variability on Colombian coffee productivity: A dynamic panel model approach. *Agricultural Systems*, *190*, Article 103126. https://doi.org/10.1016/j.agsy.2021.103126

Criollo, H., Muñoz, J., Checa, J., & Noguera, W. (2019). Initial growth of coffee (*Coffea arabica* L. var) castillo in the coffee zone of Nariño. *Revista de Ciencias Agrícolas*, *36*, 124–137. https://doi.org/10.22267/rcia.1936e.112

DaMatta, F. M., Ronchi, C. P., Maestri, M., & Barros, R. S. (2007). Ecophysiology of coffee growth and production. *Brazilian Journal of Plant Physiology*, *19*(4), 485–510. https://doi.org/10.1590/S1677-04202007000400014

Encalada, M., Soto Carreño, F., & Morales Guevara, D. (2016). Coffee (*Coffea arabica* L.) seedling growth with four shade levels under two soil and climate conditions of Ecuador. *Cultivos Tropicales*, *37*(2), 72–78. https://doi.org/10.13140/RG.2.1.4335.7681

Federación Nacional de Cafeteros de Colombia-FNC. (2021). *Publicaciones: Informe de Gestión 2021*. https://federaciondecafeteros.org/app/uploads/2022/05/IG-2021_Digital.pdf

Gaitán, A. L., Villegas, C., Rivillas, C. A., & Hincapié, E. (2011). Almácigos de café: Calidad fitosanitaria, manejo y siembra en el campo. *Avances Técnicos Cenicafé, 404*, 1–8.

Grothendieck, G. (2022). *nls2: Non-linear regression with brute force*. R package version 0.3-3. https://CRAN.R-project.org/package=nls2

Hunt, R. (1979). Plant growth analysis: The rationale behind the use of the fitted mathematical function. *Annals of Botany*, *43*(2), 245–249. https://doi.org/10.1093/oxfordjournals.aob.a085632

Hunt, R. (1990). *Basic growth analysis*. Springer.

Hunt, R., Causton, D. R., Shipley, B., & Askew, A. P. (2002). A modern tool for classical plant growth analysis. *Annals of Botany*, *90*(4), 485–488. https://doi.org/10.1093/aob/mcf214

Jaramillo, A. (2018). *El clima de la caficultura Colombiana*. FNC-Cenicafé. https://www.cenicafe.org/es/index.php/nuestras_publicaciones/libros/publicaciones_el_clima_de_la_caficultura_en_colombia

Kaufmann, K. W. (1981). Fitting and using growth curves. *Oecologia*, *49*(3), 293–299. https://doi.org/10.1007/BF00347588

León-Burgos, A. F., Unigarro, C. A., & Balaguera-López, H. E. (2022). Soil waterlogging conditions affect growth, water status, and chlorophyll "a" fluorescence in coffee plants (*Coffea arabica* L.). *Agronomy*, *12*, Article 1270. https://doi.org/10.3390/agronomy12061270

Liu, J.-H., Yan, Y., Ali, A., Yu, M.-F., Xu, Q.-J., Shi, P.-J., & Chen, L. (2018). Simulation of crop growth, time to maturity and yield by an improved sigmoidal model. *Scientific Reports*, *8*(1), Article 7030. https://doi.org/10.1038/s41598-018-24705-4

Maldonado, C. E. M., & Ángel-Giraldo, L. (2020). Resistencia genética a la enfermedad de la cereza del café en variedades cultivadas en Colombia. *Cenicafé*, *71*(1), 69–90. https://doi.org/10.38141/10778/1121

Maradiaga, W. D., Evangelista, A. W. P., Alves Junior, J., & Honorato, M. V. (2017). Growing of coffee seedlings on different substrates and fertilized with lithothamium. *Revista Facultad Nacional de Agronomía Medellín*, *70*(2), 8177–8182. https://doi.org/10.15446/rfna.v70n2.64522

Moraes, G. A. B. K., Chaves, A. R. M., Martins, S. C. V., Barros, R. S., & DaMatta, F. M. (2010). Why is it better to produce coffee seedlings in full sunlight than in the shade? A morphophysiological approach. *Photosynthetica*, *48*(2), 199–207. https://doi.org/10.1007/s11099-010-0025-4

Nab, C., & Maslin, M. (2020). Life cycle assessment synthesis of the carbon footprint of Arabica coffee: Case study of Brazil and Vietnam conventional and sustainable coffee production and export to the United Kingdom. *Geo: Geography and Environment*, *7*(2), Article e00096. https://doi.org/10.1002/geo2.96

Neiva, E., França, A. C., Grazziotti, P. H., Porto, D. W. B., Araújo, F. H. V., & Leal, F. D. S. (2019). Growth of seedlings and young plants of coffee in composts of textile industry residues. *Revista Brasileira de Engenharia Agrícola e Ambiental*, *23*, 188–195. https://doi.org/10.1590/18071929/agriambi.v23n3p188-195

Paine, C. E. T., Marthews, T. R., Vogt, D. R., Purves, D., Rees, M., Hector, A., & Turnbull, L. A. (2012). How to fit nonlinear plant growth models and calculate growth rates: An update for ecologists. *Methods in Ecology and Evolution*, *3*(2), 245–256. https://doi.org/10.1111/j.2041-210X.2011.00155.x

Plataforma Agroclimática Cafetera-Agroclima. (2019). Portal web. https://agroclima.cenicafe.org/

Poorter, H., & Garnier, E. (1996). Plant growth analysis: An evaluation of experimental design and computational methods. *Journal of Experimental Botany*, *47*(9), 1343–1351. https://doi.org/10.1093/jxb/47.9.1343

R Development Core Team (2019). *R: A language and environment for statistical computing*. R Foundation for Statistical Computing.

Rakocevic, M., & Matsunaga, F. T. (2018). Variations in leaf growth parameters within the tree structure of adult *Coffea arabica* in relation to seasonal growth, water availability and air carbon dioxide concentration. *Annals of Botany*, *122*(1), 117–131. https://doi.org/10.1093/aob/mcy042

Rendón, J. R. (2020). Administración de sistemas de producción de café a libre exposición solar. In Centro Nacional de Investigaciones de Café (Ed.), *Manejo agronómico de los sistemas de producción de café* (pp. 34–71). Cenicafé. https://doi.org/10.38141/10791/0002_2

Rodríguez-López, N. F., Martins, S. C. V., Cavatte, P. C., Silva, P. E. M., Morais, L. E., Pereira, L. F., Reis, J. V., Ávila, R. T., Godoy, A. G., Lavinski, A. O., & DaMatta, F. M. (2014). Morphological and physiological acclimations of coffee seedlings to growth over a range of fixed or changing light supplies. *Environmental and Experimental Botany*, *102*, 1–10. https://doi.org/10.1016/j.envexpbot.2014.01.008

Sadeghian, K. S. S. (2014). Manejo integrado de nutrientes para una caficultura sostenible. *Suelos Ecuatoriales*, *44*(2), 74–89.

Sadeghian, S., & Ospina-Penagos, C. (2021). Manejo nutricional de café durante la etapa de almácigo. *Avances Técnicos Cenicafé*, 532, 1–8. https://doi.org/10.38141/10779/0532

Schmildt, E. R., Amaral, J. A. T., Schmildt, O., & Santos, J. S. (2014). Análise comparativa de equações para estimativa da área foliar em cafeeiros. *Coffee Science*, *9*(2), 155–167.

Silveira, H. R. O., Santos, M. O., Alves, J. D., Souza, K. R. D., Andrade, C. A., & Alves, R. G. M. (2014). Growth effects of water excess on coffee seedlings (*Coffea arabica* L.). *Acta Scientiarum Agronomy*, *36*, 211–218. https://doi.org/10.4025/actasciagron.v36i2.17557

Souza, A. J., Guimarães, R. J., Colombo, A., Sant'Ana, J. A. V., & Castanheira, D. T. (2016). Quantitative analysis of growth in coffee plants cultivated with a water-retaining polymer in an irrigated system. *Revista Ciência Agronômica*, *47*, 162–171. https://doi.org/10.5935/1806-6690.20160019

Tatagiba, S. D., Pezzopane, J. E. M., & Reis, E. F. (2010). Crescimento vegetativo de mudas de café arábica (*Coffea arabica* L.) submetidas a diferentes níveis de sombreamento. *Coffee Science, 5*(3), 251–261. http://www.sbicafe.ufv.br/handle/123456789/5413

Torres, V., Barbosa, I., Meyer, R., Noda, A., & Sarduy, L. (2012). Criterios de bondad de ajuste en la selección de modelos no lineales en la descripción de comportamientos biológicos. *Revista Cubana de Ciencia Agrícola*, *46*(4), 345–350.

Unigarro-Muñoz, C. A., Hernández-Arredondo, J. D., Montoya-Restrepo, E. C., Medina-Rivera, R. D., Ibarra-Ruales, L. N., Carmona-González, C. Y., & Flórez-Ramos, C. P. (2015). Estimation of leaf area in coffee leaves (*Coffea* arabica L.) of the Castillo® variety. *Bragantia*, *74*(4), 412–416. https://doi.org/10.1590/1678-4499.0026

Voorend, W., Lootens, P., Nelissen, H., Roldán-Ruiz, I., Inzé, D., & Muylle, H. (2014). LEAF-E: A tool to analyze grass leaf growth using function fitting. *Plant Methods*, *10*(1), Article 37. https://doi.org/10.1186/1746-4811-10-37

Weih, M., Adam, E., Vico, G., & Rubiales, D. (2022). Application of crop growth models to assist breeding for intercropping: Opportunities and challenges. *Frontiers in Plant Science*, *13*, Article 720486. https://doi.org/10.3389/fpls.2022.720486

Discriminant analysis for estimating meristematic differentiation point based on morphometric indicators in banana (*Musa* AAA)

Análisis discriminante para estimar el punto de diferenciación meristemática basado en indicadores morfométricos en banano (*Musa* AAA)

Ana María Martínez Acosta[1]*, Daniel Gerardo Cayón-Salinas[2], and Aquiles Enrique Darghan-Contreras[3]

ABSTRACT

In the banana crop, leaf area is a fundamental trait for production; however, monitoring this variable during a cycle is difficult due to the structural characteristics of the plant, and a method for its determination is necessary. Therefore, the objective of this research was to propose a model for estimating total leaf area by measuring the cross-sectional area of the pseudostem to identify when meristematic differentiation occurs. In plants between F10 and flowering, functional leaves were measured for length, width, and dry mass. Cross-sectional area was calculated every 10 cm from the base to 70 cm, at ⅓, ½ of the plant height and up to the last pair of leaves. From the principal components, the cross-sectional measurement at 50 cm was selected, obtaining a nonlinear model for indirect estimation of leaf area. Subsequently, Fisher's linear discriminant analysis was used with the parameters associated with the number of leaves emitted and the estimated leaf area to obtain the cutoff point as the centroid of the extracted components. As an indicator for the approximate identification of the moment of meristem differentiation, the emission of leaf 12 was generated, which determines the phenological stage (vegetative-reproductive) of the plant. The results describe tools to follow up the growth in the productive units to facilitate crop monitoring, allowing the generation of differential production approaches.

Key words: allometry, pseudostem, phenological stages, non-destructive methods.

RESUMEN

En el cultivo de banano el área foliar es una característica fundamental para la producción; no obstante, el monitoreo de esta variable durante el ciclo se dificulta por las características estructurales de la planta, siendo necesario algún método para su determinación. Por lo tanto, el objetivo de esta investigación fue proponer un modelo de estimación del área foliar total, mediante la medición del área de la sección transversal del seudotallo, para identificar cuando ocurre la diferenciación meristemática. En plantas entre F10 y floración se midió en las hojas funcionales largo, ancho y masa seca. El área de la sección transversal se calculó a 10 cm de la base hasta 70 cm, a ⅓, ½ de la altura de la planta y hasta el último par de hojas. A partir de los componentes principales se seleccionó la medida de la sección transversal a 50 cm, obteniéndose un modelo no lineal de estimación indirecta del área foliar. Posteriormente se utilizó el análisis discriminante lineal de Fisher con los parámetros asociados al número de hojas emitidas y al área foliar estimada para obtener el punto de corte como centroide de los componentes extraídos. Se generó como indicador para la identificación aproximada del momento de la diferenciación del meristemo la emisión de la hoja 12, y con esto la determinación de la etapa fenológica (vegetativa-reproductiva) en la cual se encuentra la planta. Los resultados describen herramientas para hacer seguimiento al crecimiento en las unidades productivas que facilitarían el monitoreo del cultivo, permitiendo generar enfoques de producción diferenciales.

Palabras clave: alometría, seudotallo, etapas fenológicas, métodos no destructivos.

Introduction

The banana crop is vulnerable to various factors that can affect plant development and therefore yield, so it is necessary to monitor the productive status of the plantation by monitoring its yield indicators (Turner *et al*., 2007). Parker (2020) asserts that the photosynthetic capacity of plants can be estimated from the potential of the canopy to intercept light and fix carbon which, in turn, is associated with the productivity of the crop, using as reference the number of photosynthetically active leaves that develop before the emergence of the inflorescence.

Received for publication: June 18, 2022. Accepted for publication: November 11, 2022 Doi: 10.15446/agron.colomb.v40n3.103234

[1] Facultad de Ciencias Agrarias, Politécnico Colombiano Jaime Isaza Cadavid, Medellín (Colombia).
[2] Departamento de Ciencias Agrícolas, Facultad de Ciencias Agropecuarias, Universidad Nacional de Colombia, Palmira (Colombia).
[3] Departamento de Agronomía, Facultad de Ciencias Agrarias, Universidad Nacional de Colombia, Bogotá (Colombia).
* Corresponding author: ammartinez@elpoli.edu.co

Plant allometry allows the generation of one-dimensional (height) or two-dimensional (cross-sectional area) measurements that can be used to estimate some yield attributes. In general, non-destructive methods have been devised that use indirect measurements generated from mathematical or statistical models whose predictions are used as productivity indicators (Karaca *et al*., 2020). In various allometric studies, models have been developed to estimate growth for blueberries (*Vaccinium corymbosum)*, passion fruit (*Passiflora edulis*), pineapple (*Ananas comosus*), and papaya (*Carica papaya*) among other crops (Jorquera-Fontena *et al*., 2017; Souto *et al*., 2017; Santos *et al*., 2018; Oliveira *et al*., 2019).

In the Musaceae, based on growth indicators such as root characteristics, height of the mother plant or successional plant, pseudostem circumference, number of functional leaves (photosynthetically active leaves) and leaf area (LA), it is possible to estimate photosynthetic capacity, accumulation of biomass, efficiency in water use as well as variables associated with production and agronomic characteristics in germplasm selection programs (Nyombi *et al*., 2009; Martínez *et al*., 2015; Chang *et al*., 2018; Laskar *et al*., 2020; Stevens *et al*., 2020; Nowembabazi *et al*., 2021).

Dépigny *et al*. (2015) propose the OTO model for leaf area estimation in different varieties, including the number of functional leaves, length and width of the 1st, 3rd, and the last leaf to emerge. The model can be used on any accession of banana, regardless of its variety, stage of development, or growth conditions. Although the model is robust, it is limited to measurements of the leaves of the upper third of the plant, considering the characteristics of height and structure of the plant. But Martínez-Acosta *et al*. (2018) present a model to estimate the same previous variable from the measurement of the cross-sectional area of the pseudostem, avoiding *in situ* measurements of the leaves. Empirical models must be developed that facilitate the estimation of variables of a plant organ of interest, which can be obtained from easy measurements of another organ. Considering the above, this research proposes to build a model to estimate the leaf area from measurements of the pseudostem cross-sectional areas (PCSA) and calculation of the current LA, and, thus, identify the moment when meristematic differentiation occurs.

Materials and methods

The research was carried at the farm of the Banana Research Center-CENIBANANO in Carepa (7°46'22" N; 76°40'00" W, 40 m a.s.l.), Urabá (Colombia), where the annual averages of temperature, relative air humidity, rainfall, and sunshine are 28°C, 87.5%, 2650 mm, and 1700 h yr^{-1}, respectively. Sampling and processing of the samples was carried out between the calendar weeks 25 to 45 of 2018, a period with sufficient water availability to plants. Thirty-four banana (*Musa* AAA subgroup Cavendish cv. Williams) plants were randomly selected between F10 and flowering in the phenological growth stages 4050 and 6000 according to the BBCH scale (Meier, 2001). The samples were selected of plot with 1800 plants ha^{-1}; for each sampled plant, the number of leaves emitted was calculated, based on the remains of the leaf sheaths present in the pseudostem that were intrinsically associated with unequally spaced times (temporary event). Following the phyllotaxy of the plant, the total number of leaves present was counted, taking the 1st leaf as the youngest completely expanded leaf until the last functional leaf called the "oldest leaf". Finally, an empirical categorization of the phenological phase of the plant, vegetative or reproductive, was proposed based on the number of visible leaves and the morphological difference at the base of the leaf blade of the leaves present. This was used as the reference classification (Borja Agamez *et al*., 2018).

Leaf area estimation

All leaves present on each plant were cut off and numbered according to their position on the pseudostem. For each leaf, the length and width at the widest point of a leaf blade were determined. The total LA present was estimated with A) Belalcázar model (Belalcázar, 1991), B) Kumar model (Kumar *et al*., 2002) and C) calculation from the leaf dry mass LA(DM), where a 10 cm^2 or 5 cm^2 sample was taken from each leaf (depending on the size of the leaf blade), following the parameters described by Martín-Prevél (1974), the rest of the leaf was stored in paper bags. The sample and the rest of the leaf were dried in the CENIBANANO Laboratory at 65°C until reaching constant weight. Total leaf area was calculated using the ratio of mass to area in the leaf sample for the total number of leaves (assuming an even distribution of mass in the organ) (Equation 1).

$$LA = \sum_{i=1}^{n} \frac{m_i \, a_i^*}{m_i^*} \quad (1)$$

where LA = total leaf area, m_i = dry mass of the *i*-th complete leaf, m_i^* = dry mass of the sample from the *i*-th leaf, a_i^* = area of the sample from the *i*-th leaf, and *n* = number of leaves present.

Measurement of pseudostem cross-sectional area (PCSA)

For all plants, the circumference of the pseudostem was measured every 10 cm from the base of the pseudostem as

the initial point or relative zero to maximum height (MH), identified by the vertex formed by the last pair of functional leaves. Additionally, the circumference was measured from the base of the pseudostem at one-third (⅓) and one-half (½) of the MH. The height at which these last measurements were made was variable, considering that the plants were at different physiological ages, since the growth and elongation of the pseudostem is conditioned by the appearance of new leaves and the phenological stage.

With these measurements, the PCSA was estimated at different heights (assuming a cylindrical shape with a circular base), between 10 and 70 cm, at ⅓ MH, at ½ MH, and MH (Equation 2), where P_i represents the *i*-th circumference (cm) of the pseudostem corresponding to the *i*-th height. From the data collected, a data matrix of dimension 34×15 was built, for a total of 510 measurements.

$$\text{PCSA} = \frac{{P_i}^2}{4\pi};$$

$$i = \{10, 20, 30, 40, 50, 60, 70, \tfrac{1}{3}\text{MH}, \text{MH}\} \quad (2)$$

Statistical analysis

Except for the initial categorization associated with the phenological phase, a standardized principal components analysis was applied to the matrix data from which a single component was extracted, since the explained variance of this component was a little over 96%. A variable associated with the PCSA and another with the LA(DM) leaf area estimation method were chosen, based on the generated biplot (and therefore the correlation between the first component and the original variables) (Gower & Hand, 1995).

With this single pair of variables (PCSA at 50 cm height and LA(DM)), a series of linear and nonlinear models were explored, finding a nonlinear model estimated by nonlinear least squares as the best fit. Equation 3 shows the functional form, where *y* is the response variable associated with LA(DM), β_0 and β_1 are the parameters of the model to be adjusted, and *x* is the cross-sectional area of the pseudostem.

$$y = \left(\beta_0 + \beta_1\sqrt{x}\right)^2 \quad (3)$$

With this model, leaf area predictions were generated which, compared only with the observed values, yielded a very good fit. The predictions were used as a response variable in the following analysis, in which the number of the emerged leaves (indirectly associated with a strictly continuous variable because it is the time of leaf emergence) was incorporated. At first, a scatter diagram was elaborated between the predictions and the number of visible leaves that predicted the possibility of applying a Fisher's linear discriminant analysis using the categorical variable associated with the initially proposed phenological phase as a classifier. This method was applied twice, first using the LA(DM) predictions and then the emitted leaves (which, as described above, is not a count, but an identifier of a temporal event). With these runs, the discriminant equations were generated to establish the cutoff point associated with the prediction of the LA(DM) and the new leaf by matching the respective discriminant equations, to find the useful common boundary as the cutoff point.

With the initial classification of the differentiation and with the generated partition as a cutoff point, the respective confounding matrices were obtained. However, an algorithm was built not only to have a measure of the correct classifications based on the partition up to leaf 11 at the time before differentiation and from leaf 12 at the time after differentiation, but also to allow changing this partition at all possible values (from the second value taken from the emitted leaf to the penultimate). The sequence of partitions was used as a classifier and each response separately as an explanatory variable. For the correct classifications, both independent models were proposed to classify the meristem differentiation as "pre" or "post" in each row of data. The algorithm maximized the percentage of correct classifications, since the initial categorization of the phenological phase did not necessarily guarantee an optimum in the percentage of correct classifications. Finally, a diagram was developed for the optimization progress, which allowed the selection of the emitted leaf and the estimated LA that would guarantee the maximum discrimination of the phenological phase.

Results and discussion

The LA measurements between F10 and flowering were different with each method. While with the method of Kumar *et al*. (2002) LA varied from 0.07 m^2 to 14.37 m^2, with the Belalcázar method (Belalcázar, 1991) the values ranged between 0.17 m^2 and 17.22 m^2. The LA values calculated from LA(DM) were higher than the previous ones, varying between 0.21 m^2 and 22.88 m^2. Despite the differences in LA measurement with each method, the dynamics of development followed a similar pattern. A smaller leaf area was observed in the plants at F10 that could be associated with the juvenile development phase. Later a linear increase during the vegetative development phase that culminated with the floral differentiation of the apical meristem, followed by a more unstable increase

TABLE 1. Estimated coefficients for the principal components.

	Pseudostem cross sectional area*										Leaf area estimation model		
	A10	A20	A30	A40	A50	A60	A70	A⅓ MH	A½ MH	AMH	Belalcázar (1991)	Kumar *et al*., (2002)	Leaf dry mass
Principal component	0.264	0.276	0.279	0.281	0.282	0.281	0.281	0.278	0.278	0.278	0.275	0.275	0.276

* Cross-sectional areas indicated in Equation 2.

in plants close to flowering, represented the dynamics of development described by Lassoudiere (2007), Martínez and Cayón (2012), and Dépigny *et al*. (2015).

An analysis of the standardized principal components between the measures of PCSA and LA estimated by the three methods yielded a single extracted component that explained more than 96% of the variability in the data, so their loads were extracted and correlated with the different measures of LA and the succession of PCSA. Based on the generated biplot and, therefore, on the correlation between the first component and the original variables, the highest coefficients associated with the PCSA and leaf area estimation method were selected. The LA(DM) method and the PCSA measurement at 50 cm (A50) were selected as the best predictor (Tab. 1).

With the selected variables, the dispersion diagram was constructed between the to the measurement of the PCSA at 50 cm (A50), and the LA(DM) values and a nonlinear model was fitted. The model's predictions, compared to other explored models, reached the best fit. For the selection of the best model, Akaike's information criterion, AIC=137.0691, was used.

The results of the nonlinear modeling process are presented in Figure 1, which shows that the pseudostem measurement is a convenient predictor of the LA(DM) as found by Stevens *et al*. (2020).

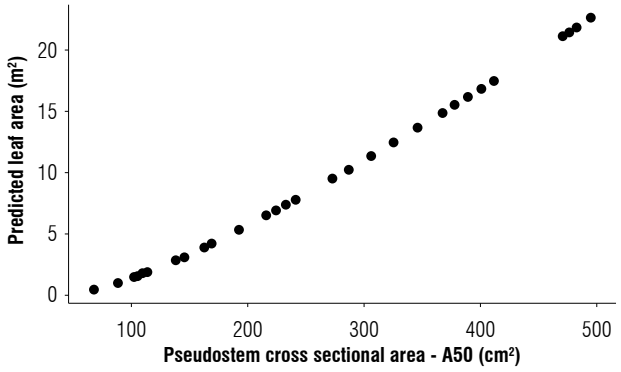

FIGURE 1. Non-linear modeling between the leaf area (LA) of banana plants cv. Williams and the pseudostem cross sectional area at 50 cm (A50).

Given that the calculation of the leaf area from the LA(DM) is a destructive methodology that demands time, effort, and resources, the indirect measurement of the LA is more convenient, because it approximates the originally estimated value without destroying the sample units as in Belalcázar (1991), Kumar *et al*. (2002) or even as in Dépigny *et al*. (2015). Although such methods adjust functional forms and result in a variable monitoring strategy, they can also show limitations due to data collection in the field, especially in plantations with tall plants, with the need to measure the 1st and the 3rd leaves. The use of PCSA can solve this difficulty in the field, in addition to being non-destructive.

Allometric relationships can potentially be affected by various abiotic and biotic factors, including genetics, ontogeny, size, age, organ structure, environment, soil moisture, and biomass accumulation (Stevens *et al*., 2020). The results show a close statistical allometric relationship between PCSA and the LA, albeit these relationships are conditional and are restricted to the situation being experienced. Although mathematically or statistically the relationships seem sensational, they are not necessarily related to reality (Briggs, 2016). Chang *et al*. (2018) validate the results obtained in this research, since they also find that the measurement of the diameter of the pseudostem is an adequate predictor of other variables in the plant, especially the LA. Thus, the final expression of the nonlinear modeling process is presented in Equation 4:

$$LA = \left(-1.73785 + 0.29079 * \sqrt{A50}\right)^2 \quad (4)$$

where LA corresponds to the measurement of the leaf area, allowing us to estimate the development of the plant based on the leaves that have emerged, and A50 to the measurement of the PCSA at 50 cm. Table 2 shows the estimation and testing of the parameters of the nonlinear model.

TABLE 2. Estimation and test of the parameters of the non linear model.

Parameters	Estimated	Standard error	t	Pr (>t)
β_0	-1.73785	0.29589	-5.873	1.57 e-06
β_1	0.29079	0.01558	18.662	< 2 e-16

Further analysis of the data revealed the approximate identification of the moment when the apical meristem changes from vegetative to reproductive condition, which depends on leaf emergence and LA. Figure 2 shows the dispersion diagram of the LA(DM) estimated by means of the nonlinear model and the emitted leaf, marking the data with the initial classification given the differentiation of the apical meristem. The graph shows the possibility of separating the points using some method that discriminates the variables.

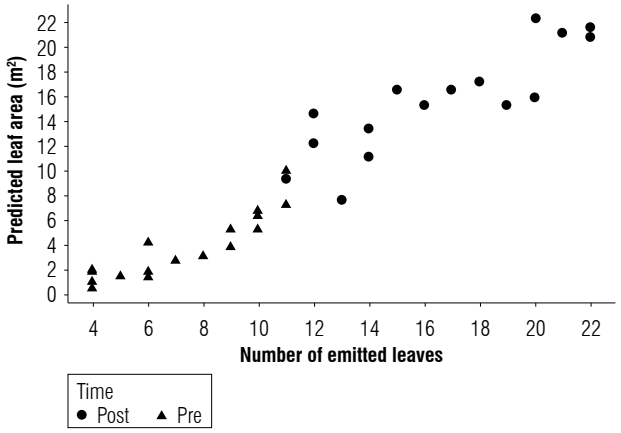

FIGURE 2. Fisher's discriminant analysis using the categorical variable associated with the phenological phase as a classifier. "Pre" corresponds before differentiation and "Post" after differentiation.

Since the number of lines that can make the separation is so large, Fisher's linear discriminant analysis was proposed to obtain the models that allow the separation and thus obtain an optimal cutoff point relative to the method used. Two discriminant functions were generated for each response (leaves emitted and estimated leaf area) and the cutoff point was estimated by these equations. The functions for LA and indirect time (t), seen from the number of leaves emitted (Equation 5), classify functions to match the first and second stage (variable = LA prediction and variable = time)

$$\begin{cases} z_{1LA} = 1.35375 + 0.323144\text{LA} \\ z_{2LA} = -10.8032 + 1.26417\text{LA} \end{cases} \quad \begin{cases} z_{1t} = 3.47146 + 0.740884\text{t} \\ z_{2t} = -14.4475 + 1.64847\text{t} \end{cases} \tag{5}$$

where z_1 and z_2 represent the ordinates of the functions for the label "1" before differentiation and "2" after differentiation for each input variable (LA and t). Equating z_1 with z_2 in each case, the cutoff point was obtained (placing a subscript c to associate it with the cutoff point in each input variable) (Tab. 3).

TABLE 3. Approximate parameters of the number of leaves emitted (t_c) and leaf area developed (LA_c) in banana plants, at the time of differentiation of the apical meristem.

Parameters	Estimated
LA_c	10.041 m²
t_c	12.09 leaves emitted

In this way, when the plant reaches an LA of 10.041 m² and has emerged up to leaf 12 (by rounding), it can be said that this is when the apical meristem changes a vegetative stage to a reproductive stage. Therefore, when the LA is less than 10.041 m², the plant is in the vegetative stage, which is indirectly identifiable before the appearance of leaf 12, corroborating what was proposed by Lassoudiere (2007) and Borja Agamez *et al*. (2018). In Figure 2, the coordinate, identified by the red dot, guarantees optimal discrimination by the method used.

The model with which the leaf area can be predicted from the PCSA and the cutoff point proposed constitute a valuable tool and information for technicians and researchers to monitor crop development of the and plan strategies that lead to improved productivity. However, as is often the case in many methods of classification and recognizing that the initial categorization was merely empirical, we proposed to fit an algorithm that would not use leaf 12 as the point of partition but would instead use different initial partition points. The comparison to obtain the percentage of correct classifications changes the initial partition, leaves the cutoff point obtained by linear discriminant, and calculates the percentage of correct classifications for all the initial or reference cut points.

Figure 3 shows the progress of the algorithm illustrating leaf emission; in leaf 12, a percentage of correct classification of 97.1% is generated, an indicator of emitted leaf previously obtained by the discriminant analysis (Tab. 2). Thus, the period from the emission of leaf 12 onwards can be considered as the approximate time of inflorescence meristem differentiation. The recording of the chronological time of appearance of leaf 12 is a midpoint that can serve as a reference in different scenarios such as the implementation of differential nutrition strategies based on phenology, for example: the contribution of minor elements or hormones before or during the process of differentiation of the apical meristem. Also, in the selection of mother plants to be eliminated, hoping that the bunch

to be harvested comes from the sucker, at a time or time of year with particular characteristics such as better market conditions, this practice is known as crop transfer.

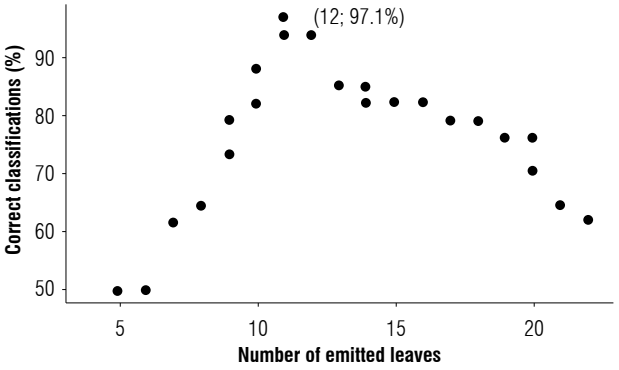

FIGURE 3. Progress of the correct classifications using the cut-off point obtained as a separator of the vegetative or reproductive phase.

Conclusions

The leaf area of the banana plants was successfully estimated based on measurements of the cross-sectional area of the pseudostem using an allometric approach. The availability of a tool to measure banana plant development, based on the estimation of leaf area prior to the inflorescence emission and during the crop cycle, constitutes a bioindicator that can be associated with production parameters and global yield estimation. It is also a practical input for researchers and technicians linked to the banana production sector to monitor plantations, facilitating the implementation of differential production approaches and support for decision making in agronomic management in the field.

Although the model proved to be reliable for estimating leaf area in banana cv. Williams, it should be validated for application to other Cavendish cultivars. Further studies should be carried out in Musaceae to establish allometric equations to relate other plant development traits with easily obtainable non-destructive measurements.

Conflict of interest statement

The authors declare that there is no conflict of interests regarding the publication of this article.

Author's contributions

AMMA formulated the overarching research goals, AMMA, EDC and DGCS designed the experiments, EDC contributed to the data analysis, AMMA and EDC wrote the article, DGCS carried out the critical review. All authors reviewed the final version of the manuscript.

Literature cited

Belalcázar, S. (1991). El cultivo del plátano (*Musa* AAB Simmonds) en el trópico. Cali, ICA – CIID – CDCQ – INIBAP. Manual de Asistencia Técnica No. 50.

Borja Agamez, W., Osorio, J. D., Herrera, N., & Sánchez, J. D. (2018). Fundamentos en fenología de banano Cavendish (*Musa* AAA) en cultivo establecido. *Boletín Técnico Cenibanano*, *1*, 1–4.

Briggs, W. (2016). *Uncertainty. The soul of modeling, probability & statistics*. Springer. https://link.springer.com/book/10.1007/978-3-319-39756-6

Chang, S., Wu, Z., Sun, W., Qiao, L., Zeng, Q., Zhang, J., & Shu, H. (2018). A method to predict banana pseudostem's strength at seedling stage. *Advances in Bioscience and Biotechnology*, *9*(9), 391–396. https://doi.org/10.4236/abb.2018.99027

Dépigny, S., Achard, R., Lescot, T., Djomessi, M. T., Tchotang, F., Ngando, D. E., & Poix, C. (2015). In vivo assessment of the active foliar area of banana plants (*Musa* spp.) using the OTO model. *Scientia Horticulturae*, *181*, 129–136. https://doi.org/10.1016/j.scienta.2014.10.044

Gower, J. C., & Hand, D. J. (1995). *Biplots. Monographs on statistics & applied probability*. Chapman & Hall.

Jorquera-Fontena, E., Génard, M., Ribera-Fonseca, A., & Franck, N. (2017). A simple allometric model for estimating blueberry fruit weight from diameter measurements. *Scientia Horticulturae*, *219*, 131–134. https://doi.org/10.1016/j.scienta.2017.03.009

Karaca, C., Büyüktaş, D., & Şehir, S. (2020). Determination of leaf area of some vegetable plants grown under greenhouse condition by non-destructive methods. *Horticultural Studies*, *38*(1), 23–28. https://doi.org/10.16882/hortis.841745

Kumar, N., Krishnamoorthy, V., Nalina, L., & Soorianathasundharam, K. (2002). Nuevo factor para estimar el área foliar total en banano. *Infomusa*, *11*(2), 42–43.

Laskar, S. Y., Weldesemayat Sileshi, G., Jyoti Nath, A., & Kumar Das, A. (2020). Allometric models for above and below-ground biomass of wild *Musa* stands in tropical semi evergreen forests. *Global Ecology and Conservation*, *24*, Article e01208. https://doi.org/10.1016/j.gecco.2020.e01208

Lassoudiere, A., (2007). *Le bananier et sa culture*. Quae, Collection Savoir-faire.

Martin-Prevel, P. (1974). Les methodes d'echantillonnage pour l'analyse foliaire du bananier: resultats d'une enquete internationale et propositions en vue d'une reference commune. Fruits. In A. Lopez, & J. Espinosa (Eds.), *Manual on the nutrition and fertilization of banana* (pp. 583–588). Potash and Phosphate Institute of Canada.

Martínez, A. M., & Cayón, D. G. (2011). Dinámica del crecimiento y desarrollo del banano (*Musa* AAA Simmonds cvs. Gran Enano y Valery). *Revista Facultad Nacional de Agronomía Medellín*, *64*(2), 6055–6064.

Martínez, C., Cayón, G., & Ligarreto, G. (2015). Physiological attributes of banana and plantain cultivars of the Colombian Musaceae collection. *Agronomía Colombiana*, *33*(1), 29–35. https://doi.org/10.15446/agron.colomb.v33n1.45935

Martínez-Acosta, A. M., Jorquera-Fontena, E., Hernández-Arredondo J. D., & Franck, N. (2018). Sección transversal del

pseudotallo como estimador del área foliar total en banano (*Musa* AAA). Un estudio preliminar. *XXXII Reunión Argentina de Fisiología Vegetal y XVI Congreso Latinoamericano de Fisiología Vegetal* (pp. 116).

Meier, W. (2001). *Growth stages of mono and dicotyledonous plants*. BBCH Monograph. Federal Biological Research Centre for Agriculture and Forestry. https://doi.org/10.5073/20180906-074619

Nowembabazi, A., Taulya G., & Tinzaara, W. (2021). Allometric functions for apple banana leaf area and above ground biomass. *African Journal of Agricultural Research*, *17*(9), 1229–1236. https://doi.org/10.5897/AJAR2021.15478

Nyombi, K., van Asten, P. J. A., Leffelaar, P. A., Corbeels, M., Kaizzi, C. K., & Giller, K. E. (2009). Allometric growth relationships of East Africa highland bananas (*Musa* AAA-EAHB) cv. Kisansa and Mbwazirume. *Annals of Applied Biology*, *155*(3), 403–418. https://doi.org/10.1111/j.1744-7348.2009.00353.x

Oliveira, V. S., Santos K. T. H., Ambrósio, T. J., Santos, J. S. H., Santana W. R., Malikouski, R. G., Nascimento A. L., Santos G. P., Schmildt O., & Schmildt, E. R. (2019). Mathematical modeling for leaf area estimation from papaya seedlings 'Golden THB'. *Journal of Agricultural Science*, *11*(5), 496–505. https://doi.org/10.5539/jas.v11n5p496

Parker, G. (2020). Tamm review: Leaf Area Index (LAI) is both a determinant and a consequence of important processes in vegetation canopies. *Forest Ecology and Management*, *477*, Article 118496. https://doi.org/10.1016/j.foreco.2020.118496

Santos, M. P., Maia V. M., Oliveira F. S., Pegoraro, R. F., Santos S. R., & Aspiazú, I. (2018). Estimation of total leaf area and D leaf area of pineapple from biometric characteristics. *Revista Brasileira de Fruticultura, 40*(6), Article e-556. https://doi.org/10.1590/0100-29452018556

Souto, A. G. L., Cordeiro, M. H. M., Rosado, L. D. S., Santos., C. E. M., & Bruckner, C. H. (2017). Non-destructive estimation of leaf area in passion fruit (*Passiflora edulis* L.). *Australian Journal of Crop Science*, *11*(12), 1534–1538. https://doi.org/10.21475/AJCS.17.11.12.PNE662

Stevens, B., Diels, J., Brown, A., Bayo, S., Ndakidemi, P. A., & Swennen, R. (2020). Banana biomass estimation and yield forecasting from non-destructive measurement for two contrasting cultivars and water regimes. *Agronomy*, *10*(9), Article 1435. https://doi.org/10.3390/agronomy10091435

Turner, D. W., Fortescue, J. A., & Thomas, D. S. (2007). Environmental physiology of the bananas (*Musa* spp.). *Brazilian Journal of Plant Physiology*, *19*(4), 463–484. https://doi.org/10.1590/S1677-04202007000400013

Leaf area prediction models from growth measurements in Andean blueberry (*Vaccinium meridionale* Swartz) in the nursery

Modelos de predicción de área foliar a partir de mediciones de crecimiento en agraz (*Vaccinium meridionale* Swartz) en vivero

Mariam Vásquez-Martínez[1*], Pedro Lizarazo-Peña[2], Enrique Darghan[1], Liz Patricia Moreno-Fonseca[1], and Stanislav Magnitskiy[1]

ABSTRACT

The Andean blueberry is a high-Andean wild fruit species consumed in fresh or processed form that has high potential due to its antioxidant capacity. Leaf area describes the photosynthetic capacity of plants and is employed as a variable in multiple physiological studies; however, in Andean blueberry *(Vaccinium meridionale* Swartz*)*, its direct measurement is costly. The aim of this research was to propose models for estimating the leaf area in young Andean blueberry plants using morphometric variables. In the study, 436 Andean blueberry plants of different ages (10 to 26 months) obtained with different methods of asexual propagation (tissue culture or cuttings) were used. Variables, such as dry weight per organ, leaf area, plant height, number of vegetative shoots and number of leaves, were measured. Simple and multiple regressions were performed and the "weighted least squares" technique was used to meet the regression assumptions. Five models with coefficients of determination (R^2) greater than 0.81 were proposed. Two models were of the multiple type and employed the number of leaves together with the dry weight of leaves or the total dry weight as predictor variables. The other models were linear and used total dry weight, dry weight of leaves or number of leaves as explanatory variables of leaf area; the number of leaves was a particularly interesting variable due to its non-destructive nature. The models presented could be a useful tool for estimating leaf area in future studies in Andean blueberry.

Key words: average leaf area, regression analysis, weighted least squares, Andean species, Ericaceae.

RESUMEN

El agraz es un frutal silvestre altoandino de consumo en fresco o procesado que presenta alto potencial debido a su capacidad antioxidante. El área foliar describe la capacidad fotosintética de las plantas y se emplea como variable en múltiples estudios fisiológicos; no obstante, en agraz (*Vaccinium meridionale* Swartz) su medición directa resulta dispendiosa. El objetivo de esta investigación fue plantear modelos para estimar el área foliar en plantas jóvenes de agraz, empleando variables de tipo morfométrico. Se utilizaron 436 plantas de agraz de diferentes edades (entre 10 y 26 meses) obtenidas a partir de propagación asexual (estacas o cultivo de tejidos). Se midieron variables como peso seco por órgano, área foliar, altura de la planta, número de brotes vegetativos y número de hojas. Se realizaron regresiones simples y múltiples y se utilizó la técnica de "mínimos cuadrados ponderados" para cumplir con los supuestos de la regresión. Se plantearon cinco modelos con coeficientes de determinación (R^2) superiores a 0.81. Dos modelos fueron de tipo múltiple y emplearon el número de hojas junto con el peso seco de hojas o el peso seco total como variables predictoras. Los otros tres modelos fueron de tipo lineal y utilizaron el peso seco total, el peso seco de hojas o número de hojas como variables explicativas del área foliar, siendo el número de hojas particularmente interesante por su carácter no destructivo. Los modelos presentados pueden ser una herramienta útil para estimar el área foliar en futuras investigaciones en agraz.

Palabras clave: área foliar promedio, análisis de regresión, mínimos cuadrados ponderados, especies andinas, Ericaceae.

Introduction

The Andean blueberry (*Vaccinium meridionale* Swartz) (Ericaceae) is a woody shrub that grows spontaneously in the mountainous areas of Colombia, Ecuador, Peru, Venezuela, and Jamaica (Muñoz *et al*., 2009; Torres *et al*., 2009; Maldonado Celis *et al*., 2017). The Andean blueberry plants have a high domestication potential for fruit consumption in fresh and industrial processing due to the fruit's antioxidant activity and high content of phenolic compounds including anthocyanins, which can exceed those found in commercial species such as blueberries (Bernal *et al*., 2014; Maldonado Celis *et al*., 2017; Garzón *et al*., 2020).

Received for publication: September 30, 2022. Accepted for publication: December 10, 2022. Doi: 10.15446/agron.colomb.v40n3.105039

[1] Facultad de Ciencias Agrarias, Universidad Nacional de Colombia, Bogotá (Colombia).
[2] Facultad de Ingeniería, Universidad El Bosque, Bogotá (Colombia).
* Corresponding author: mavasquezma@unal.edu.co

The nursery material corresponds to plants cultivated for subsequent transplanting to the field (Singh *et al*., 2017); this is decisive in the quality and productivity of crops (Sánchez-Aguilar *et al*., 2016), so multiple studies focus on this phase. In Andean blueberry propagated from seeds, the nursery stage of growth ends after approximately 26 months (Torres *et al*., 2012). For asexually propagated Andean blueberry, few reports indicate the duration of the nursery period. According to González *et al*. (2018), a duration of 5 months is an adequate period for a rooted cutting of Andean blueberry to reach a size of around 20 cm in height and be suitable for transplanting to the field. Medina-Cano *et al*. (2015) report a period between 15 and 18 months from preparing the cuttings to their transplanting to the final site. Due to the taxonomic relationship of Andean blueberry with blueberry (*V. corymbosum*), reports for early growth of blueberry may be adjusted to Andean blueberry. Generally, in blueberries propagated from cuttings or by tissue culture, the nursery stage lasts from 18 to 24 months; after this period the plants are considered ready to be transplanted to the final site (Bryla & Machado, 2011; Bryla & Strik, 2015). In young plants of Andean blueberry, initial growth is characterized by extensive leaf formation. Vegetative growth progresses through formation and differentiation of axillar buds, followed by expansion and development of leaf blades. Finally, young leafy shoots are developed, characterized by the presence of leaves, prominent elongation of branches and leaf expansion, and formation of new axillary buds that can be differentiated into vegetative or reproductive organs (Medina-Cano *et al*., 2019).

The leaf area (LA) quantifies the total leaf surface that a plant possesses; this variable is of high importance in research in biology, plant physiology, agronomy, and ecology (Cabezas-Gutiérrez *et al*., 2009; Weraduwage *et al*., 2015). The LA is used as a response or predictor variable in processes such as light interception for photosynthesis and transpiration for efficient water use, and as an indicator of growth and productivity (Kucharik *et al*., 1998; Montoya-Restrepo *et al*., 2017). At the plant community level, LA is the basis for estimating light interception indicators, such as the leaf area index (LAI) used in function-adjusted growth analysis (Cabezas-Gutiérrez *et al*., 2009; Benedetto & Tognetti, 2016; Hunt, 2017).

The methods to estimate LA in plants can be classified into direct and indirect groups (Yan *et al*., 2019). The direct or destructive methods limit the possibility of measuring the same individual as a function of time in growth studies and require intensive labor, as they involve removing the leaves of a plant to measure them with different techniques. Direct LA measurement can be done with LI-3000C portable leaf area meter (LI-COR, Lincoln, NE, USA) or the Portable Laser Leaf Area Meter (CID Bio-Science, Camas, WA, USA). The use of these meters is limited because of their cost. As an alternative, the use of images is a strategy that allows estimating values from the use of image processing software such as ImageJ (Rasband, 1997) used in various studies (Schneider *et al*., 2012; Easlon & Bloom, 2014; Milić *et al*., 2018; Suarez Salazar *et al*., 2018; Cosmulescu *et al*., 2020; Wakui & Kudo, 2021), Adobe Photoshop (Adobe Systems Incorporated, 1990), and AutoCAD (Autodesk, 1982), which are based on the use of a scale and the manual segmentation of images to differentiate the background of leaves.

The LA estimation is useful when the number of experimental units or observations is small or the same experimental unit is monitored, such as in perennial or timber crops, or where direct measurement of LA is costly (Montoya *et al*., 2017). Indirect methods obtain an approximation to LA from mathematical models based on non-destructive morphometric measurements and indicators of growth including: i) the ratio of length and width of leaves, number of leaves, and combination of these variables (NeSmith, 1991; Igathinathane *et al*., 2006; Fallovo *et al*., 2008; Spann & Heerema, 2010; Celik *et al*., 2011; Cabezas-Gutiérrez & Peña-Baracaldo, 2012; Suárez Salazar *et al*., 2018; León-Burgos *et al*., 2022), and ii) models or relationships with other variables such as leaf dry weight (Akram-Ghaderi & Soltani, 2007; Huang *et al*., 2019) among other variables. One of the limitations in using mathematical models is their specificity at the level of variety, cultivar, phenological stages (Pire & Venezuela, 1995) and stratum in the canopy (Brito *et al*., 2007). This generally requires direct methodologies for the model validation (Yan *et al*., 2019), ignoring, in some cases, the use of other growth variables related to LA that could increase the precision of the LA estimation.

The Andean blueberry has small, simple, alternate, coriaceous, lanceolate or oblong-lanceolate leaves, with a serrated margin, cuneate leaf base and acute apex (Ehlenfeldt *et al*., 2022). In blueberries, structural traits of leaves and stems can correlate with yield parameters (Barai *et al*., 2022), while, for the Andean blueberry, no studies have been carried out in this regard. Additionally, leaves can be one of the by-products of the Andean blueberry cultivation (Zapata-Vahos *et al*., 2015) since they have a high content of polyphenols and other substances of nutraceutical and medicinal importance (Borda-Yepes *et al*., 2019). Direct measurement of LA in Andean blueberry plants is difficult

due to the high number of leaves and their small size (Ehlenfeldt *et al*., 2022), resulting in a slow and meticulous procedure. In other *Vaccinium* species (*V. corymbosum, V. virgatum*, and others), models have been developed for the measurement of leaf area. However, these species are deciduous, while the Andean blueberry is an evergreen perennial plant; therefore, it is important to develop specific models for the Andean blueberry that allow a better estimation of this variable given the difficulty of direct LA measurement and the scarcity of alternative methods for estimating its LA. The purpose of this research was to establish five models to estimate LA in young Andean blueberry plants. These models employed various growth variables and used experimental and statistical validation.

Materials and methods

Plant material and experiment establishment

The experiment was carried out between 2019 and 2021 under greenhouse conditions at the Faculty of Agricultural Sciences of the Universidad Nacional de Colombia, Bogotá, at an altitude of 2,550 m a.s.l., with average air temperature 18.6±10°C, average relative humidity 66±26% (ELMA DT-171 datalogger, Elma instruments, Rytternarken, Denmark). In total, 436 Andean blueberry plants propagated asexually were used in the vegetative stage of growth, with ages from 10 to 26 months (Tab. 1). The leaf area (LA) of 54,492 leaves was measured. The first group of plants was obtained by rooting of apical cuttings of wild plants from the municipalities of Guachetá, Cundinamarca (2800 m a.s.l., 5°26′71.8" N and 73°42′09.2" W) and San Miguel de Sema, Boyacá (2572 m a.s.l., 5°36′09.3" N and 73°45′23.8" W); rooted cuttings were planted in 2.0 L plastic pots with a substrate (3:1:0.3 v/v/v): sand + perlite + Klasmann® peat without nutrients. The second and third groups were plants propagated *in vitro* by proliferation of axillary buds in a commercial nursery in the municipality of Rionegro, Antioquia (24°C, 80% relative humidity, 2800 m a.s.l.); the plants were planted in 2.6 L plastic pots with sand + Klasmann® peat without nutrients (5:1 v/v). Phytosanitary management was carried out preventively, with monthly application of a garlic-chili based pest repellent (70 g L^{-1}) (Alisín® - Sáfer Agrobiológicos S.A.S), and a chlorothalonil-based protective fungicide (720 g L^{-1}), both at a dosage of 1 ml L^{-1}.

Nitrogen and phosphorous fertilizations were carried out with doses between 0 to 2.7 and 0 to 1.3 g/plant per 5 months, respectively. The range of fertilization with N and P varied because these plants were the object of another fertilization trial with these mineral nutrients. The rest of the fertilization plan was carried out in the same proportion for all plants (1.25 K_2O, 0.73 CaO, 1.08 MgO g/plant per 5 months and 18.15 Fe, 12.45 Mn, 6.21 $H_3B_2O_3$, 0.70 Zn, and 0.70 Cu mg/plant per 5 months). The total fertilizer dose was divided into 4 applications realized at 3, 8, 12, and 16 weeks after transplanting the plants into plastic pots. Fertilizer sources were: urea ($CO(NH_2)_2$), calcium nitrate ($Ca(NO_3)_2$), di-ammonium phosphate ($(NH_4)_2HPO_4$), triple super phosphate ($Ca(H_2PO_4)_2xH_2O$, potassium sulfate (K_2SO_4), calcium sulfate ($CaSO_4$), magnesium sulfate heptahydrate ($MgSO_4x7H_2O$), iron sulfate ($FeSO_4$), boric acid (H_3BO_3), zinc sulfate ($ZnSO_4$), copper sulfate ($CuSO_4$), and manganese sulfate ($MnSO_4$). Fertilization doses were established in accordance with the research by González *et al*. (2018) and studies conducted on plants of the genus *Vaccinium* (Percival & Privé, 2002; Jeliazkova & Percival, 2003; Percival *et al*., 2003; Nestby *et al*., 2014; Maqbool *et al*., 2017) and a pre-assay of this research.

TABLE 1. Characteristics of the Andean blueberry plants used in the experiment.

Propagation type	Group	Age (months)	Number of plants
Cuttings	1	10	50
In vitro	2	14	70
		16	68
		18	68
	3	22	72
		24	63
		26	45

Evaluated variables

A descriptive analysis of the average leaf area (ALA) calculated from the total LA of each plant divided by the number of leaves was carried out to compare the groups of plants. Regressions were made from non-destructive variables such as height (H), measured from the base of the stem to the last apical vegetative shoot, number of vegetative shoots (NS), which, in the case of *V. meridionale*, are reddish in color due to the presence of anthocyanin pigments, and number of leaves (NL) of each plant (Medina-Cano *et al*., 2015; González *et al*., 2018). Similarly, regressions were performed for destructive variables such as dry weight per organ (DW) and LA, the latter as an explanatory variable.

To determine the total DW per plant, the plants were separated into roots, stems, and leaves and dried in a muffle

oven at 75°C until constant weight. Subsequently, the following were determined: the root dry weight (RDW), leaf dry weight (LDW), stem dry weight (SDW) of plants propagated by cuttings, dry weight of the branches originating from stems in plants propagated *in vitro* (BSDW) and the total plant dry weight (TPDW) by adding the weight of all organs (Becerra *et al*., 2022). The leaf area (LA) of each plant was determined from digital image processing using the software ImageJ® v. 1.52 (Schneider *et al*., 2012). The photographs were taken with a mobile phone 25 MP camera at a height of 60 cm.

Statistical analysis

Statistical analysis was performed using the statistical software R (version 3.5.1.) and the respective libraries according to the statistical procedures described below. An exploratory analysis was carried out from the average LA of a single leaf to compare the groups of plants according to age. A descriptive analysis was performed from scatter diagrams to identify patterns in the relationships of variables. Pearson correlations were used to identify and quantify the linear relationship between variables with respect to LA. The plots were made using the "ggplot2" library (Wickham, 2016) and the correlation matrix was obtained with the "GGally" library extension (Schloerke *et al*., 2021).

From the variables with the highest correlation, various simple or multiple linear regression models were explored. In order to establish or propose a model that involves only non-destructive variables, models were tested with the predictor variables NL, H and NS, and LA as a response. Compliance with the regression assumptions was evaluated for all models. As morphometric variables and performance indicators are usually highly correlated, multicollinearity was evaluated from the variance inflation factor (VIF) with the "DescTools" library (Signorell, 2018). Similarly, linearity was studied using Pearson's correlation and residual normality using the Kolmogorov-Smirnov normality test, both from the "stats" library (R Core Team, 2022). Heteroscedasticity was evaluated using the "Non-constant Variance Score Test" from the "car" library (Fox & Weisberg, 2019) and the presence of influential data was evaluated using the Cook distance criterion. In cases where some of the regression assumptions were not met, the weighted least squares technique was used (PennState, 2021). Finally, the models that met the assumptions were compared based on their predictions using the root mean square error (Root Mean Square Error, RMSE).

Results and discussion

Determination of the average leaf area (ALA) has been used to estimate the total leaf area in commercial blueberry plants and wild blueberries (Fallovo *et al*., 2008; Celik *et al*., 2011; Lancheros, 2012; Becerra *et al*., 2022) and perennial crops such as cherry (*Prunus avium*) and coffee (*Coffea arabica*) (Cittadini & Peri, 2006; Taugourdeau *et al*., 2014). For the consolidated database of the Andean blueberry, ALA varied between 0.03 cm^2 (first quartile) and 1.85 cm^2 (fourth quartile), with a median of 0.94 cm^2 and a mean of 0.93 cm^2 (Fig. 1). However, the mean ALA presented differences between the study groups, being 0.44 cm^2 for group 1 in which all plants were propagated by cuttings, 0.92 cm^2 for group 2 and 1.07 cm^2 for group 3; plants in these last two groups were propagated *in vitro*.

Between the groups, differences were observed in the ALA related to the type of propagation (Fig. 1). The plants propagated by cuttings presented lower ALA (group 1: 0.45 ± 0.27 cm^2) compared to plants propagated *in vitro* (group 2: 0.92 ± 0.26 cm^2, group 3: 1.03 ± 0.22 cm^2). The ALA for the group of plants propagated by cuttings coincides with the range of 0.1 to 0.3 cm^2 described by Lancheros (2012) for plants propagated by seeds.

Variations in ALA were reported in wild and domesticated blueberries depending on the method of propagation, with tall and medium-tall blueberry plants obtained *in vitro* growing faster and having a greater number of stems, more lateral branches, and a greater number of shoots as well as higher canopy area and plant dry weight compared to plants obtained by stem cuttings (Marino *et al*., 2014). Blueberry (*V. corymbosum* L.) plants micropropagated *in vitro* produced more and longer shoots than plants obtained from semi-woody cuttings (Litwinczuk *et al*., 2005). This coincides with the present research, which observed shorter primary branches and shorter internodes in plants propagated by cuttings as compared to longer primary branches of *in vitro* propagated plants. Additionally, *in vitro* propagated plants of Andean blueberry had a planophyllous, almost runner-type branch formation, which promotes higher leaf production (Fig. 2). The higher number of shoots per plant in the *in vitro* propagated plants could also be due to the differences in plant age or size between the two propagation methods during this study.

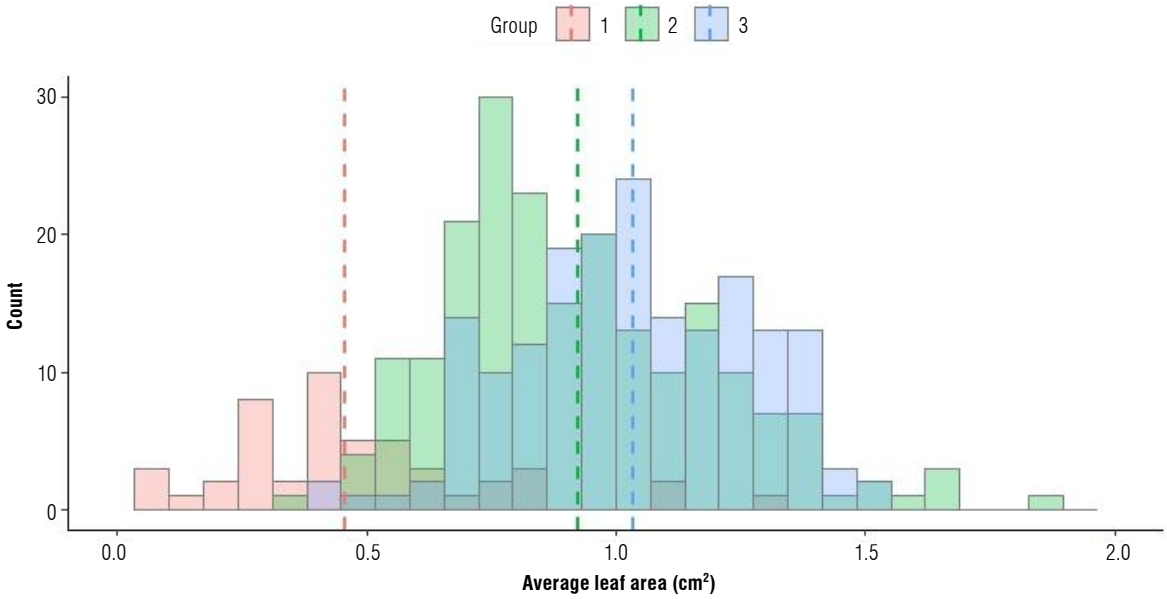

FIGURE 1. Histogram of the average leaf area for each of the Andean blueberry (*Vaccinium meridionale* Swartz) plant groups. Group 1: Young plants 10 months old (red) propagated by cuttings. Group 2: young plants 14 to 18 months old (blue) and group 3: young plants 22 to 26 months old (green) propagated in vitro. Dotted lines represent mean of each group. n=436.

The ALA differed according to age; plants 10 (0.45 ± 0.27 cm^2) and 14 (0.75 ± 0.18 cm^2) month-old had lower ALA values, while plants 16 (0.99 ± 0.24 cm^2), 18 (1.03 ± 0.27 cm^2), 22 (0.99 ± 0.23 cm^2), 24 (1.01 ± 0.22 cm^2), and 26 (1.13 ± 0.20 cm^2) month-old had a similar average ALA value (Fig. 3).

Most of the variables evaluated presented linear relationships with LA, except for plant height (H), number of vegetative shoots (NS), and root dry weight (RDW) (Fig. 4). Although in different plant species a linear relationship between LA and H has been reported (Calvo-Alvarado *et al*., 2008; Fanourakis *et al*., 2014), in Andean blueberry this relationship was not observed, apparently, due to the relatively low rate of growth of this species.

For the consolidated data, LA presented the highest Pearson correlation values with leaf dry weight (LDW) (0.95), total plant dry weight (TPDW) (0.95) and number of leaves (NL) (0.92) variables. The NL relationship with LA differed by groups, being similar between the groups of *in vitro* propagated plants (group 2: 0.88, group 3: 0.92) and higher than the young plants propagated by cuttings (group 1: 0.60), which suggests that the relationship between LA and NL differs according to the type of propagation (Fig. 2). Considering that the variables LDW, TPDW and NL presented the highest correlation values according to the methodology proposed by Mukaka (2012) and that the correlation between the groups was similar, models for leaf area prediction were proposed based on LDW, TPDW and NL, while the other variables were discarded.

The linear and multiple models initially proposed failed to meet some of the assumptions, but two of the multiple and three of the linear models (Tab. 2) from their weighting with the errors, using the weighted least squares technique, did meet the assumption. This technique is useful for observations that present non-constant variances in the errors (PennState, 2021) and was employed by Panigrahi and Sankar Das (2020), where they used this method to improve the remote estimation of the leaf area index and canopy water content in rice plants under water stress.

The multiple models (1 and 2) described in Table 3 had higher determination coefficients and a lower error, which shows their high capacity to estimate LA; however, their use implies the measurement of two variables, which depending on the case were LDW and NL or TPDW and NL. Considering the parsimony criterion, the use of linear models can be an interesting alternative, since this requires a single variable. Although models 3 and 4 use a destructive variable, it is experimentally easier and more accessible to weigh the plant organ than to make a direct measurement of LA. The Andean blueberry has numerous small-sized leaves (Ehlenfeldt *et al*., 2022), which makes it difficult to directly measure the LA or to perform other types of non-destructive measurements such as leaf length or width (Lancheros, 2012).

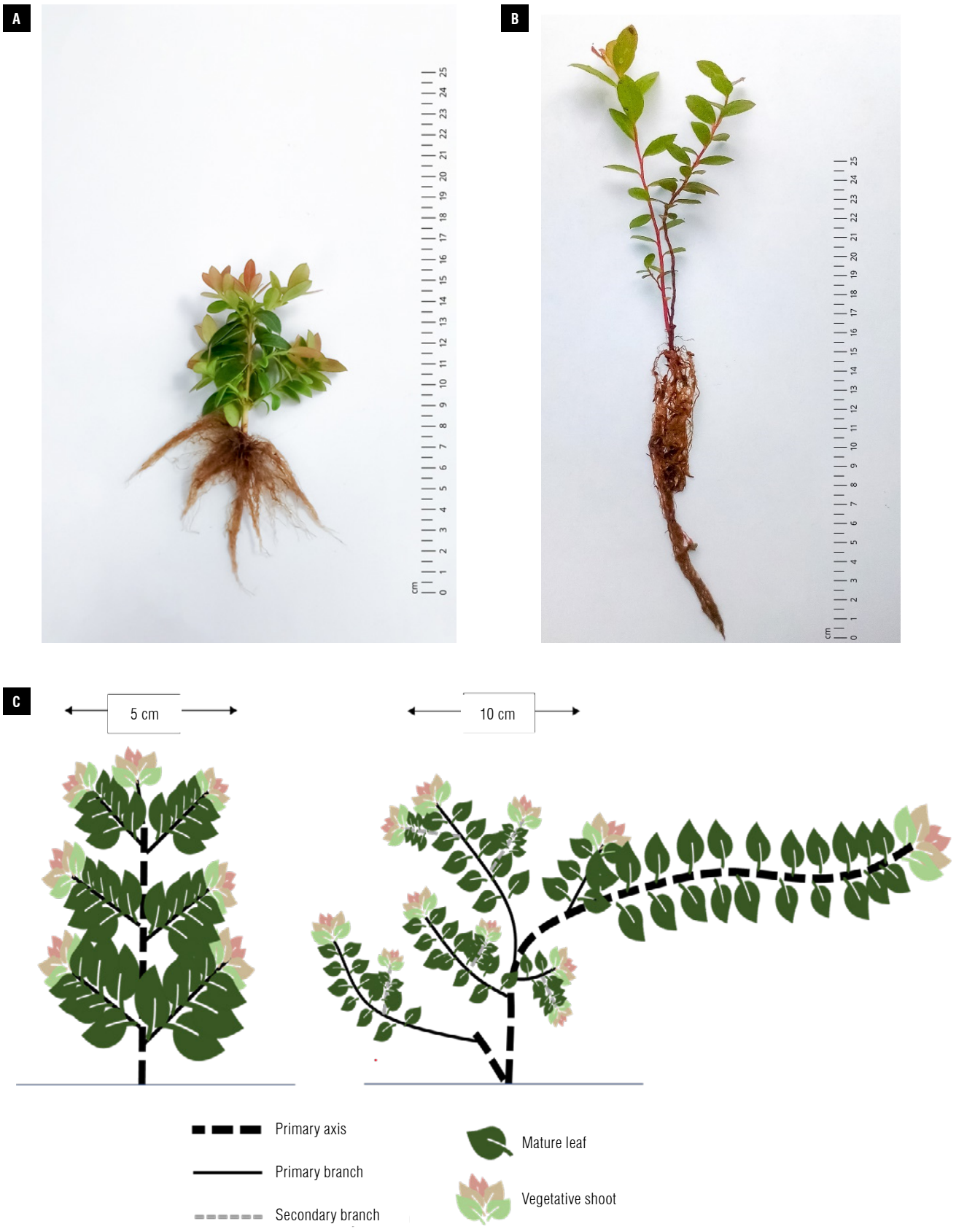

FIGURE 2. Photographs (A and B) and schematic representation (C) of the architecture of young Andean blueberry (*Vaccinium meridionale* Swartz) propagated from cuttings (A) and *in vitro* (B). The boxes in Fig. 2C indicate the scale in cm.

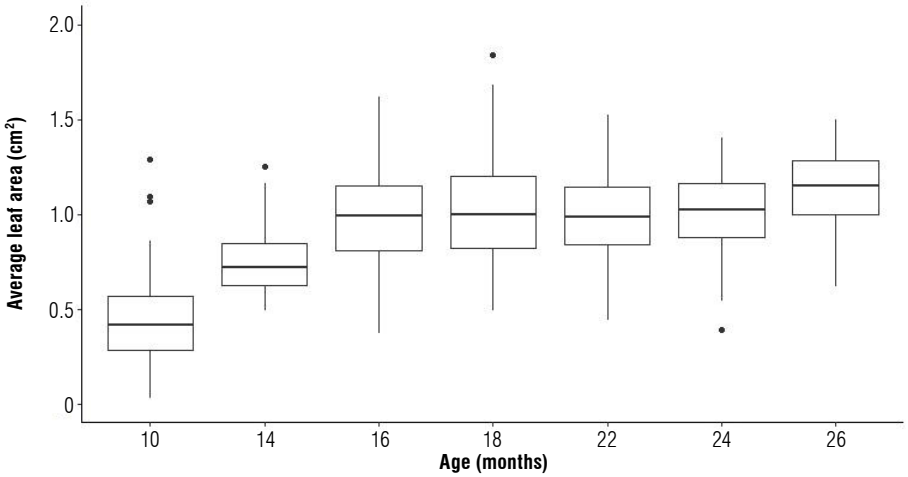

FIGURE 3. Box-and-whisker plot for average leaf area (ALA) in young Andean blueberry (*Vaccinium meridionale* Swartz) plants according to their age. Plants 10 months old propagated from cuttings and plants 14 to 26 months old propagated *in vitro*. n=436.

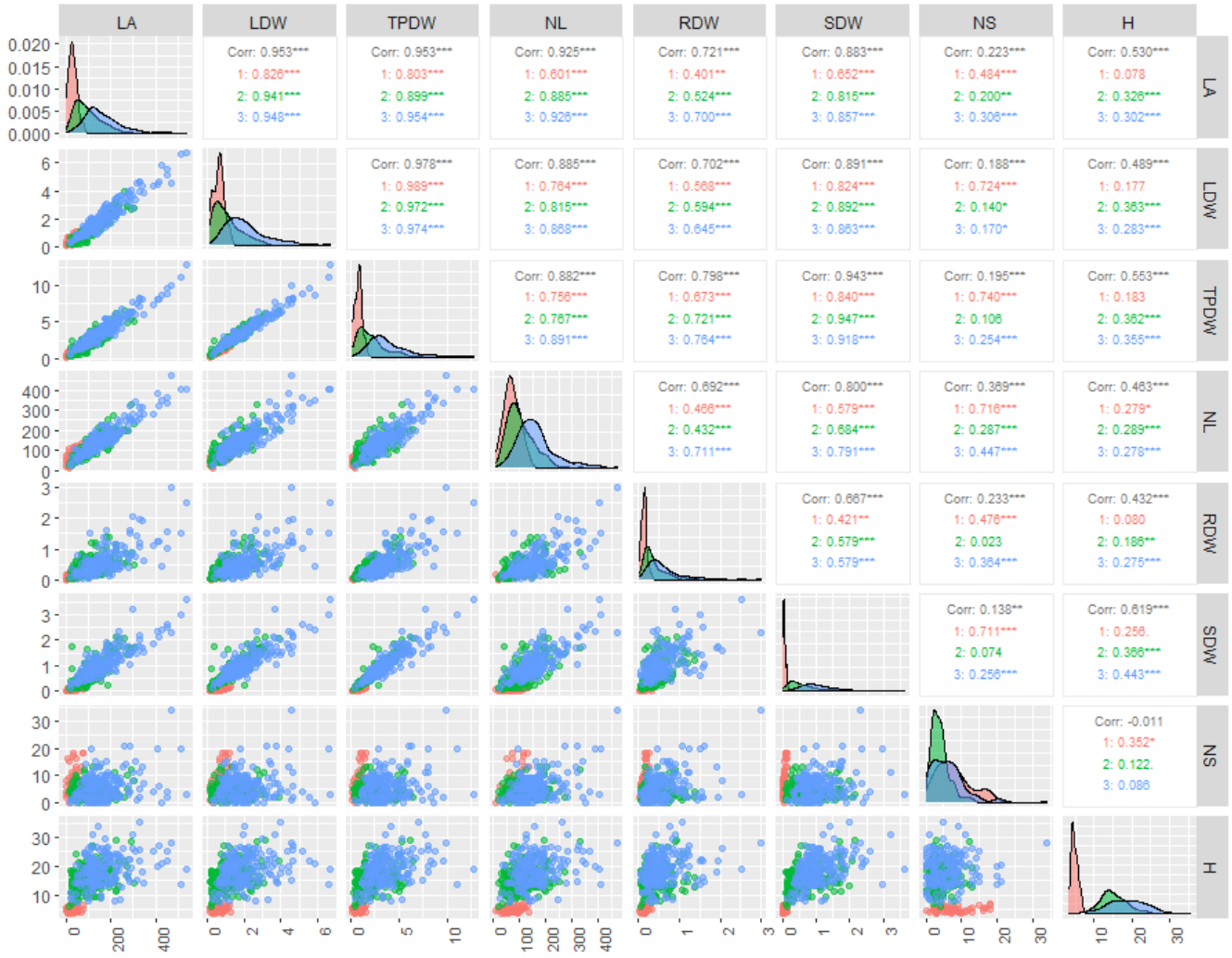

FIGURE 4. Dispersion, distribution, and Pearson correlation by pairs for the variables leaf area (LA), leaf dry weight (LDW), total plant dry weight (TPDW), number of leaves (NL), root dry weight (RDW), stem dry weight (SDW), number of shoots (NS), and height (H) of young plants of Andean blueberry (*Vaccinium meridionale* Swartz). Group 1: young plants 10 months old (red) propagated by cuttings. Group 2: young plants 14 to 18 months old (blue) and group 3: young plants 22 to 26 months old (green) propagated *in vitro* and the consolidation of these groups (black). n=436.

TABLE 2. Regression models with the best fit for estimating leaf area in young plants of the Andean blueberry.

N°	Model	R^2	R^2 adjusted	RMSE
1	LA = (28.392 × TPDW) + (0.465 × NL) -12.752	0.9182	0.9178	21.740
2	LA = (51.119 × LDW) + (0.457 × NL) -10.766	0.8104	0.8100	21.753
3	LA = (77.870 × LDW) + 7.191	0.8735	0.8732	26.579
4	LA = (43.474 × TPDW) + 5.229	0.8733	0.8730	26.791
5	LA = (1.117 × NL) - 18.730	0.8104	0.8100	33.702

LA: Leaf area per plant, cm^2; LDW: Leaf dry weight of an individual plant, mg; TPDW: Total plant dry weight, mg; NL: Number of leaves per plant. R^2: Coefficient of determination; R^2 adj: Coefficient of determination adjusted for multiple variables; RMSE: Root Mean Square Error.

The leaf dry weight (LDW) is considered the most appropriate criterion to estimate plant photosynthetic assimilation, as it is closely related to the LA (Taiz *et al*., 2018). This is in agreement with Akram-Ghanderi and Soltani (2007) who showed that, for cotton, the power equation best described the relationship between LA and LDW. Finally, model 5 is an LA estimation alternative that uses a non-destructive variable, such as the number of leaves (NL). Similar studies in perennial crops, such as grapevines (Lopes & Pinto, 2005) and coffee (Montoya *et al*., 2017), show that models based on the NL result in an easy-to-measure and economical alternative to estimate LA. This has also been reported in semi-annual crops such as corn by Dwyer and Stewart (1986) and Elings (2000); the latter author highlighting that this relationship is true if the average LA of a single leaf is known and the plant has leaves of similar size, as is the case of the Andean blueberry (Ehlenfeldt *et al*., 2022).

Conclusions

The differences found in plant architecture and the average leaf area in young Andean blueberry plants depending on the propagation method (by cuttings or *in vitro*) must be considered for the planning of agronomic practices, such as pruning, studying the canopy architecture (plant density) and frequency of agronomic labors. This research proposes five models for an adequate estimation of leaf area that used destructive and non-destructive variables, and their combination. The adjustment of the models using weighted least squares fulfilled the assumptions for some of the proposed models. The use of the models developed in this research, especially the one that uses number of leaves (a non-destructive variable), could facilitate future studies for the determination of leaf area in this species.

Acknowledgments

The authors express their gratitude to the Faculty of Agricultural Sciences, Universidad Nacional de Colombia (Bogotá), especially to the Center for Research and Rural Extension (Centro de Investigación y Extension Rural - CIER), for the partial financing of the research within the framework of the project "Support for registered research groups that contribute to strengthening research in the Faculty of Agricultural Sciences of the Bogota campus" (QUIPU No. 207010012262) through the Horticulture research group of Minciencias. We are also grateful to the producers of the Andean blueberry from the municipalities of Guachetá (Cundinamarca) and San Miguel de Sema (Boyacá), who permitted the collection of plant cuttings from their properties and to C.I. Agroberries nursery located in Rionegro (Antioquia), who supplied *in vitro* propagated plants.

Author's contributions

MVM: conceptualization, research, writing - original draft, visualization, writing, and editing. PLP: conceptualization, visualization, statistical analysis, writing, and editing. ED: conceptualization, statistical analysis, writing, and editing. LPMF: supervision, writing, and editing. SM: supervision, project administration, writing, and editing. All authors have read and approved the final version of the manuscript.

Conflict of interest statement

The authors declare that there is no conflict of interests regarding the publication of this article.

Literature cited

Adobe Systems Incorporated. (1990). *Adobe Photoshop*. Microsoft Windows.

Autodesk. (1982). *AutoCAD*. Microsoft Windows.

Akram-Ghaderi, F., & Soltani, A. (2007). Leaf area relationships to plant vegetative characteristics in cotton (*Gossypium hirsutum* L.) grown in a temperate sub-humid environment. *International Journal of Plant Production*, *1*(1), 63–71.

Barai, K., Calderwood, L., Wallhead, M., Vanhanen, H., Hall, B., Drummond, F., & Zhang, Y. J. (2022). High variation in yield among wild blueberry genotypes: Can yield be predicted by leaf and stem functional traits? *Agronomy*, *12*(3), Article 617. https://doi.org/10.3390/agronomy12030617

Becerra, A. D., Quevedo-Rubiano, S., Magnitskiy, S., & Lancheros, H. O. (2022). Morphological responses of Andean blueberry (*Vaccinium meridionale* Swartz) plants growing in three environments at different altitudes. *Revista Colombiana de Ciencias Hortícolas*, *16*(3), Article e15034.

Benedetto, D., & Togmetti, J. (2016). Técnicas de análisis de crecimiento de plantas: su aplicación a cultivos intensivos. *Revista de Investigaciones Agropecuarias*, *42*(3), 258–282.

Bernal, L. J., Melo, L. A., & Díaz Moreno, C. (2014). Evaluation of the antioxidant properties and aromatic profile during maturation of the blackberry (*Rubus glaucus* Benth) and the bilberry (*Vaccinium meridionale* Swartz). *Revista Facultad Nacional de Agronomía Medellín*, *67*(1), 7209–7218. https://doi.org/10.15446/rfnam.v67n1.42649

Borda-Yepes, V. H., Chejne, F., Daza-Olivella, L., Alzate-Arbelaez, A. F., Rojano, B. A., & Raghavan, V. G. S. (2018). Effect of microwave and infrared drying over polyphenol content in *Vaccinium meridionale* (Swartz) dry leaves. *Journal of Food Process Engineering*, *42*(1), Article e12939. https://doi.org/10.1111/jfpe.12939

Brito, E., Romero, E. R., Casen, S. D., Alonso, L. G., & Digonzelli, P. A. (2007). Métodos no destructivos de estimación del área foliar por tallo en la variedad LCP 85-384 de caña de azúcar. *Revista Industrial y Agrícola de Tucumán*, *84*(2), 29–32.

Bryla, D. R., & Machado, R. M. A. (2011). Comparative effects of nitrogen fertigation and granular fertilizer application on growth and availability of soil nitrogen during establishment of highbush blueberry. *Frontiers in Plant Science*, *2*, Article 46. https://doi.org/10.3389/fpls.2011.00046

Bryla, D. R., & Strik, B. C. (2015). Nutrient requirements, leaf tissue standards, and new options for fertigation of northern highbush blueberry. *HortTechnology*, *25*(4), 464–470. https://doi.org/10.21273/horttech.25.4.464

Cabezas-Gutiérrez, M., & Peña-Baracaldo, F. (2012). Estimación del área foliar del arándano (*Vaccinium corymbosum*) por medio de un método no destructivo. *Revista U.D.C.A Actualidad & Divulgación Científica*, *15*(2), 373–379. https://doi.org/10.31910/rudca.v15.n2.2012.837

Cabezas-Gutiérrez, M., Peña, F., Duarte, H. W., Colorado, J. F., & Lora Silva, R. (2009). Un modelo para la estimación del área foliar en tres especies forestales de forma no destructiva. *Revista U.D.C.A Actualidad & Divulgación Científica*, *12*(1), 121–130. https://doi.org/10.31910/rudca.v12.n1.2009.648

Calvo-Alvarado, J. C., McDowell, N. G., & Waring, R. H. (2008). Allometric relationships predicting foliar biomass and leaf area:sapwood area ratio from tree height in five Costa Rican rain forest species. *Tree Physiology*, *28*(11), 1601–1608. https://doi.org/10.1093/treephys/28.11.1601

Celik, H., Serhat-Odabas, M., & Odabas, F. (2011). Leaf area prediction models for highbush blueberries (*Vaccinium corymbosum* L.) from linear measurement. *Journal of Microbiology, Biotechnology and Food Sciences*, *33*(1), 16–21.

Cittadini, E. D., & Peri, P. L. (2006). Estimation of leaf area in sweet cherry using a non-destructive method. *Revista de Investigaciones Agropecuarias*, *35*(1), 143–150.

Cosmulescu, S., Scrieciu, F., & Manda, M. (2020). Determination of leaf characteristics in different medlar genotypes using the ImageJ program. *Horticultural Science*, *47*(2), 117–121. https://doi.org/10.17221/97/2019-HORTSCI

Easlon, H. M., & Bloom, A. J. (2014). Easy Leaf Area: Automated digital image analysis for rapid and accurate measurement of leaf area. *Applications in Plant Sciences*, *2*(7), Article 1400033. https://doi.org/10.3732/apps.1400033

Ehlenfeldt, M. K., Polashock, J. J., Rowland, L. J., Ogden, E., & Luteyn, J. L. (2022). Fertile intersectional hybrids of 4x Andean blueberry (*Vaccinium meridionale*) and 2x lingonberry (*V. vitis-idaea*). *HortScience*, *57*(4), 525–531. https://doi.org/10.21273/hortsci16285-21

Fallovo, C., Cristofori, V., De-Gyves, E. M., Rivera, C. M., Rea, R., Fanasca, S., Bignami, C., Sassine, Y., & Rouphael, Y. (2008). Leaf area estimation model for small fruits from linear measurements. *HortScience*, *43*(7), 2263–2267. https://doi.org/10.21273/hortsci.43.7.2263

Fanourakis, D., Briese, C., Max, J. F. J., Kleinen, S., Putz, A., Fiorani, F., Ulbrich, A., & Schurr, U. (2014). Rapid determination of leaf area and plant height by using light curtain arrays in four species with contrasting shoot architecture. *Plant Methods*, *10*(1), 1–11. https://doi.org/10.1186/1746-4811-10-9

Fox, J., & Weisberg, S. (2011). *An R companion to applied regression* (2nd ed.). Sage, Thousand Oaks CA. http://socserv.socsci.mcmaster.ca/jfox/Books/Companion

Garzón, G. A., Soto, C. Y., López-R, M., Riedl, K. M., Browmiller, C. R., & Howard, L. (2020). Phenolic profile, in vitro antimicrobial activity and antioxidant capacity of *Vaccinium meridionale* Swartz pomace. *Heliyon*, *6*(5), Article e03845. https://doi.org/10.1016/j.heliyon.2020.e03845

González, L. K., Rugeles, L. N., & Magnitskiy, S. (2018). Effect of different sources of nitrogen on the vegetative growth of Andean blueberry (*Vaccinium meridionale* Swartz). *Agronomía Colombiana*, *36*(1), 58–67. https://doi.org/10.15446/agron.colomb.v36n1.69304

Huang, W., Ratkowsky, D. A., Hui, C., Wang, P., Su, J., & Shi, P. (2019). Leaf fresh weight versus dry weight: Which is better for describing the scaling relationship between leaf biomass and leaf area for broad-leaved plants? *Forests*, *10*(3), Article 256. https://doi.org/10.3390/f10030256

Hunt, R. (2017). Growth analysis, Individual plants. In B. Thomas, B. G. Murray, & D. J. Murphy (Eds.). *Encyclopedia of applied plant sciences* (2nd ed., Vol. 1, pp. 421–429). Academic Press.

Igathinathane, C., Prakash, V. S. S., Padma, U., Babu, G. R., & Womac, A. R. (2006). Interactive computer software development for leaf area measurement. *Computers and Electronics in Agriculture*, *51*(1–2), 1–16. https://doi.org/10.1016/j.compag.2005.10.003

Jeliazkova, E. A., & Percival, D. C. (2003). N and P fertilizers, some growth variables, and mycorrhizae in wild blueberry (*Vaccinium angustifolium*). *Acta Horticulturae*, *626*, 297–304. https://doi.org/10.17660/actahortic.2003.626.41

Kassambara, A. (2020). Factoextra: Extract and visualize the results of multivariate data analyses. R package versión 1.0.7. https://CRAN.R-project.org/package=factoextra

Kucharik, C. J., Norman, J. M., & Gower, S. T. (1998). Measurements of branch area and adjusting leaf area index indirect measurements. *Agricultural and Forest Meteorology*, *91*(1–2), 69–88. https://doi.org/10.1016/S0168-1923(98)00064-1

Lancheros, H. (2012). Caracterización de las micorrizas nativas en agraz *Vaccinium meridionale* Swartz y evaluación de su efecto sobre el crecimiento plantular [MSc Thesis, Universidad Nacional de Colombia]. https://repositorio.unal.edu.co/handle/unal/12135

León-Burgos, A. F., Ramírez, C., Rendón Sáenz, J. R., Imbachi-Quinchua, L. C., Unigarro-Muñoz, C. A., & Balaguera-López, H. E. (2022). Fitting growth curves of coffee plants in the nursery stage of growth: A functional approach. *Agronomia Colombiana*, *40*(3), 344–353. https://doi.org/10.15446/agron.colomb.v40n3.101333

Litwinczuk, W., Srzegorz, G., & Wrona, D. (2005). Field performance of highbush blueberries (*Vaccinium x corymbosum* L.) cv. "Herbert" propagated by cuttings and tissue culture. *Scientia Horticulturae*, *106*, 162–169. https://doi.org/10.1016/j.scienta.2005.02.025

Lopes, C., & Pinto, P. A. (2005). Easy and accurate estimation of grapevine leaf area with simple mathematical models. *Vitis - Journal of Grapevine Research*, *44*(2), 55–61.

Maldonado Celis, M. E., Franco Tobón, Y. N., Agudelo, C., Arango, S. S., & Rojano, B. (2017). Andean berry (*Vaccinium meridionale* Swartz). In E. M. Yahia (Ed.), *Fruit and vegetable phytochemicals: Chemistry and human health* (2nd ed., pp. 869–881). https://doi.org/10.1002/9781119158042.ch40

Marino, S. R., Williamson, J. G., & Olmstead, J. W. (2014). Vegetative growth of three southern highbush blueberry cultivars obtained from micropropagation and softwood cuttings in two Florida locations. *HortScience*, *49*(5), 556–561. https://doi.org/10.21273/hortsci.49.5.556

Maqbool, R., Percival, D., Zaman, Q., Astatkie, T., Adl, S., & Buszard, D. (2017). Leaf nutrients ranges and berry yield optimization in response to soil-applied nitrogen, phosphorus and potassium in wild blueberry (*Vaccinium angustifolium* Ait.). *European Journal of Horticultural Science*, *82*(4), 166–179. https://doi.org/10.17660/eJHS.2017/82.4.2

Medina Cano, C. I., Lobo Arias, M., Castaño Colorado, Á. A., & Cardona, L. E. (2015). Análisis del desarrollo de plantas de mortiño (*Vaccinium meridionale* Swartz.) bajo dos sistemas de propagación: clonal y sexual. *Ciencia & Tecnología Agropecuaria*, *16*(1), Article 390. https://doi.org/10.21930/rcta.vol16_num1_art:390

Medina Cano, C. I., Martínez Bustamante, E., & López Orozco, C. A. (2019). Phenological scale for the mortiño or agraz (*Vaccinium meridionale* Swartz) in the high Colombian Andean area. *Revista Facultad Nacional de Agronomia Medellin*, *72*(3), 8897–8908. https://doi.org/10.15446/rfnam.v72n3.74460

Milić, B., Tarlanović, J., Keserović, Z., Magazin, N., Miodragović, M., & Popara, G. (2018). Bioregulators can improve fruit size, yield and plant growth of northern highbush blueberry (*Vaccinium corymbosum* L.). *Scientia Horticulturae*, *235*, 214–220. https://doi.org/10.1016/j.scienta.2018.03.004

Montoya Restrepo, E. C., Hernández Arredondo, J. D., Unigarro Muñoz, C. A., & Flórez Ramos, C. P. (2017). Estimación del área foliar en café variedad Castillo® a libre exposición y su relación con la producción. *Cenicafé*, *68*(1), 55–61.

Mukaka, M. (2012). Statistics corner: A guide to appropriate correlation coefficient in medical research. *Malawi Medical Journal*, *24*(3), 69–71.

Muñoz, J. D., Martínez, L. J., & Ligarreto, G. A. (2009). Caracterización de los ambientes agroecológicos del agraz o mortiño (*Vaccinium meridionale* Swartz), en la zona altoadina de Colombia. In G. A. Ligarreto (Ed.), *Perspectivas del cultivo de agraz o mortiño (Vaccinium meridionale Swartz) en la zona altoandina de Colombia (*pp. 29–56). Universidad Nacional de Colombia. Facultad de Agronomía.

NeSmith, D. S. (1991). Nondestructive leaf area estimation of rabbiteye blueberries. *HortScience*, *26*(10), Article 1332. https://doi.org/10.21273/hortsci.26.10.1332

Nestby, R., Martinussen, I., Krogstad, T., & Uleberg, E. (2014). Effect of fertilization, tiller cutting and environment on plant growth and yield of European blueberry (*Vaccinium myrtillus* L.) in Norwegian forest fields. *Journal of Berry Research*, *4*(2), 79–95. https://doi.org/10.3233/JBR-140070

Panigrahi, N., & Sankar Das, B. (2020). Evaluation of regression algorithms for estimating leaf area index and canopy water content from water stressed rice canopy reflectance. *Information Processing in Agriculture*, *8*(2), 284–298. https://doi.org/10.1016/j.inpa.2020.06.002

PennState Eberly College of Science. (2021, January 20). *Lesson 13: Weighted Least Squares & Robust Regression*. https://online.stat.psu.edu/stat501/lesson/13

Percival, D. C., & Privé, J. P. (2002). Nitrogen formulation influences plant nutrition and yield components of lowbush blueberry (*Vaccinium angustifolium* Ait.). *Acta Horticulturae*, *574*, 347–353. https://doi.org/10.17660/actahortic.2002.574.52

Percival, D. C., Janes, D. E., Stevens, D. E., & Sanderson, K. (2003). Impact of multiple fertilizer applications on plant growth, development, and yield of wild lowbush blueberry (*Vaccinium angustifolium* Aiton). *Acta Horticulturae*, *626*, 423–429. https://doi.org/10.17660/actahortic.2003.626.57

Pire, R., & Valenzuela, I. (1995). Estimación del área foliar en *Vitis vinifera* L. "French Colombard" a partir de mediciones lineales en hojas. *Agronomía Tropical*, *45*(1), 143–154.

Sánchez-Aguilar, H., Aldrete, A., Vargas-Hernández, J., & Ordaz-Chaparro, V. (2016). Influencia del tipo y color de envase en el desarrollo de plantas de pino en vivero. *Agrociencia*, *50*(4), 481–492.

Schloerke, B., Cook, D., Larmarange, J., Briatte, F., Marbach, M., Thoen, E., Elberg, A., Toomet, O., Crowley, J., Hofmann, H., & Wickham, H. (2021, June 21). GGally: Extension to 'ggplot2'. Version 2.1.2. https://CRAN.R-project.org/package=GGally

Schneider, C. A., Rasband, W. S., & Eliceiri, K. W. (2012). NIH Image to ImageJ: 25 years of image analysis. *Nature Methods*, *9*(7), 671–675. https://doi.org/10.1038/nmeth.2089

Signorell, A. (2018). DescTools: Tools for descriptive statistics. R package version 0 .99. 24. https://cran.r-project.org/web/packages/DescTools/index.html

Singh, R. R., Meena, L. K., & Singh, P. (2017). High tech nursery management in horticultural crops: A way for enhancing income. *International Journal of Current Microbiology and Applied Sciences*, *6*(6), 3162–3172. https://doi.org/10.20546/ijcmas.2017.606.372

Shi, P., Ratkowsky, D. A., Li, Y., Zhang, L., Lin, S., & Gielis, J. (2018). A general leaf area geometric formula exists for plants - Evidence from the simplified Gielis equation. *Forests*, *9*(11), Article 714. https://doi.org/10.3390/f9110714

Spann, T. M., & Heerema, R. J. (2010). A simple method for non-destructive estimation of total shoot leaf area in tree fruit crops. *Scientia Horticulturae*, *125*(3), 528–533. https://doi.org/10.1016/j.scienta.2010.04.033

Suárez Salazar, J. C., Melgarejo, L. M., Duran Bautista, E. H., Di Rienzo, J. A., & Casanoves, F. (2018). Non-destructive estimation of the leaf weight and leaf area in cacao (*Theobroma cacao* L.). *Scientia Horticulturae*, *229*, 19–24. https://doi.org/10.1016/j.scienta.2017.10.034

Taiz, L., Zeiger, E., Moller, I. M., & Murphy, A. (2018). *Fundamentals of plant physiology*. Oxford University Press.

Taugourdeau, S., le Maire, G., Avelino, J., Jones, J. R., Ramirez, L. G., Jara Quesada, M., Charbonnier, F., Gómez-Delgado, F., Harmand, J. M., Rapidel, B., Vaast, P., & Roupsard, O. (2014). Leaf area index as an indicator of ecosystem services and management practices: An application for coffee agroforestry. *Agriculture, Ecosystems and Environment*, *192*, 19–37. https://doi.org/10.1016/j.agee.2014.03.042

Torres, W. S., Montoya, I. A., & Ligarreto, G. A. (2009). Aspectos sociales y económicos de la producción de agraz o mortiño (*Vaccinium meridionale* Swartz). In G. A. Ligarreto, *Perspectivas del cultivo de agraz o mortiño (Vaccinium meridionale Swartz) en la zona altoandina de Colombia* (pp. 113–134).

Torres, W. S., Rubio, E. W., & G. A. Ligarreto. (2012). Agraz o mortiño (*Vaccinium meridionale* Swartz). In G. Fischer (Ed.), *Manual para el cultivo de frutales en el trópico* (pp. 905–914). Produmedios.

Wakui, A., & Kudo, G. (2021). Ecotypic differentiation of a circumpolar Arctic-alpine species at mid-latitudes: Variations in the ploidy level and reproductive system of *Vaccinium vitis-idaea*. *AoB PLANTS*, *13*(3), Article plab015. https://doi.org/10.1093/aobpla/plab015

Weraduwage, S. M., Chen, J., Anozie, F. C., Morales, A., Weise, S. E., & Sharkey, T. D. (2015). The relationship between leaf area growth and biomass accumulation in *Arabidopsis thaliana*. *Frontiers in Plant Science*, *6*, Article 167. https://doi.org/10.3389/fpls.2015.00167

Wickham, H. (2016). ggplot2: Elegant graphics for data analysis. Springer-Verlag New York. https://ggplot2.tidyverse.org

Yan, G., Hu, R., Luo, J., Weiss, M., Jiang, H., Mu, X., Xie, D., & Zhang, W. (2019). Review of indirect optical measurements of leaf area index: Recent advances, challenges, and perspectives. *Agricultural and Forest Meteorology*, *265*, 390–411. https://doi.org/10.1016/j.agrformet.2018.11.033

Zapata-Vahos, I. C., Villacorta, V., Maldonado, M. E., Castro-Restrepo, D., & Rojano, B. (2015). Antioxidant and cytotoxic activity of black and green tea from *Vaccinium meridionale* Swartz leaves. *Journal of Medicinal Plants Research*, *9*(13), 445–453. https://doi.org/10.5897/JMPR2014.5744

Spectral behavior of banana with *Foc* R1 infection: Analysis of Williams and Gros Michel clones

Comportamiento espectral de banano con infección de *Foc* R1: análisis de clones Williams y Gros Michel

Estefanía Macias-Echeverri[1*], Lilliana María Hoyos-Carvajal[1], Verónica Botero-Fernández[2], Sebastián Zapata-Henao[3], and Juan Carlos Marín-Ortiz[4]

ABSTRACT

Fusarium wilt is the greatest threat to Musaceae production worldwide; remote sensing techniques based on reflectance spectroscopy are proposed for its detection. The spectral response of leaves of healthy plants and plants infected with *Fusarium oxysporum* f. sp. *cubense* Race 1 (*Foc* R1) from two banana cultivars during the incubation period of the disease were characterized. Spectra of 400-1000 nm were measured in healthy and *Foc* R1-infected plants on Gros Michel (GM: susceptible) and Williams (W: resistant) bananas with an Ocean Optics HR2000+ portable spectrometer. Similar general patterns were obtained in the spectra for both cultivars for the Vis, around 25% in the green region, but, as the foliar development progressed, reflectance decreased throughout the entire spectral range, close to 12.5% (green region of Vis range) on leaf 4 of both. Four wavelengths were discriminant for the healthy plants in the cultivars. Additionally, reflectance increased in the infected plants in the incubation period throughout the range, decreasing rapidly once the first visible symptoms appeared. The results suggested that an increase in reflectance at discriminating wavelengths can be used to diagnose diseased plants in the asymptomatic period, and a rapid decrease in this suggests the onset of the symptomatic phase.

Key words: early detection, spectrum, vascular disease, fungus, *Fusarium* wilt.

RESUMEN

La marchitez por *Fusarium* es la mayor amenaza para la producción mundial de musáceas; para su detección se proponen técnicas de detección remota basadas en espectroscopía de reflectancia. Se caracterizó la respuesta espectral de hojas de plantas sanas e infectadas con *Fusarium oxysporum* f. sp. *cubense* Raza 1 (*Foc* R1) en dos cultivares de banano, durante el periodo de incubación de la enfermedad. Se midieron los espectros de 400-1000 nm en plantas sanas e infectadas con *Foc* R1 de banano Gros Michel (GM: susceptible) y Williams (W: resistente) con un espectrómetro portátil Ocean Optics HR2000+. Se obtuvieron patrones generales en los espectros similares para ambos cultivares en el Vis, alrededor del 25% en la región del verde, pero al avanzar el desarrollo foliar disminuyó la reflectancia en todo el rango espectral, cerca al 12.5% (región verde del rango Vis) en la hoja cuatro de ambos. Cuatro longitudes de onda fueron discriminantes para plantas sanas en los cultivares. Adicionalmente, la reflectancia aumentó en las plantas infectadas en el periodo de incubación en todo el rango, disminuyendo rápidamente una vez se presentaron los primeros síntomas visibles. Los resultados sugirieron que un aumento de la reflectancia en longitudes de onda discriminantes puede usarse para diagnosticar plantas enfermas en el periodo asintomático y una rápida disminución sugiere el inicio de la fase sintomática.

Palabras clave: detección temprana, espectro, enfermedad vascular, hongo, marchitez por *Fusarium*.

Introduction

Plants are the main source of food for humans and animals worldwide (Ratnadass *et al*., 2012; Barbedo, 2013). However, during cultivation, they are affected by different types of diseases that reduce production and quality and, therefore, decrease their economic value (Dordas, 2008; Martinelli *et al*., 2015). Plant infections in the agricultural and food sectors have been reported to account for more than 30% of total production losses in most developing countries (Rizzo *et al*., 2021). Losses can be reduced or eradicated through early detection, monitoring and management of

Received for publication: July 29, 2022. Accepted for publication: November 25, 2022 Doi: 10.15446/agron.colomb.v40n3.103969

[1] Facultad de Ciencias Agrarias, Universidad Nacional de Colombia, Medellín (Colombia).
[2] Facultad de Minas, Universidad Nacional de Colombia, Medellín (Colombia).
[3] Centro Nacional de Investigaciones en Banano-CENIBANANO, Carepa (Colombia).
[4] Grupo de Investigación Fitotecnia Tropical, Universidad Nacional de Colombia, Medellín (Colombia).
* Corresponding author: emaciase@unal.edu.co

diseases (Zhang *et al*., 2019). To date, studies have reported that there are more than 50,000 plant diseases worldwide, parasitic and non-parasitic (Pimentel, 2011).

Plantains and bananas are fundamental in the diet of African and Latin American countries. In the world, only 15% of the total production is exported to non-producing regions and the remaining product is traded in national markets for local consumption (Varma & Bebber, 2019). For 2019, world banana exports, excluding cooking bananas, reached a maximum of 20.2 million t, with this product being fourth in consumption worldwide after wheat, rice, and corn (FAO, 2020).

The disease known as banana Fusarium wilt, or fusariosis, is a disease caused by *Fusarium oxysporum* f. sp. *cubense* race 1 (*Foc* R1), which has more recently been intensified by *Foc* tropical race 4 (*Foc* TR4) in Cavendish banana (Wang *et al*., 2020), recently classified as *Fusarium odoratissimum* by Maryani *et al*. (2018), who currently consider this the greatest threat to global production of Musaceae in general. It is a disease in which the pathogen invades, colonizes, and blocks the xylem vessels of the roots and interrupts the translocation of water and nutrients, causing severe wilting (Li *et al*., 2014). Its typical symptoms include yellowing and wilting of the leaves, vascular discoloration within the rhizome and pseudostem, and death of the infected plant (Ploetz, 2006). There is no known effective chemical control to treat this fungus, and, since it is a vascular pathogen, its detection and diagnosis are complex.

In recent decades, the development and application of various non-invasive techniques for plant disease detection that is sensitive, consistent, fast, and cost-effective have increased (Zhang *et al*., 2019). The most popular are: fluorescence spectroscopy, visible/near-infrared spectroscopy (VIS/NIR), fluorescence imaging, and hyperspectral imaging (Sankaran *et al*., 2010). Several studies have already been carried out regarding spectroscopy, especially with the use of VIS radiation in the detection of diseases in symptomatic plants (Mahlein *et al*., 2013, Abu-Khalaf & Salman, 2014; Szuvandzsiev *et al*., 2014, Thomas *et al*., 2018). Some of this research has focused on early detection of plant diseases (Marín *et al*., 2018) and detection of diseases that can "mask" symptoms (Abdulridha *et al*., 2019).

Knowing the location, extent, and severity of the appearance of diseases and pests is essential to guide phytosanitary procedures. Conventional monitoring and diagnosis of diseases and pests in the field are laborious, subjective, and generally inefficient, while remote sensing techniques can monitor plant diseases and pests on a large scale and early (Mahlein, 2016).

Vascular-type diseases, such as *Fusarium* wilt, are difficult to detect early. Other types of diseases, such as localized or superficial ones, can be detected with the observation of symptoms; however, for vascular-type diseases, visible symptoms indicate that the fungus or pathogenic organism has already invaded the vascular tissue (García-Bastidas *et al*., 2020). By observing interactions between the pathogen and hosts, a variety of symptoms and damage to plants can be identified, providing a basis for monitoring with remote sensing (Zhang *et al*., 2019). However, early detection requires the ability to identify those characteristics that make each infection unique, even in the absence of external symptoms. The behavior of healthy plants must be compared with that of diseased plants for successful diagnoses (Zhang *et al*., 2012).

An early detection system based on spectroscopy techniques can reduce losses in crops with more speed, sensitivity, and selectivity by avoiding propagation of diseases, avoiding the sowing of plants carrying the pathogen, and avoiding the need to destroy samples for analysis (Chaerle & Van der Straeten, 2000). The main objective of this research was to characterize the spectral response of healthy plants and plants infected with *Foc* R1 from two banana groups (one susceptible and one resistant) using reflectance spectroscopy during the incubation period of the infection.

Materials and methods

Plant material and location

Gros Michel (GM) and Williams (W) banana plants of *in vitro* origin were purchased from a commercial nursery. The study was carried out at the Universidad Nacional de Colombia, Medellin campus. Twenty ml of a general hydroponic solution formula were used every 8 d, containing (milli-equivalents): NO_3^- (12.0), PO_4^{3-} (1.0), K (1.7), Mg (1.5), Ca (2.8) and SO_4^{2-} (0.5), and micro-equivalents of Fe (70.0), Mn (18.0), Zn (7.7), Cu (1.5), B (27.5), and Mo (0.5). The plants were planted in 2 kg nursery bags, with a 1:1 mixture (v/v) of peat (Mikskaar MKS1) and coconut fiber (commercial products) as substrate. The internal environmental conditions in the greenhouse during the experiment were: average temperature of 32°C and 80% relative air humidity.

Microorganisms

The Varonesa strain of *Foc* R1 was used, provided by the Centro de Investigaciones del Banano (CENIBANANO)

and isolated from symptomatic pseudostems of Manzano banana (AAB) plants collected from the "Varonesa" commercial farm (7°63'23" N, 76°36'20" W) in Urabá, Colombia.

Plant inoculation

The *Foc* R1 Varonesa strain was multiplied in a Potato Dextrose Agar (PDA) culture medium. After 7 d of growth, its surface was washed with sterile, distilled water to obtain a suspension with a concentration of $1x10^6$ conidia/ml. For the infection, the methodology proposed by Jie *et al*. (2009) was used: when the plants reached the 1030 development stage according to the BBCH scale, a scalpel was used to make a cut at the base of the root of each plant, which was immediately inoculated with 15 ml of the conidia suspension.

Spectroscopy

Reflectance spectra were obtained with a USB2000+ portable spectroscope (Ocean Optics, Largo, FL) with an HL-2000-HP tungsten halogen light source (wavelength range 360-2400 nm), a model WS-1 diffuse reflectance standard (reflectivity > 98% in the 250-1,500 nm range), and a QR600-7-VID-125F 600 µm premium grade reflectance probe (Ocean Optics, Largo, FL, USA). The measurements were taken in a closed environment when the plants had five functional leaves with the optical fiber on the adaxial surface of the leaf, obtaining three spectra for each leaf. The integration time was 6 s, with an average of 5 readings per measurement and an "interval time" of 2000 µs.

The time range of the measurements corresponded to the incubation period of the disease, defined as that from inoculation to the development of the first symptoms.

Statistical analysis

A completely randomized design was used to compare two treatments: susceptible (GM) and resistant (W) plants, both inoculated with Foc R1 and uninoculated.

Reflectance measurements were taken every 2 d after infection. Four data sets with 140 spectra each (28 leaves per treatment) were collected for each sampling day (560 spectra/sampling day).

Spectra with noise, distortion or reading errors were eliminated. The selection for removal was confirmed with an analysis of outliers identified in a principal component analysis (PCA) without data pretreatment. The variant normal standard transformation (SNV) provided good grouping of the plants in the treatments according to the results of the tests.

After pretreatment, the data were analyzed with the RELIEF-type classification algorithm and with the wavelengths that had the greatest weight. A linear discriminant analysis (LDA) was performed for the classifications. All analyses were performed with the Software R-project® version 4.1.2 (De Mendiburu, 2022).

Results

Difference in the spectral response of healthy Williams and Gros Michel banana plants

The general behavior of the reflectance of both cultivars was similar in the Vis spectrum; however, the W had a lower reflectance in the NIR range. A detailed analysis showed that the spectral response of the leaves varied according to the stage of development. The first leaf, with an expanding leaf lamina (according to the BBCH 1000 scale), had a higher reflectance, around 25% in the Vis for both, with respect to the rest of the leaves. However, in the NIR, the values increased by 87% for W and 75% for GM. As the stage of the leaf development advanced to other positions (2^{nd}, 3^{rd}, and 4^{th} leaves), the reflectance decreased throughout the entire spectral range, to values close to 12.5% in leaf 4 in both clones (Fig. 1A-B).

The RELIEF type classification algorithm defined a greater weight (0.10) for four reflectance regions. This algorithm "assumes" that these variables are strongly relevant if they easily distinguish between two observations of different classes, that is, between GM and W in this specific case (Fig. 1C). The wavelengths selected from the RELIEF-type algorithm in the discriminant analysis correctly classified 98% of the plants in the early plant development stages (Fig. 1D).

Spectral response of healthy plants and plants infected with *Foc* R1

Figure 2 shows the spectral response of leaves from healthy banana plants and plants inoculated with *Foc* R1 from 7 d post-inoculation (dpi). No change was observed in the average reflectance spectra during the first week. In the GM (susceptible) plants inoculated with *Foc* R1, reflectance increased during the incubation period of the disease (Fig. 2A-C) in the entire range of the measured spectrum, exceeding 50% in the Vis range and 96% in the NIR range, as compared to the uninoculated plants. Once the symptoms of the disease became visible, *i.e*., after the incubation period was over, the reflectance rapidly decreased throughout the entire spectral range (Fig. 2D). For W (resistant), the spectral response of the leaves of healthy plants inoculated with *Foc* R1 did not show significant variation during the

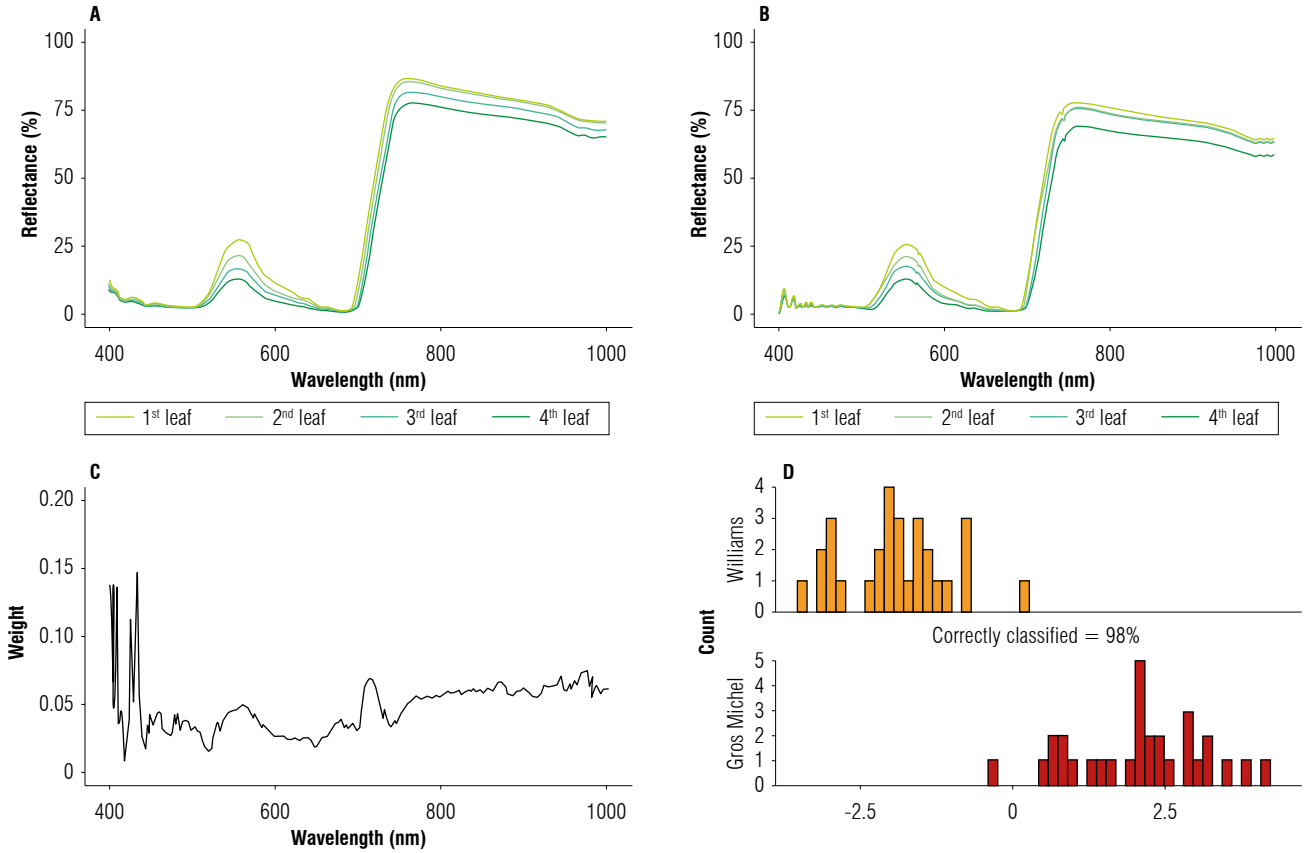

FIGURE 1. Spectral response with healthy Williams and Gros Michel banana plant leaves at 8 weeks of age. A) Reflectance spectra of the first four leaves measured in the Williams; B) Reflectance spectra of the first four leaves measured in the Gros Michel; C) Weights defined by the RELIEF type algorithm for all wavelengths in the measured range (400-1000 nm); D) Linear Discriminant Analysis using the evaluated plant as discrimination classes.

first 21 dpi (Fig. 2E-G); however, reflectance decreased throughout the range starting at the fourth week (Fig. 2).

Relationship between the spectral response and the intensity of vascular wilt symptoms in Gros Michel plants susceptible to *Foc* R1

Table 1 shows the spectral response to *Foc* R1 of a group of leaves and its evolution in symptoms in GM banana plants. From the spectral point of view, three states were denoted in the Vis: a first, basal state (category 0), a second state of reflectance elevation resulting from the loss of photosynthetic pigments (categories 1, 2, 3 and 4), and a third state for a drop in reflectance to minimum values throughout the measured range (categories 5 and 6) (Fig. 3). Category 0 had a reflectance of 13% in the Vis, a basis for comparison of the evolution of subsequent responses, which corresponds to an uninoculated plant. After 10 dpi and until day 27, categories 1, 2 and 3 had a spectral response in the Vis that increased up to 70%. The leaves remained active but reflected most of the incident energy, which was observed until category 4. Once category 5 was reached, the reflectance had a value of 63% in the Vis, which rapidly decreased over 48 h, reaching 3% (category 6), indicating that the organ was not functional.

Reflectance differed in the NIR (700 to 1000 nm), with values oscillating between 57 and 68% in categories 0 to 3. Starting at category 4, it increased to 68% and then dropped to 9% in category 6.

The healthy susceptible plants (category 0) had reflectance percentages of 13% in the Vis and 58% in the NIR. This variable increased by up to 70% in the Vis and 68% in the NIR in category 4 leaves, where the leaf blade had yellowing. Then, in the final stage of the infection, a rapid deterioration of the leaves was observed, coinciding with a decrease in reflectance values to less than 10% in the entire spectral range (category 6) (Fig. 3).

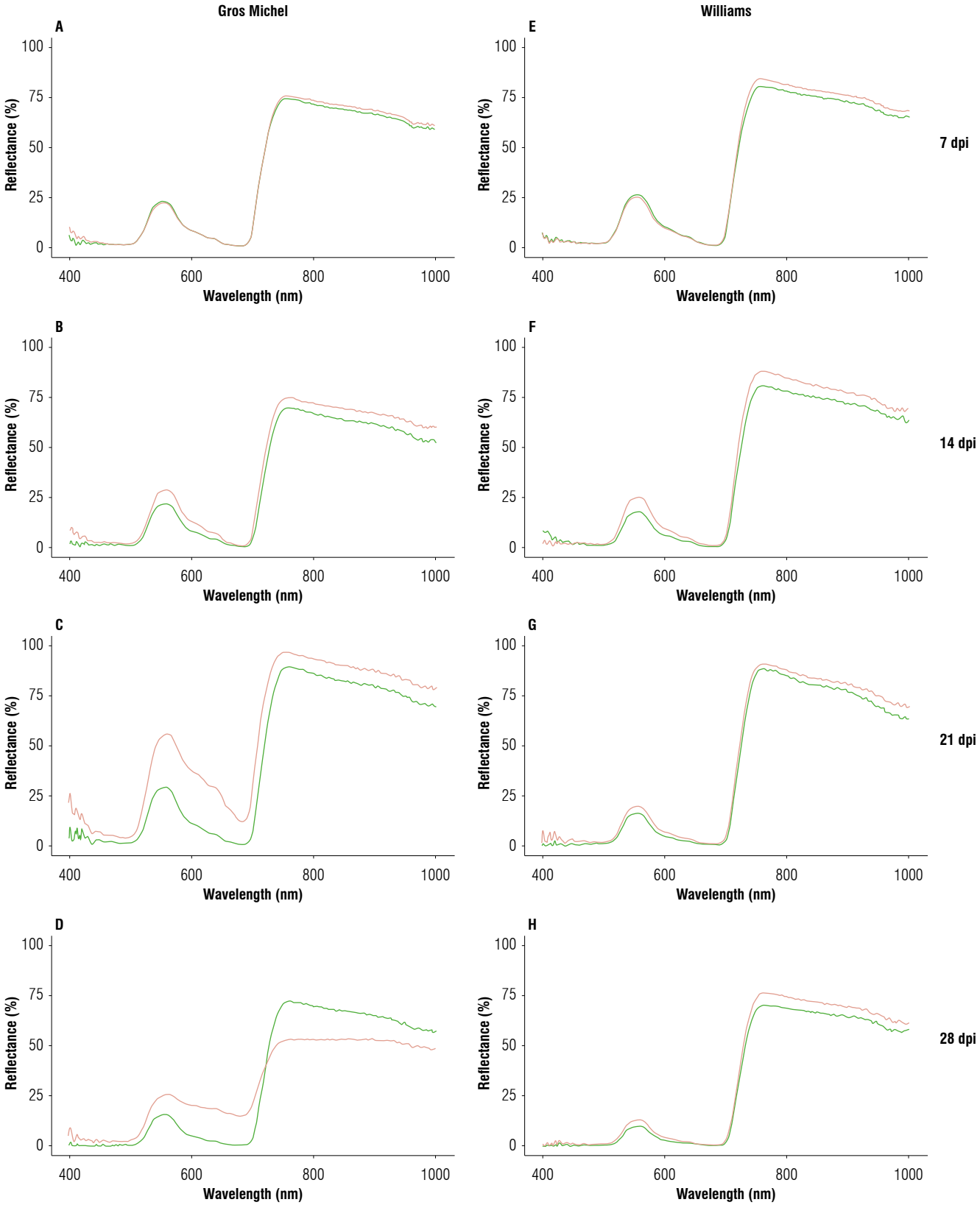

FIGURE 2. Reflectance spectra from leaves of Gros Michel (A-D) and Williams (E-H) cultivars at 7, 14, 21, and 28 dpi. Green line: control plants; orange line: plants infected with *Foc* R1.

TABLE 1. Symptoms and spectral response of the Gros Michel plants susceptible to *Foc* R1 infection.

Category	dpi	Visible symptoms on leaf lamina	Spectral response: reflectance (%)	
			Vis (400-700 nm)	NIR (700-1000 nm)
0	0	No symptoms: homogeneous dark green, fully expanded	0% at 400 nm (blue) 13% at 550 nm (green) 0% at 700 nm (red)	58% at 750 nm - 48% at 1000 nm
1	10	Homogeneous light green throughout the leaf, fully expanded	0% at 400 nm (blue) 20% at 550 nm (green) 0% at 700 nm (red)	63% at 750 nm - 51% at 1000 nm
2	20	Light yellow on the edge and light green in the center, fully expanded	3% at 400 nm (blue) 35% at 550 nm (green) 3% at 700 nm (red)	58% at 750 nm - 48% at 1000 nm
3	24	Bright yellow in more than 90% of the leaf, green areas near the main vein. Fully expanded	6% at 400 nm (blue) 55% at 550 nm (green) 25% at 700 nm (red)	57% at 750 nm - 43% at 1000 nm
4	27	Homogeneous pale yellow throughout the leaf, with loss of turgor in small areas. Leaf edge necrosis	7% at 400 nm (blue) 70% at 550 nm (green) 70% at 700 nm (red)	68% at 750 nm - 52% at 1000 nm
5	31	Pale yellow with loss of turgor in more than 80% of the leaf. Necrosis on the edge and large central areas of the leaf	7% at 400 nm (blue) 63% at 550 nm (green) 63% at 700 nm (red)	62% at 750 nm - 52% at 1000 nm
6	33	Homogeneous brown throughout the leaf. Loss of turgor and necrosis throughout the leaf	0% at 400 nm (blue) 3% at 550 nm (green) 5% at 700 nm (red)	9% at 750 nm - 9% at 1000 nm

Reflectance percentages at each wavelength are approximate.

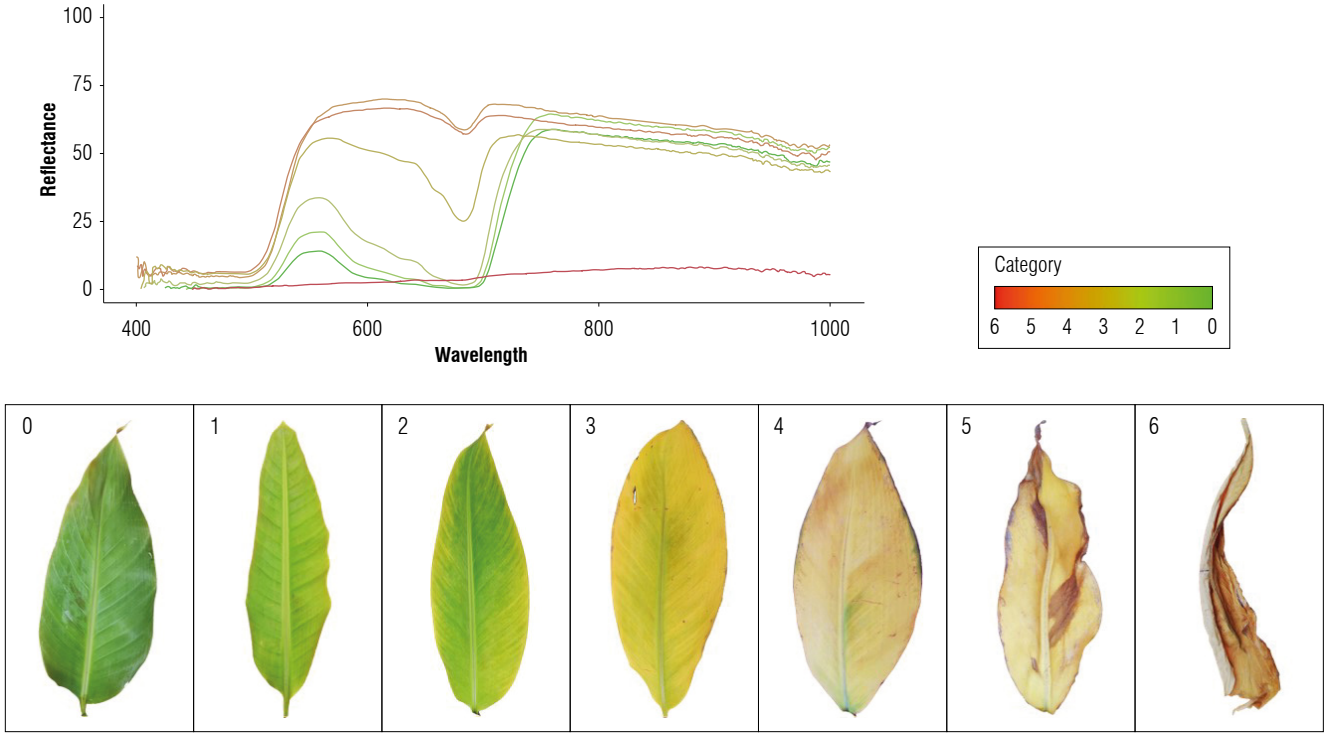

FIGURE 3. Spectral categorization of the Gros Michel plants susceptible to *Foc* R1 infection.

Discussion

Differences in the spectral response in healthy plants of Williams (resistant) and Gros Michel (susceptible)

The reflectance graphs for the first four leaves of both cultivars are similar in the Vis spectrum, as reported by Sinha *et al*. (2020), who spectrally characterized 12 banana genotypes. However, reflectance varies as a function of many leaf properties, such as leaf shape and thickness, pigment content, nutrient status, age, moisture content, and phenological stage (Hatfield *et al*., 2008; Martínez & Solís, 2018). In this case, the curves of both cultivarshad low reflectivity in the Vis spectrum, as described by Mather and Koch (2011), who confirmed that vigorous vegetation has low reflectivity in the visible spectrum, with a relative maximum around 550 nm, because the reflectance of a wavelength in this range decreases with an increase in the content of chlorophyll in the leaf (Hatfield *et al*., 2008), indicating that the incident light is being used.

As the phenological stage of leaves progresses, there is a general decrease in the entire spectrum; in the Vis range this is due to the increase in the chlorophyll content to the maximum possible for a mature leaf (Dray *et al*., 2012; Castañeda *et al*., 2018), which decreases when senescence begins. Leaves in early stages of development may have a different spectral imprint than mature leaves because they have less cellulose and lignin in the cell wall than mature leaves (Durgante *et al*., 2013) and because the pigments and leaf blade are just reaching their full potential for development peaks (Durgante *et al*., 2013). Changes in the carotenoid content of leaves and their ratio to chlorophyll are widely used to diagnose the physiological state of plants during development, senescence, acclimatization, and adaptation to different environments and types of stress (Young & Britton, 1990; Demmig-Adams *et al*., 1996).

On the other hand, the spectral reflectance in the broad portion of Vis and NIR has been related to plant chlorophyll content, leaf health and water content, while the red edge band (NIR) has been related to photosynthesis and foliar nitrogen (Verrelst *et al*., 2015; Féret *et al*., 2017, Silva-Perez *et al*., 2018). In the NIR, healthy vegetation has high reflectivity, which gradually decreases towards the mid-infrared (Mather & Koch, 2011). In this case, although the two cultivars peaked in this range of the spectrum, the W reached higher reflectance in the NIR range (infrared spectrum, 700-1000 nm). Specifically, the spongy mesophyll has cavities that scatter most of the incident energy in the near-infrared band of the electromagnetic spectrum (Mather, 2004). For this reason, any healthy leaf will have high reflectivity in the near infrared but very low reflectivity in the visible spectrum (Chuvieco, 2008). A large difference was observed between the Vis bands (especially in the red light) and the near infrared. Some authors have studied the importance of this relationship, proposing as a general principle that the greater the contrast between these bands (red and near infrared), the greater the vigor of the observed plants (Chuvieco, 2008). Here, the leaves of the healthy plants of the two cultivars presented very similar curves in the measured spectral range, with differences in the infrared spectrum, possibly, because of subtle differences in the structure of their tissues and the water content they can store (Chuvieco, 2008).

The differential spectral response measured in the cultivars identified specific wavelengths that can be used for their classification. In recent decades, this technology has been used to discriminate closely related forest species, using discriminant analysis of spectral data, which confirmed the existence of spectral signatures in species, with a correct identification rate of over 96% (Durgante *et al*., 2013). Sohn *et al*. (2021) used Vis-NIR spectroscopy to discriminate *Amaranthus* sp. with an accuracy rate of up to 99.7%, recommending the use of this technology for species recognition even in juvenile stages. In addition, these authors suggested the use of Vis-NIR spectroscopy in combination with pre-processing, spectral libraries, and appropriate models for the identification and discrimination of varieties and plant species.

Spectral response of plants infected with *Foc* R1

Infection by *F. oxysporum* causes a series of physiological and morphological changes, both internally and externally (Pérez *et al*., 2014). Likewise, stress will manifest itself as a variation in the spectral response of healthy plants (Chuvieco, 2008).

In the GM plants, an increase in reflectance was initially observed throughout the spectrum. When a banana plant is infected by *Foc* R1, there are structural and biochemical changes that result in plant senescence (Dong *et al*., 2014). Plant wilting is generally attributed to vessel obstruction or systemic toxicity (Berestetskiy, 2008). The plugging theory has been proposed for the specific case of *Foc* R1 infections, which suggests that the vessels of infected plant become clogged with fungal hyphae, callose, tylose, and gel, which hinders water transport and, finally, causes a water deficit (Pivonia *et al*., 2002). When the water content in the leaves decreases, reflectivity increases, especially in the mid-infrared light, since there is no plant water to absorb energy (Chuvieco, 2008). Additionally, in the

colonization process of plants, microorganisms can secrete phytotoxins capable of reducing the vital activity of plant cells. For example, there are toxins that have their site of action in the cytoplasmatic membrane, with the formation of transmembrane ion channels being the mechanism of action (Feigin *et al*., 1996). The formation of these channels causes alteration in the ion transport, the massive exit of electrolytes from the interior of the cells and, finally, death (Lavermicocca *et al*., 1997).

Likewise, when a plant is infected, chlorophyll degrades faster than carotenoids (Sanger, 1971). This effect generates an increase in the reflectance of the red-light wavelengths because of the reduction of absorbed chlorophyll. The loss of chlorophyll in a leaf produces greater reflectivity between the blue and red wavelengths (which is why the leaf turns yellow) because carotenes and xanthophylls, which absorb blue light and reflect green and red light, are dominant (Boyer *et al*., 1988). Finally, when a leaf is senescent, its internal cellular structure deteriorates, with lower reflectivity in the near infrared spectrum (Martínez & Solís, 2018). When leaves die, brown pigments (tannins) appear, and leaf reflectance and transmittance in the wavelength range between 400 nm and 750 nm decrease (Boyer *et al*., 1988). This behavior was observed in the leaves of the susceptible cultivar, where the accumulation of internal and external symptoms ended with senescence.

In the W leaves, a constant trend was observed for the reflectance throughout the spectrum during the study. However, although these plants are resistant, they were still subjected to inoculation stress, where the roots were injured, and *Foc* R1 structures were added. For this reason, a slight increase in the reflectance was noted in the infrared peak, which stabilized, resulting in a similar curve to that in the control plants. This can be attributed to a temporary accumulation of anthocyanins in response to inoculation; since these pigments serve as stress indicators for many plant species, their detection and quantitative evaluation provide information on the response and adaptation of plants to different types of stress (Chalker-Scott, 1999). In short, this group is stressed by the presence of the pathogen, being tolerant rather than resistant.

Relationship between the spectral response and the intensity of vascular wilt symptoms in Gros Michel plants susceptible to *Foc* R1

The data related the spectral response with the intensity of the symptoms of vascular wilt in Gros Michel. Pérez *et al*. (2014) proposed a scale of external and internal symptoms for banana plants in greenhouses, in which five important stages in the infection process are considered; the description of these stages was accompanied by photographs and a description of typical external and internal symptoms for each one. In the present study, a complementary scale was proposed with the description of the reflectance obtained between 400 and 1000 nm in banana plants infected by *Foc* R1 under greenhouse conditions. Although it is similar to that of Pérez *et al*. (2014), it offers greater detail for monitoring the progress of the disease. The spectral characterization, complementary to other diagnostic methods, facilitates the diagnosis and identification of diseased plants in early stages.

To conclude, it is necessary to identify discriminating wavelengths in the NIR since, in the initial stages, the appearance of symptoms is very subtle. Wavelengths must be specific to the phenomenon to differentiate between healthy and sick plants. Categories based on the intensity of the visible symptoms observed during the different stages of the infection are recommended.

Conclusions

A method for detecting and discriminating the spectral response of two varieties of banana plants was tested using reflectance spectroscopy in healthy plants and in *Foc* R1-infected plants. The results showed that Vis-NIR spectroscopy, in combination with appropriate pre-processing methods and multivariate data analysis, is an efficient tool for effectively classifying GM and W banana plants. Spectral fingerprints for the plants were elucidated in each variety for leaves in different stages of development. The differences in the Vis range of the spectrum were very evident.

The results suggested that the biochemical and biophysical changes generated in banana plants by *Foc* R1 infection can be detected and discriminated before visible symptoms appear using reflectance spectroscopy in the VIS/NIR ranges. Specifically, Gros Michel plants (susceptible to *Foc* R1) infected by *Foc* R1 presented a spectrum that differentiated them from healthy plants of the same variety and from Williams plants in the asymptomatic period of the disease. The spectral characterization differentiated diseased plants, making it an objective tool for diagnosis of banana wilt and its identification in early stages. Additionally, it is possible to improve the precision and efficiency of this diagnostic method for plant diseases with a scale of symptoms based on the spectral response of leaves in each stage of pathogenesis development.

Acknowledgments

The authors thank the Universidad Nacional de Colombia for funding and the Centro de Investigaciones del Banano (CENIBANANO/AUGURA) for supplying the *Foc* R1 strain to inoculate the plants.

Conflict of interest statement

The authors declare that there is no conflict of interests regarding the publication of this article.

Author's contributions

LMHC and JCMO designed the experiments; EME, JCMO and LMHC carried out the field and laboratory experiments; EME, JCMO, LMHC and VBF contributed to the data analysis; and EME, JCMO and LMHC wrote the article. All authors reviewed the final version of the manuscript.

Literature cited

Abdulridha, J., Batuman, O., & Ampatzidis, Y. (2019). UAV-based remote sensing technique to detect citrus canker disease utilizing hyperspectral imaging and machine learning. *Remote Sensing*, *11*(11), Article 1373. https://doi.org/10.3390/rs11111373

Abu-Khalaf, N., & Salman, M. (2014). Visible/Near infrared (VIS/NIR) spectroscopy and multivariate data analysis (MVDA) for identification and quantification of olive leaf spot (OLS) disease. *Palestine Technical University Research Journal*, *2*(1), 1–8. https://doi.org/10.53671/pturj.v2i1.21

Barbedo, J. G. A. (2013). Digital image processing techniques for detecting, quantifying and classifying plant diseases. *SpringerPlus*, *2*(1), Article 660. https://doi.org/10.1186/2193-1801-2-660

Berestetskiy, A. O. (2008). A review of fungal phytotoxins: from basic studies to practical use. *Applied Biochemistry and Microbiology*, *44*(5), Article 453. https://doi.org/10.1134/s0003683808050013

Boyer, M., Miller, J., Belanger, M., Hare, E., & Wu, J. (1988). Senescence and spectral reflectance in leaves of northern pin oak (*Quercus palustris* Muenchh.). *Remote Sensing of Environment*, *25*(1), 71–87. https://doi.org/10.1016/0034-4257(88)90042-9

Castañeda, C. S., Almanza-Merchán, P. J., Pinzón, E. H., Cely, G. E., & Serrano, P. A. (2018). Estimación de la concentración de clorofila mediante métodos no destructivos en vid (*Vitis vinífera* L.) cv. Riesling Becker. *Revista Colombiana de Ciencias Hortícolas*, *12*(2), 329–337. https://doi.org/10.17584/rcch.2018v12i2.7566

Chaerle, L., & Van Der Straeten, D. (2000). Imaging techniques and the early detection of plant stress. *Trends in Plant Science*, *5*(11), 495–501. https://doi.org/10.1016/s1360-1385(00)01781-7

Chalker-Scott, L. (1999). Environmental significance of anthocyanins in plant stress responses. *Photochemistry and Photobiology*, *70*(1), 1–9. https://doi.org/10.1111/j.1751-1097.1999.tb01944.x

Chuvieco, E. (2008). *Teledetección ambiental. La observación de la tierra desde el espacio* (3rd ed.). Ariel.

De Mendiburu, F. (2022, February). *Agricolae: Statistical procedures for agricultural research*. R v. 4.1. 2. http://cran.r-project.org/package=agricolae

Demmig-Adams, B., Gilmore, A. M., & Adams III, W. W. (1996). *In vivo* functions of carotenoids in higher plants. *The FASEB Journal*, *10*(4), 403–412. https://doi.org/10.1096/fasebj.10.4.8647339

Dong, X., Xiong, Y., Ling, N., Shen, Q., & Guo, S. (2014). Fusaric acid accelerates the senescence of leaf in banana when infected by *Fusarium*. *World Journal of Microbiology and Biotechnology*, *30*(4), 1399–1408. https://doi.org/10.1007/s11274-013-1564-1

Dordas, C. (2008). Role of nutrients in controlling plant diseases in sustainable agriculture. A review. *Agronomy for Sustainable Development*, *28*(1), 33–46. https://doi.org/10.1051/agro:2007051

Dray, F. A., Center, T. D., & Mattison, E. D. (2012). *In situ* estimates of waterhyacinth leaf tissue nitrogen using a SPAD-502 chlorophyll meter. *Aquatic Botany*, *100*, 72–75. https://doi.org/10.1016/j.aquabot.2012.03.005

Durgante, F. M., Higuchi, N., Almeida, A., & Vicentini, A. (2013). Species spectral signature: discriminating closely related plant species in the Amazon with near-infrared leaf-spectroscopy. *Forest Ecology and Management*, *291*, 240–248. https://doi.org/10.1016/j.foreco.2012.10.045

FAO (The Food and Agriculture Organization of the United Nations). (2020). *Análisis del mercado del banano. Panorama general de febrero de 2020*. http://www.fao.org/3/ca9212es/ca9212es.pdf

Feigin, A. M., Takemoto, J. Y., Wangspa, R., Teeter, J. H., & Brand, J. G. (1996). Properties of voltage-gated ion channels formed by syringomycin E in planar lipid bilayers. *The Journal of Membrane Biology*, *149*(1), 41–47. https://doi.org/10.1007/s002329900005

Féret, J. B., Gitelson, A. A., Noble, S. D., & Jacquemoud, S. (2017). PROSPECT-D: towards modeling leaf optical properties through a complete lifecycle. *Remote Sensing of Environment*, *193*, 204–215. https://doi.org/10.1016/j.rse.2017.03.004

García-Bastidas, F. A., Quintero-Vargas, J. C., Ayala-Vasquez, M., Schermer, T., Seidl, M. F., Santos-Paiva, M., Noguera, A. M., Aguilera-Galvez. C., Wittenberg, A., Hofstede, R., Sørensen, A., & Kema, G. H. J. (2020). First report of Fusarium wilt Tropical Race 4 in Cavendish bananas caused by *Fusarium odoratissimum* in Colombia. *Plant Disease*, *104*(3), 994–994. https://doi.org/10.1094/pdis-09-19-1922-pdn

Hatfield, J. L., Gitelson, A. A., Schepers, J. S., & Walthall, C. L. (2008). Application of spectral remote sensing for agronomic decisions. *Agronomy Journal*, *100*(S3), S-117–S-131. https://doi.org/10.2134/agronj2006.0370c

Jie, L., Zifeng, W., Lixiang, C., Hongming, T., Patrik, I., Zide, J., & Shining, Z. (2009). Artificial inoculation of banana tissue culture plantlets with indigenous endophytes originally derived from native banana plants. *Biological Control*, *51*(3), 427–434. https://doi.org/10.1016/j.biocontrol.2009.08.002

Lavermicocca, P., Iacobellis, N. S., Simmaco, M., & Graniti, A. (1997). Biological properties and spectrum of activity of *Pseudomonas syringae* pv. Syringaetoxins. *Physiological and Molecular Plant Pathology*, *50*(2), 129–140. https://doi.org/10.1006/pmpp.1996.0078

Li, M. H., Xie, X. L., Lin, X. F., Shi, J. X., Ding, Z. J., Ling, J. F., Xi, P. G., Zhou, J. N., Leng, Y., Zhong, S., & Jiang, Z. D. (2014). Functional characterization of the gene *FoOCH1* encoding a putative α-1, 6-mannosyltransferase in *Fusarium oxysporum* f. sp. *Cubense*. *Fungal Genetics and Biology*, *65*, 1–13. https://doi.org/10.1016/j.fgb.2014.01.005

Mahlein, A. K. (2016). Plant disease detection by imaging sensors–parallels and specific demands for precision agriculture and plant phenotyping. *Plant Disease*, *100*(2), 241–251. https://doi.org/10.1094/pdis-03-15-0340-fe

Mahlein, A. K., Rumpf, T., Welke, P., Dehne, H. W., Plümer, L., Steiner, U., & Oerke, E. C. (2013). Development of spectral indices for detecting and identifying plant diseases. *Remote Sensing of Environment*, *128*, 21–30. https://doi.org/10.1016/j.rse.2012.09.019

Marín, J. C., Hoyos-Carvajal, L., & Botero-Fernández, V. (2018). Detección de plantas asintomáticas de *Solanum lycopersicum* L. infectadas con *Fusarium oxysporum* usando espectroscopia de reflectancia VIS. *Revista Colombiana de Ciencias Hortícolas*, *12*(2), 436–446. https://doi.org/10.17584/rcch.2018v12i2.7293

Martinelli, F., Scalenghe, R., Davino, S., Panno, S., Scuderi, G., Ruisi, P., Villa, P., Stroppiana, D., Boschetti, M., Goulart, L. R., Davis, C. E., & Dandekar, A. M. (2015). Advanced methods of plant disease detection. A review. *Agronomy for Sustainable Development, 35*(1), 1–25. https://doi.org/10.1007/s13593-014-0246-1

Martínez, R., & Solís, G. A. (2018). Caracterización espectral y detección de flecha seca en palma africana en Puntarenas, Costa Rica. *Revista Geográfica de América Central*, *2*(61), 349–377. https://doi.org/10.15359/rgac.61-2.13

Maryani, N., Lombard, L., Poerba, Y. S., Subandiyah, S., Crous, P. W., & Kema, G. H. J. (2018). Phylogeny and genetic diversity of the banana Fusarium wilt pathogen *Fusarium oxysporum* f. sp. *cubense* in the Indonesian centre of origin. *Studies in Mycology*, *91*(1), 79–99. https://doi.org/10.1016/j.simyco.2018.06.003

Mather, P. (2004). *Computer processing of remotely-sensed images* (2nd ed.). John Wiley & Sons.

Mather, P., & Koch, M. (2011). Pre-processing of remotely-sensed data. In P. Mather, & M. Koch, *Computer processing of remotely-sensed images*: *An introduction* (4th ed., pp. 87–124). John Wiley & Sons. https://doi.org/10.1002/9780470666517.ch4

Pérez Vicente, L. F., Dita, M., & Martínez De La Parte, E. (2014). *Technical manual: Prevention and diagnostic of Fusarium wilt (Panama disease) of banana caused by Fusarium oxysporum f. sp. cubense Tropical Race* 4 *(TR4)*. FAO.

Pimentel, D. (2011). *Biological invasions: economic and environmental costs of alien plant, animal, and microbe species* (2nd ed). CRC Press.

Pivonia, S., Cohen, R., Katan, J., & Kigel, J. (2002). Effect of fruit load on the water balance of melon plants infected with *Monosporascus cannonballus*. *Physiological and Molecular Plant Pathology*, *60*(1), 39–49. https://doi.org/10.1006/pmpp.2001.0375

Ploetz, R. C. (2006). *Fusarium* wilt of banana is caused by several pathogens referred to as *Fusarium oxysporum* f. sp. *cubense*. *Phytopathology*, *96*(6), 653–656. https://doi.org/10.1094/phyto-96-0653

Ratnadass, A., Fernandes, P., Avelino, J., & Habib, R. (2012). Plant species diversity for sustainable management of crop pests and diseases in agroecosystems: a review. *Agronomy for Sustainable Development*, *32*(1), 273–303. https://doi.org/10.1007/s13593-011-0022-4

Rizzo, D. M., Lichtveld, M., Mazet, J. A., Togami, E., & Miller, S. A. (2021). Plant health and its effects on food safety and security in a one health framework: Four case studies. *One Health Outlook*, *3*(1), 1–9. https://doi.org/10.1186/s42522-021-00038-7

Sanger, J. E. (1971). Quantitative investigations of leaf pigments from their inception in buds through autumn coloration to decomposition in falling leaves. *Ecology*, *52*(6), 1075–1089. https://doi.org/10.2307/1933816

Sankaran, S., Mishra, A., Ehsani, R., & Davis, C. (2010). A review of advanced techniques for detecting plant diseases. *Computers and Electronics in Agriculture*, *72*(1), 1–13. https://doi.org/10.1016/j.compag.2010.02.007

Silva-Perez, V., Molero, G., Serbin, S. P., Condon, A. G., Reynolds, M. P., Furbank, R. T., & Evans, J. R. (2018). Hyperspectral reflectance as a tool to measure biochemical and physiological traits in wheat. *Journal of Experimental Botany*, *69*(3), 483–496. https://doi.org/10.1093/jxb/erx421

Sinha, P., Robson, A., Schneider, D., Kilic, T., Mugera, H. K., Ilukor, J., & Tindamanyire, J. M. (2020). The potential of in-situ hyperspectral remote sensing for differentiating 12 banana genotypes grown in Uganda. *ISPRS Journal of Photogrammetry and Remote Sensing*, *167*, 85–103. https://doi.org/10.1016/j.isprsjprs.2020.06.023

Sohn, S. I., Oh, Y. J., Pandian, S., Lee, Y. H., Zaukuu, J. L. Z., Kang, H. J., Ryu, T. H., Cho, W. S., Cho, Y. S., & Shin, E. K. (2021). Identification of *Amaranthus* species using Visible-Near-Infrared (Vis-NIR) spectroscopy and machine learning methods. *Remote Sensing*, *13*(20), Article 4149. https://doi.org/10.3390/rs13204149

Szuvandzsiev, P., Helyes, L., Lugasi, A., Szántó, C., Baranowski, P., & Pék, Z. (2014). Estimation of antioxidant components of tomato using VIS-NIR reflectance data by handheld portable spectrometer. *International Agrophysics*, *28*(4), 521–527. https://doi.org/10.2478/intag-2014-0042

Thomas, S., Kuska, M. T., Bohnenkamp, D., Brugger, A., Alisaac, E., Wahabzada, M., Behamnn, J., & Mahlein, A. K. (2018). Benefits of hyperspectral imaging for plant disease detection and plant protection: a technical perspective. *Journal of Plant Diseases and Protection*, *125*(1), 5–20. https://doi.org/10.1007/s41348-017-0124-6

Varma, V., & Bebber, D. P. (2019). Climate change impacts on banana yields around the world. *Nature Climate Change*, *9*(10), 752–757. https://doi.org/10.1038/s41558-019-0559-9

Verrelst, J., Camps-Valls, G., Muñoz-Marí, J., Rivera, J. P., Veroustraete, F., Clevers, J. G., & Moreno, J. (2015). Optical remote sensing and the retrieval of terrestrial vegetation bio-geophysical properties – A review. *ISPRS Journal of Photogrammetry and Remote Sensing*, *108*, 273–290. https://doi.org/10.1016/j.isprsjprs.2015.05.005

Wang, D., Peng, C., Zheng, X., Chang, L., Xu, B., & Tong, Z. (2020). Secretome analysis of the banana Fusarium wilt fungi *Foc R1* and *Foc TR4* reveals a new effector OASTL required for full pathogenicity of *Foc TR4* in banana. *Biomolecules*, *10*(10), Article 1430. https://doi.org/10.3390/biom10101430

Young, A. J., & Britton, G. (1990). Carotenoids and oxidative stress. In M. Baltscheffsky (Ed.), *Current research in photosynthesis* (pp. 3381–3384). Springer. https://doi.org/10.1007/978-94-009-0511-5_759

Zhang, J., Huang, Y., Pu, R., Gonzalez-Moreno, P., Yuan, L., Wu, K., & Huang, W. (2019). Monitoring plant diseases and pests through remote sensing technology: A review. *Computers and Electronics in Agriculture*, *165*, Article 104943. https://doi.org/10.1016/j.compag.2019.104943

Zhang, J., Pu, R., Huang, W., Yuan, L., Luo, J., & Wang, J. (2012). Using in-situ hyperspectral data for detecting and discriminating yellow rust disease from nutrient stresses. *Field Crops Research*, *134*, 165–174. https://doi.org/10.1016/j.fcr.2012.05.011

Biological studies of *Puccinia lantanae,* a potential biocontrol agent of "Lippia" (*Phyla nodiflora* var. *minor*)

Estudios biológicos en *Puccinia lantanae*, posible agente de biocontrol de"Lippia" (*Phyla nodiflora* var. *minor*)

Guadalupe Traversa[1]*, Alejandro Joaquín Sosa[2], Guillermo Rubén Chantre[3], and María Virginia Bianchinotti[3]

ABSTRACT

Phyla nodiflora var. *minor* (syn. *P. canescens* (Kunth) Greene) known *as* "lippia" is an invasive weed with considerable impact on agricultural systems and conservation areas in Australia. The rust fungus *Puccinia lantanae* Farl. has been proposed as a potential biocontrol agent of *Lantana camara.* As it was previously found in *Lippia* s.l. in Argentina, we aim to study: (i) its geographical distribution in Argentina, Bolivia, and Chile; (ii) teliospore germination and basidiospore formation under different incubation temperatures; (iii) the effect of teliospore age on germination capacity; (iv) the effect of heat shock on teliospore germination and basidiospore formation; and (v) the pathogenicity of the rust fungus on *P. nodiflora*. Field surveys were conducted in Argentina, Bolivia, and Chile. *In vitro* experimental assays of germination and pathogenicity were performed. The rust was found in four provinces of Argentina (Jujuy, Salta, Formosa, and Entre Rios) and was not found in Bolivia and Chile. *Puccinia lantanae* showed the maximum values of teliospore germination and basidiospore formation at 20°C. The effect of aging and heat shock treatments significantly reduced teliospore germination. Pathogenicity tests showed that *P. nodiflora* var. *minor*, *reptans*, and *nodiflora* were infected with the "Formosa" isolate. The isolates "Salta" and "Entre Rios" infected var. *minor* and *reptans,* being potential candidates for biocontrol.

Key words: spores, biological control, invasive species, specificity.

RESUMEN

Phyla nodiflora var. *minor* (syn. *P. canescens* (Kunth) Greene), conocida comúnmente como "lippia" es una maleza invasora que genera un grave impacto en los sistemas agrícolas y áreas protegidas en Australia. La roya, *Puccinia lantanae* Farl., ha sido propuesta como un potencial agente de biocontrol de *Lantana camara*. Este hongo fue encontrado en *Lippia* s.l. en Argentina; por esta razón, proponemos estudiar (i) su distribución geográfica en Argentina, Bolivia y Chile; (ii) la germinación de teliosporas y la formación de basidiosporas bajo diferentes temperaturas de incubación; (iii) el efecto de la edad de las teliosporas sobre la capacidad de germinación; (iv) el efecto del choque térmico sobre la germinación de teliosporas y la formación de basidiosporas; (v) la patogenicidad de la roya sobre *P. nodiflora*. Se realizaron ensayos *in vitro* de germinación y de patogenicidad. La roya se encontró en cuatro provincias de Argentina (Jujuy, Salta, Formosa y Entre Ríos), y no se encontró en Bolivia y Chile. La germinación de las teliosporas y la formación de basidiosporas fueron máximas a 20°C. El efecto de la edad de las teliosporas y los tratamientos de choque térmico redujeron significativamente la germinación de estas. *P. nodiflora* var. *minor*, *reptans* y *nodiflora* fueron infectadas con el aislado "Formosa". Los aislados "Salta" y "Entre Rios", infectaron a la var. *minor* y *reptans* siendo candidatos potenciales de biocontrol.

Palabras clave: esporas, control biológico, especies invasoras, especificidad.

Introduction

Phyla nodiflora var. *minor* (synonym *P. canescens* (Kunth) Greene) (Verbenaceae), commonly known as "lippia" in Australia, is a notorious weed of riparian and floodplain production and conservation areas with considerable impact on rural production, land values, and ecosystem services. It is a perennial plant with a prostrate habit and creeping stems that can root at each node, which favors spreading and increasing in density. This invasive plant was commercially introduced in Australia as an ornamental species during the second half of the XIX century and has invaded 5.3 million ha of the "Murray-Darling" basin floodplain. The greatest invasions and impacts occur in the Murray-Darling Basin´s northern catchment, but also throughout the basin and elsewhere in Australia. In the

Received for publication: July 08, 2022. Accepted for publication: December 15, 2022 Doi: 10.15446/agron.colomb.v40n3.103562

[1] Departamento de Agronomía, Universidad Nacional del Sur (UNS), Bahía Blanca (Argentina).
[2] Fundación para el Estudio de Especies Invasivas (FuEDEI), Hurlingham (Argentina).
[3] Centro de Recursos Naturales Renovables de la Zona Semiárida (CERZOS) - UNS, Consejo Nacional de Investigaciones Científicas y Técnicas (CONICET) - Centro Científico Tecnológico (CCT), Bahía Blanca (Argentina).
* Corresponding author: guadalupe.traversa@uns.edu.ar

Murray-Darling Basin, the weed costs the grazing industry an estimated Australian dollar AUD $38 million per year and the environment AUD $1.8 billion per year (Earl, 2003).

Current short term and unsustainable control methods include the use of herbicides, cultivation, and grazing management (Julien *et al*., 2012). The use of herbicides is restricted by the presence of susceptible crops along waterways. *Phyla nodiflora* var. *minor* may be managed by cultivation, however, in many areas the practice is not sustainable as there is a significant risk of soil loss associated with cultivation of areas adjacent to waterways (Earl, 2003). Biological control was proposed as part of the weed management in reserve areas, woodlands, forests, and along stream banks.

Originally, two species were recognized in Australia, *Phyla nodiflora* and *Phyla canescens* (Munir, 1993). Although *Phyla nodiflora* has a worldwide distribution, the condition of being native to Australia (Gross *et al*., 2017) has implications for the selection of biological control agents. The South American genus *Phyla* Lour (Verbenaceae), originally included in the genus *Lippia* L., currently comprises five species (O'Leary & Múlgura, 2012). Following the taxonomic revision of the genus *Phyla* Lour provided by O'Leary & Múlgura (2012), three varieties of *P. nodiflora* are recognized: *P. nodiflora* (L.) Greene var. *nodiflora*, *P. nodiflora* var. *minor* (Hook.) O'Leary & Múlgura, and *P. nodiflora* var. *reptans* (Kunth) Moldenke. According to Sosa *et al*. (2017), the variety *minor* is an invasive weed in Australia, while the variety *nodiflora* is the native Australian form (formerly known as *P. nodiflora*).

The *P. nodiflora* plant is native to South America with the center of origin probably in Central and Northern Argentina (Julien *et al*., 2012). It is likely that many specific antagonists can be found in this region, and they can be proposed as potential biological control agents against this weed. Systematic surveys on the three varieties of *P. nodiflora* are scarce, and only a few arthropods (Cabrera *et al*., 2016) and pathogens are mentioned as natural enemies (Viégas, 1961; Ellis, 1976; Farr *et al*., 1989).

Puccinia lantanae Farl. (Pucciniales, Basidiomycota) was described as infecting *P. nodiflora* var. *minor* (formerly *Lippia canescens=P. canescens*) in Argentina (Lindquist, 1982). Julien *et al*. (2012) registered this rust damaging *P. nodiflora* under natural conditions in the field in Argentina. *Puccinia lantanae* is an autoecius (completes the life cycle on a single host) microcyclic rust, for which only the teleutosporic stage is known (Cummins & Hiratsuka, 2003). This rust has been reported on *Lippia* spp. in South America (*fide* Jackson, 1932; Lindquist, 1982). Particularly, in Argentina, the geographic distribution range of *P. lantanae* in *Lantana* spp. and *Lippia* spp. includes Buenos Aires, Entre Ríos, Corrientes, Misiones, Tucumán and Salta provinces (Hernández & Hennen, 2002). Previous studies suggest its potential use as a biocontrol agent of *Lantana camara* L., considered a weed with serious impact (Barreto *et al*., 1995).

Rusts are considered very attractive biocontrol agents due to their high specificity and the impressive biocontrol successes in some species (Morin *et al*., 2006), with different pathotypes specialized on different plant species and even in some cases on different genotypes within the same plant species. Additionally, there is evidence of distinct races of *P. lantanae* that attack only one species and are even specific to biotypes within that species (Rentería & Ellison, 2004).

Field surveys in the native range and knowledge of the biology of putative biological agents are essential components of a biocontrol program (Fourie & Wood, 2018). Extensive collecting and research on this rustwere performed in Brazil and Peru (Barreto *et al*., 1995; Ellison & Cortat, 2011), but similar studies do not exist for Argentina or bordering countries. Temperature is one of the environmental limitations of the disease development in the field (Agrios, 2005); its effect on teliospore germination and basidiospore production is crucial in the epidemiology of microcyclic rust disease.

In this research, we aim to study: i) the geographic distribution of *P. lantanae* on *P. nodiflora* in Argentina and two bordering countries (Bolivia and Chile), (ii) the effect of different incubation temperatures, aging and heat shock on teliospore germination and basidiospore formation, and (iii) the pathogenicity of the rust fungus on *P. nodiflora* var. *minor*, *P. nodiflora* var. *reptans*, and *P. nodiflora* var. *nodiflora*.

Materials and methods

Field surveys and collection of rust isolates

Field trips were performed to study the geographic distribution of *Puccinia lantanae* in Argentina, Bolivia, and Chile. Both rust and *P. nodiflora* (var. *minor*, *reptans*, and *nodiflora*) plant material was collected from different locations. Roadside surveys were conducted in Argentina from December 2004 to January 2011 (41°S northwards). As *P. nodiflora* var. *minor* is a small and prostrate plant and often grows in the understory, it is difficult to observe from

a moving vehicle. Therefore, inspection sites were assigned according to the following criteria: the first site was randomly selected within the first 50 km away from Buenos Aires along main routes and subsequent inspections were systematically placed every 50, 100 and 180 km, giving a total of 217 visited sites during 6 years of field survey (Fig. 1). Plant specimens from all locations were collected and dried for further identification. Whenever a rust infected plant population was found, material was collected and placed between pieces of newspaper in a plant press for further study in the laboratory (Tab. 1). Each collection of the rust is termed "isolate". A GPS reading was taken to record the site location. Some sites were visited more than once in different seasons.

In the laboratory, field collected samples of infected plants with rust were processed. Freehand razor blade cuts were performed on infected leaves. The cuts were placed in water or potassium hydroxide in an aqueous solution 5%. A coverslip was placed over the cuts (Waller *et al*., 2002). Fifty teliospores were measured (width and length) (Anikster *et al*., 2004) using a compound microscope (Olympus CX 31).

Source and maintenance of plants

New *P. nodiflora* individuals of each variety were obtained to establish rust cultures with isolates of different locations and to conduct pathogenicity tests. Healthy stem cuts with three to four nodes (with leaves) were buried in 10 cm-diameter plastic pots containing steam sterilized soil and organic substrate mixture (1:1, w/w) leaving two nodes over the soil surface. *Phyla nodiflora* propagules were grown for 15 d at 25°C and 100% relative humidity (RH) (humid chamber), and thereafter at 25°C and 60% RH until the four-five leaf stage.

Rust inoculation methodology

The leaf disc inoculation method proposed by Morin *et al*. (1993) was used for all inoculation experiments. The host plants (3 months old) from which leaf discs were collected were *P. nodiflora* var. *nodiflora* (350), *P. nodiflora* var. *reptans* (264), and *P. nodiflora* var. *reptans* (205). Each leaf disc was covered by a mass of spores (telia) of the rust 5 mm in diameter. Ten circular discs of leaf with telia (3-4 weeks old) were placed on the surface of 2% water agar (WA) in a 9 cm diameter Petri dish base, with the telia on the side

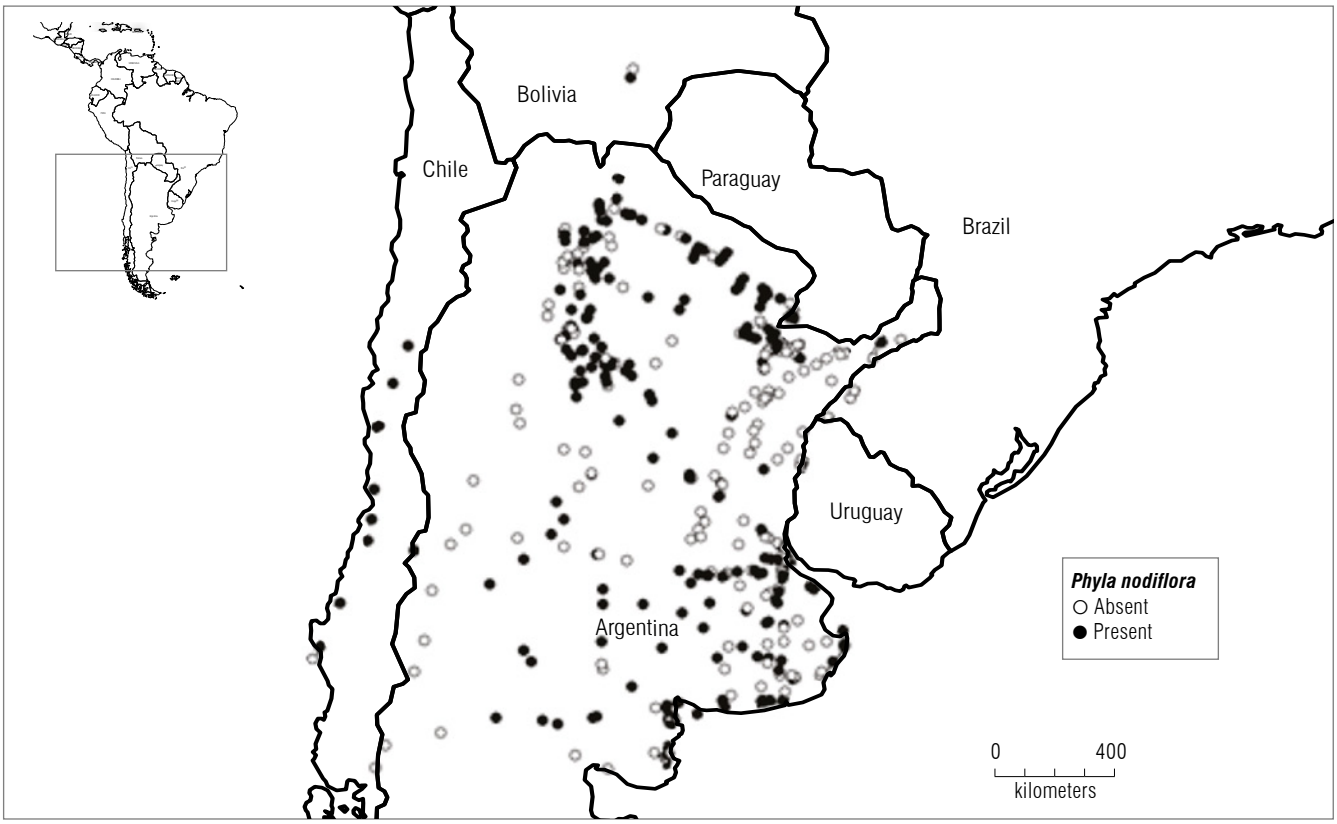

FIGURE 1. Distribution of *Phyla nodiflora* var. *minor, reptans*, and *nodiflora* in southern South America. Circles indicated sites visited to sample the plants. Solid circles: plant present, empty circles: plant absent. Data from Chile were obtained by A. Sosa.

away from the water agar. The base of the dish was inverted and fixed to the top of a plastic pot with holes. Three young, healthy plants of *P. nodiflora* were placed in a plant pot. The pot with the plants was sealed to the pot containing the telia inverted with masking tape and incubated at 20°C for 48 h in the dark. The inside of the pots as well as the plants was sprayed with a fine mist of sterile distilled water. The pot chambers were then placed inside an inoculation chamber. This consisted of a cube shaped polyethylene boxes with the floor covered with water-soaked newspaper to provide around 100% RH.

After 48 h, the plants were transferred to the glasshouse (24±2°C, 12-h dark/12-h light (fluorescent, 1400 Lux) regime, at around 75% RH), until telia started to develop. For conservation purposes, infected leaves collected from both field surveys and pathogenicity tests were preserved inside paper bags at 3±0.5°C with silica gel to avoid the germination of teliospores.

Isolation and maintenance of rust isolates

Rust cultures were established from a single telium (Thomas *et al*., 2021) from rust-infected material collected at sites 205 (Salta province), 264 (Entre Rios province) and 350 (Formosa province) (Supplementary material). A single telium isolate was obtained using the leaf disc method. The single telium isolate was used to inoculate a plant of the same origin of the telium (site where the rust was collected). Healthy *P. nodiflora* plants were inoculated monthly with *P. lantanae* to ensure a continuous supply of mature telia throughout the experiments.

Biology of *P. lantanae*

Morphological characterization and microscopy

For light microscope observations, a drop of water was placed on a slide, the sori were scraped with a sterile needle and the teliospores were transferred into the drop of water. A coverslip was placed over it.

An Olympus SP350 camera was attached to the microscope eyepieces and photos were taken to illustrate the morphology of the telia and teliospores and characterize the pre-infection development (*i.e*., from teliospore to basidiospore production) of the rust fungus.

For scanning electron microscope observations, a 2.5% glutaraldehyde fixation was performed in 0.067 M phosphate buffer (pH 7.2) and then washed with phosphate buffer (15 min, 3 times). Gradual dehydration was conducted with alcohol and acetone and then critical point drying was done (E3000, Polaron) using CO_2. The samples were mounted in stubs. Finally, gold was evaporated (300 Å) using an Argon plasma metal evaporator (91000 Model 3, Pelco). Microphotographs were taken with a LEO EVO 40 scanning electron microscope at 7.0 kV potential (Mercer & Birbeck, 1972).

Germination studies

Effect of temperature on teliospore germination and basidiospore formation

Twenty days after teliospores had developed on plants, they were scraped from leaves bearing mature telia and further suspended in 5 ml of sterile distilled water (SDW). Aliquots of 0.10 ml were transferred to 9 cm diameter Petri dishes containing water agar (WA) medium were incubated at 10, 15, 20, 25, and 30°C in several growth chambers, one for each temperature. The Petri dishes were wrapped in aluminum foil to exclude light and sealed with adhesive tape. Teliospore germination was examined after 4, 7, 11, 20, 24, and 48 h of incubation. A completely randomized factorial design was used (N=90, n=3). The Petri dish was placed under the compound microscope (Olympus CX 31) at (16x and 40x of lenses eyepiece and objective) 640x, and germination percentages were recorded by randomly selecting 50 teliospores per replicate. A teliospore was considered germinated when the germ tube was observed. Basidiospore formation was determined as the percentage of teliospores producing basidiospores (*i. e*., that has at least one basidiospore in the metabasidium or next to it) (Morin *et al*., 1992b) at 10, 15, 20, 25, and 30°C after 24 h of incubation. Pictures of the Petri dishes were taken using a camera (Olympus SP 350) attached to the Olympus CX 31 microscope. Dishes were sampled destructively.

Effect of heat shock on teliospore germination and basidiospore formation

An experiment was performed in order to test the hypothesis that a heat shock during incubation (*i.e*., high temperature exposure) would influence the capacity of teliospore germination and/or basidiospore formation. Spores were exposed to three different incubation temperature regimes (3 h at 30°C + 21 h at 20°C; 6 h at 30°C + 18 h at 20°C; 24 h at 20°C). Teliospore germination and basidiospore formation were registered after 4, 7, 11, 20, and 24 h of incubation using the same procedure described above. A completely randomized factorial design was used (n=3) (n: number of replicates).

Effect of teliospore age on germination capacity

Final germination was assessed on WA after 48 h of incubation at 20°C after different periods of storage: 2, 5, 7,

12, and 18 months. Storage time was defined as the time between the harvest of the teliospores until the end of storage. The leaves with telia collected from inoculated plants were kept inside paper bags with silica gel in a refrigerator at 3.0±0.5°C. A completely randomized factorial design was used (n=3).

Pathogenicity tests

Pathogenicity tests determine the ability of a pathogen to provoke diseases. These tests are essential studies when a rust is proposed as a potential biocontrol of a weed (Fourie & Wood, 2018). The tests were conducted to confirm if *P. lantanae* could infect the three varieties of *P. nodiflora*. Also, the level of *in vitro* damage was determined.

Telia collected from fields and obtained from the laboratory plants were used for inoculations. Three experiments were designed. Telia taken from plants of *P. nodiflora* var. *nodiflora* (site 350) and from *P. nodiflora* var. *reptans* (from sites 264 and 205) (see Supplementary material) were inoculated on plants of the three varieties (plants from sites 205, 264, 345, 350). Those plant specimens inoculated with telia of the same origin, were considered as positive controls for the pathogenicity test.

Pathogenicity tests were performed using the leaf disc method (Morin *et al*., 1993). Infection was checked daily and ranked using categories proposed by Ellison *et al*. (2008): 0 - without macroscopic symptoms; 1 - chlorosis; 2 - between 1-5 telia on leaves and stems, localized infection; 3 - more than 5 telia, until semi-systemic infection.

Statistical analysis

Germination percentages and basidiospore formation data were analyzed with ANOVA followed by a mean comparison test (protected LSD Fisher, $P<0.05$). Analyses of variance were performed using InfoStat software (Di Rienzo *et al*., 2013).

Results and discussion

Field surveys and collection of rust isolates

Puccinia lantanae was found only in locations from Argentina (Entre Rios, Formosa, Jujuy, and Salta). None of the populations of *P. nodiflora* in Bolivia or Chile showed symptoms of rust infection. To give a definitive conclusion on the distribution of the rust infecting *Phyla* in South America, it would be necessary to make more extensive collecting. The rust was observed only in five sites. Its prevalence was low (2%). Mostly it was collected on plants belonging to the var. *reptans* (four sites) and it was found infecting *P. nodiflora* var. *nodiflora* in only one site of the several visited. The prevalence of the rust was 2%.

TABLE 1. Rust collection sites and dates. Pnr: *Phyla nodiflora* var. *reptans.* Pnn: *Phyla nodiflora* var. *nodiflora*.

Site	Host	Date
205. Rt 34.11 km S Pichanal. Salta province	Pnr	12 December 2005 20 June 2007 26 January 2008 23 July 2008 30 March 2009 13 November 2009 22 July 2010 13 January 2011 28 August 2011
264. Parque Nacional Predelta, Entre Ríos province	Pnr	1 June 2006 24 February 2009 10 November 2009 10 January 2011
292. 7 km N Gral. San Martin. Parque Nacional Calilegua. Jujuy province	Pnr	28 August 2006 11 November 2006 11 February 2007 20 June 2007 27 January 2008
300. Dique Itiyuro. 3 km S Salvador Mazza. Salta province	Pnr	21 June 2007
350. Rt 81, Km 1682, 60 km NO Guillermo Juarez. Formosa province	Pnn	24 July 2008 22 February 2009 12 November 2009 17 February 2010 22 July 2010 12 January 2011

Telia were observed in pustules of 5 mm of diameter. On leaves, telia were mostly hypophyllous, rounded, isolated, or arranged in concentric circles causing early defoliation of infected plants (Fig. 2A). Symptoms on leaves were characterized by chlorotic spots on the adaxial side corresponding with telia on the abaxial side. Under high humidity conditions, germination of basidiospores was evidenced as a hyaline layer covering the telia (Fig. 2B).

Biology of *Puccinia lantanae*

Morphological characterization and microscopy

The rust produced one- and two-celled golden-brown teliospores (Fig. 2C). The one-celled were ovoid to ellipsoidal, 17-28.5 x 13.5-23 µm. The two-celled spores were ellipsoidal to clavate, constricted at the septum,

23-36 x 12-23 µm, with thick walls, 1.5-2 µm laterally, and 5-7 µm at the apices. Two-celled spores with an oblique septum were rarely observed. In all the teliospores, the pedicel was persistent, sometimes eccentrically inserted (Fig. 2D). A germ pore was often clear on the distal end of the cells (Fig. 2F). When germinating, two-celled teliospores formed one or two germ tubes as observed in other *Puccinia* species (Alexopoulos *et al*., 1996) (Fig. 2G). Occasionally, germ tubes ramified, but these did not develop metabasidia (Fig. 2H). Basidiospores were hyaline, ellipsoidal to shortly oval (Fig. 2E).

The commonest teliospores (about 75-80% of the population) were one-celled. Thomas *et al*. (2021) also considered this type as the dominant one on *Lantana camara*, recording abundances of up to 96%. The one-celled spores showed the same mean size as the teliospores formed by the same rust species on *L. camara*, but the two-celled spores were narrower than those measured on that host (Thomas *et al*., 2021). The constriction at the septum was reported by Barreto *et al*. (1995) also in teliospores developing on *L. camara*. Therefore, the rust species of the present research was confirmed through morphological studies.

Germination studies

Effect of temperature on teliospore germination and basidiospore formation

Two processes were observed, (i) germination of teliospores with germ tube and (ii) four-celled metabasidia (Fig. 2I), and formation of basidiospore. Not all the teliospores germinated and not all the germ tubes developed a metabasidium with basidiospores.

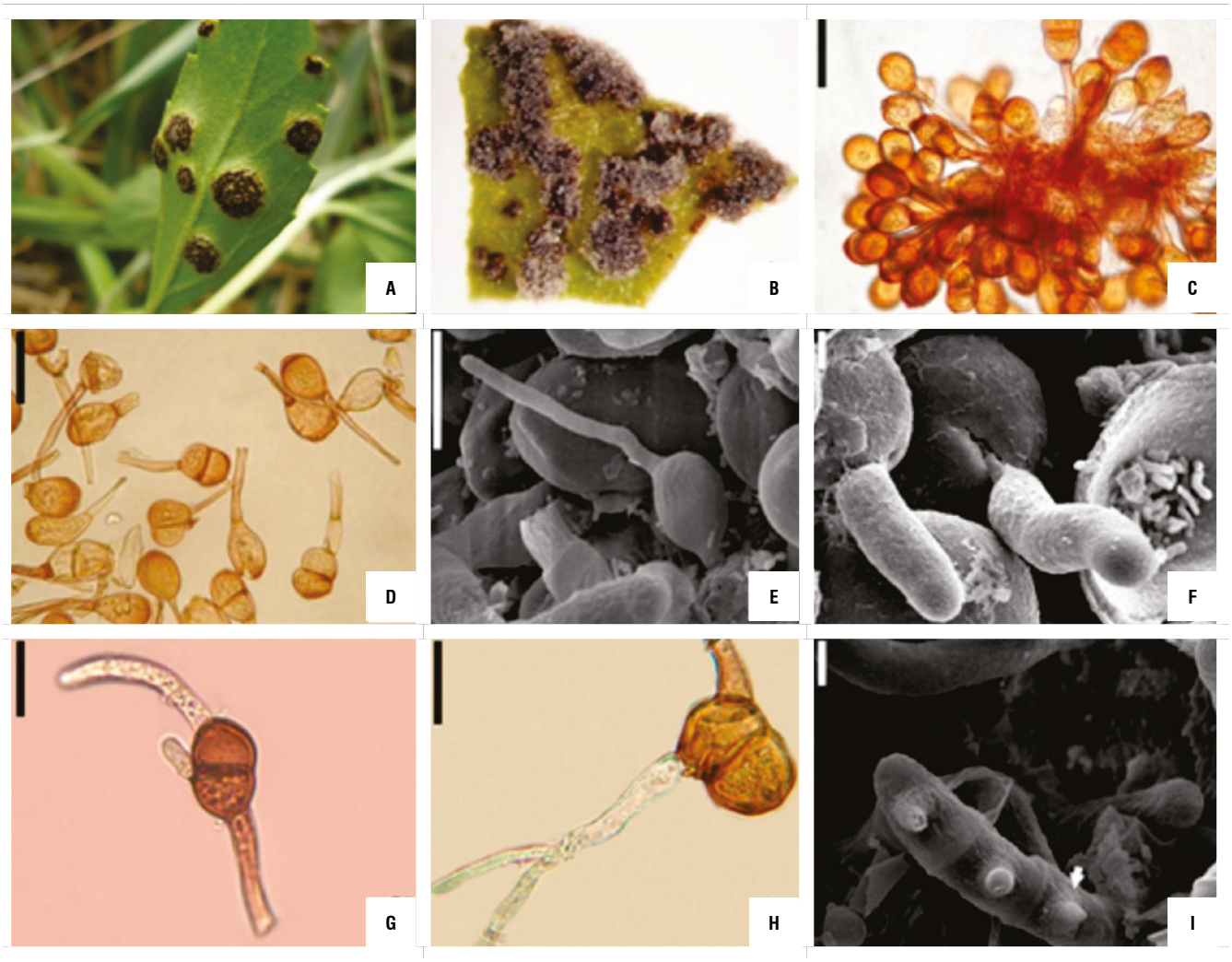

FIGURE 2. Telia of *Puccinia lantanae*. A) Infection symptoms in the field, B) Hyaline formation over telia of an infected leaf, C) One-celled and two-celled teliospores, D) Pedicel eccentrically inserted, E) Germinated basidiospore, F) Germ pore, G) Two-celled teliospores form two germ tubes, H) Ramification of germ tube, I) Metabasidia with conical sterigma. Bars: C and D: 30 μm, E: 10 μm, F: 2 μm, G: 20 μm, H: 15 μm, I: 3 μm.

Teliospore germination was influenced predominantly by temperature. As observed in Figure 3, the highest germination values were registered at 20°C at each incubation time ($P<0.05$). The same result was obtained by Thomas *et al.* (2021), working with an Amazonian pathotype of *P. lantanae* on *L. camara*. According to Thomas *et al.* (2021), the maximum infection on *L. camara* was obtained at 20°C. In the present study, the lowest germination figures were obtained at 30°C, while no infection was found on *L. camara* at 30°C (Thomas *et al.*, 2021). The germination started over a period ranging between four and 7 h of incubation (Fig. 3). Koutsidou (personal communication, August 21, 2020) obtained similar germination rates working with the Amazonian isolate of *P. lantanae* from *L.camara*.

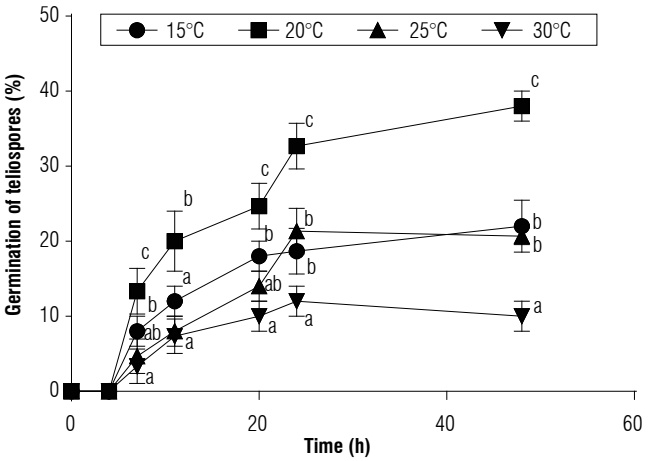

FIGURE 3. Germination of teliospores of *Puccinia lantanae* at different constant temperature regimes as a function of incubation time. Different letters indicate statistical differences among means (protected LSD Fisher test, $P<0.05$) at each incubation time. No teliospore germination was registered at 10°C. Bars show standard error.

The percentage of teliospores that produced basidiospores was determined at 10, 15, 20, 25, and 30°C (Fig. 4). No basidiospores formed at 10°C. At 20°C most of the teliospores formed metabasidia and produced basidiospores. Basidiospore development was inhibited or prevented by extreme temperatures. As observed in Figure 4, the optimum temperature for basidiospore formation was 20°C. Wide metabasidia with long sterigmata and long germ tubes did not form basidiospores. Similarly, Morin *et al.* (1992a) observed the branching of the germ tube, long germ tubes and wide basidia while working with *Puccinia xanthii* Schw. Abnormal germination can occur when telia are exposed to either sub or supraoptimal temperatures. However, the nuclear state of the mycelium which is formed from the long germ tubes needs to be addressed to establish its effective infection capacity.

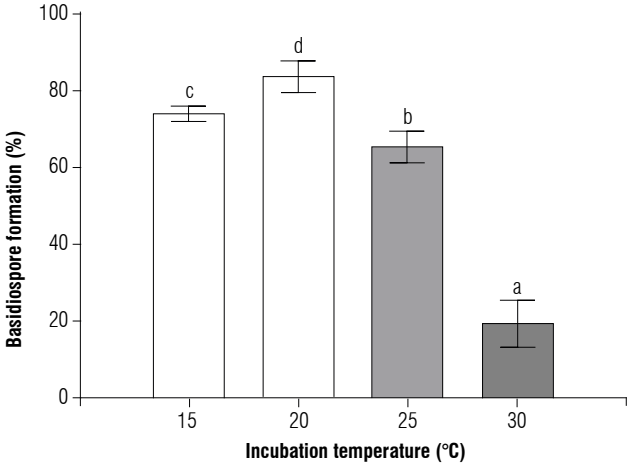

FIGURE 4. Basidiospore development of *Puccinia lantanae* at different constant temperature regimes after 24 h of incubation. Different letters indicate statistical differences among means (protected LSD Fisher test, $P<0.05$). Bars show standard error (n=3).

After 24 h of incubation at 20°C, four conical sterigma developed (Fig. 2I). Most of the basidiospores germinated while still joined to the sterigma or close to it as a common cytological phenomenon in WA.

Effect of heat shock on teliospore germination and basidiospore formation

The effect of high temperatures on the germination of teliospores was evaluated. Teliospore germination and basidiospore formation were influenced by the interaction between temperature and incubation time. Both heat shock treatments significantly reduced teliospore germination (75% in average) and basidiospore formation (64% in average) compared to the control (Figs. 5-6). Basidiospores

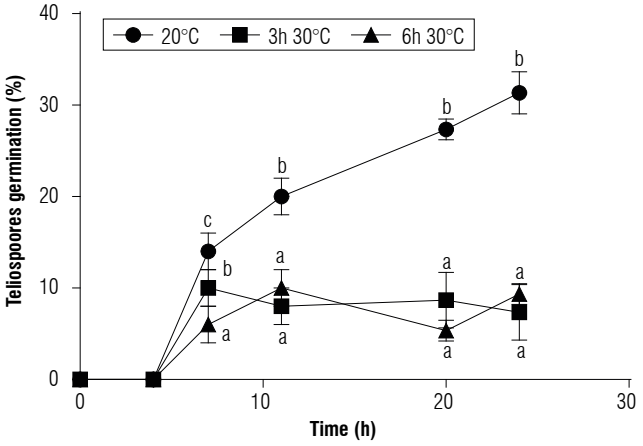

FIGURE 5. Effect of heat shock on germination of teliospores of *Puccinia lantanae*. Teliospores were incubated at 20°C for 24 h (control), 3 h at 30°C + 21 h at 20°C, or 6 h at 30°C + 18 h at 20°C. Different letters indicate statistical differences among means (protected LSD Fisher test, $P<0.05$) at each incubation time. Bars show standard error (n=3).

formed in a sequential manner under high humidity conditions (Fig. 6) as well as in *P. araujiae*, thus, increasing the period over which the inoculum is produced and is available for new infections to take place (Anderson *et al*., 2016). Similar observations were reported by Morin *et al*. (1993) in *P. xanthii*.

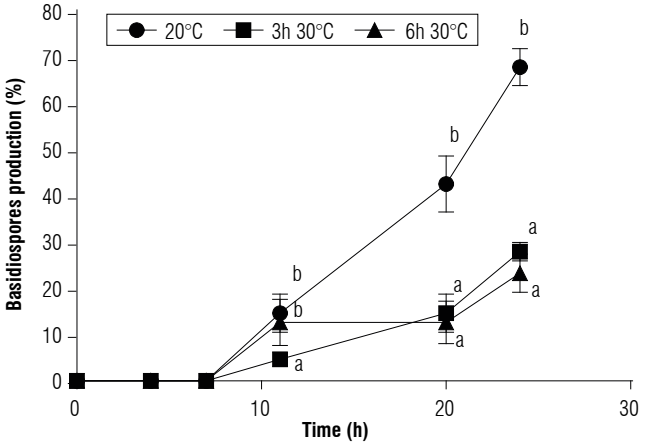

FIGURE 6. Effect of heat shock on formation of basidiospores of *Puccinia lantanae*. Teliospores were incubated at 20ºC for 24 h (control), 3 h at 30ºC + 21 h at 20ºC, or 6 h at 30ºC + 18 h at 20ºC. Different letters indicate statistical differences among means (protected LSD Fisher test, $P<0.05$) at each incubation time. Bars show standard error (n=3).

Effect of teliospores storage on germination

Storage on teliospore germination showed a negative exponential pattern (Fig. 7). A 50% reduction on germination was recorded after 7.2 months of storage at 3.0±0.5ºC.

Pathogenicity tests

The first symptoms of *P. lantanae* on *P. nodiflora* plants were visible after 15-20 d. Sporulation occurred mainly

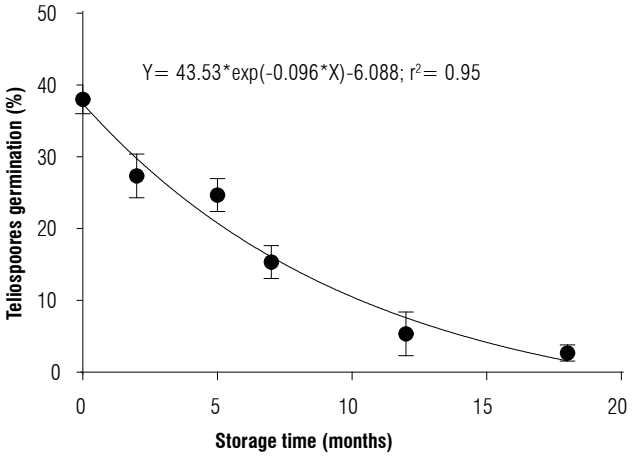

FIGURE 7. Effect of teliospore age of *Puccinia lantanae* on germination after 48 h of incubation at 20ºC. Different letters indicate statistical differences among means (protected LSD Fisher test, $P<0.05$). Bars show standard error (n=3).

on the lower surface of the leaves. The rust caused significant damage to *P. nodiflora*, infecting leaf, petiole, and stem tissues, resulting in cankering and stem die-back as premature leaf drop.

The different symptoms that the three varieties of *Phyla nodiflora* plants developed after being inoculated with teliospores from different sample sites are shown in Table 2. Inoculation was considered successful when plants exhibited low or high levels of infection (Reaction 2 and 3). Only the *Puccinia lantanae* isolate R350n ("Formosa isolate") produced infection on all the varieties of *P. nodiflora*. *Phyla nodiflora* var. *nodiflora* was the variety that exhibited most resistance to infection. The rust isolates R264r ("Entre Rios isolate") and R205r ("Salta isolate"), both from *P. nodiflora* var. *reptans,* were successfully inoculated on *P.*

TABLE 2. Results of the inoculations with *Puccinia lantanae* on *Phyla nodiflora* (leaf disc method).

Experiment Nº	Inoculum source (site of origin)	Inoculated on	Reaction				Plants with symptoms	Plants inoculated (N: total number)
			0[1]	1	2	3		
1	R350n[2]	Pnr205[3]	0	4	12	2	16	18
		Pnm345	1	0	10	7	17	18
		Pnn350	4	6	8	0	14	18
2	R264r	Pnm345	0	3	4	11	18	18
		Pnn350	13	5	0	0	5	18
		Pnr264	2	5	0	11	16	18
3	R205r	Pnr205	0	3	3	12	18	18
		Pnm345	0	2	10	6	18	18
		Pnn350	11	7	0	0	7	18

[1] Reaction: (0) plants without symptoms, (1) chlorotic spots, (2) low level of sporulation (localized infection, 1-5 pustules) and (3) high level of disease (more than 5 pustules until semisistemic infection).

[2] Strain of the fungus. For example: R350n means that the strain of the rust (R) was originally found in site 350 on var. *nodiflora* plants.

[3] Inoculated plants, for example: Pnr205 means that *Phyla nodiflora* var. *reptans* was obtained from site 205.

N: 162

nodiflora var. *minor* and *P. nodiflora* var. *reptans*. These rust isolates would be potential candidates for biocontrol of the target weed.

Conclusions

The rust *Puccinia lantanae* exhibited pathogenicity on three varieties of *Phyla nodiflora,* including *P. nodiflora* var. *minor*, which is a weed with serious impact in Australia. However, some features of the fungal biology could alter its effectivity. The rust showed a mesophilic behavior; higher temperatures negatively influenced both the germination of teliospores as the development of basidiospores. In addition, aging also affected teliospores, diminishing their capacity of germination after five months of storage. Of the three isolates of *P. lantanae* studied, two are promising candidates for biocontrol of the weed but one should be disregarded as it infects *P. nodiflora* var. *nodiflora*, which is native to Australia. This study demonstrates that there are differences between isolates of the same pathogen, which is why in-depth genetical studies of potential agents are necessary as part of a biocontrol study.

Acknowledgments

We thank Dr. Mic Julien and Dr. Louise Morin for their useful advice. We acknowledge Dr. Victoria Cardo for her fieldwork assistance. GT held a scholarship from CSIRO Entomology (Australia) to develop a thesis. This research was supported by grants from Agencia Nacional de Promoción Científica y Tecnológica MINCyT (PICT-2016-1575) and CSIRO Entomology.

Conflict of interest statement

The authors declare that there is no conflict of interests regarding the publication of this article.

Author´s contributions

GT and GC designed the study. GT developed research within six-year field surveys and wrote the manuscript. AS performed field surveys with GT. GC and VB performed statistical analyses and in collaboration with AS contributed to manuscript content and revisions. All authors reviewed the final version of the manuscript.

Literature cited

Agrios, G. N. (2005). *Plant pathology*. Elsevier.

Alexopoulos, C. J., Mims, C. W., & Blackwell, M. (1996). *Introductory mycology*. John Willey and Sons, Inc.

Anderson, F. E., López, S. P. S., Sánchez, R. M., Fuentealba, C. G. R., & Barton, J. (2016). *Puccinia araujiae*, a promising classical biocontrol agent for moth plant in New Zealand: biology, host range and hyperparasitism by *Cladosporium uredinicola*. *Biological Control*, *95*, 23–30. https://doi.org/10.1016/j.biocontrol.2015.12.015

Anikster, Y., Szabo, L. J., Eilam, T., Manisterski, J., Koike, S. T., & Bushnell, W. R. (2004). Morphology, life cycle biology, and DNA sequence analysis of rust fungi on garlic and chives from California. *Phytopathology*, *94*(6), 569–577.

Barreto, R. W., Evans, H. C., & Ellison, C. A. (1995). The mycobiota of the weed *Lantana camara* in Brazil, with particular reference to biological control. *Mycological Research*, *99*(7), 769–782. https://doi.org/10.1016/S0953-7562(09)80725-9

Cabrera, N., Sosa, A., Telesnicki, M., & Julien, M. (2016). Morphology of juvenile stages of Kuschelinabergi (Harold) with biological information (Coleoptera, Chrysomelidae, Alticini). *ZooKeys*, (561), Article 51. https://doi.org/10.3897/zookeys.561.5950

Cummins, G. B., & Hiratsuka, Y. (2003). *Illustrated genera of rust fungi* (3rd ed.). APS Press.

Di Rienzo, J. A., Casanoves, F., Balzarini, M. G., González, L., Tablada, M., & Robledo C. W. (2013). *InfoStat version 2013*. Grupo InfoStat, Universidad Nacional de Córdoba. https://www.infostat.com.ar

Earl, J. (2003). *The distribution and impacts of lippia (*Phyla canescens*) in the Murray Darling system* (Report). Agricultural Information & Monitoring Services.

Ellis, M. B. (1976). *More dematiaceous hyphomycetes*. Commonwealth Mycological Institute. https://doi.org/10.1079/9780851983653.0000

Ellison, C. A., & Cortat, G. (2011). *Assessment of the suitability of the rust fungus Puccinia lantanae for release as a classical biological control agent against Lantana camara in Australia* (Report VM10038). CABI.

Ellison, C. A., Evans, H. C., Djeddour, D. H., & Thomas, S. E. (2008). Biology and host range of the rust fungus *Puccinia spegazzinii*: a new classical biological control agent for the invasive, alien weed *Mikania micrantha* in Asia. *Biological Control*, *45*(1), 133–145. https://doi.org/10.1016/j.biocontrol.2007.12.001

Farr, D. F., Bills, G. F., Chamuris, G. P., & Rossman, A. Y. (1989). *Fungi on plants and plant products in the United States*. APS Press.

Fourie, A., & Wood, A. R. (2018). The rust fungus *Puccinia arechavaletae*, a potential biological control agent of balloon vine (*Cardiospermum grandiflorum*) in South Africa. I: Biology. *Australasian Plant Pathology*, *47*(4), 379–387. https://doi.org/10.1007/s13313-018-0569-5

Gross, C. L., Fatemi, M., Julien, M., McPherson, H., & Van Klinken, R. (2017). The phylogeny and biogeography of *Phyla nodiflora* (Verbenaceae) reveals native and invasive lineages throughout the world. *Diversity*, *9*(2), Article 20. https://doi.org/10.3390/d9020020

Hernández, J. R., & Hennen, J. F. (2002). Rust fungi (Uredinales) of northwest Argentina. *SIDA*, *Contributions to Botany*, *20*(1), 313–338.

Jackson, H. S. (1932). The rusts of South America based on the Holway collections—VI. *Mycologia*, *24*(1), 62–186.

Julien, M., Sosa, A., Traversa, G., & Van Klinken, R. (2012). *Phyla canescens* (Kunth) Greene–lippia. In J. Cullen, M. Julien, & R. McFadyen (Eds.), *Biological control of weeds*

in Australia (pp. 463–471). CSIRO Publishing. https://doi.org/10.1071/9780643104204

Lindquist, J. C. (1982). *Royas de la República Argentina y zonas limítrofes*. Instituto Nacional de Tecnología Agropecuaria.

Mercer, E. H., & Birbeck, M. S. (1972). *Electron microscopy: a handbook for biologists*. Blackwell Scientific.

Morin, L., Auld, B. A., & Brown, J. F. (1993). Host range of *Puccinia xanthii* and postpenetration development on *Xanthium occidentale*. *Canadian Journal of Botany*, *71*(7), 959–965. https://doi.org/10.1139/b93-108

Morin, L., Brown, J. F., & Auld, B. A. (1992a). Effects of environmental factors on teliospore germination, basidiospore formation, and infection of *Xanthium occidentale* by *Puccinia xanthii*. *Phytopathology*, *82*(12), 1443–1447. https://doi.org/10.1094/phyto-82-1443

Morin, L., Brown, J. F., & Auld, B. A. (1992b). Teliospore germination, basidiospore formation and the infection process of *Puccinia xanthii* on *Xanthium occidentale*. *Mycological Research*, *96*(8), 661–669. https://doi.org/10.1016/s0953-7562(09)80494-2

Morin, L., Neave, M., Batchelor, K., & Reid, A. (2006). Biological control: a promising tool for managing bridal creeper, *Asparagus asparagoides* (L.) Druce, in Australia. *Plant Protection Quarterly*, *21*(2), 69–67. https://www.cabi.org/isc/abstract/20063166393

Munir, A. A. (1993). A taxonomic revision of the genus *Phyla* Lour. (Verbenaceae) in Australia. *Journal of the Adelaide Botanic Garden*, *15*(2), 109–128.

O'Leary, N., & Múlgura, M. E. (2012). A taxonomic revision of the genus *Phyla* (Verbenaceae). *Annals of the Missouri Botanical Garden*, *98*(4), 578–596. https://doi.org/10.3417/2009120

Rentería, J. L., & Ellison, C. (2004). Potential biological control of *Lantana camara* in the Galapagos using the rust *Puccinia lantanae*. *SIDA, Contributions to Botany*, *21*(2), 1009–1017.

Sosa, A. J., Cardo, M. V., & Julien, M. H. (2017). Predicting weed distribution at the regional scale in the native range: environmental determinants and biocontrol implications of *Phyla nodiflora* (Verbenaceae). *Weed Research*, *57*(3), 193–203.

Thomas, S. E., Evans, H. C., Cortat, G., Koutsidou, C., Day, M. D., & Ellison, C. A. (2021). Assessment of the microcyclic rust *Puccinia lantanae* as a classical biological control agent of the pantropical weed *Lantana camara*. *Biological Control*, *160*, Article 104688. https://doi.org/10.1016/j.biocontrol.2021.104688

Viégas, A. P. (1961). *Índice de fungos da América do Sul*. Instituto Agronomico.

Waller, J. M., Lenné, J. M., & Waller, S. J. (Eds.). (2002). *Plant pathologist's pocketbook* (No. 632.3/W198). CABI Publishing.

Supplementary material

TABLE S1. Sites visited to sample *P. nodiflora* var. *minor*, *P. nodiflora* var. *reptans* and *P. nodiflora* var. *nodiflora* and *P. lantanae* in southern South America. ND stands for no data available.

GPS	Code	Latitude (South)	Longitude (West)	Country	GPS	Code	Latitude (South)	Longitude (West)	Country
10	1	25.51	64.98	Argentina	203	32	24.27	64.85	Argentina
11R	2	ND	ND	Argentina	204	33	24.00	64.55	Argentina
18	3	27.51	64.89	Argentina	205	34	23.40	64.30	Argentina
33	4	37.17	59.42	Argentina	206	35	23.93	64.04	Argentina
34	5	36.85	59.89	Argentina	207	36	24.99	64.59	Argentina
53	6	29.14	59.24	Argentina	208	37	25.03	64.58	Argentina
81	7	27.43	58.85	Argentina	209	38	24.91	64.42	Argentina
92	8	37.19	59.05	Argentina	210	39	25.50	63.60	Argentina
126	9	35.01	58.75	Argentina	211	40	25.82	62.82	Argentina
128	10	32.08	60.59	Argentina	212	41	26.22	61.86	Argentina
144	11	34.60	60.96	Argentina	213	42	27.22	62.10	Argentina
150	12	27.94	63.41	Argentina	214	43	27.93	65.59	Argentina
180	13	22.87	64.36	Argentina	215	44	31.55	61.44	Argentina
184	14	29.61	57.22	Argentina	216	45	28.31	63.36	Argentina
186	15	34.46	60.04	Argentina	217	46	35.45	58.79	Argentina
187	16	34.45	61.87	Argentina	218	47	40.17	62.65	Argentina
188	17	34.13	63.40	Argentina	219	48	40.71	64.07	Argentina
189	18	33.60	65.30	Argentina	220	49	40.26	65.11	Argentina
190	19	33.30	65.88	Argentina	221	50	39.17	66.13	Argentina
191	20	32.85	65.47	Argentina	222	51	39.09	67.57	Argentina
192	21	32.29	65.69	Argentina	223	52	39.55	69.31	Argentina

Continued

GPS	Code	Latitude (South)	Longitude (West)	Country	GPS	Code	Latitude (South)	Longitude (West)	Country
193	22	31.80	65.00	Argentina	224	53	40.66	71.35	Argentina
194	23	30.62	65.47	Argentina	225	54	39.93	71.06	Argentina
195	24	29.70	66.80	Argentina	226	55	37.62	70.16	Argentina
196	25	28.45	66.87	Argentina	227	56	36.64	69.83	Argentina
197	26	27.22	66.82	Argentina	228	57	35.08	69.59	Argentina
198	27	26.06	65.95	Argentina	229	58	33.62	69.01	Argentina
199	28	25.58	65.57	Argentina	230	59	33.12	68.53	Argentina
200	29	24.72	65.50	Argentina	231	60	33.43	66.94	Argentina
201	30	23.92	65.46	Argentina	232	61	37.36	59.10	Argentina
202	31	23.68	65.44	Argentina	233	62	37.58	58.74	Argentina
234	63	38.54	58.64	Argentina	270	93	27.87	63.97	Argentina
235	64	38.52	60.51	Argentina	271	94	27.99	64.01	Argentina
236	65	38.71	60.45	Argentina	272	95	22.97	64.37	Argentina
237	66	38.98	61.28	Argentina	273	96	25.25	64.47	Argentina
243	67	30.05	59.53	Argentina	274	97	25.23	64.05	Argentina
244	68	29.02	59.17	Argentina	276	98	24.23	63.98	Argentina
245	69	28.34	58.43	Argentina	277	99	24.73	64.20	Argentina
246	70	27.97	57.58	Argentina	278	100	24.73	64.21	Argentina
247	71	27.63	56.83	Argentina	279	101	24.72	64.64	Argentina
248	72	27.77	55.81	Argentina	280	102	25.91	61.71	Argentina
249	73	27.75	57.25	Argentina	282	103	38.59	61.89	Argentina
250	74	27.55	58.52	Argentina	283	104	37.33	57.06	Argentina
251	75	27.12	58.97	Argentina	284	105	36.85	56.69	Argentina
252	76	26.48	58.28	Argentina	285	106	36.34	56.74	Argentina
253	77	26.48	58.29	Argentina	289	107	33.93	64.44	Argentina
254	78	26.02	58.39	Argentina	291	108	23.87	65.45	Argentina
255	79	25.58	59.23	Argentina	292	109	23.75	64.85	Argentina
256	80	25.23	59.87	Argentina	293	110	25.74	64.94	Argentina
257	81	25.34	59.94	Argentina	294	111	26.51	64.75	Argentina
258	82	25.62	60.08	Argentina	295	112	26.46	64.74	Argentina
259	83	27.07	59.71	Argentina	297	113	36.26	61.69	Argentina
260	84	30.07	58.00	Argentina	298	114	24.10	64.82	Argentina
261	85	30.60	58.47	Argentina	299	115	22.74	63.82	Argentina
262	86	31.24	59.24	Argentina	300	116	22.10	63.73	Argentina
263	87	31.71	60.53	Argentina	301	117	16.19	67.72	Bolivia
264	88	32.11	60.63	Argentina	302	118	16.22	67.68	Bolivia
265	89	32.11	60.63	Argentina	303	119	16.18	67.73	Bolivia
267	90	33.15	59.29	Argentina	304	120	16.21	68.85	Bolivia
268	91	24.73	64.64	Argentina	305	121	18.91	63.39	Bolivia
269	92	30.12	62.10	Argentina	306	122	18.64	63.29	Bolivia
310	123	34.56	59.37	Argentina	342	152	29.71	63.73	Argentina
311	124	34.46	59.51	Argentina	343	153	30.92	62.68	Argentina
312	125	34.63	60.51	Argentina	344	154	31.53	61.54	Argentina
313	126	34.60	61.01	Argentina	345	155	38.70	62.27	Argentina
314	127	34.84	61.50	Argentina	346	156	39.08	64.56	Argentina
315	128	35.51	63.00	Argentina	347	157	23.03	63.90	Argentina
316	129	35.91	62.82	Argentina	350	158	23.70	62.31	Argentina
317	130	36.90	62.39	Argentina	351	159	25.76	59.12	Argentina
318	131	38.01	63.34	Argentina	352	160	26.16	59.35	Argentina

Continued

GPS	Code	Latitude (South)	Longitude (West)	Country	GPS	Code	Latitude (South)	Longitude (West)	Country
321	132	36.70	64.28	Argentina	354	161	26.84	59.05	Argentina
322	133	35.50	64.10	Argentina	355	162	27.10	58.96	Argentina
323	134	35.04	64.26	Argentina	357	163	27.90	59.27	Argentina
324	135	29.88	61.26	Chile	359	164	36.76	56.70	Argentina
325	136	27.37	70.34	Chile	370	165	39.05	64.39	Argentina
326	137	28.56	70.81	Chile	371	166	39.30	65.66	Argentina
327	138	29.94	70.34	Chile	372	167	39.28	65.67	Argentina
328	139	31.87	71.40	Chile	373	168	37.33	66.49	Argentina
329	140	32.83	71.48	Chile	374	169	36.96	66.72	Argentina
330	141	33.52	71.60	Chile	375	170	34.86	67.78	Argentina
331	142	33.82	70.17	Chile	376	171	34.09	66.71	Argentina
332	143	35.46	72.48	Chile	378	172	26.77	59.71	Argentina
333	144	36.84	73.10	Chile	379	173	26.77	59.71	Argentina
334	145	37.25	73.32	Chile	381	174	26.95	59.85	Argentina
336	146	27.71	64.47	Argentina	382	175	25.54	60.02	Argentina
337	147	26.81	65.24	Argentina	383	176	25.49	59.98	Argentina
338	148	23.92	65.46	Argentina	386	177	24.34	61.13	Argentina
339	149	24.06	65.42	Argentina	387	178	27.41	58.84	Argentina
340	150	27.95	64.22	Argentina	388	179	27.33	58.44	Argentina
341	151	28.30	64.18	Argentina	390	180	27.39	64.31	Argentina
391	181	26.21	64.63	Argentina	ND12	200	38.39	62.85	Argentina
392	182	24.54	65.37	Argentina	ND13	201	37.86	63.80	Argentina
401	183	24.78	65.04	Argentina	ND14	202	37.12	64.29	Argentina
403	184	26.23	65.24	Argentina	ND15	203	36.40	64.28	Argentina
404	185	27.68	65.23	Argentina	ND16	204	35.95	64.28	Argentina
405	186	28.62	65.10	Argentina	ND17	205	34.11	64.38	Argentina
406	187	28.51	64.87	Argentina	ND18	206	34.16	64.38	Argentina
407	188	28.63	64.09	Argentina	ND19	207	34.72	64.42	Argentina
ND1	189	ND	ND	Argentina	ND20	208	33.28	64.42	Argentina
ND2	190	ND	ND	Argentina	ND21	209	33.00	64.16	Argentina
ND3	191	ND	ND	Argentina	ND22	210	33.02	63.59	Argentina
ND4	192	34.80	61.97	Argentina	ND23	211	33.12	63.08	Argentina
ND5	193	34.88	62.65	Argentina	ND24	212	33.21	62.59	Argentina
ND6	194	35.06	62.99	Argentina	ND25	213	33.30	62.05	Argentina
ND7	195	ND	ND	Argentina	ND26	214	33.59	61.47	Argentina
ND8	196	36.50	62.63	Argentina	ND27	215	33.84	61.73	Argentina
ND9	197	37.66	62.45	Argentina	ND28	216	34.18	61.51	Argentina
ND10	198	38.03	62.31	Argentina	ND29	217	34.58	61.00	Argentina
ND11	199	38.49	62.38	Argentina					

Ocimum gratissimum L.: A natural alternative against fungi associated with bean and maize seeds during storage

Ocimum gratissimum L.: una alternativa natural contra hongos asociados con semillas de frijol y maíz durante el almacenamiento

Juliana Trindade Lima[1], Antonio Fernando de Souza[2], and Hildegardo Seibert França[3]*

ABSTRACT

The aim of the study was to evaluate *in vitro* antioxidant and antifungal activities of the ethanolic extract and its fractions from *Ocimum gratissimum* leaves. The ethanolic extract was obtained by maceration in ethanol and subsequent fractionation with solvents of increasing polarity (hexane, dichloromethane, ethyl acetate and butanol). The Minimum Inhibitory Concentration (MIC) was determined for the ethanol extract and dichloromethane fraction. The antioxidant capacity was evaluated by DPPH (2,2-diphenyl-1-picryl-hydrazyl-hydrate) and ABTS (2,2'-azino-bis(3-ethylbenzothiazoline-6-sulfonic acid)) free radical scavenging methods, and by FRAP (Ferric Reducing Antioxidant Power). The *in vitro* antifungal effect was determined by the agar diffusion method on *Aspergillus* sp. and *Rhizopus* sp. fungi associated with corn and bean seeds during storage. The best samples with antifungal effect were determined by gas chromatography-mass spectrometry (GC/MS). The ethanolic extract had strong antioxidant capacity for all tested methods (DPPH 371.10±2.98 µg ml^{-1}, ABTS 182.43±1.10 µg ml^{-1}, FRAP 262.39±3.61 TEAC). Regarding the antifungal activity, the ethanolic extract and dichloromethane fraction resulted in total suppression (100%) of fungal growth and MIC ranged from 0.625 to 1.25 mg ml^{-1}. In the GC/MS analysis, 22 substances were detected in all samples evaluated, with predominance of eugenol. These results indicated high biological potential of this plant as a biofungicide.

Key words: antifungal activity, antioxidant capacity, *Aspergillus*, *Rhizopus*.

RESUMEN

El objetivo del estudio fue evaluar *in vitro* las actividades antioxidantes y antifúngicas del extracto etanólico y sus fracciones a partir de las hojas de *Ocimum gratissimum*. El extracto etanólico se obtuvo por maceración en etanol y posterior fraccionamiento con disolventes de polaridad creciente (hexano, diclorometano, acetato de etilo y butanol). La Concentración Mínima Inhibitoria (CMI) se determinó para el extracto de etanol y la fracción de diclorometano. La capacidad antioxidante se evaluó mediante los métodos de eliminación de radicales libres DPPH (2,2-difenil-1-picril-hidrazil-hidrato) y ABTS (ácido 2,2'-azino-bis(3-etilbenzotiazolina-6-sulfónico)) por PARF (Poder Antioxidante Reductor Férrico). El efecto antifúngico *in vitro* se determinó mediante el método de difusión de agar sobre hongos *Aspergillus* sp. y *Rhizopus* sp. asociados con semillas de frijol y maíz durante el almacenamiento. Las mejores muestras con efecto antifúngico se determinaron por cromatografía de gases acoplada a espectrometría de masas (CG/EM). El extracto etanólico presentó fuerte capacidad antioxidante para todos los métodos probados (DPPH 371.10±2.98 µg ml^{-1}, ABTS 182.43±1.10 µg ml^{-1}, PARF 262.39±3.61 TEAC). En cuanto a la actividad antifúngica, el extracto etanólico y la fracción de diclorometano mostraron supresión total (100%) del crecimiento fúngico y la CMI varió de 0.625 a 1.25 mg ml^{-1}. En el análisis CG/EM se detectaron 22 sustancias en todas las muestras evaluadas, con predominio de eugenol. Estos resultados indicaron un alto potencial biológico de esta planta como biofungicida.

Palabras clave: actividad antifúngica, capacidad antioxidante, *Aspergillus*, *Rhizopus*.

Introduction

It is estimated that at least 15% of losses during seed storage occur due to product contamination by insects and fungi (Silva *et al*., 2021). Extracts and essential oils from plants have demonstrated ability to inhibit the action of phytopathogens or the production of mycotoxins; these promising biofungicides could mitigate the use of chemical pesticides (Mohr *et al*., 2017). This is due to the presence of compounds from the secondary metabolism of plants. These chemical compounds, such as terpenes, phenolics, and alkaloids are important biological agents that can play

Received for publication: November 16, 2022. Accepted for publication: December 31, 2023 Doi: 10.15446/agron.colomb.v40n3.105851

[1] Graduate Program in Plant Biology, Vitória Campus, Federal University of Espirito Santo, Vitória (Brazil).
[2] Santa Teresa Campus, Federal Institute of Espírito Santo, Santa Teresa (Brazil).
[3] Vila Velha Campus, Federal Institute of Espírito Santo, Vila Velha (Brazil).
* Corresponding author: hildegardo.franca@ifes.edu.br

antifungal roles against species of the genus *Aspergillus*, *Rhizopus*, *Penicillium*, *Colletotrichum* as well as antioxidant roles (Elisée *et al*., 2020).

Natural plant-based products are a more appropriate strategy in agricultural management when compared to commercial fungicides, as they are biodegradable, prevent pathogen resistance, and are less harmful to human health (Chowdhary *et al*., 2018). However, the composition and activity of the bioactive components of plants vary according to genotype, geographic location, and vegetative stage, as well as method, solvent and temperature used in the extraction process (Onyebuchi & Kavaz, 2020). The extraction of secondary metabolites can be performed using a fractionation technique with solvents of different polarities to concentrate chemical groups in distinct fractions with completely different chemical characteristics in a single plant (Mann, 2012).

Ocimum gratissimum L., popularly known as clove basil, is an aromatic herb that belongs to the Lamiaceae family and is found in South America, Africa, and Asia (Mohr *et al*., 2017). It is used as a food condiment and in folk medicine; the infusion of leaves is prepared for the treatment of fever, flu, and kidney problems (Matos, 2007; Penido *et al*., 2016). It has a diversity of chemical groups with proven biological activities due to its anti-inflammatory (Dzoyem *et al*., 2021), insecticidal (Benelli *et al*., 2019), antibacterial (Hamma *et al*., 2020), antioxidant (Onyebuchi & Kavaz, 2020) and antifungal properties against several species of fungi, among them *Aspergillus niger, Botryodiplodia theobromae, Rhizopus stolonifer, Fusarium oxysporium, Penicillium expansum,* and *Colletotrichum* spp. (Uchegbu *et al*., 2019).

The chemical profile of these compounds includes the presence of flavonoids, tannins, sterols, terpenoids, saponins, and alkaloids (Hamma *et al*., 2020). Previous studies have shown that the ethanolic extracts and essential oils obtained from *O. gratissimum* leaves are rich in phenolic compounds with antioxidant and antimicrobial action against various pathogens (Dambolena *et al*., 2010; Elisée *et al*., 2020; Onyebuchi & Kavaz, 2020). The leaves are rich in essential oils, whose main components contain eugenol, thymol, and linalool, with antimicrobial activities already documented in the literature (Faria *et al*., 2006; Mohr *et al*., 2017).

Most studies on the control of phytopathogens have focused on the biological properties of essential oils; there are few data based on extracts and their fractionation from *O. gratissimum* leaves against phytopathogens (Dambolena *et al*., 2010; Mohr *et al*., 2017; Elisée *et al*., 2020). Therefore, the aim of the present study was to evaluate the *in vitro* antifungal and antioxidant capacity and the chemical profile of the most active samples from *O. gratissimum* leaves.

Materials and methods

Collection and botanical identification of the plant species

Collection and botanical identification of *O. gratissimum* L. leaves were done at the Engenheiro Agrônomo Reginaldo Conde (FERC) Experimental Farm of the Institute for Research, Technical Assistance and Rural Extension of Espírito Santo (INCAPER), Viana, Espírito Santo, Brazil, in October 2019.

Preparation of the ethanolic extract and its fractions

The plant extract was prepared at the Laboratory of the Federal Institute of Espírito Santo (Ifes), Vila Velha campus (Brazil). Leaves were dried in an oven with air circulation at 40°C for 24 h and then crushed. To obtain the ethanolic extract (EEtOH), leaves were macerated in 96% ethanol at 1:10 w/v ratio (dryer plant: ethanol), at room temperature and protected from light. Subsequently, the extract was filtered, and the solvent removed on a rotary evaporator (Buchi Rotavapor R-3 CH 9230 Flawil 1, Switzerland). The recovered solvent was added to the leaf residue and crushed again until the plant drug was depleted. The concentrated residue (EEtOH) obtained was stored in amber glass under refrigeration at 4°C. To obtain fractions of different polarities, part of the EEtOH was resuspended in the ethanol-water mixture v/v (8:2) and submitted to successive liquid-liquid partitions with organic solvents of increasing polarities; after total removal of solvents, the following fractions were obtained: hexane (FHex), dichloromethane (FDCM), ethyl acetate (FAce), *n*-butanol (FBuOH), and the aqueous residual (FAq).

Antifungal activity

Mycelial growth inhibition percentage

The experimental design was completely randomized, in a 6x3 +2 factorial scheme, with three replicates. Factor A was composed of six different extracts (EEtOH; FHex; FDCM; FAce; FBuOH and FAq) and factor B was composed of three concentrations (0.1; 5.0, and 10.0 mg ml^{-1}), plus two additional treatments, negative control, and positive control. The negative control did not contain EEtOH or fraction and the positive control was Cercobin® commercial fungicide

based on thiophanate methyl (Dimethyl 4,4'-(o-phenylene) (3-thioallophanate) at 0.8 mg ml^{-1}.

For the *in vitro* antifungal activity evaluation, the agar diffusion method according to Barros *et al*. (1995) was used. The ethanolic extract and fractions were tested on *Aspergillus* sp. and *Rhizopus* sp., isolated from traditional bean and corn seeds and identified at the Laboratory of Diagnosis of Plant Diseases of Federal Institute of Espírito Santo (Ifes), Santa Teresa campus.

Sterilized stock solutions (15 mg ml^{-1}) were diluted in sterilized Potato-Dextrose-Agar (PDA) medium, in a melting state, to obtain final concentrations of 0.1, 5.0, or 10.0 mg ml^{-1} for each sample. Then, the final solutions were poured into 5 cm diameter Petri dishes. The fungi were spiked into the center of each Petri dish. Plates were incubated in a growth chamber (BOD) at 25°C, 12 h photoperiod, until the mycelial growth of the respective fungi in the negative control treatment reached the edge of the plate. Mycelial growth was evaluated by daily measurement of the diameter (in cm) of colonies. The mycelial growth inhibition percentage (GIP) was estimated using the equation (Kordali *et al*., 2003):

$$GIP(\%) = \frac{D_c - D_t}{D_c} \times 100$$

where D_c is average mycelial diameter of the negative control (cm) and D_t is average mycelial diameter of treatments (cm).

Determination of the Minimum Inhibitory Concentration (MIC)

The most promising (due to preview antifungal action in susceptibility tests) samples from *O. gratissimum* leaves were selected for the determination of the Minimum Inhibitory Concentration (MIC). The MIC of the main component of both samples, eugenol, was also evaluated.

The EEtOH and the FDCM were added to PDA to make a 5 mg ml^{-1} stock solution. Serial dilution was performed to obtain concentrations of 5.0, 2.5, 1.25, 0.625, 0.3125, and 0.1 mg ml^{-1}; then the agar diffusion method was performed, as previously mentioned. For evaluation of pure eugenol, a stock solution of 1.0 mg ml^{-1} of pure eugenol in 0.5% DMSO (dimethyl sulfoxide) was prepared; subsequently serial dilutions were performed with final concentrations of 1.0, 0.75, 0.5, 0.25, and 0.125 mg ml^{-1}. They were then incubated for 48 h at 25°C and the fungal growth was observed. The lowest concentration, which inhibits the visible growth of the tested organism after macroscopic evaluation, was determined as Minimum Inhibitory Concentration (MIC) (Talibi *et al*., 2012). All determinations were tested in triplicate.

In vitro antioxidant capacity

DPPH test

The antioxidant capacity of the EEtOH and fractions using the 2,2-diphenyl-1-picryl hydrazyl (DPPH) free radical scavenging was determined according to Casagrande *et al*. (2007), with modifications. Five hundred µl of 250 µM DPPH ethanolic solution was mixed to 30 µl of solutions containing decreasing concentrations of the extracts in ethanol (1000, 500, 250, 125, and 62.5 µg ml^{-1}) plus 1,000 µl of 0.1 M acetate buffer and 1,000 µl of absolute ethanol. The so-called "blank" solution was prepared with ethanol-DPPH mixture. After 30 min of incubation at room temperature, the absorbance was read against a blank at 517 nm in a spectrophotometer. The DPPH radical scavenging activity was expressed as inhibition percentage:

$$IC\%_{(DPPH)} = 100 - \frac{A_{SAMPLE}}{A_{CONTROL}} \times 100$$

where A_{SAMPLE} is the absorbance of treatments, and $A_{CONTROL}$ is the absorbance of control (containing all reagents, except treatment sample).

The antioxidant activity was evaluated based on the IC_{50} value (µg ml^{-1}) extract concentration necessary to scavenge 50% of the DPPH free radical by linear regression using concentration values (µg ml^{-1}) versus inhibition percentage (IC%).

ABTS test

The antioxidant capacity of the EEtOH and fractions was determined using the 2,2-azinobis (3-ethylbenzothiazoline-6-sulfonic acid) (ABTS) free radical according to Sánchez-González *et al*. (2005). $ABTS^{+\bullet}$ cation was produced by reacting 7 mM ABTS stock solution with 2.45 mM potassium persulfate. The mixture was stored in a dark bottle at room temperature for 16 h. The ABTS solution was diluted in phosphate buffer (pH 7.4) to an absorbance of 0.7 at 730 nm. The samples were resuspended in ethanol, generating solutions with concentrations ranging from 62.5 to 1,000.0 µg ml^{-1}. After adding 10 µL of each sample standard to 4 ml of diluted $ABTS^{+\bullet}$ solution, absorbance readings at 730 nm were performed after 6 min of reaction in the spectrophotometer. The antioxidant capacity was

calculated by the inhibition percentage of the ABTS radical activity (IC% (ABTS)), according to the following equation:

$$IC\%_{(ABTS)} = 100 - \frac{A_{SAMPLE}}{A_{CONTROL}} \times 100$$

where A_{SAMPLE} is the absorbance of treatments and $A_{CONTROL}$ is the absorbance of control (containing all reagents except the treatment sample).

The antioxidant activity was evaluated based on the IC_{50} value (μg ml^{-1}) of the extract concentration necessary to scavenge 50% of the ABTS free radical by linear regression using concentration values (μg ml^{-1}) versus percentage inhibition (IC%).

Iron reduction assay (FRAP)

The antioxidant capacity of the EEtOH and fractions was evaluated by reducing iron (FRAP) based on the method of Sánchez-González *et al*. (2005), with some modifications. This method is based on the reduction of the ferric ion (Fe^{3+}) to the ferrous ion (Fe^{2+}) by antioxidant molecules present in the extracts and subsequent formation of a colored complex of the Fe^{2+} and 4,6-tripyridyl-s-triazine (TPTZ). The FRAP reagent was prepared as follows: 2.5 ml of a 10 mM solution of TPTZ in 40 mM HCl were added to 2.5 mL of $FeCl_3.6H_2O$ and 25 mL of 0.3 mM acetate buffer pH 3.6. The solution was incubated at 37°C for 30 min in a water bath. For the evaluation of the antioxidant capacity, 900 μl of the previously prepared FRAP reagent was mixed with 90 μl of distilled water and 10 μl of the sample or standard. The samples were incubated at 37°C for 30 min and the reading was performed at 595 nm in a UV-Visible spectrophotometer (Biospectro SP-220). Standard solutions with different concentrations of Trolox (0.5, 1.0, 2.5, 5.0, 10.0, 15.0, and 20.0 μmol) were used for calibration. Results were expressed as μmol Trolox equivalent/g sample (TEAC - Trolox equivalent antioxidant capacity).

Analysis by gas chromatography coupled to a mass spectrometer

The analyses by gas chromatography coupled with mass spectrometry (GC/MS) were performed at the Laboratory of Chromatography of LabPetro, Federal University of Espírito Santo. The nonpolar fractions that showed the greatest biological effects were analyzed by a gas chromatograph coupled to an Agilent 7890B mass spectrometer (Agilent, CA, USA) and a model 5977A MSD mass detector with electronic ionization of 70 eV. The column used was a 30 m x 250 μm x 0.25 μm HP-5 column. The injector was set to a temperature of 290°C and the detector to 310°C. Elution was done on a heating ramp, starting of 40°C with a heating rate of 5°C/min to 280°C, followed by a heating rate of 15°C/min to 310°C, remaining at that temperature for 10 min.

For characterization, a C10 to C40 alkane standard was used and submitted to the same chromatographic conditions. Compounds were identified through comparison with the National Institute of Standards and Technology (NIST) database library followed by comparison of literature retention rates (NIST, 2018).

Statistical analysis

Mycelial growth inhibition percentage data were submitted to analysis of variance (ANOVA). The interaction between factors was analyzed; later the Tukey test ($P<0.05$) was applied for the factorial group, and the Dunnett test ($P<0.05$) was applied for the comparison of means of the factorial group with additional treatments (positive and negative control), using Assistat 7.6 software.

The antioxidant activity was evaluated using ANOVA followed by the Tukey test ($P<0.05$) using Assistat 7.6 software. All experiments were completed in triplicate to ensure reproducibility.

Results and discussion

The mycelial growth inhibition percentage

Antifungal activity of the samples of *O. gratissimum* at different concentrations against *Aspergillus* sp. and *Rhizopus* sp. fungi is shown in Table 1. For the variable growth inhibition percentage (GIP), there was a significant interaction between the concentrations of the plant extracts tested. The results indicate that EEtOH and FDCM at 5 and 10 mg ml^{-1} had high antifungal activity, with complete suppression (100%) of the mycelial growth of *Aspergillus* sp. and *Rhizopus* sp. These were the only treatments against *Aspergillus* sp. and *Rhizopus* sp. with antifungal activity higher than treatment synthetic fungicide, in 0.8 mg ml^{-1}. Among the polar fractions, FAce at 10 mg ml^{-1} was the most active with GIP of 37.4 and 61% for *Aspergillus* sp. and *Rhizopus* sp., respectively.

Minimum Inhibitory Concentration (MIC)

The MIC results of the most activity samples of *O. gratissimum* and eugenol are found in Table 2. The MIC ranged from 0.625 to 1.25 mg ml^{-1}. The samples FDCM exhibited the lowest MIC with a value of 0.625 mg ml^{-1} for *Aspergillus* sp. and *Rhizopus* sp., while for EEtOH, the MIC for

TABLE 1. Mycelial growth inhibition percentage (GIP) of *Aspergillus* sp. and *Rhizopus* sp. submitted to different ethanolic extract concentrations (mg ml^{-1}) and fractions from *Ocimum gratissimum* leaves.

Treatments	*Aspergillus* sp.			*Rhizopus* sp.		
	0.1	5	10	0.1	5	10
EEtOH	8.6 b	100 a	100 a	5.2 a	100 a	100 a
FHex	7.6 bc	40.7 b	52.5+ b	4.9 a	36 c	47.7 c
FDCM	11.9 a	100 a	100 a	6.1 a	100 a	100 a
FAce	3.7 d	19.3 c	37.4 c	4.7 a	44.5 b	61 b
FBuOH	8.3 b	11.3 d	21.8 d	0* b	3.1 d	8.6+ d
FAq	5.5 cd	10.5 d	19.6 d	0* b	1.5* d	2.8 e
DMSO	0	0	0	0	0	0
Thiophanate methyl	54	54	54	9.8	9.8	9.8

EEtOH: ethanolic extract; FHex: hexane fraction; FDCM: dichloromethane fraction; FAce: ethyl acetate fraction; FBuOH: butanol fraction; FAq: aqueous fraction; DMSO: negative control. Means followed by different lowercase letters in the column differ statistically from each other by the Tukey's test ($P<0.05$). Means followed by * and + do not differ statistically from DMSO and fungicide treatments, respectively (Dunnett; $P>0.05$).

Aspergillus sp. was 1.25 mg ml^{-1} and for *Rhizopus* sp. it was 0.625 mg ml^{-1}. Preliminary chemical analysis showed eugenol as major compounds in the sample of the EEtOH and FDCM, MIC was done with eugenol pure, and the result was 0.125 mg ml^{-1}.

TABLE 2. Minimum Inhibitory Concentration (MIC, mg ml^{-1}) of samples from *Ocimum gratissimum* leaves and eugenol pure solutions.

Samples	*Aspergillus* sp.	*Rhizopus* sp.
EEtOH	1.25	0.625
FDCM	0.625	0.625
Eugenol	0.125	0.125

EEtOH: ethanolic extract; FDCM: dichloromethane fraction.

Antioxidant capacity

The antioxidant potential of *O. gratissimum* extracts was studied by means of synthetic radical tests, DPPH and ABTS, and by the FRAP assay, as with the results shown in Table 3. The antioxidant potential of extracts by DPPH and ABTS consisted of the ability to eliminate free radicals by donating a hydrogen atom or an electron. The antioxidant capacity is related to the degree of discoloration of the reaction solution with the synthetic free radical (Re *et al.,* 1999; Sousa *et al.,* 2007).

The EEtOH partition exhibited the highest antioxidant capacity for both DPPH and ABTS assays, followed by nonpolar fractions, FHex and FDCM, respectively. Low potential was identified in polar fractions, with FAce significantly lower among all extracts evaluated in the DPPH and ABTS assays. FAq was the only extract that did not show significant potential for scavenging the ABTS radical. The FRAP assay defines antioxidant as any substance in the reaction medium with reducing power by donating a hydrogen atom (Duh *et al.,* 1999). Thus, EEtOH presented the highest reducing power and as the polarity is increased, the reduction capacity of samples is smaller, with FAq showing the lowest value.

TABLE 3. Antioxidant activity by DPPH, ABTS, and FRAP of the ethanolic extract and fractions from *Ocimum gratissimum* leaves.

Treatments	DPPH IC_{50} (μg ml^{-1})	ABTS IC_{50} (μg ml^{-1})	FRAP (TEAC)
EEtOH	371.1±2.98 e	182.43±1.1 e	262.39±3.61 a
FHex	405.60±3.21 e	325.86±3.49 d	229.88±1.65 b
FDCM	707.11±2.75 d	370.00±1.76 c	111.51±5.03 c
FAce	2088.33±13.52 a	641.06±8.05 a	39.62±1.63 e
FBuOH	905.96±5.64 c	495.66±5.63 b	64.13±2.29 d
FAq	1748.52±8.36 b	4816.50±20.35 ns	27.32±1.9 f

EEtOH: ethanolic extract; FHex: hexane fraction; FDCM: dichloromethane fraction; FAce: ethyl acetate fraction; FBuOH: butanol fraction; FAq: aqueous fraction; ns: not significant. Means followed by different lowercase letters in the column differ statistically from each other by the Tukey's test ($P<0.05$).

Identification by GC/MS

In the GC/MS chromatographic profile EEtOH samples and their nonpolar fractions from *O. gratissimum* leaves, 22 substances were identified, shown in Table 4. From chromatograms, the presence of eugenol as the major substance in all samples was observed, with the highest relative percentage (61.26%) in the FDCM fraction, followed by the EEtOH extract (59.61%) and FHex fraction (37.65%).

The *Aspergillus* sp. and *Rhizopus* sp. fungi can accelerate the deterioration process of stored seeds (Silva *et al*., 2021). The present study demonstrated *in vitro* antifungal activity of the EEtOH and FDCM samples from *O. gratissimum* leaves at 5 mg ml^{-1} against *Aspergillus* sp. and *Rhizopus* sp. fungi associated with seeds in the storage phase, which indicates biological potential of extracts obtained from this plant. Onaebi *et al.* (2020), using the EEtOH at 100 mg ml^{-1} from *O. gratissimum* leaves, found reductions in the growth of *Aspergillus flavus* (51.93%) and *Aspergillus niger*

TABLE 4. Compounds identified by gas chromatography coupled to mass spectrometer from the ethanolic extract and the hexane and dichloromethane fractions from *Ocimum gratissimum* leaves.

Ocimum gratissimum samples with % of chromatogram areas						
Number	**Retention time (min)**	**Identified compounds**	**KI[a]**	**EEtOH**	**FHex**	**FDCM**
1	17.499	Eugenol	1357	59.61	37.65	61.26
2	17.945	a-Copaene	1374	-	0.83	-
3	18.168	(-)-β-Bourbonene	1382	-	0.51	-
4	18.531	Vanillin	1396	-	-	1.22
5	19.045	Caryophyllene	1416	1.32	2.28	-
6	20.617	Germacrene D	1478	1.91	1.5	-
7	21.686	δ-Cadinene	1522	-	1.21	-
8	23.061	Caryophyllene oxide	1580	-	1.42	-
9	25.432	Germacra-4(15),5,10(14)-trien-1α-ol	1683	-	0.74	-
10	26.537	Coniferyl alcohol	1734	-	-	0.86
11	28.758	Phytol derivative	1839	1.52	0.94	-
12	31.207	n-Hexadecanoic acid	1963	-	0.63	-
13	31.861	Ethyl hexadecanoate	1994	0.85	1.72	-
14	34.045	Phytol	2112	3.08	6.97	-
15	34.528	Methyl α-linolenate	2139	-	2.03	1.11
16	34.938	Linoleic acid ethyl ester	2162	-	0.65	-
17	35.052	Ethyl linoleate	2169	1.7	3.14	-
18	35.545	Octadecanoic acid, 17-methyl-, methyl ester	2196	-	0.45	-
19	43.255	Squalene	2832	4.72	10.24	-
20	44.682	Vitamin E	3151	0.81	2.88	-
21	45.445	Chondrillasterol	3297	-	3.18	-
22	45.803	γ-Sitosterol	3356	-	3.05	-
Total (%)				75.52	82.02	64.45

[a] Retention index obtained as a standard reference of ν-alkanes using HP-5MS column. EEtOH = Ethanolic extract, FHex = Hexane fraction, and FDCM = Dichloromethane fraction.

(23.7%), but the same did not occur for *Rhizopus delemar* (0%); the difference from the present study may be due the extract preparation.

The fraction FDCM and the EEtOH extract showed the best antifungal activities, and the GC/MS analysis indicates eugenol as the major compound. Eugenol is a phenylpropanoid commonly found in essential oils extracted from *O. gratissimum* leaves and, due to its nonpolar characteristic, it was easily identified in the less polar fractions and in the ethanolic extract in this study. Eugenol is related to several biological activities, mainly against phytopathogens (Faria *et al.,* 2006; Dambolena *et al.,* 2010).

There are numerous studies with essential oils of *O. gratissimum*; however, research for ethanolic extracts and fractions of different polarities is scarce (Zareiyan & Khajehsharif, 2022). In our experiment, the MIC results showed that eugenol has higher activity than EEtOH and FDCM samples. Ethanol is a non-selective solvent in the process of extracting compounds from plants, thus allowing for a greater chemical diversity of constituents in the extracts obtained, but at low concentrations. On the other hand, fractions obtained from the fractionation process with selective solvents of different polarities have higher concentrations and lower diversity of phytochemicals and are more selective in terms of polarity, thus the DCM sample had higher concentrations of the compounds with antifungal activity. Nwofor *et al.* (2021) presented the MIC of 100 mg ml^{-1} for methanolic extracts of *O. gratissimum* against *Penicillium citrinum, Aspergillus aculeatus, Aspergillus fumigatus, Curvularia kusanol*, *and Absidia* spp.

The EEtOH showed the highest antioxidant capacity among samples used in the DPPH, ABTS and FRAP methods. Ouyang *et al*. (2013) showed antioxidant activities of methanolic extracts and ethyl acetate fraction from *O. gratissimum* leaves using the same methods as in this study.

In our study, the non-polar fractions demonstrated more antioxidant capacity than polar fractions. This could be explained by the presence of eugenol substance in all samples and other antioxidants like squalene and vitamin E.

The results of this study confirmed that *O. gratissimum* extracts have antifungal and antioxidant activity, but the type of solvent can interfere with the chemical composition and biological properties. The mechanism of action is likely related to the presence of eugenol. In addition, extracts can scavenge free radicals, which could reduce seed deterioration during storage. However, it is still necessary to verify the *in vivo* efficacy and improve the activity with the release of the active ingredient at the specific site of action.

Acknowledgments

The authors would like to thank the Coordination for the Improvement of Higher Education Personnel (CAPES) for the scholarship – Financial Code 001, the Espírito Santo Research and Innovation Support Foundation (FAPES) APES/SEAG (Process 76449130/16) and the Federal Institute of Espirito Santo (IFES) for financial support from PRODIF.

Conflict of interest statement

The authors declare that there is no conflict of interests regarding the publication of this article.

Author's contributions

JTL carried out the field and laboratory experiments and contributed to writing of the manuscript. AFS designed the experiments and revised the manuscript. HSF designed the methodology, obtained the financial support for the project leading to this publication and reviewed the final edition and style. All authors have read and approved the final version of the manuscript.

Literature cited

Barros, S. T., Oliveira, N. D., & Maia, L. C. (1995). Efeito de extrato de alho (*Allium sativum*) sobre o crescimento micelial e germinação de conídios de *Curvularia* spp. e *Alternaria* spp. *Summa Phytopathologica*, *21*(2), 168–170.

Benelli, G., Pavela, R., Maggi, F., Wandjou, J. G. N., Fofie, N. G. B. Y., Koné-Bamba, D., Sagratini, G., Vittori, S., & Caprioli, G. (2019). Insecticidal activity of the essential oil and polar extracts from *Ocimum gratissimum* grown in Ivory Coast: Efficacy on insect pests and vectors and impact on non-target species. *Industrial Crops and Products*, *132*, 377–385. https://doi.org/10.1016/j.indcrop.2019.02.047

Casagrande, R., Georgetti, S. R., Verri Jr, W. A., Borin, M. F., Lopez, R. F. V., & Fonseca, M. J. V. (2007). *In vitro* evaluation of quercetin cutaneous absorption from topical formulations and its functional stability by antioxidant activity. *International Journal of Pharmaceutics*, *328*(2), 183–190. https://doi.org/10.1016/j.ijpharm.2006.08.006

Chowdhary, K., Kumar, A., Sharma, S., Pathak, R., & Jangir, M. (2018). *Ocimum* sp.: Source of biorational pesticides. *Industrial Crops and Products*, *122*, 686–701. https://doi.org/10.1016/j.indcrop.2018.05.068

Dambolena, J. S., Zunino, M. P., López, A. G., Rubinstein, H. R., Zygadlo, J. A., Mwangi, J. W., Thoithim G.N., Kibwage, I. O., Mwalukumbi, J. M., & Kariuki, S. T. (2010). Essential oils composition of *Ocimum basilicum* L. and *Ocimum gratissimum* L. from Kenya and their inhibitory effects on growth and fumonisin production by *Fusarium verticillioides*. *Innovative Food Science & Emerging Technologies*, *11*(2), 410–414. https://doi.org/10.1016/j.ifset.2009.08.005

Duh, P. D., Du, P. C., & Yen, G. C. (1999). Action of methanolic extract of mung bean hulls as inhibitors of lipid peroxidation and non-lipid oxidative damage. *Food and Chemical Toxicology, 37*(11), 1055–1061. https://doi.org/10.1016/S0278-6915(99)00096-4

Dzoyem, J. P., Nganteng, D. N. D., Melong, R., Wafo, P., Ngadjui, B., Allémann, E., & Delie, F. (2021). Bioguided identification of pentacyclic triterpenoids as anti-inflammatory bioactive constituents of *Ocimum gratissimum* extract. *Journal of Ethnopharmacology*, *268*, Article 113637. https://doi.org/10.1016/j.jep.2020.113637

Elisée, K. K., Pintea, A., Constantin, O. O., Odagiu, A., David, N. J., & Joseph, D. A. (2020). Total phenolic compounds extraction in leaves of *Ocimum gratissimum* L. and their potential activity against some agricultural contaminants. *Asian Research Journal of Agriculture*, *13*(4), 1–10. https://doi.org/10.9734/arja/2020/v13i430108

Faria, T. D. J., Ferreira, R. S., Yassumoto, L., Souza, J. R. P. D., Ishikawa, N. K., & Barbosa, A. D. M. (2006). Antifungal activity of essential oil isolated from *Ocimum gratissimum* L. (eugenol chemotype) against phytopathogenic fungi. *Brazilian Archives of Biology and Technology*, *49*(6), 867–871. https://doi.org/10.1590/S1516-89132006000700002

Hamma, I. I., Tafinta, I. Y., Abdulmalik, A., Theophilus, J., & Abubakar, M. (2020). Phytochemical screening and antibacterial activity of the crude extract of scent leaf (*Ocimum gratissimum*) on *Escherichia coli* and *Staphylococcus aureus*. *Asian Plant Research Journal*, *5*(2), 1–7. https://doi.org/10.9734/aprj/2020/v5i230101

Kordali, S., Cakir, A., Zengin, H., & Duru, M. E. (2003). Antifungal activities of the leaves of three *Pistacia* species grown in Turkey. *Fitoterapia*, *74*(1-2), 164–167. https://doi.org/10.1016/S0367-326X(02)00320-9

Mann, A. (2012). Phytochemical constituents and antimicrobial and grain protectant activities of clove basil (*Ocimum gratissimum* L.) grown in Nigeria. *International Journal of Plant Research*, *2*(1), 51–58. https://doi.org/10.5923/j.plant.20120201.08

Matos, F. (2007). *Plantas medicinais-guia de seleção e emprego de plantas medicinais usadas em fitoterapia no nordeste do Brasil*. Universidade Federal do Ceará.

Mohr, F. B. M., Lermen, C., Gazim, Z. C., Gonçalves, J. E., & Alberton, O. (2017). Antifungal activity, yield, and composition of *Ocimum gratissimum* essential oil. *Genetics and Molecular Research*, *16*(1), Article gmr16019542. https://doi.org/10.4238/gmr16019542

National Institute of Standards and Technology (NIST). (2018). *NIST Chemistry WebBook*. https://webbook.nist.gov/chemistry

Nwofor, C. N., Oyeka, A. C., Onyenwe, E. N., & Fajana A. (2021). Phytochemical analysis and *in vitro* screening of antifungal activity of *Jatropha multifida, Euphorbia hirta*, *Occimum gratissimum and Mitracarpus scaber* leaves extract. *GSC Biological and Pharmaceutical Sciences*, *14*(3), 98–112. https://doi.org/10.30574/gscbps.2021.14.3.0023

Onaebi, C., Onyeke, C., Osibe, D., Ugwuja, F., Okoro, A., & Onyegirim, P. (2020). Antimicrobial activity of *Ocimum gratissimum* L. and *Carica papaya* L. against postharvest pathogens of avocado pear (*Persea americana* Mill.). *Journal of Plant Pathology*, 102, 319–325. https://doi.org/10.1007/s42161-019-00420-5

Onyebuchi, C., & Kavaz, D. (2020). Effect of extraction temperature and solvent type on the bioactive potential of *Ocimum gratissimum* L. extracts. *Scientific Reports*, *10*(1), Article 21760. https://doi.org/10.1038/s41598-020-78847-5

Ouyang, X., Wei, L., Pan, Y., Huang, S., Wang, H., Begonia, G. B., & Ekunwe, S. I. (2013). Antioxidant properties and chemical constituents of ethanolic extract and its fractions of *Ocimum gratissimum*. *Medicinal Chemistry Research*, *22*(3), 1124–1130. https://doi.org/10.1007/s00044-012-0113-z

Penido, A. B., Morais, S. M. D., Ribeiro, A. B., & Silva, A. Z. (2016). Ethnobotanical study of medicinal plants in Imperatriz, State of Maranhão, Northeastern Brazil. *Acta Amazonica*, *46*(4), 345–354. https://doi.org/10.1590/1809-4392201600584

Re, R., Pellegrini, N., Proteggente, A., Pannala, A., Yang, M., & Rice-Evans, C. (1999). Antioxidant activity applying an improved ABTS radical cation decolorization assay. *Free Radical Biology and Medicine*, *26*(9-10), 1231–1237. https://doi.org/10.1016/S0891-5849(98)00315-3

Sánchez-González, I., Jiménez-Escrig, A., & Saura-Calixto, F. (2005). *In vitro* antioxidant activity of coffees brewed using different procedures (Italian, espresso and filter). *Food Chemistry*, *90*(1-2), 133–139. https://doi.org/10.1016/j.foodchem.2004.03.037

Silva, A. O. D., Silva, A. O. D., Gomes, J. A., Oliveira, R. C. D., Silva, D. A. S., & Viégas, I. D. J. M. (2021). Armazenamento de grãos na agricultura familiar: principais problemáticas e formas de armazenamento na região nordeste paraense. *Research, Society and Development*, *10*(1), Article e36610111835. https://doi.org/10.33448/rsd-v10i1.11835

Sousa, C. M. D. M., Silva, H. R., Vieira-Jr., G. M., Ayres, M. C. C., Costa, C. L. S. D., Araújo, D. S., Cavalcante, L. C. D., Barros, E. D. S., Araújo, P. B. D. M., Brandão, M. S., & Chaves, M. H. (2007). Fenóis totais e atividade antioxidante de cinco plantas medicinais. *Química Nova*, *30*(2), 351–355. https://doi.org/10.1590/S0100-40422007000200021

Talibi, I., Askarne, L., Boubaker, H., Boudyach, E. H., Msanda, F., Saadi, B., & Aoumar, A. A. B. (2012). Antifungal activity of some Moroccan plants against *Geotrichum candidum*, the causal agent of postharvest citrus sour rot. *Crop Protection, 35*, 41–46. https://doi.org/10.1016/j.cropro.2011.12.016

Uchegbu, R. I., Akalazu, J. N., & Sokwaibe, C. E. (2019). An evaluation of the chemical compositions and antifungal activity of *Ocimum gratissimum* (Nchuanwu) leaves against some plant pathogens. *Asian Journal of Applied Chemistry Research, 2*(3-4), 1–7. https://doi.org/10.9734/ajacr/2018/v2i3-430078

Zareiyan, F., & Khajehsharifi, H. (2022). *In-vitro* phytochemical analysis of essential oil and methanolic and hydromethanolic extracts of *Ocimum gratissimum*. *Journal of Plant Biochemistry and Biotechnology, 31*, 894–906. https://doi.org/10.1007/s13562-022-00768-3

Nitrous oxide flux from soil with *Urochloa brizantha* under nitrogen fertilization in Honduras

Flujo de óxido nitroso del suelo con *Urochloa brizantha* bajo fertilización nitrogenada en Honduras

Breno Augusto Sosa Rodrigues[1*], Diego Tobar López[2], Yuly Samanta García Vivas[1], Josué Mauricio Flores Cocas[1], Noé Humberto Paiz Gutiérrez[1], and Elsa Gabriela Zelaya Méndez[1]

ABSTRACT

The emission of nitrous oxide is considerable in livestock systems, influenced by nitrogen fertilization and edaphoclimatic conditions. The aim of the research was to measure the flux of nitrous oxide (N_2O) from the soil under *Urochloa brizantha* with nitrogen fertilization. In the pastures, a randomized complete block design was established with four replicates and three treatments, consisting of 2 m^2 plots with *U. brizantha* fertilized with urea, bokashi and without fertilizer application. The gas samples were collected over three months between the rainy and dry seasons using the static closed chamber methodology. The samples related to the soil and plants were taken at a depth of 15 cm under undisturbed conditions every month, to quantify: gravimetric moisture, ammonium, nitrate, total carbon, total nitrogen, carbon/nitrogen ratio, and plant dry matter (DM). The ANAVA registered a significant difference between treatments for N_2O, with the application of urea promoting higher accumulated flows (0.37 mg N_2O m^{-2} h^{-1}), followed by bokashi (0.34 mg N_2O m^{-2} h^{-1}) and lastly by the control (0.27 mg N_2O m^{-2} h^{-1}). The daily emission of the gas fluctuated in the rainy season, when soil moisture promoted higher emission peaks compared to the dry season. The fractions of nitrogen, carbon and DM were not affected by the treatments. The use of urea and the anaerobic conditions of soil due to the rains generated higher N_2O values, while the organic amendment, bokashi, was the best alternative for the greenhouse gas mitigation and soil conservation.

Key words: livestock, bokashi, greenhouse gases, soil nitrogen.

RESUMEN

La emisión de óxido nitroso es considerable en sistemas ganaderos, influenciada por la fertilización nitrogenada y condiciones edafoclimáticas. El objetivo del ensayo fue medir el flujo de óxido nitroso (N_2O) del suelo bajo *Urochloa brizantha* con fertilización nitrogenada. En las pasturas se estableció un diseño de bloques completos al azar con cuatro repeticiones y tres tratamientos, consistentes en parcelas de 2 m^2 con *U. brizantha* fertilizada con urea, bokashi y sin aplicación de fertilizantes. Las muestras del gas se recolectaron a lo largo de tres meses entre la época lluviosa y seca con la metodología de cámaras cerradas estáticas. Las muestras relacionadas al suelo y plantas se tomaron a una profundidad de 15 cm en condiciones inalteradas cada mes, para cuantificar: humedad gravimétrica, amonio, nitrato, carbono total, nitrógeno total, relación carbono/nitrógeno y materia seca de plantas (MS). El ANAVA registró diferencia significativa entre tratamientos para el N_2O, siendo la aplicación de urea la que promovió mayores flujos acumulados (0.37 mg N_2O m^{-2} h^{-1}), luego el bokashi (0.34 mg N_2O m^{-2} h^{-1}) y por último el testigo (0.27 mg N_2O m^{-2} h^{-1}). La emisión diaria del gas fue fluctuante en el periodo lluvioso, cuando la humedad en el suelo promovió mayores picos de emisión en comparación con la estación seca. Las fracciones de nitrógeno, carbono y MS no fueron afectadas por los tratamientos. El uso de la urea y las condiciones anaeróbicas del suelo por las lluvias generaron mayores valores del N_2O, mientras que la enmienda orgánica, bokashi, fue la mejor alternativa mitigadora de los gases de efecto de invernadero y de conservación del suelo.

Palabras clave: ganadería, bokashi, gases de efecto de invernadero, nitrógeno del suelo.

Introduction

The production of food without generating high levels of environmental pollution is one of the great challenges of humanity. The agricultural sector, especially livestock, contributes 18% of the total emission of greenhouse gases (GHG) into the atmosphere; at the same time, it is responsible for 37% of methane (CH_4) emissions and 65% of nitrous oxide (N_2O) (Steinfeld *et al*., 2006; FAO, 2013). Within the objectives of sustainable development of the Paris Agreement, countries have committed to reduce emissions from the different productive sectors (CMNUCC, 2017).

Received for publication: May 31, 2022. Accepted for publication: December 17, 2022 Doi: 10.15446/agron.colomb.v40n3.102963

[1] National Autonomous University of Honduras, La Ceiba (Honduras).
[2] Tropical Agricultural Research and Teaching Center, Turrialba (Costa Rica).
* Corresponding author: breno.sosa@unah.edu.hn

In Honduras, the agricultural sector has a significant influence on GHG emissions. From 1990 to 2014, synthetic fertilization (8.3%), manure applied to the soil (4%), and pastures (22.7%) were the agricultural activities that most influenced the GHG emission from soils in livestock systems (FAO, 2017). The National Climate Change Strategy of Honduras (ENCC) promotes the use of technologies, laws, training and generation of information in the industrial and agro-environmental sector; however, preventing increases in GHG emissions from the soil is complex and difficult, in a reality of low agricultural technology, extreme poverty, continuous deforestation, soil degradation, and excessive use of agrochemicals in agroecosystems (ENCC, 2022).

Grazing is the main livestock production system in the region and has been identified as a source of N_2O due to deposition of animal waste in pastures, use of nitrogenous fertilizers (Pastrana *et al*., 2011), harvest residues, and compaction of soils, among others (Millard *et al*., 2004). It is estimated that between 75 and 90% of the nitrogen (N) consumed by grazing livestock is excreted through urine and manure (Luo *et al*., 2010). Considering that N_2O has 298 greater global warming potential (IPCC, 2007) compared to CO_2, its impact has importance for global warming.

The GHG emissions from the soil, especially N_2O, depend on the biological cycle of N, soil management, and the particular edaphoclimatic conditions of each region (Uchida *et al*., 2011; Sosa, 2013). Therefore, it is appropriate to generate mitigation, soil conservation and economically competitive strategies for the producer.

Various authors have made valuable contributions to understanding the N-soil-atmosphere relationship. Silva *et al*. (2013) found that degraded pastures emit higher N_2O compared to silvopastoral systems. Ibrahim *et al*. (2010) recorded that silvopastoral systems are a mitigating alternative to emission, comparable to natural forest. Bastidas *et al*. (2020) found that increases in synthetic nitrogen fertilization improved the agronomic performance of four pastures, including *Urochloa humidicola*, however, the emission of N_2O increased. Organic amendments, such as biochar, generate positive effects in mitigating nitrous oxide as well as improving chemical properties of the soil (Jiang *et al*., 2020).

In order to increase knowledge about the dynamics of this gas and the factors that model its expression in livestock systems, this research sought to quantify the N_2O flux from the soil planted with *Urochloa brizantha* and fertilized with bokashi and urea.

Materials and methods

Characterization of the experimental area

This study was carried out between October 2016 and April 2017 in pastures of *Brachiaria* of the Regional University Center of the Atlantic Coast (CURLA) of the National Autonomous University of Honduras (UNAH) located in the municipality of La Ceiba, department of Atlántida, Honduras at 15°47'20" N and 87°51'15" W, altitude of 26 m. The climate conditions of the experiment site were: average temperature of 26.2°C, relative air humidity of 95%, and average annual rainfall of 3,230 mm (Climatemps, 2017) distributed in the rainy season, from mid-September to February, when approximately 70% of the precipitation falls. The Oxisol (Soil Taxonomy, 2014) was analyzed (Tab. 1) at a depth of 0-20 cm before establishing the experiment.

TABLE 1. Initial physicochemical properties of the soil with pastures.

Property	Unit	Value	Level
pH		5.34	Low
$Al^{3+} + H^+$	$cmol_+ kg^{-1}$	0.89	High
OM	$g kg^{-1}$	25.6	Medium
N total	%	0.24	High
NH_4^+	$mg kg^{-1}$	0.13	Low
NO_3^-	$mg kg^{-1}$	26.95	Low
C:N		10.45	Medium
EC	$dS m^{-1}$	0.13	Low
K	$cmol_+ kg^{-1}$	0.33	Low
Ca		1.17	Low
Mg		0.5	Low
Na		0.05	Low
P	$mg kg^{-1}$	7.09	Low
S		5.82	Low
B		0.09	Low
Fe		56.35	High
Mn		46.4	High
Cu		1.26	Medium
Zn		1.57	Medium
Apparent density	$g cm^3$	1.12	No compaction
Real density		2.65	Constant
Total porosity	%	54.7	Good
Volumetric humidity		19.5	--
Texture	--	Clay loam	Easy labor

pH: aqueous solution 1:1; EC: saturated extract, conductance; Al+H: extraction with KCl; macro and microelements: plasma Mehlich-3; texture: pipette; bulk density: bevelled cylinder; real density: pycnometer; porosity and moisture: mathematical formula. The soil analysis was carried out at the Western Hemisphere Analytical Laboratory (WHAL) of the Standard Fruit company and the CURLA soil laboratory, Atlantis, Honduras, 2017.

To analyze the chemical properties of the soil, international criteria were used (Molina & Meléndez, 2002). The high levels of exchangeable acidity, Fe, Mn, low pH and the amount of organic matter (Tab. 1) should be noted, as they can interfere with the availability and absorption of mineral nutrients as well as with biological activity, and, therefore, with crop yield. The physical properties were suitable for tillage (texture), facilitating root development (apparent density and total porosity) and moisture retention.

Experiment description

The experimental units consisted of field plots with an area of 2 m^2, in which *Urochloa brinzantha* (Hochst. ex A. Rich.) R. D. var. brizantha, established approximately 6 years ago, was planted sown at a rate of seed 2.5 kg ha^{-1} and fertilized with different N sources (treatments) under a randomized complete block design with four replicates (Tab. 2).

TABLE 2. Treatments established to analyze the flux of N_2O from the soil planted with pastures and nitrogen fertilization.

Treatments	Nitrogen dose	
	(g m^{-2})	(kg ha^{-1})
Pastures without fertilization	-	-
Pastures with bokashi	878.5	59.47
Pastures with urea	26.0	59.47

Fertilization with organic and synthetic N sources was carried out twice, at the beginning of the rainy season (November 2016) and in the dry season (April 2017). In the treatments with the chemical synthesis fertilization, this was done by applying the urea fertilizer at a dose of 26 g m^{-2}, according to the 59.47 kg ha^{-1} of N required by the crop (Hernández, 2009). For the treatments with addition of organic compost bokashi type, the calculated and applied dose was 878.5 g m^{-2}, in order to provide the same amount of N as the conventional fertilizer, according to chemical analysis performed on bokashi (total N=1.36 %, pH=7.45, C=16.75 and C:N=12.36) in the WHAL laboratory (Honduras).

The materials used to make the bokashi were 200 kg of chicken manure, 50 kg of rice husks, 200 kg of forest land, 150 kg of cow dung, 22.65 kg of charcoal, 9.06 kg of rice semolina, 0.9 kg of yeast, 1.89 L of molasses, 1.35 kg of calcium carbonate, 2.26 kg of ash, 2.26 kg of rock meal, and moisture was regulated by fist test. All the ingredients were mixed randomly and homogeneously. After 21 d, the product was harvested, turning it once every 24 h until day 14, letting it rest for the third week, monitoring its humidity and temperature regularly to ensure quality. Then it was sieved and packed in 25 or 50 kg bags.

In order to be as homogeneous as possible, the area of the base of the chamber was taken into account for the application of the appropriate amount of treatment in the quadrant; 0.234 g of the conventional treatment and 7.9 g of the organic fertilizer were applied inside the base of the chamber, and the rest outside of it.

The harvest of the pastures was done monthly, making cuts manually at an approximate height of 10 cm above the soil. In the 1 m^2 area, where the chamber was established, disturbing the soil was avoided as much as possible during the samplings. In a parallel area where the chamber was established, soil samples were obtained from the 1 m^2 of the soil surface at a depth of 10 cm to measure chemical properties, such as C and N contents, and physical properties. such as moisture, which affect the dynamics of nitrous oxide.

Evaluated variables

In the dry and rainy season of the year, variables related to the soil were quantified: ammonium, nitrate and total N were determined by Mehlich-3 plasma detection, and total carbon by LOI (Loss of ignition method) (Jones, 1999); volumetric moisture (Jaramillo, 2002) was determined taking compound samples made up of five subsamples from each useful plot of the treatments.

To analyze the productivity of the pasture, the pasture was harvested from 1 m^2 of each experimental unit fresh 30 d after cut, at a height of 10 cm, simulating grazing. A 250 g sample was then taken and dried in an oven for 3 d at 70°C to determine the percentage of plant dry matter (DM).

For the analysis of GHG fluxes from the soil and the atmosphere, the Closed-Chamber Technique (CCT) was used (Pastrana *et al.*, 2011; Klein and Harvey, 2012; Sosa, 2013). The CCT is a standard at the international level and is in the process of being validated for the Central American region.

The chambers were made of a PVC tube, with a diameter of 24.0 cm and 38.0 cm in height, with an acrylic cover and a circular design; in the latter, with two holes: one with a rubber septum used to introduce the thermometer and the other for sampling, without internal ventilation. The chambers were lined with an insulating membrane of aluminized polyethylene foam 9 mm thick, to avoid direct sunlight and heating of the chambers.

To install the chambers in the 12 experimental units under field conditions, the PVC ring/base was placed at a depth of 10 cm in the soil, placing it 1 d before sampling, to restore soil conditions when disturbed. The chambers were

then mounted on the rings and hermetically sealed with an elastic band.

Prior to taking the samples in the treatments, the calibration curve was carried out in a range of 12 h (6:00 am – 6:00 pm), with samples every 2 h for 2 d. to calculate the average gas emission and the schedule where this most often occurs.

Once the calibration was done, the sampling time was defined at 10:00 am similar to Arguedas *et al*. (2019) in Costa Rica. For the collection of the samples in each treatment, the internal air of the chamber was mixed by pumping the air syringes. The sample was then transferred to a 20 ml vacuum "vial" tube, to be later transported to the laboratory. Sampling lasts for 1 h, taking three samples per chamber at three different times: T0: when installing the chamber; T20 = 20 min; and T40 = 40 min. Additionally, for each day of sampling, two air samples are taken outside the chamber, at the same height of the sampling, to be used as a "blank" in the laboratory.

Sampling frequency: two months of sampling were scheduled in the rainy season, between December 2016 and January 2017, and one month in the dry season, between March and April 2017. Table 3 shows the schedule carried out according to the sampling days:

TABLE 3. Monthly schedule for taking nitrous oxide samples.

No. sampling	1	2	3	4	5	6	7	8	9	10
Sampling day of the month	1	2	3	4	5	9	12	17	24	29

Analysis of the samples

The samples were sent to the INTA-CR Gas Chromatograph, located in Alto de Ochomogo, Cartago (Costa Rica) for subsequent study and estimation of the N_2O flux and the emission factor, according to the methodology described by Venterea *et al*. (2012) described below:

Once the GHG concentration has been quantified (in parts per million), the N_2O flux was calculated as a function of area and time. To calculate the flux of N_2O, the following ideal gas equation was used:

$$g\,N_2O = \frac{Pa*V*MW*ppm}{R*T*1000000} \quad (1)$$

where:

Pa=pressure in Pascal

V=chamber volume in m^3

MW=molecular weight of N_2O in g/mol

ppm=weight of N_2O at the collection T of the sample

R=Units in $Pa*m^3/mol*K$

T=Temperature in degrees Kelvin

The linear flux was calculated using the equation:

$$Linear\ mg\,N_2O\,m^2\,h^{-1} = \frac{(g\,T40 - g\,T20) + (g\,T20 - g\,T0)*1000}{(Area * Time)} \quad (2)$$

where:

g T40 = g N_2O of T40

g T20 = g N_2O of T20

g T0 = g N_2O of T0

Area = Chamber area, cm^2

Time = Time to collect the gas sample, 0, 20 or 40 min.

Statistical analysis

Data were analyzed with the SAS program using an analysis of variance (PRoC GLm) (SAS Institute Inc., 2002), to determine differences in treatments, followed by the Tukey's multiple range test; the analysis of variance detected differences with a probability level of 5%.

Results and discussion

Accumulated flux of N_2O under nitrogen fertilization

The analysis of variance recorded significant differences for the nitrous oxide flux in the treatments evaluated in the pastures (Fig. 1), differentiated by the highest emission due to chemical synthesis fertilizer, followed by bokashi and finally, by the pasture without fertilization. Soil moisture is one of the factors that modulates the emission or sink action of N_2O; however, the existing variability in the soil and the contributions of rain generated conditions that masked the effect of the treatments, shown and explained later in Table 4. The contribution of N to the system soil is a key factor in the nitrification and denitrification processes, which release the highest percentage of N_2O into the atmosphere. Millard *et al*. (2004) and Uchida *et al*. (2011) consider that the application of nitrogenous fertilizers significantly promotes the emissions of this gas from the soil. For their part, Harty *et al*. (2016) and Montenegro (2020) verify the promoting effect of urea on the emission of N_2O, however, the stimulus represents 0.5 to 1% of the N applied. The entry of N into the system, regardless of the source, accelerates the mineralization of the nutrient, producing inorganic fractions that, accompanied by aeration and present humidity, generate N_2O.

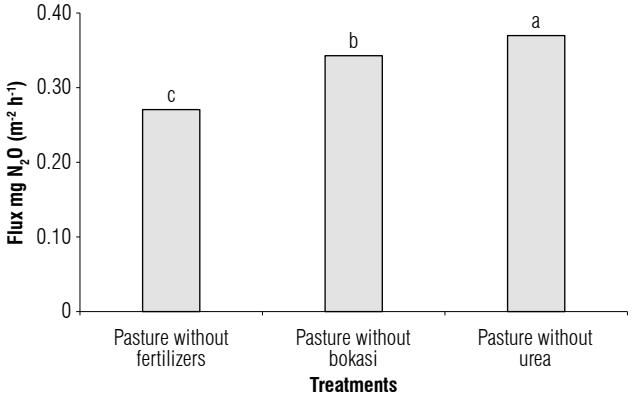

FIGURE 1. Flux of accumulated nitrous oxide in the pasture system under study. Letters indicate statistically significant differences ($P<0.05$) according to Tukey's test.

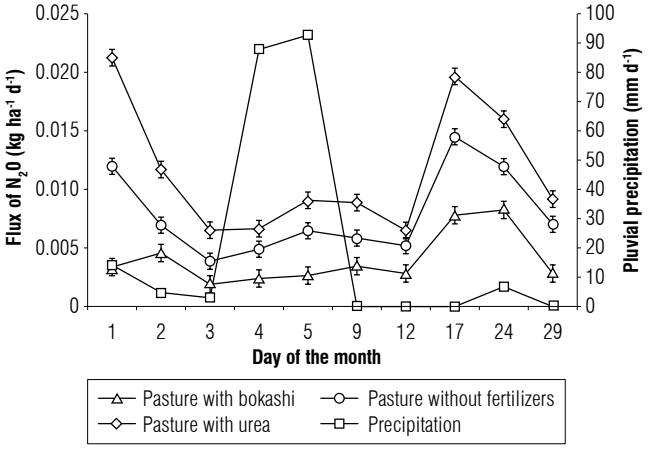

FIGURE 2. Accumulated flux of N_2O in the rainy season under nitrogen fertilization on first sampling. Error bars is standard error.

Dynamics of N_2O emitted from the soil according to the climatic season

The emission of N_2O was variable throughout the rainy season (209 mm/month) evaluated on each day sampled (Fig. 2). The trend was similar among the treatments analyzed, with the highest emission at the beginning of the month, after application of the fertilizers that correspond to each treatment. Emissions decreased in the following days, with another peak on day 17, coincident with a rainfall event of 180 mm on two consecutive days; possibly, the rainfall generated anaerobic conditions in the soil with clay loam texture.

Anaerobic conditions favor the production of the analyzed GHG. Rowlings *et al*. (2015) and Oertel *et al*. (2016) consider the role played by soil moisture in gas emission to be fundamental; when the pore spaces are filled with water, values exceed 55%. In this sense, biological denitrification predominates in conditions of low oxygen concentration, allowing the action of anaerobic heterotrophic soil bacteria that use nitrates as electron acceptors instead of O_2 in their respiration processes, and organic carbon as electron donor, with final products of NO_2, NO, N_2O, and N_2 (McNeill & Unkovich, 2007).

After the first month of measurement of the gas emission, the pastures were cut to a height of 10 cm, simulating grazing. For this second month of measurement (Fig. 3), the incidence of rainfall was lower than the previous one, with 4.2 mm accumulated. The daily flux of N_2O was low until day 9, when emission increased between treatments, coinciding with the increase in rainfall, and then gradually decreased. It is possible that the lower contribution of water to the soil affects the lower emission of N_2O (Nogueira *et al*., 2015), at which the soil mineralization process focuses more on nitrification in dry periods, when the volumes of water are lower compared to the rainy season. A similar assessment is reported by Montenegro (2020), stating that the variations observed in N_2O emissions are explained by the effect of the seasons of the year, which affect the fluctuation of water levels in soil pores. In this research, when rainfall increased, N_2O emissions increased y low oxygenation conditions in the soil promote GHG production.

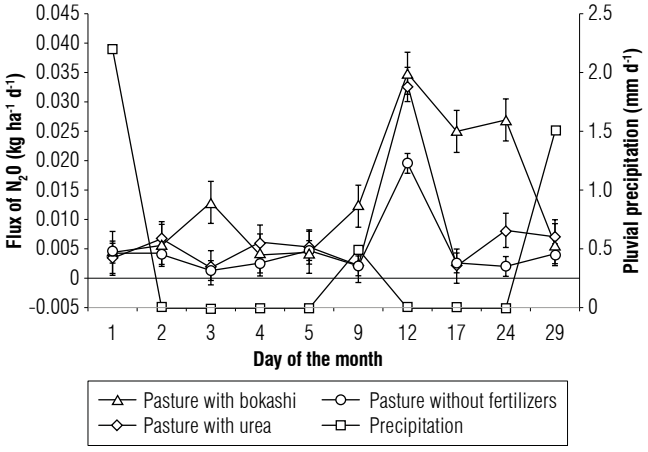

FIGURE 3. Accumulated flux of N_2O in the rainy season under nitrogen fertilization on second sampling. Error bars is standard error.

For the only sampling of gas emission in the dry season (Fig. 4), very marked fluctuations were recorded between treatments. After the second fertilization before sampling, the high values seen from day 1 in the rainy season were not obtained. During the month of evaluation, with no precipitation (0 mm rainfall) recorded, nitrification predominated, supported by the supply of N in fertilization, whose respective availability of ammonium and nitrate stimulates the activity of nitrifying bacteria (Madigan *et al*.,

2003; Sosa, 2013). A higher emission of N_2O was recorded from d 4; it is possible that the lack of water limits the production of the gas. However, Mcneill and Unkovich (2007) stated that nitrifying bacteria can release ammonium and nitrates, both under aerobic and anaerobic conditions, concentrating the activity on the soil surface, which contains more humus.

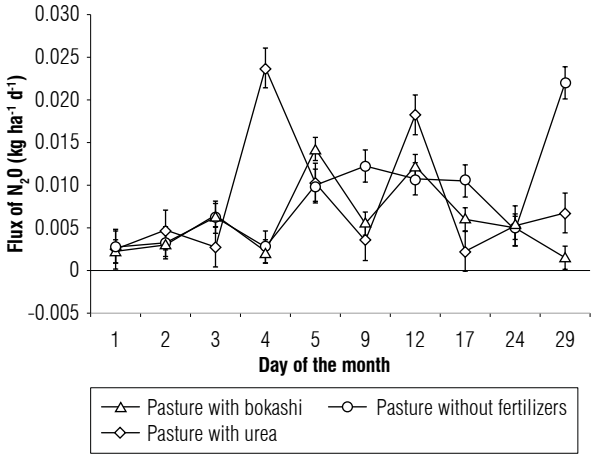

FIGURE 4. Accumulated flux of N_2O in the dry season under nitrogen fertilization at first sampling. Error bars is standard error.

Nitrogen fractions such as ammonium and nitrate, carbon, C:N ratio, soil moisture, and plant dry matter were analyzed; the ANAVA found no significant differences between treatments, blocks, and samplings (Tab. 4). There are multiple reports on variations of these edaphic parameters (Uchida *et al*., 2011; Nogueira *et al*., 2015; Rowlings *et al*., 2015; Montenegro, 2020), product of their interaction with the stimuli formulated and executed in studies; however, in the present research, the soil and climatic conditions masked the response of the variables analyzed.

It is worth mentioning that, although there was no statistical difference, the fractions of N (NO_3^- or NH_4^+) and C regulate the emission of GHG. In this sense, the availability of inorganic N ($NO_3^- + NH_4^+$) from the soil in the treatments was similar throughout the study, registering a mineralization range of 0.8 to 1.35%; this process is mediated by ammonifying and nitrifying bacteria, obtaining similar values of ammonium and nitrate in the experimental units. Even so, nitrate concentrations were higher than the concentrations of ammonium, regardless of the season, indicating that nitrification prevailed, possibly generating more N_2O. Butterbach-Balh *et al*. (2013) provided a panorama of relationships between microorganisms, plant species, climate, and soil types that regulate the emission of N_2O.

Conclusions

Nitrogen fertilization in the pastures stimulated the emission of N_2O; the organic amendment, bokashi, generated less flow from the soil with respect to urea, and, therefore, a possible mitigation strategy.

The flux of nitrous oxide varied during each month of the dry and rainy seasons, with soil moisture and nitrogen availability as the modulating factors of the greatest magnitudes of the emission. The variables related to the soil (total C, total N, ammonium, nitrate and humidity) are very dynamic over time, making it impossible to show the effect of the treatments.

Conflict of interest statement

The authors declare that there is no conflict of interests regarding the publication of this article.

TABLE 4. Biomass production and contents of C and N in the soil in the livestock system.

Sampling	Pasture/treatment	DM ($g\ m^{-2}$)	C total (%)	N total (%)	C/N ratio	NO_3^- ($mg\ kg^{-1}$)	NH_4^+ ($mg\ kg^{-1}$)	$NO_3^-+NH_4^+$ ($mg\ kg^{-1}$)	Soil moisture (%)
First month of the rainy season	Pasture with bokashi	13.08	2.57	0.23	11.04	22.51	0.12	22.63	17.96
	Pasture without fertilization	17.40	2.46	0.24	10.45	26.95	0.13	27.08	18.93
	Pasture with urea	20.63	2.45	0.23	10.52	25.92	0.13	26.05	16.44
Second month of the rainy season	Pasture with bokashi	21.15	2.74	0.27	10.40	25.75	0.12	27.54	17.92
	Pasture without fertilization	21.68	2.70	0.27	10.15	26.50	0.12	26.62	18.93
	Pasture with urea	19.82	2.64	0.27	9.75	28.17	0.13	21.45	16.44
Dry season month	Pasture with bokashi	99.84	2.73	0.28	10.02	23.46	0.14	23.59	17.96
	Pasture without fertilization	108.24	2.74	0.27	10.17	32.00	0.13	32.13	18.93
	Pasture with urea	134.85	2.66	0.24	11.14	28.71	0.13	25.92	16.44

DM: plant dry matter.

Author's contributions

BASR supervised the research and the writing of the article. YSGV gave ideas for the formulation and execution of the research. DTL obtained financing and supervised the research. JMC supervised research. NHP and EGZ carried out the research. All authors have read and approved the final version of the manuscript.

Literature cited

Arguedas Acuña, F., Jiménez-Araya, J., & Abarca Monge, S. (2019). Momento óptimo del día para muestrear óxido nitroso en el trópico muy húmedo de Costa Rica. *Alcances Tecnológicos*, *12*(2), 33–46. https://doi.org/10.35486/at.v12i2.90

Bastidas, M., Villegas, D., Ruden, A., Mazabel, J., Enciso, K., Gutiérrez Solís, J. F., & Arango, J. (2020). *Determinación de la eficiencia en el uso del nitrógeno (UEN) por principales pasturas forrajeras de trópico bajo en respuesta a diferentes fertilizantes nitrogenados-Informe final de resultados* (Report). Alianza Bioversity International - CIAT.

Butterbach-Bahl, K., Baggs, E. M., Dannenmann, M., Kiese, R., & Zechmeister-Boltenstern, S. (2013). Nitrous oxide emissions from soils: how well do we understand the processes and their controls?. *Philosophical Transactions of the Royal Society B: Biological Sciences, 368*(1621), Article 20130122. https://doi.org/10.1098/rstb.2013.0122

Climatemps. (2017). *La Ceiba Climate and temperature*. http://www.la-ceiba.climatemps.com/index.php

CMNUCC (Convención Marco de las Naciones Unidas sobre el Cambio Climático). (2017). *Acuerdos internacionales sobre acción por el clima*. http://www.consilium.europa.eu/es/policies/climate-change/international-agreements-climate-action/

ENCC (Estrategia Nacional de Cambio Climático). (2022). *Propuesta de lineamientos para una Estrategia Nacional de Adaptación y Mitigación al Cambio*. SERNA.

FAO (Food and Agriculture Organization of the United Nations). (2013). *Climate-smart agriculture sourcebook*. http://www.fao.org/docrep/018/i3325e/i3325e.pdf

FAO (Food and Agriculture Organization of the United Nations) (2017). *FAOSTAT. Base de datos emisiones de CO_2-eq del sector agropecuario de Honduras*. http://www.fao.org/faostat/es/#country/95

Harty, M. A., Forrestal, P. J., Watson, C. J., McGeough, K. L., Carolan, R., Elliot, C., Krol, D., Laughlin, R. J., Richards, K. G., & Lanigan, G. J. (2016). Reducing nitrous oxide emissions by changing N fertiliser use from calcium ammonium nitrate (CAN) to urea based formulations. *Science of the Total Environment*, *563–564*, 576–586. https://doi.org/10.1016/j.scitotenv.2016.04.120

Hernández, E. G. (2009). *Evaluación agronómica y calidad analítica del Brachiaria brizantha cv marandú a diferentes fuentes de fertilización en Olancho, fase III* [Undegraduate thesis, Universidad Nacional de Agricultura]. Catacamas.

Ibrahim, M. A., Guerra, L., Casasola Coto, F., & Neely, C. (2010). Importance of silvopastoral systems for mitigation of climate change and harnessing of environmental benefits. In *Grassland carbon sequestration: management, policy and economics. Proceedings of the workshop on the role of grassland carbon sequestration in the mitigation of climate change* (Vol. 11). FAO.

IPCC (Intergovernmental Panel on Climate Change). (2007). *Summary for Policymakers. Climate Change 2007: Synthesis Report of Fourth Assessment Report of the Intergovernmental Panel on Climate Change*. Cambridge University Press.

Jiang, Y., Kang, Y., Han, C., Zhu, T., Deng, H., Xie, Z., & Zhong, W. (2020). Biochar amendment in reductive soil disinfestation process improved remediation effect and reduced N_2O emission in a nitrate-riched degraded soil. *Archives of Agronomy and Soil Science*, *66*(7), 983–991. https://doi.org/10.1080/03650340.2019.1650171

Jones, J. J. B. 1999. *Soil analysis handbook of reference methods*. CRS Press.

Klein, C., & Harvey, M. (Eds.). 2012. *Nitrous oxide chamber methodology guidelines*. Global Research Alliance on Agricultural Greenhouse Gases.

Luo, J., de Klein, C. A. M., Ledgard, S. F., & Saggar, S. (2010). Management options to reduce nitrous oxide emissions from intensively grazed pastures: a review. *Agriculture, Ecosystems & Environment*, *136*(3-4), 282–291. https://doi.org/10.1016/j.agee.2009.12.003

Madigan, M. T., Martinko, J. M., & Parker, J. (Eds.). (2003). *Biología de los microorganismos* (10th ed.). Pearson-Prentice Hall.

Mcneill, A., & Unkovich, M. (2007). *The nitrogen cycle in terrestrial ecosystems*. In P. Marschner, & Z. Rengel (Eds.), *Nutrient cycling in terrestrial ecosystems* (pp. 37–64). Springer-Verlag. https://doi.org/10.1007/978-3-540-68027-7_2

Millard, N., Ndufa., J. K., Cadisch., G., & Baggs, E. M. (2004). Nitrous oxide emissions following incorporation of improved-fallow residues in the humid tropics. *Global Biogeocheical Cycles, 18*(1), Article 1032. https://doi.org/10.1029/2003GB002114

Molina, E., & Meléndez, G. (2002). *Tabla de interpretación de análisis de suelos*. Centro de Investigaciones Agronómicas, Universidad de Costa Rica.

Montenegro, J. (2020). Efecto de diferentes fuentes de nitrógeno en la emisión de óxido nitroso en plantaciones de café en Costa Rica. *Revista de Ciencias Ambientales*, *54*(2), 111–130. https://doi.org/10.15359/rca.54-2.6

Nogueira, A. K. S., Rodrigues, R. A. R., Castro, B. S., Nogueira, T. F., Silva, J. J. N., Behling, M., Mombach, M., Armacolo, N., & Silveira, J. G. (2015). Emissões de óxido nitroso e metano do solo em áreas de recuperação de pastagens na Amazonia matogrossense. *Química Nova*, *38*(7), 937–943. https://doi.org/10.5935/0100-4042.20150109

Oertel, C., Matschullat, J., Zurba, K., Zimmermann, F., & Erasmi, S. (2016). Greenhouse gas emissions from soils – A review. *Geochemistry*, *76*(3), 327–352. https://doi.org/10.1016/j.chemer.2016.04.002

Pastrana, I., Reza, S., Espinosa, M., Suárez, E., & Díaz, E. (2011). Efecto de la fertilización nitrogenada en la dinámica del óxido nitroso y metano en *Brachiaria humidicola* (Rendle) Schweickerdt. *Ciencia y Tecnología* Agropecuaria, *12*(2), 134–142. https://doi.org/10.21930/rcta.vol12_num2_art:223

Rowlings, D. W., Grace, P. R., Scheer, C., & Liu, S. (2015). Rainfall variability drives interannual variation in N_2O emissions from

a humid, subtropical pasture. *Science of the Total Environment*, *512–513*, 8–18. https://doi.org/10.1016/j.scitotenv.2015.01.011

Silva Parra, A., Gómez Isuasti, A. S., Landazury, B., & Preciado, B. (2013). Evaluación de gases de efecto invernadero (GEI) en sistemas ganaderos asociados con pasto kikuyo (*Pennisetum clandestinum* Hoechst Ex Chiov). *Revista Colombiana de Ciencia Animal, 6*(1), 36–43.

Soil Taxonomy. (2014). *Claves para la taxonomía de suelos* (12th ed.). United Sates Department of Agriculture. Natural Resources Conservation Service. https://www.nrcs.usda.gov/sites/default/files/2022-10/Spanish-Keys-to-Soil-Taxonomy.pdf

Sosa, B. A. (2013). *Dinámica del nitrógeno del suelo en sistemas de maíz Zea mays L. y soya Glycine max* L. *bajo el efecto de abonos verdes* [Doctoral dissertation, Universidad Nacional de Colombia, sede Palmira]. https://repositorio.unal.edu.co/handle/unal/33721

Steinfeld, H., Gerber, P., Wassenaar, T., Castel, V., Rosales, M., & Haan, C. (2006). *Livestock's long shadow. Environmental issues and options*. FAO, Food and Agriculture Organization of the United Nations.

Uchida, Y., Clough, T. J., Kelliher, F. M., Hunt, J. M., & Sherlock, R. R. (2011). Effects of bovine urine, plants and temperature on N_2O and CO_2 emissions from a sub-tropical soil. *Plant and Soil*, *345*, 171–186. https://doi.org/10.1007/s11104-011-0769-z

Venterea, R. T., Parkin, T. B., Cárdenas, L., Petersen, S. O., & Pedersen, A. R. (2012). Data analysis considerations. In C. de Klein, & M. Harvey (Eds.), *Nitrous oxide chamber methodology guidelines* (pp. 95–121). Global Research Alliance on Agricultural Greenhouse Gases.

Effect of different fertilizers on yield and grain composition of maize in the tropical rainforest zone

Efecto de diferentes fertilizantes sobre el rendimiento y composición del grano de maíz en la zona de selva tropical

Oluwatosin Komolafe[1*] and Moses Adewole[1]

ABSTRACT

This study assessed the quality of selected organic-based fertilizers (OBF) (neem-fortified (NM) and cow dung compost (CD)) and compared them with an inorganic fertilizer (IF) NPK 20-10-10 to determine the growth response and grain composition of maize. The field study was conducted in the early and late cropping seasons of 2015 at the Teaching and Research Farm of the Obafemi Awolowo University, Ile-Ife, Nigeria. The experiment, laid out in a randomized complete block design, consisted of six treatments: 100% NM and 100% CD, each at the rate of 3 and 6 t ha^{-1}, IF at 0.3 t ha^{-1} (inorganic fertilizer recommendation for local maize production), and zero fertilizer application as control. The highest grain yield of maize (1.87 ± 0.13 t ha^{-1}) was obtained with IF and the lowest one (1.01 ± 0.10 t ha^{-1}) with zero fertilizer application. Maize grain yield from the repeated experiment without treatments applications reduced by about 50 and 75% for OBFs and IF and control plots, respectively. Low crude fiber, 2.62-4.13% obtained using OBFs was a good indicator of maize quality. Organic-based fertilizers demonstrated superior effects on the quality of maize grains when compared to the inorganic fertilizer.

Key words: organic amendment, *Zea mays*, inorganic fertilizer, nutritional content, soil quality, composted manure.

RESUMEN

Este estudio evaluó la calidad de fertilizantes orgánicos seleccionados (FOS) (fortificados con neem (NM) y compost de estiércol de vaca (CD)) y los comparó con un fertilizante inorgánico NPK 20-10-10 (IF) para determinar la respuesta de crecimiento y composición del grano de maíz. El estudio de campo se realizó en las temporadas de cultivo tempranas y tardías de 2015 en la Granja de Enseñanza e Investigación de la Universidad Obafemi Awolowo, Ile-Ife, Nigeria. El experimento, establecido en un diseño de bloques completos al azar, constó de seis tratamientos: 100% NM y 100% CD, cada uno a razón de 3 y 6 t ha^{-1}, IF a 0.3 t ha^{-1} (recomendación de fertilización inorgánica para la producción local de maíz), y cero aplicación de fertilizantes como control. El mayor rendimiento de grano de maíz (1.87 ± 0.13 t ha^{-1}) se obtuvo con IF y el menor (1.01 ± 0.10 t ha^{-1}) con cero aplicación de fertilizante. El rendimiento de grano de maíz del experimento repetido sin aplicaciones de tratamientos se redujo en aproximadamente un 50 y un 75% para las parcelas FOS e IF y de control, respectivamente. El bajo contenido de fibra cruda, 2.62-4.13% obtenido mediante FOS, fue un buen indicador de la calidad del maíz. Los fertilizantes orgánicos demostraron efectos superiores en la calidad de los granos de maíz en comparación con el fertilizante inorgánico.

Palabras clave: enmienda orgánica, *Zea mays*, fertilizante inorgánico, contenido nutricional, calidad del suelo, estiércol compostado.

Introduction

Soil nutrient depletion is a worldwide environmental challenge having serious negative impact on food security and soil quality. Soil nutrient depletion involves loss of organic matter and reduced soil nutrient levels (Osujieke *et al*., 2020). This could lead to reduced crop yield and loss of agricultural lands. For sustainable long-term productivity and a better agricultural environment, maintenance of soil quality is necessary (Johnston & Poulton, 2018). Crop production in sub-Saharan Africa (SSA) has faced various limitations. Among them are climate change and low soil fertility. However, low soil fertility status has been the most challenging in this region for many decades. It has been a major reason for increased food insecurity, which is evident in the declining food production per capita from smallholder farms (Mango *et al*., 2017; Ayito *et al*., 2018).

Many factors, both natural and artificial, have been identified as the reasons for such low soil quality. Some of them include soil erosion, overgrazing, and indiscriminate vegetation removal. Other factors that contribute to soil

Received for publication: September 30, 2022. Accepted for publication: December 14, 2022 Doi: 10.15446/agron.colomb.v40n3.105046

[1] Institute of Ecology and Environmental Studies, Obafemi Awolowo University, Ile-Ife (Nigeria).
* Corresponding author: komolafeolaoluwa@ymail.com

nutrient depletion through physico-climatic processes in tropical Africa and particularly SSA include loss of soil nitrogen and phosphorus through wind and water erosion as well as leaching of nitrogen and potassium (Slama *et al*., 2020). Others are unsustainable tillage practices and continuous cropping with low or no fertilizer inputs. Continuous cropping without fertilizer inputs, or wrong or inadequate fertilizer applications have led to further reduction in soil quality (Choudhary *et al*., 2018).

Fertilizer is any organic or inorganic material that is added to a soil to supply one or more plant nutrients essential to the growth of plants and also to improve soil condition (Cai *et al*., 2019). Fertilizer application is an important farming practice. It has led to improved crop production and has increased the acceptance of other sustainable practices that enhance crop production. Hence, fertilizer application has been integrated into many agricultural programs and has become a key element for improving crop production in most countries.

Liu *et al*. (2019) observed that an improvement in soil fertility is needed to increase agricultural productivity. They further observed that enhanced soil fertility will lead to improvement in food security and increased income for many farmers. Therefore, to reduce nutrient depletion in soils, application of fertilizers (organic or inorganic) in required dosages and with appropriate methods are necessary (Adewole & Adeoye, 2008). However, sustaining soil quality depends on the ability to enhance nutrient recycling in soils (Schröder *et al*., 2016).

Addition of different soil amendments in response to declining soil fertility has been studied by many scientists (Diacono & Montemurro, 2011; Syuhada *et al*., 2016; Jjagwe *et al*., 2020). An inorganic fertilizer improves crop yield, soil pH, total nutrient content and increased nutrient availability, while the use of an organic fertilizer, such as manure, leads to improved soil conditions for longer periods of time, particularly with continuous maize crop cultivation (Oladele *et al*., 2019).

Maize (*Zea mays*) is an important agricultural crop in the SSA and ranks as the most important cereal crop, with Nigeria as the largest African producer (IITA, 2018). It is a staple food for more than 1.2 billion people in SSA and Latin America (IITA, 2018). Its importance could be attributed to its capability to be grown all through the year. Globally, the demand for maize sometimes surpasses supply as a result of the various domestic uses and importance (Ten Berge *et al*., 2019). In most African countries, maize production per capita has not been on the same level with the population growth over the past 60 years (Smale & Jayne, 2003). Therefore, with maize a strategic and important crop, its production must be maintained at adequate levels to ensure food security and self-sufficiency at both household and national levels (Santpoort, 2020). Maize is also a crop that requires a high amount of mineral nutrients for its growth and its productivity is largely dependent on soil nutrient management (Kannan *et al*., 2013). Therefore, there is a need to take appropriate steps to ensure increased maize production by improving the physical and chemical properties of the soil. This can be achieved through appropriate farming practices such as the use of appropriate fertilizers and sound agronomic practices. This study, therefore, compared the efficacy of selected organic and inorganic fertilizers on the growth response and nutrient composition of maize on an Alfisol of a forest ecological zone in Southwestern Nigeria. A drought-tolerant maize variety was used as an improved seed technology to help flatten economic burden often associated with frequent droughts in the study area.

Materials and methods

The study was carried out at the Teaching and Research Farm, Obafemi Awolowo University (OAU), Ile-Ife, Osun State, Nigeria in the early (April - July) and late (August - November) seasons of 2015. The research farm was located at 07°30'0" N and 04°30'0" E, at an elevation of 268 m a.s.l. The study area falls within the lowland tropical rainforest (Adesina, 1989). The experimental sites had a total annual rainfall of 1165.2 mm and an average annual temperature of 35.2°C (Komolafe, 2015). The early seasons have an average temperature of 28.57°C and 141 mm of precipitation, the late seasons have average temperature of 26.49°C and 144.29 mm of precipitation (Climate Change Knowledge Portal, 2021).

Experimental site

The experimental site was cleared manually, and pre-cropped soil samples were collected at a depth of 0-15 cm for analysis. A drought-tolerant maize variety, DT-SYN-8W obtained from the Institute of Agricultural Research and Training, Ibadan, Nigeria was the test crop. Neem-fortified organic fertilizer sourced from Alesinloye Waste Recycling Complex of Ibadan (Nigeria) and fortified with neem leaves and NPK 20-10-10 inorganic fertilizer were procured from an open market in Ibadan. Fresh cow dung was obtained from the Beef Unit of the Teaching and Research Farm, OAU, Ile-Ife and composted aerobically. The experiment consisted of six treatments laid out in a

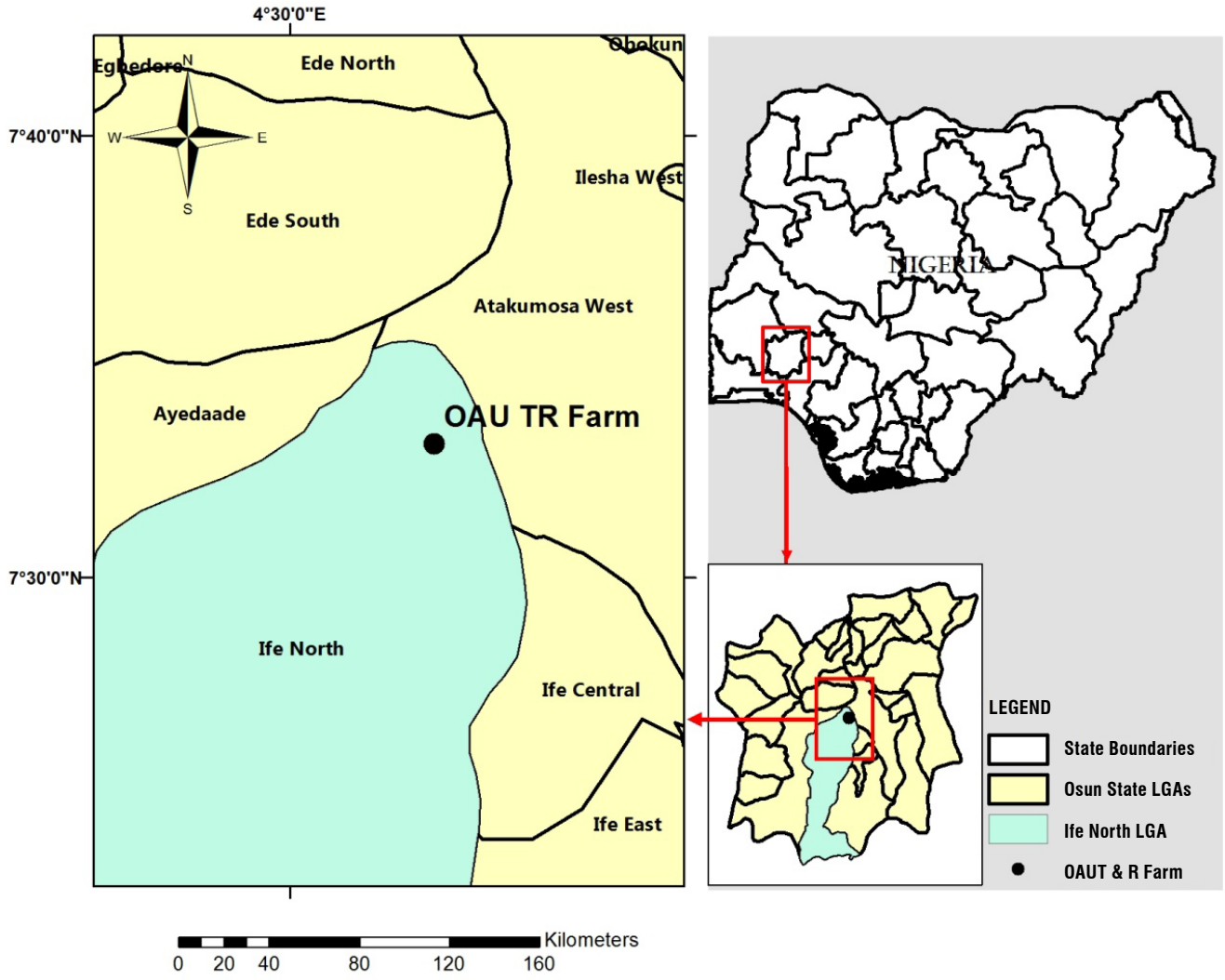

FIGURE 1. Map of Nigeria showing the study area.

randomized complete block design. The treatments were: 100% neem-fortified organic fertilizer (NM) and 100% cow dung compost (CD), each at the rate of 3 or 6 t ha^{-1}, NPK (20-10-10) at 0.3 t ha^{-1} (inorganic fertilizer recommendation for local maize production) and zero fertilizer application as control.

The experimental site consisted of three 23.0 x 2.5 m blocks; each block was in turn divided into six plots of 3.0 x 2.5 m with an alley of 1.0 m between blocks and 1.0 m within plots. Each treatment plot was replicated thrice to give a total of 18 plots. The test crop was sown at three seeds per hill using 75 x 50 cm planting distance. All the treatments, except NPK (20-10-10), were applied at sowing. The NPK fertilizer was applied two weeks after planting. Maize seedlings were later thinned to two seeds per hole at two weeks after sowing (WAS) to give a total of 53,333 maize plants per ha. Manual weeding using a handheld hoe was carried out at 2 and 5 weeks after sowing. Maize ears from each treatment plot were harvested, threshed, and stored for grain yield weight determination. The experiment was repeated during the late maize cropping season to identify any improvements or changes in the performance of the crops over time due to the earlier treatments. Post-cropped soil samples were collected immediately after maize harvesting in the late cropping season.

Analysis of soil properties

The following chemical properties of the sampled soil, neem-fortified organic fertilizer and cow dung compost were determined using standard methods (Page *et al.*, 1982). Soil pH was determined in a 1:1 soil to water suspension using the Dwyer model WPH1 waterproof pH

tester. Particle size distribution was determined using the hydrometer method. Soil organic carbon was determined using the Walkley and Black method. The exchangeable cations were determined using 1 M Ammonium acetate buffered at pH 7.0 as extractant. The K^+ and Na^+ concentrations in the soil were read on a Gallenkamp flame photometer while Ca^{2+} and Mg^{2+} concentrations in the soil extracts were read on a Perkin-Elmer Model 403 atomic absorption spectrophotometer (AAS). Exchangeable acidity was determined by the titration method after extraction with KCl. Total nitrogen was determined using macro-Kjedahl method. Available phosphorus was determined by the ascorbic acid molybdate blue method as described by Murphy and Riley. Micronutrients (Zn, Mn, Cu, B, and Fe) and As were extracted using 0.1 M HCl (Juo, 1982) and their concentrations in the soil extracts were read on the AAS. Dried maize grains (at 12% percentage moisture) were subjected to proximate composition using the methods from AOAC (1990).

Statistical analysis

Collected data were analyzed using ANOVA (analysis of variance) and their treatment means were calculated by Duncan's Multiple Range Test (DMRT) method using GraphPad Prism 5 and SAS. Descriptive statistics was used to determine the reduction in the grain yield of maize between the two cropping seasons.

Result and discussion

Experimental site and the organic fertilizers used

The soil texture was sandy loam with 792.00, 114.00, and 94.00 g kg^{-1} of sand, clay, and silt, respectively (Tab. 1). The soil pH (1:1 soil-H_2O) of the experimental site was 7.86, indicating an alkaline condition. Other soil properties included: 22.51 g kg^{-1} of organic carbon, 2.12 g kg^{-1} of total nitrogen, 1.63 mg kg^{-1} of available phosphorus and 21.01 cmol kg^{-1} of cation exchange capacity, but mostly dominated by Ca^{2+}. The micronutrient contents of Zn, Mn, Cu, and Fe were 1.28, 30.80, 1.65, and 141.00 mg kg^{-1}, respectively. The neem-fortified organic fertilizer had 148.88 and 16.50 g kg^{-1} organic carbon and total nitrogen, respectively, and a carbon-nitrogen ratio of 9.02. Other values of the neem-fortified organic fertilizer were: 31.37 mg kg^{-1} of available phosphorus, and 13.30, 16.97 and 0.33 cmol kg^{-1} of available K, Ca and Mg, respectively. The Zn, As and B in neem-fortified organic fertilizer had values 1.73, 2.10 and 1.30 mg kg^{-1}, respectively. Except for the carbon-nitrogen ratio, available P and Mg, all other parameters were lower in the cow dung compost than in the neem-fortified organic fertilizer. In this study, the soil organic carbon and total nitrogen are considered moderate, according to the ratings of the Developing Agri-input Markets in Nigeria (DAIMINA) (Singh, 2002). These, however, may not be adequate for optimum production of maize, as low grain yield of maize is the current realizable scenario by most resource-poor Nigerian farmers (IITA, 2018).

TABLE 1. Properties of pre-cropped soil and two organic fertilizers used.

Property	Soil	NM	CD
pH (1:1 soil-water)	7.86	-	-
Organic carbon (g kg^{-1})	22.51	148.88	135.37
Total N (g kg^{-1})	2.12	16.50	11.60
C/N	-	9.02	11.67
Available P (mg kg^{-1})	1.63	31.37	35.15
Exchangeable cations (cmol kg^{-1})			
Na^+	0.27	-	-
K^+	0.20	13.30	1.45
Ca^{2+}	20.15	16.97	1.11
Mg^{2+}	0.39	0.33	0.58
CEC	21.01	-	-
Exchangeable acidity (cmol kg^{-1})	0.40	-	-
Zn (mg kg^{-1})	1.28	1.73	0.05
Mn (mg kg^{-1})	30.80	-	-
Cu (mg kg^{-1})	1.65	-	-
As (mg kg^{-1})	-	2.10	1.30
B (mg kg^{-1})	-	1.30	0.80
Fe(mg kg^{-1})	141.00	-	-
Sand (g kg^{-1})	792.00	-	-
Clay (g kg^{-1})	114.00	-	-
Silt (g kg^{-1})	94.00	-	-
Textural class	Sandy loam		-

NM = Neem-fortified organic fertilizer, CD = Cow dung compost.

Shehu *et al.* (2018) and Lucas *et al.* (2019) worked extensively on nutrient requirements for enhanced grain yield of maize in Nigeria and Brazil, respectively. These authors observed that near moderate soil organic matter can be related to inherently high sandy nature of the parent material and low capacity to store carbon. This could also be the reason for low total N and cation exchangeable capacity, as soil organic carbon plays a vital role in soil fertility maintenance. The neem-fortified organic fertilizer with low C/N ratio had better opportunity to mineralize and release its essential nutrients for maize use faster than cow dung compost with higher C/N ratio. Syuhada *et al.* (2016) observed a similar scenario in their study, where biochar with small fractions of carbon mineralized later than synthetic fertilizers with fast release of nutrients. Seman-Varner *et al.* (2019) and Jjagwe *et al.* (2020) also observed better response from low

C/N ratio amendments of plant- and animal-based manure than those with high C/N ratio.

Effects of organic and inorganic fertilizer applications on grain yield

The effects of organic and inorganic fertilizer applications on the grain yield and percentage reduction of maize during the two cropping seasons are presented in Table 2. The application of NPK 20-10-10 gave significantly (P<0.05) highest grain yield, 1.87 t ha^{-1}; while the control plot had the least significant grain yield (1.01 t ha^{-1}) of maize from the early cropping season. Except for NPK 20-10-10 and control plots that had reduced grain yield of maize by over 75%, other plots with organic-based fertilizers had about 50% reduction of the grain yield of maize in the late cropping season.

The inorganic fertilizer NPK 20-10-10 gave significantly highest grain yield of maize during the early cropping season because of its ability to release nutrient elements faster than most organic-based fertilizers, resulting in high maize grain yield in the early cropping season. The neem-fortified organic fertilizer that had higher maize grain yield than cow dung compost could be due to the faster mineralization and releasing tendency in neem-fortified organic fertilizer. This agrees with Slomon *et al*. (2018), who stated that breakdown and mineralization of the neem amendment result in the release of nutrients to the soil, thus, improving the soil nutrients and subsequently improving the crop yield. The higher the quantity of organic-based fertilizer used, the higher the grain yield of maize. During the repeat experiment in the late cropping season, about 50% reduction was observed with organic-based treatment applications, while over 75% reduction was observed with NPK 20-10-10 and zero treatment applications. Lower percentage reduction obtained with organic-based fertilizers was due to their nutrient slow-releasing effect in maize crop production.

Effects of organic and inorganic fertilizer applications on the grain composition and grain yield of maize

The compositions of the harvested maize grain in the early and late cropping seasons are presented in Table 3. Crude protein 8.12-11.99%, crude fat 2.16-4.13%, reducing sugar 3.27-7.08%, vitamin C 2.86-3.85%, and crude fiber 2.62-4.13% were enhanced with the addition of organic-based fertilizers, compared to the inorganic fertilizer or zero treatment application. Except for crude fiber, lower values were obtained with inorganic fertilizer and zero treatment applications.

In this study, the early maize cropping season produced better grain quality than the late cropping season. The early maize cropping season generally occurs during the rainy period, when more soil moisture will be available for nutrient element mobility and their uptake by maize plants than in the late cropping season. Maize grains from early cropping season had higher crude fiber and vitamin C than maize grains from the late cropping season, and these might have been influenced by higher nutrient element' mobility and their uptake by the maize plant. Low crude fiber is useful in quality assessment of maize grain as this enhances the utilization of nitrogen and accumulation of micronutrients useful for human nutrition (Obinna-Echem *et al*., 2018).

Effects of organic and inorganic fertilizer applications on post-cropped soil properties of the maize field are presented in Table 4. Most of the soil parameters, such as organic carbon, total nitrogen, available phosphorus, and CEC, increased after maize harvesting of the late cropping season when organic-based fertilizers were applied to soil. These soil parameters, however, decreased with NPK 20-10-10 and zero treatment applications. Also, the soil parameters increased with increase in treatment applications. The soils became more acidic after the late maize cropping season.

TABLE 2. Mean (± SD) grain yield (t ha^{-1}) and percentage reduction of maize during two cropping seasons.

Treatment	Early cropping season	Late cropping season	Percentage reduction
NM3	1.27 ± 0.13 ab	0.64 ± 0.15 a	49.6
CD3	1.10 ± 0.15 ab	0.50 ± 0.14 a	54.5
NM6	1.53 ± 0.17 ab	0.77 ± 0.13 a	49.7
CD6	1.42 ± 0.23 ab	0.72 ± 0.13 a	49.3
NPK 20-10-10	1.87 ± 0.13 a	0.40 ± 0.15 ab	78.6
Control	1.01 ± 0.10 b	0.25 ± 0.10 b	75.2

NM3 = Neem-fortified organic fertilizer at 3 t ha^{-1}, CD3 = Cow dung compost at 3 t ha^{-1}, NM6 = Neem-fortified organic fertilizer at 6 t ha^{-1}, and CD6 = Cow dung compost at 6 t ha^{-1}. Mean values with the same letter(s) down the column are not significantly different by Duncan's Multiple Range test at P<0.05.

TABLE 3. Grain composition of maize harvested in the early and late cropping seasons.

Treatments	Crude protein (%)	Crude fat (%)	Crude fiber (%)	Ash (%)	Moisture (%)	Total sugar (%)	Reducing sugars (%)	Vitamin C (%)
Early cropping season								
NM3	9.74 a	4.10 a	2.92 b	4.24 a	13.06 a	10.40 a	7.08 a	3.85 a
CD3	8.12 b	3.42 a	3.93 b	3.54 a	10.89 c	8.67 bc	5.90 bc	3.21 ab
NM6	10.45 a	4.13 a	4.10 a	4.72 a	13.30 a	11.87 a	8.00 a	4.05 a
CD6	8.24 b	3.48 a	4.13 a	3.63 a	10.23 c	9.13 ab	6.16 b	3.12 b
NPK 20-10-10	5.96 d	2.45 c	5.11 a	2.61 c	7.55 d	6.59 c	4.45 c	2.28 c
Control	8.86 c	3.21 b	4.95 a	3.82 b	11.53 b	9.61 b	6.28 b	3.01 b
Late cropping season								
NM3	10.81 a	2.59 a	2.62 b	2.51 a	10.81 b	11.78 a	3.92 c	3.43 a
CD3	9.01 b	2.16 a	3.24 a	2.09 a	9.01 bc	9.82 b	3.27 d	2.86 b
NM6	11.99 a	3.03 a	3.28 a	2.74 a	13.61 a	12.87 a	6.11 a	3.81 a
CD6	9.23 b	2.33 a	3.36 a	2.11 a	10.12 b	9.90 b	4.70 b	2.93 b
NPK 20-10-10	7.38 d	1.86 c	4.26 a	1.69 b	8.10 c	7.92 c	3.76 cd	2.34 c
Control	8.05 c	2.20 ab	4.03 a	2.08 a	10.86 b	8.21 bc	3.94 c	3.21 ab

NM3 = Neem-fortified organic fertilizer at 3 t ha^{-1}, CD3 = Cow dung compost at 3 t ha^{-1}, NM6 = Neem-fortified organic fertilizer at 6 t ha^{-1}, CD6 = Cow dung compost at 6 t ha^{-1}. Mean values with the same letter(s) in the same column are not significantly different by Duncan's Multiple Range Test at $P<0.05$.

TABLE 4. Effects of organic and inorganic fertilizers on post-cropped soil properties.

Property	NM3	CD3	NM6	CD6	NPK 20-10-10	Control
pH	7.56±0.12	7.60±0.15	7.63±0.17	7.65±0.05	7.33±0.17	7.03±0.07
Organic C (g kg^{-1})	42.63±1.04	33.81±0.85	49.46±0.64	43.16±1.00	19.43±0.27	13.59±0.11
Total N (g kg^{-1})	4.12±0.27	3.25±0.20	4.61±0.19	3.72±0.27	1.85±0.25	1.22±0.15
Available P (mg kg^{-1})	4.84±0.23	2.99±0.18	5.57±0.25	4.64±0.15	3.13±0.17	2.98±0.13
Exchangeable bases (cmol kg^{-1})						
Na^+	0.54±0.06	0.41±0.05	0.65±0.05	0.54±0.06	0.36±0.04	0.33±0.07
K^+	0.44±0.04	0.34±0.04	0.34±0.05	0.29± 0.01	0.34±0.06	0.23±0.07
Ca^{2+}	6.02±0.15	4.63±0.14	5.99±0.11	4.99±0.11	3.32±0.10	3.15±0.10
Mg^{2+}	0.68±0.15	0.52±0.11	0.67±0.13	0.56±0.14	0.36±0.04	0.30±0.05
Micronutrients (mg kg^{-1})						
Zn	1.82±0.28	1.40±0.20	1.56±0.22	1.30±0.10	1.20±0.05	1.15±0.05
Mn	30.11±2.25	23.16±1.45	29.64±0.45	24.70±0.24	17.28±0.12	16.20±0.17
Cu	1.50±0.05	1.16±0.02	1.36±0.04	1.13±0.07	0.95±0.05	0.95±0.04
Fe	132.90±3.25	102.20±2.80	107.60±3.20	89.80±2.20	90.67±1.13	86.50±1.77

NM3 = Neem-fortified organic fertilizer at 3 t ha^{-1}, CD3 = Cow dung compost at 3 t ha^{-1}, NM6 = Neem-fortified organic fertilizer at 6 t ha^{-1}, and CD6 = Cow dung compost at 6 t ha^{-1}.

Conclusions

Organic-based fertilizers vary in nutrient composition and mineralization rate depending on their organic materials make-up. The two organic-based (neem-fortified and cow dung compost) fertilizers have longer-lasting and more positive effects on soil properties, particularly soil organic carbon, total nitrogen, and CEC than the inorganic fertilizer (NPK 20-10-10). Also, neem-fortified organic fertilizer demonstrated superior influence on soil properties and grain yield of maize, and there was a direct relationship on the quantity of added fertilizer and grain yield of maize. Organic-based fertilizers demonstrated superior effects on the quantity and quality of maize grains than the inorganic fertilizer.

Conflict of interest statement

The authors declare that there is no conflict of interests regarding the publication of this article.

Author's contributions

OK and MA designed the experiments. OK conducted the research process, specifically performing the experiments and data collection, applied statistical techniques to analyze study data, and wrote the original draft. MA oversaw and led the research activity planning and execution and verified the overall replication/reproducibility of results/experiments and other research outputs. MA also revised the manuscript. All authors reviewed the final version of the manuscript.

Literature cited

Adesina, F. A. (1989). Plant species characteristics and vegetation dynamics in the tropics. *International Journal of Environmental Studies, 33*(1-2), 67–78. https://doi.org/10.1080/00207238908710481

Adewole, M. B., & Adeoye, G. O. (2008). Comparative study of blanket fertilizer application and nutrients' critical level fertilizer application to cassava/maize intercrop. *Ife Journal of Science, 10*(2), 293–296.

Association of Official Analytical Chemists (AOAC). (1990). *Official methods of analysis of the analytical chemists* (15th ed., Vol. 2). Washington, DC.

Ayito, E. O., Iren, O. B., & John, K. (2018). Effects of neem-based organic fertilizer, NPK and their combinations on soil properties and growth of okra (*Abelmoschus esculentus*) in a degraded ultisol of Calabar, Nigeria. *International Journal of Plant & Soil Science, 24*(5), 1–10. https://doi.org/10.9734/IJPSS/2018/43027

Cai, A., Xu, M., Wang, B., Zhang, W., Liang, G., Hou, E., & Luo, Y. (2019). Manure acts as a better fertilizer for increasing crop yields than synthetic fertilizer does by improving soil fertility. *Soil and Tillage, 189*, 168–175. https://doi.org/10.1016/j.still.2018.12.022

Choudhary, M., Panday, S. C., Meena, V. S., Singh, S., Yadav, R. P., Mahanta, D., Mondai, T., MIshra, P. K., Bisht, J. K., & Pattanayak, A. (2018). Long-term effects of organic manure and inorganic fertilization on sustainability and chemical soil quality indicators of soybean-wheat cropping system in the Indian mid-Himalayas. *Agriculture, Ecosystems & Environment, 257*, 38–46. https://doi.org/10.1016/j.agee.2018.01.029

Climate Change Knowledge Portal. (2021). Country Nigeria. https://climateknowledgeportal.worldbank.org/country/nigeria

Diacono, M., & Montemurro, F. (2011). Long-term effects of organic amendments on soil fertility. In E. Lichtfouse, M. Hamelin, M. Navarrete, & P. Debaeke (Eds.), *Sustainable agriculture* (Vol. 2, pp. 761–786). Springer. https://doi.org/10.1007/978-94-007-0394-0_34

International Institute of Tropical Agriculture (IITA). (2018, October 15). *Maize* (*Zea mays*). https://www.iita.org/cropsnew/maize

Jjagwe, J., Chelimo, K., Karungi, J., Komakech, A. J., & Lederer, J. (2020). Comparative performance of organic fertilizers in maize (*Zea mays* L.) growth, yield and economic results. *Agronomy*, *10*(1), Article 69. https://doi.org/10.3390/agronomy10010069

Johnston, A. E., & Poulton, P. R. (2018). The importance of long-term experiments in agriculture: their management to ensure continued crop production and soil fertility; the Rothanmsted experience. *European Journal of Soil Science, 69*(1), 113–125. https://doi.org/10.1111/ejss.12521

Juo, A. S. R. (1982). *Selected methods for soil and plant analysis*. International Institute of Tropical Agriculture (IITA).

Kannan, R. L., Dhivya, M., Abinaya, D., Krishna, R. L., & Krishnakumar, S. (2013). Effect of integrated nutrient management on soil fertility and productivity in maize. *Bulletin of Environment, Pharmacology and Life Sciences, 2*(8), 61–67.

Komolafe, O. O. (2015). *Effect of two tillage practices and fertilizer use on soil properties and the yield of maize* [MSc thesis. Institute of Ecology and Environmental Studies, Obafemi Awolowo University].

Liu, H., Khan, M. Y., Carvalhais, L. C., Delgado-Baquerizo, M., Yan, L., Crawford, M., Dennis, P. G., Singh, B., & Schenk, P. M. (2019). Soil amendments with ethylene precursor alleviate negative impacts of salinity on soil microbial properties and productivity. *Scientific Reports*, 9, Article 6892. https://doi.org/10.1038/s41598-019-43305-4

Lucas, F. T., Borges, B. M. M. N., & Coutinho, E. L. M. (2019). Nitrogen fertilizer management for maize production under tropical climate. *Agronomy Journal, 111*(4), 2031–2037. https://doi.org/10.2134/agronj2018.10.0665

Mango, N., Siziba, S., & Makate, C. (2017). The impact of adoption of conservation agriculture on smallholder farmers' food security in semi-arid zones of southern Africa. *Agriculture and Food Security,* 6, Article 32. https://doi.org/10.1186/s40066-017-0109-5

Obinna-Echem, P., Barber, L., & Enyi, C. (2018). Proximate composition and sensory properties of complementary food formulated from malted pre-gelatinized maize, soybean and carrot flours. *Journal of Food Research, 7*(2), 17–24. https://doi.org/10.5539/jfr.v7n2p17

Oladele, S. O., Adeyemo, A. J., & Awodun, M. A. (2019). Influence of rice husk biochar and inorganic fertilizer on soil nutrients availability and rain-fed rice yield in two contracting soils. *Geoderma, 336*, 1–11. https://doi.org/10.1016/j.geoderma.2018.08.025

Osujieke, D. N., Ibrahim, N. B., & Onwu, C. A. (2020). Nutrient depletion, organic matter loss, soil acidification, sodicity and salinization resulted due to nature interactions. Causes and way forward: A review. *Merit Research Journal of Agriculture and Soil Science, 8*(1), 1–14. https://doi.org/10.5281/ZENODO.3633797

Page, A. L., Miller, R. H., & Keeney, D. R. (1982). *Methods of soil analysis, Part 2, chemical and microbiological properties*. American Society of Agronomy, Inc.

Santpoort, R. (2020). The drivers of maize area expansion in sub-Saharan Africa. How policies to boost maize production overlook the interest of smallholder farmers. *Land*, *9*(3), Article 68. https://doi.org/10.3390/land9030068

Schröder, J. J., Schulte, R. P. O., Creamer, R. E., Delgado, A., van Leeuwen, L., Lehtinen, T., Rutgers, M., Spiegel, H., Staes, J., Tóth, G., & Wall, D. G. (2016). The elusive role of soil quality in nutrient cycling: a review. *Soil Use and Management, 32*(4), 476–486. https://doi.org/10.1111/sum.12288

Seman-Varner, R., Varco, J. J., & O'Rourke, M. E. (2019). Winter cover crop and fall-applied poultry litter effect on winter cover and soil nitrogen. *Agronomy Journal, 111*(6), 3301–3309. https://doi.org/10.2134/agronj2019.02.0133

Shehu, B. M., Merckx, R., Jibrin, J. M., Kamara, A. Y., & Rurinda, J. (2018). Quantifying variability in maize yield response to nutrient applications in the Northern Nigerian Savanna. *Agronomy, 8*(2), Article 18. https://doi.org/10.3390/agronomy8020018

Singh, H. B. (2002). The role of manures and fertilizers in crop production. Developing Agri-input Markets in Nigeria (DAIMINA); International Center for Soil Fertility and Agricultural Development.

Slama, F., Gargouri-Ellouze, E., & Bouhlila, R. (2020). Impact of rainfall structure and climate change on soil and groundwater salinization. *Climatic Change, 163*, 395–413. https://doi.org/10.1007/s10584-020-02789-0

Smale, M., & Jayne, T. (2003). *Maize in Eastern and Southern Africa: Seeds of success in retrospect* (Discussion Paper No 97). Environmental and Production Technology Division, International Food Policy Research Institute.

Syuhada, A. B., Shamshuddin, J., Fauziah, C. I., Rosenani, A. B., & Arifin, A. (2016). Biochar as soil amendment: Impact on chemical properties and corn nutrient uptake in a Podzol. *Canadian Journal of Soil Science, 96*(4), 400–412. https://doi.org/10.1139/cjss-2015-0044

Slomon, S., Afolami, S. O., Popoola, T. O. S., Atungwu, J. J., Odeyemi, S. & Daramola, F. Y. (2018). Screen house assessment of neem-fortified cassava peel powder for controlling nematodes and yield improvement of sugarcane (*Saccharum officinarum*). *International Multidisciplinary Research Journal*, *8*, 15–12.

Ten Berge, H. F. M., Hijbeek, R., Van Loon, M. P., Rurinda, J., Tesfaye, K., Zingore, S., Craufurd, P., van Heerwaarden, J., Brentrup, F., Schröder, J. J., Boogaard, H. L., De Groot, H. L. E., & Van Ittersum, M. K. (2019). Maize crop nutrient input requirements for food security in sub-Saharan Africa. *Global Food Security, 23*, 9–21. https://doi.org/10.1016/j.gfs.2019.02.001

Characterization and classification of lulo (*Solanum quitoense* Lam.) fruits by ripening stage using partial least squares discriminant analysis (PLS-DA)

Caracterización y clasificación de frutos de lulo (*Solanum quitoense* Lam.) por estado de maduración mediante análisis discriminante de mínimos cuadrados parciales (PLS-DA)

Sofía Marcela González-Bonilla[1] and María Remedios Marín-Arroyo[1]*

ABSTRACT

Lulo or naranjilla (*Solanum quitoense* Lam.) is a tropical fruit with great potential for its contents of antioxidant and biofunctional compounds and sensory characteristics. Nowadays, the different methodologies to classify the ripening stage of lulo fruits are prone to bias and can hinder adequate characterization of the fruit maturity stage as they do not use measurements. The aim of this research was to define an accurate method for classifying lulo fruits by ripening stage based on non-destructive parameters and to determine their main characteristics according to the ripening stage. Hierarchical cluster analysis was carried out to classify fruits according to their maturity index (MI) into two (MI2) and three (MI3) homogeneous groups of individuals. Using partial least squares discriminant analysis (PLS-DA), with the non-destructive parameters showing significant differences between groups, classification functions by ripening stage were established. The PLS-DA correctly classified 89.47% of the fruits in the MI2 classification and 78.95% in the MI3 classification. The predictive power of the models was tested with fruits other than those used to establish the prediction equations, obtaining a correct classification in 75% of the cases. It is possible to classify lulo fruits objectively with a limited number of non-destructive parameters that constitutes a useful tool from harvesting to consumption.

Key words: naranjilla, maturity index, ripening stage prediction, tropical fruits.

RESUMEN

El lulo o naranjilla (*Solanum quitoense* Lam.) es una fruta tropical con un gran potencial debido a su contenido de compuestos antioxidantes, biofuncionales y características sensoriales. Actualmente las diferentes formas de clasificación por estado de maduración del fruto de lulo son propensas a sesgos y dificultan una adecuada caracterización de la madurez del fruto ya que no utilizan un método de medida. El objetivo de esta investigación fue proponer un método para clasificar los frutos de lulo por estado de madurez a partir de parámetros no destructivos y determinar las principales características según su madurez. Se realizaron análisis de clúster jerárquicos para clasificar los frutos según el índice de madurez (MI), en dos (MI2) y tres (MI3) grupos homogéneos de individuos. Mediante análisis discriminante por mínimos cuadrados parciales (PLS-DA), con los parámetros no destructivos que mostraron diferencias significativas entre grupos, se establecieron funciones de clasificación según su grado de madurez. El PLS-DA clasificó correctamente el 89.47% de los frutos en la clasificación MI2 y el 78.95% en la clasificación MI3. El poder predictivo de los modelos se comprobó con frutos distintos a los utilizados para establecer las ecuaciones de predicción, obteniendo una clasificación correcta en el 75% de los casos. Es posible clasificar frutos de lulo de forma objetiva con un número limitado de parámetros no destructivos, lo que constituye una herramienta útil desde la cosecha de los frutos hasta su consumo.

Palabras clave: naranjilla, índice de madurez, predicción del estado de madurez, frutos tropicales.

Introduction

In recent years, interest in tropical fruits has increased in non-producing countries, leading to a growing market for these fruits. Global production of tropical fruits was estimated to be approximately 100.2 million t in 2018 with an annual increase of 4% from 2017 to 2018 (FAO, 2020). Tropical fruits comprise more than 2700 species and are an important source of economic growth, food security, and nutrition in rural production areas (Altendorf, 2017).

Import demand in developed countries for these fruits has evolved with migration, as consumers tend to maintain their food preferences. The volume of world trade in major tropical fruits in 2021 rose to a record of USD 10.5 billion

Received for publication: June 8, 2022. Accepted for publication: October 19, 2022 Doi: 10.15446/agron.colomb.v40n3.103082

[1] Institute for Innovation & Sustainable Food Chain Development, Universidad Pública de Navarra, Campus Arrosadia, Pamplona (Spain).
* Corresponding author: remedios.marin@unavarra.es

in constant 2014-2016 dollar terms, marking an expansion of approximately 8% from 2020 (FAO, 2022). In addition, increased awareness among consumers about the health and nutritional benefits of tropical fruits is increasing the demand for diversity of minor fruit production in developed markets (Altendorf, 2018).

Lulo or naranjilla (*Solanum quitoense* Lam.) is a tropical fruit that belongs to the Solanaceae family. The main lulo varieties are *septentrionale,* produced mainly in Colombia, Panama, and Costa Rica, and *quitoense* produced in southern Colombia and Ecuador (Ramírez *et al*., 2021). "Lulo Castilla", "lulo de Castilla" or "Castilla variety" are appellatives used to refer to the native material used in the planting of lulo in Colombia. These denominations may correspond to different ecotypes propagated from seeds extracted by producers and, therefore, have no certification, given the existence of only one registered cultivar in Colombia, "La Selva" (Lobo Arias *et al*., 2007).

Lulo arouses great interest in the global market due to its sensory characteristics such as aroma, refreshing acidic flavor (Hinestroza-Córdoba *et al*., 2020) and the striking yellowish-green color of the juice. Lulo is a low-calorie fruit characterized by its high contents of potassium and vitamin C. The antioxidant compounds and other biofunctional compounds found in this fruit can help control hypertension (Forero *et al*., 2016).

Lulo fruits are round or oval, depending on the variety, and fruit weight (W) varies between 35 g (Bernal & Díaz, 2006) and 210 g (Ochoa-Vargas, 2016). Axial diameter (AD) is between 3 cm and 9 cm and longitudinal diameter (LD) is between 3 cm and 8 cm (Bernal & Diaz, 2006). In color, lightness (L*) varies between 37 (Acosta *et al*., 2009) and 61 (Forero *et al*., 2014), with color coordinate green-red (a*) between -10 and 52 (Mejía *et al*., 2012), color coordinate blue-yellow (b*) between 31 (Mejía *et al*., 2012) and 62 (Forero *et al*., 2014), chroma (C*) between 47 (Mejía *et al*., 2012) and 53 (Gancel *et al*., 2008), and hue (h) between 67 (Gancel *et al*., 2008) and 179 (Mejía *et al*., 2012). In biochemical characteristics, the pH of juice can vary between 2.4 and 3.5 (Morillo-Coronado *et al*., 2019), titratable acidity (TA) is between 2.6% (Acosta *et al*., 2009) with 4% citric acid (Forero *et al*., 2014, Ochoa-Vargas *et al*., 2016), and total soluble solid (TSS) contents is between 6.5 ºBrix (Almanza-Merchán *et al*., 2016) and 13.6 ºBrix (Jaime-Guerrero *et al*., 2022).

One of the key factors affecting the distribution of the lulo crops is the fluctuation in fruit quality and in the maturity stages, due to the ratio between soluble solids and organic acid content (Ochoa-Vargas *et al*., 2016). The ripening of lulo fruits is a complex process due to multiple factors, such as metabolic pathways associated with the development of color, flavor, texture, aroma, and nutritional value (minerals, vitamins, fibers, and antioxidants) (Ramírez *et al*., 2018). During the ripening, an increase of yellow-orange and loss of green color is observed (Andrade-Cuvi *et al*., 2015).

There are different ways of classifying "lulo de Castilla" by ripening stage, all of them visual. These are commonly used to set the optimal harvest date of the fruits for export, fresh consumption, or use as raw material for the food industry, etc. The Colombian Technical Standard (NTC 5093) establishes the requirements that "lulo de Castilla" must meet for its use and establishes a visual classification into six stages of ripening by color change: green fruit (color 0) to an orange fruit (color 5) (ICONTEC, 2002). Another type of classification uses the color percentage, from 100% green (1) to 100% orange (5) (Andrade-Cuvi *et al*., 2015).

These visual classification methods can hardly be considered objective for several reasons: environmental lighting conditions are not specified to perform the classification, the surface of green or orange areas specified by the classifications is subjective since no measurement method is established, and the perception of color will be influenced by interindividual differences in the subjects performing the classification. For these reasons, the present research aims to determine the main physicochemical characteristics of the lulo fruits. The authors hypothesized that it is possible to objectively classify lulo fruits according to their stages of maturity from external characteristics of the fruits that can be determined quantitatively.

Materials and methods

Fruit material

The fruits used in this study were "lulo de Castilla" (*Solanum quitoense* Lam.), originally from Colombia and exported by the company Heaven's Fruits to Spain. The fruit was purchased from a local retailer in 2 kg lots, on different dates to ensure more representative sampling. The fruits were then taken to the laboratory of the Avances en Enología y Tecnología Alimentaria (Aenoltec) research group of the Universidad Pública de Navarra in Pamplona, Navarra (Spain), where the experiments were carried out. Eight different lots were purchased; and from each lot between five and seven fruits were randomly selected. A total of 52 fruits were chosen, of which 40 were used to

establish the classification models, and the remaining 12 fruits were used to test the predictive power of the models.

Visual classification by stage of maturation

The lulo fruits were visually classified by ripening stage (Fig. 1) following the Colombian Technical Standard (NTC 5093): color 0, a dark green fruit, physiologically ripe; color 1, dark green fruit with light green shades; color 2, green fruit with some orange shades; color 3, orange fruit with green glimpses towards the center of the fruit; color 4, orange fruit with few green glimpses; and color 5, orange fruit (ICONTEC, 2002). To minimize the influence of the different factors (environmental conditions, operator) in the classification, four photographs (top, bottom, and two sides) of each fruit were taken under controlled conditions with DigiEye equipment (VeriVide Ltd.,United Kingdom) that uses a computer-controlled digital camera (Nikon) allowing high-quality repeatable images of both two and three-dimensional samples. The photographs were used to classify the fruits always under the same conditions.

External physical characteristics

The analyses detailed below were performed on the whole fruits. Weight (W) of the individual fruits was measured with the use of a balance (Cobos Jt-300c, Spain). LD and AD were measured with a digital micrometer (Mitutoyo Corp., Japan). The relationships between weight and dimensions (W/LD and W/AD) were calculated.

DigiEye equipment (VeriVide Ltd., United Kingdom) with standard illuminant D65 and using the CIELAB scale was used for color measurement. The measurement method described by Matusiak (2015) was followed. The equipment was calibrated first with a white folder (Model No Digital uniformity Card, Issue DEUCOO2) and subsequently with a color folder (Model No Digitizer Calibration Chart, version No 3.6). Calibration values were $\Delta E^*<5$ points, median <1 (usually 0.7); R, G, and B with values between 225 ± 5. Color coordinates L*, a*, b*, $C^* = \sqrt{a^2 + b^2}$, and h were measured. Reflectance was measured from 400 to 700 nm in 10 nm intervals. The area under the curve (AUC), the maximum peak percent reflectance, and the wavelength at which it occurs were determined. For the determination of each parameter, five measurements were made per photograph, obtaining a total of 20 measurements per fruit.

Juice extraction

After external characterization, juice was extracted. For this purpose, the fruits were split in half, and juice, seeds and placenta were extracted manually. The juice was separated with the aid of a 710 µm sieve (Retsch, Germany).

Physicochemical analysis

The analyses detailed below were performed on the extracted juice.

The pH was measured by AOAC method 945.10 with a potentiometer equipped with a glass electrode (Crison GLP 22, series 530013, European Union) (AOAC, 2005a). TSS was determined by AOAC method 932.12 (AOAC, 2005b), with a refractometer (RX-700 CX, Japan). Data were expressed in ºBrix. The determination of TA was made according to the procedure of the UNE 12147 standard. Results were expressed in g citric acid/100 ml of lulo juice

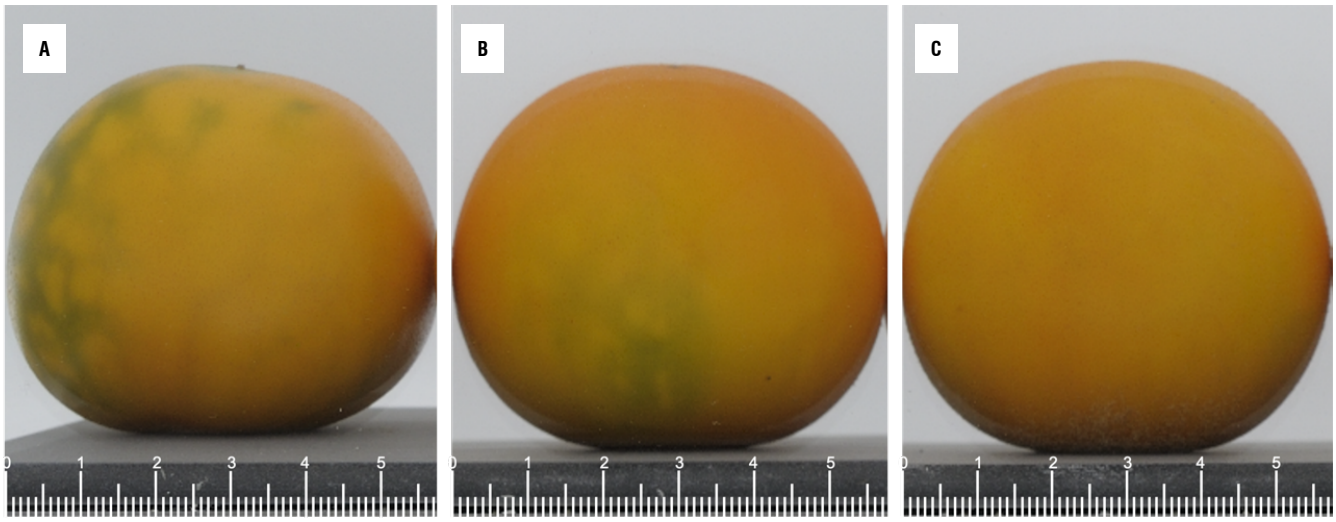

FIGURE 1. Lulo fruits at stages of ripening: A) 3, B) 4, and C) 5 according to the Colombian Technical Standard (NTC 5093). The scale is in cm.

(Asociación Española de Normalización (UNE), 1997). The maturity index (MI) was calculated as the TSS/TA ratio. All analyses were carried out in triplicate.

Statistical analysis

The first step of the statistical analysis was to perform a descriptive analysis of all the variables to determine outliers using box plots. After eliminating outliers that were out of range, a hierarchical agglomerative cluster analysis was performed with Euclidean distance, according to the Ward agglomeration method and truncation by several classes to define homogeneous groups of individuals according to the experimentally determined MI. Commonly, fruits for export are harvested at a medium ripening stage to avoid loss of weight and firmness during transit. Since we have been working with fruits for export, lulo are usually harvested as they belong to group Color 3 of the Colombian Technical Standard NTC 5093. So, it was only possible to have fruits of ripening groups 3, 4, and 5 according to the standard. Therefore, in this research, a truncation was performed in two and three groups (MI2 and MI3, respectively) since the analyzed fruits corresponded only to the three highest maturity groups defined by ICONTEC in the NTC 5093 standard.

To determine significant differences between the dependent variables (external physical and physicochemical characteristics of the lulo fruits) in the different ripening groups according to the Instituto Colombiano de Normas Técnicas y Certificación (ICONTEC) classification and the MI classifications obtained from the cluster analysis, an ANOVA was performed followed by Tukey´s multiple comparison analysis with a significance level of 5% (P<0.05).

Subsequently, with the non-destructive parameters that showed significant differences between the groups by ripening stage, a partial least squares discriminant analysis (PLS-DA) was performed to try to establish functions to classify the fruits according to their ripening stage. The method was applied on centered and reduced values with a 95% confidence interval. The discriminant analysis was carried out for the new classifications established by the MI, using as predictive variables the non-destructive parameters with significant differences between groups by the ripening stage. The predictive analysis was performed with a new set of 12 fruits. All analyses were performed with XLSTAT 2021.2.1.1116 software (Addinsoft).

Results

The values obtained for the external measurements and physicochemical analysis were in the following ranges: W (83.36-119.80 g), LD (49.27-58.83 mm), AD (55.10-64.13 mm), L* (47.32-58.37), color coordinate a* (12.29-34.69, red zone), color coordinate b* (54.91-80.15, yellow zone), C* (62.21-86.47), h (60.36-75.73), pH (2.84-3.23), TSS (6.32-11.47 ºBrix), and TA (1.99-4.07 g citric acid/100 ml).

The maximum reflectance percentages, whose values varied between 30.45 and 53.55%, were measured as 600 nm (R600).

With the parameters measured, the following indexes were calculated (the range of variation obtained is indicated in parentheses): W/LD (1.66-2.26 g mm^{-1}), W/AD (1.49-1.93 g mm^{-1}), MI (1.57-6.20 ºBrix/(g citric acid/100 ml) and AUC (43.93-75.36%).

Table 1 contains the results of the cluster analysis performed for the groups of fruits by ripening stage using the MI as a variable.

The grouping of the fruits into two clusters (A and B) provides two heterogeneous groups in which, according to the maximum distance to the centroid and intragroup variation (Tab. 1), there is greater variability among fruits in group B. In the grouping of three clusters (A, B1, and B2), there are three groups with greater homogeneity in

TABLE 1. Results of the cluster analysis performed for the groupings of lulo fruits in two or three groups by maturity index (MI).

Group	Number of fruits	Centroid	Minimum distance to centroid	Maximum distance to centroid	Intragroup variation
Distribution in two groups					
A	16	2.137	0.014	0.570	0.054
B	22	3.093	0.003	1.130	0.143
Distribution in three groups					
A	16	2.137	0.014	0.570	0.054
B1	9	2.754	0.018	0.208	0.018
B2	13	3.329	0.038	0.893	0.093

terms of maximum distance to the centroid and intragroup variation.

When comparing the maturity groups of the new classifications (MI2 and MI3), group A had the same centroid (2.137) and distances (0.014 minimum and 0.570 maximum) in both classifications. This indicates that the same 16 lulo fruits were classified in the same class in both the second and third maturity groups. Group A in both classifications obtained the lowest MI compared to the other groups, and it corresponds to the group with the lowest fruit maturity. According to the centroid contents in the MI3 classification, the most mature lulo fruits belonged to group B2.

Table 2 summarized the results of the ANOVA analysis followed by Tukey's multiple comparisons test, performed to identify the parameters in which the groups in each of the classifications differed significantly ($P<0.05$).

ICONTEC groups significantly differed ($P<0.05$) in color parameters (coordinates L*, a*, b* C*, h*, R600, and AUC), TSS content and MI. In the case of classification by MI, all variables except DL, L*, b*, C* and the W/AD index showed significant differences ($P<0.05$) between groups.

Discriminant analyses were performed with the PLS-DA method to establish the functions that best classify the ripening stages of the fruits, with the external parameters that have shown significant differences ($P<0.05$) between the groups established by MI (W, AD, W/LD, a*, and h coordinate, R600, AUC). The explanatory variables with the greatest influence on the model (W, AD, and W/LD) were selected and discriminant analyses were again performed using only these variables. The classification functions obtained are presented in Table 3.

The MI2 clustering correctly classified 89.47% of the lulo fruits, while the MI3 clustering correctly classified 78.95%.

The predictive power of the equations obtained was assessed with a new set of 12 fruits. When two ripening stage groups (MI2) were considered, 75% of the fruits were correctly classified, and when three groups (MI3) were considered, 33% were correctly classified. Figures 2 and 3 show

TABLE 2. Mean values and standard error of physical and physicochemical characteristics of "lulo de Castilla" (*Solanum quitoense* Lam.) at different ripening stages according to the ICONTEC classification and maturity index (MI) classifications in two and three groups (MI2 and MI3).

Parameters [2]	ICONTEC classification[1]			MI2 classification [1,2]		MI3 classification [1,2]		
	Group 3 (n=13)	Group 4 (n=14)	Group 5 (n=11)	Group A (n=16)	Group B (n=22)	Group A (n=16)	Group B1 (n=9)	Group B2 (n=13)
W (g)	101.8 ± 3.2^{a}	105.5 ± 2.0^{a}	101.1 ± 3.1^{a}	98.5 ± 2.6^{a}	106.1 ± 1.7^{b}	98.5 ± 2.6^{a}	109.1 ± 2.9^{b}	104.1 ± 2.0^{ab}
LD (mm)	53.3 ± 0.6^{a}	53.8 ± 0.6^{a}	52.3 ± 0.6^{a}	53.3 ± 0.6^{a}	53.1 ± 0.4^{a}	53.3 ± 0.6^{a}	53.8 ± 0.5^{a}	52.6 ± 0.6^{a}
AD (mm)	59.2 ± 0.7^{a}	60.0 ± 0.5^{a}	59.3 ± 0,7^{a}	58.1 ± 0.5^{a}	60.6 ± 0.4^{b}	58.1 ± 0.5^{a}	60.6 ± 0.8^{b}	60.5 ± 0.4^{b}
W/LD	1.9 ± 0.0^{a}	2.0 ± 0.0^{a}	1.9 ± 0.0^{a}	1.8 ± 0.0^{a}	2.0 ± 0.0^{b}	1.8 ± 0.0^{a}	2.0 ± 0.0^{b}	2.0 ± 0.0^{b}
W/AD	1.7 ± 0.0^{a}	1.8 ± 0.0^{a}	1.7 ± 0.0^{a}	1.7 ± 0.0^{a}	1.7 ± 0.0^{a}	1.7 ± 0.0^{a}	1.8 ± 0.0^{a}	1.7 ± 0.0^{a}
L*	51.8 ± 0.6^{a}	55.1 ± 0.5^{b}	55.8 ± 0.4^{b}	53.2 ± 0.7^{a}	54.9 ± 0.5^{a}	53.2 ± 0.7^{a}	54.3 ± 0.8^{a}	55.3 ± 0.6^{a}
a*	21.2 ± 1.0^{a}	29.1 ± 0.8^{b}	31.5 ± 0.4^{b}	24.4 ± 1.3^{a}	29.1 ± 0.9^{b}	24.4 ± 1.3^{a}	28.4 ± 1.6^{ab}	29.6 ± 1.2^{b}
b*	63.7 ± 1.4^{a}	65.5 ± 1.7^{a}	72.3 ± 1.6^{b}	66.1 ± 1.6^{a}	67.4 ± 1.4^{a}	66.1 ± 1.6^{a}	68.1 ± 2.9^{a}	69.9 ± 1.4^{a}
C*	67.6 ± 1.3^{a}	71.9 ± 1.6^{a}	79.0 ± 1.5^{b}	70.8 ± 1.7^{a}	73.6 ± 1.5^{a}	70.8 ± 1.7^{a}	74.1 ± 3.0^{a}	73.3 ± 1.6^{a}
h (º)	71.8 ± 0.9^{b}	66.0 ± 0.7^{a}	66.3 ± 0.6^{a}	69.9 ± 1.1^{b}	66.8 ± 0.6^{a}	69.2 ± 1.1^{b}	67.5 ± 1.1^{ab}	66.3 ± 0.7^{a}
R600 (%)	38.7 ± 1.0^{a}	47.5 ± 1.0^{b}	50.6 ± 0.5^{b}	42.6 ± 1.5^{a}	47.4 ± 1.1^{b}	42.6 ± 1.5^{a}	46.5 ± 2.1^{ab}	48.1 ± 1.3^{b}
AUC (%)	56.5 ± 1.6^{a}	69.3 ± 1.4^{b}	71.6 ± 0.8^{b}	61.7 ± 2.1^{a}	68.4 ± 1.5^{b}	61.7 ± 2.1^{a}	66.7 ± 2.4^{ab}	69.6 ± 1.9^{b}
pH	3.0 ± 0.0^{a}	3.0 ± 0.0^{a}	3.1 ± 0.0^{a}	3.0 ± 0.0^{a}	3.1 ± 0.0^{b}	3.0 ± 0.0^{a}	3.1 ± 0.0^{b}	3.1 ± 0.0^{b}
TSS (ºBrix)	8.0 ± 0.4^{a}	9.0 ± 0.4^{ab}	9.7 ± 0.2^{b}	7.5 ± 0.3^{a}	9.8 ± 0.1^{b}	7.5 ± 0.3^{a}	9.4 ± 0.2^{b}	10.0 ± 0.2^{b}
TA (g citric acid/100 ml)	3.4 ± 0.1^{a}	3.4 ± 0.1^{a}	3.2 ± 0.1^{a}	3.5 ± 0.1^{b}	3.2 ± 0.1^{a}	3.5 ± 0.1^{b}	3.4 ± 0.1^{b}	3.0 ± 0.1^{a}
MI (ºBrix/(g citric acid/100 ml)	2.4 ± 0.1^{a}	2.7 ± 0.2^{ab}	3.0 ± 0.2^{b}	2.1 ± 0.1^{a}	3.1 ± 0.1^{b}	2.1 ± 0.1^{a}	2.8 ± 0.1^{b}	3.3 ± 0.1^{c}

[1] For each classification, values in the same row with different letters indicate statistically significant differences ($P<0.05$) according to Tukey's test.

[2] W: weight; LD: longitudinal diameter; AD: axial diameter; W/LD: ratio weight/longitudinal diameter; W/LD: ratio weight/axial diameter; L*: lightness; a*: color coordinate green-red; b*: color coordinate blue-yellow; C*: chroma; h: hue; R600: percent reflectance at a wavelength at 600 nm; AUC: area under the curve of percent reflectance from 400 to 700 nm; TSS: total soluble solids; TA: titratable acidity; MI: maturity index; MI2: classification of 2 groups by maturity index; MI3: classification of 3 groups by maturity index; ICONTEC: Colombian Institute of Technical Standards and Certification; A and B: groups obtained from grouping the fruits in two clusters; A, B1, and B2: groups obtained from grouping the fruits in three clusters.

TABLE 3. Classification functions and percentage of correctly classified fruits obtained by PLS-DA.

Classification function	Fruits correctly classified (%)
For MI2 classification, with 3 quantitative variables (weight, axial diameter, weight/longitudinal diameter ratio).	
$F(A)= 8.42+4.00*10^{-2}*W-0.11*AD-2.84*W/LD$ $F(B)=-7.42-4.00*10^{-2}*W-0.11*AD+2.84*W/LD$	89.47
For MI3 classification, with 3 quantitative variables (weight, axial diameter, weight/longitudinal diameter ratio).	
$F(A)=8.42+4.00*10^{-2}*W-0.11*AD-2.84*W/LD$	
$F(B1)=1.40+1.18*10^{-2}*W-0.10*AD+1.82*W/LD$	78.95
$F(B2)=-8.82-5.17*10^{-2}*W+0.21*AD+1.02*W/LD$	

W: weight; AD: axial diameter; W/LD: weight/longitudinal diameter ratio.

the totality of the fruits (used to establish the classification models and to test the predictive power of the models) on the t1, t2 and t1, t3 axes generated in the PLS-DA analysis. They allowed visualizing the better discrimination in the case of two groups classified (MI2) by maturation stage.

Discussion

The fruits used in this research were characterized by medium weight, low height, and medium-high width, a tendency to red and yellow, low tonality, medium C* coordinate, TSS in the medium range, and pH and TA in the medium-high range. When compared to other studies performed with "lulo de Castilla", the fruits used had a weight above average, low height and medium width (Bernal & Díaz, 2016).

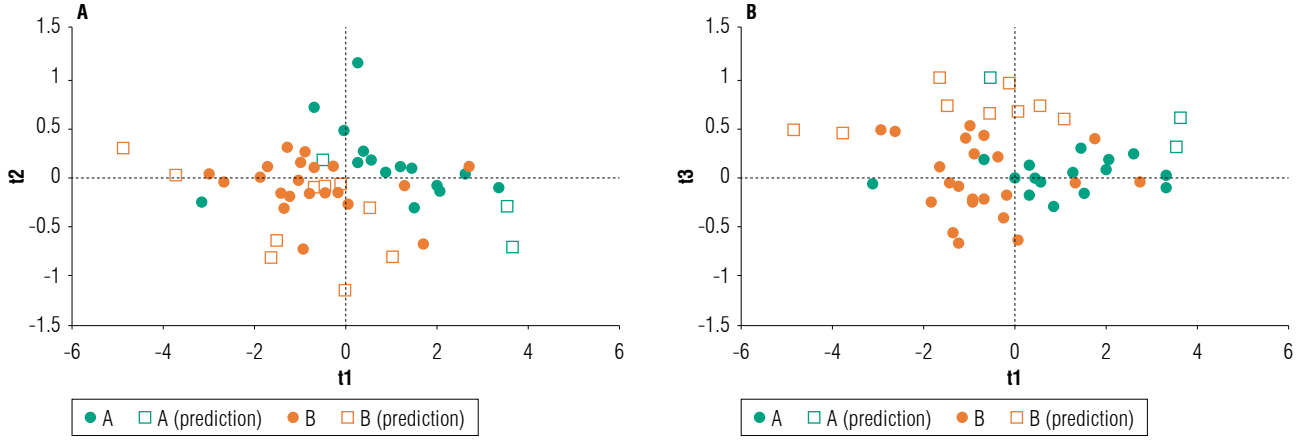

FIGURE 2. Classification with two groups (MI2) by maturation stage (A group=16 fruits and B group=22 fruits) and the classification of new fruits used to evaluate the prediction model (A group=3 fruits and B group=9 fruits). A) Observations on axes one and two; B) Observations on axes one and three.

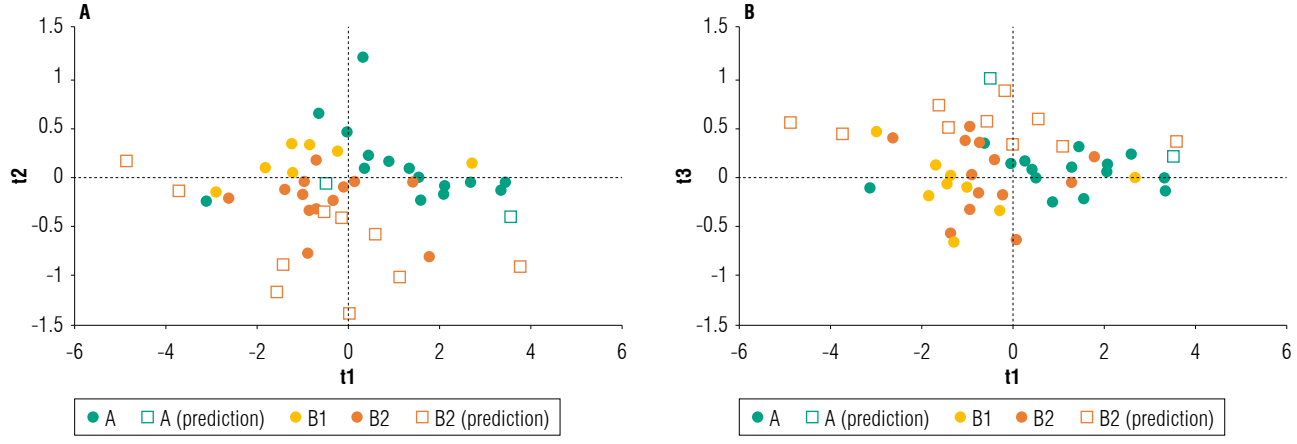

FIGURE 3. Classification with three groups (MI3) by maturation stage (A group=16 fruits, B1 group=9 fruits and B2 group=13 fruits) and the classification of new fruits used to evaluate the prediction model (A group=2 fruits and B2 group =10 fruits). A) Observations on axes one and two; B) Observations on axes one and three.

Color was in a medium range in the green-red coordinate (a*): it was high in lightness, lower in h and higher in blue-yellow (b*) and C* coordinates (Mejía *et al*., 2012). TA and pH were in the medium-high range and TSS in medium range (Mejía *et al.,* 2012; Molano-Díaz *et al,* 2022).

It is of great importance to obtain fruits with optimally mature characteristics for their use by consumers. To determine the optimum moment of maturity, there are different indexes; but, in the case of fruits, one of the most used indexes is the ratio between sugar and acid content, since this ratio gives many fruits their characteristic flavor and it is an easy indicator of commercial and organoleptic maturity (Angón-Galván *et al*., 2006).

MI (TSS/AT) increases during maturity, when organic acids decrease as they are used as substrates for respiratory processes and/or TSS increase (Andrade-Cuvi *et al.,* 2015). The reduction of TA and/or TSS content can be used as a standard criterion to detect fruit ripening. The MI (TSS/TA) is a good indicator of fruit maturity as it increases significantly during ripening (Ochoa-Vargas *et al.,* 2016).

Considering that the ICONTEC classification is based on external changes in fruit color, it makes sense to distinguish significant differences between groups in the variables related to color (coordinates L*, a*, b* C*, h*, R600, and AUC); However, color is not enough to characterize the stage of the lulo fruit maturation (Mejia *et al.,* 2012). In this research, no differences between ICONTEC classification groups were observed in parameters W, LD, AD, W/LD, W/AD, TA. An overlapping of groups was observed in physicochemical characteristics such as pH, TSS, and MI. In particular, the MI does not allow differentiating group 4 from groups 3 and 5. These facts show the deficiencies of the classification by color, since the groups obtained by this method do not show a clear relationship with the distinct stages of maturation. The ICONTEC method of classifying lulo fruits by ripening stages lacks specific methodology (environmental lighting conditions not specified; percentage areas of green, yellow, or orange color not detailed) to aid an objective classification. This classification is only visual, and depends on the color perception of the person doing the grouping, influenced by interindividual differences (Emery & Webster, 2019; Jeong & Jeong, 2021). In addition, this includes the difficulty of classifying the lulo fruits in intermediate groups since the fruits had different green and orange tones.

As MI was the criterion used to establish the groups MI2 and MI3, both classifications were discriminated by MI. For the rest of the parameters, even though in both classifications there were differences between the groups on the same parameters (W, AD, W/LD, a*, h, R600, AUC, pH, TSS, and TA), the classification into three groups did not discriminate well in the more mature groups (B1, B2), except for TA. When the lulo fruits get closer to full maturity the acids are utilized as substrates for respiratory processes and/or being transformed into sugars reflecting an increase in TSS (Ochoa-Vargas *et al*., 2016). These facts were better observed in the MI2 grouping. The more advanced the stage of ripening, the greater the weight of the fruits. Significant differences were found in the MI2 classification groups. On average, the values obtained for W were higher than those reported by Gancel *et al*. (2008) and lower than those of Ochoa-Vargas *et al*. (2016) and Jaime-Guerrero (2022). In other varieties of lulo, Forero *et al*. (2014) presented W data for the *quitoense* variety higher than for the "lulo de Castilla" used in this study. In other research (González Loaiza *et al*., 2014), W was not a determining parameter to differentiate the lulo fruits at different ripening stages since no significant differences (P<0.05) were found in the W of 100%, 50%, and 15% green lulo fruits.

No differences in LD were found between groups for any classification, while AD showed a significant increase between groups A and B (MI2). The data obtained for the dimensions were similar to those reported by Obregón-La Rosa *et al.* (2021). The W/AD value was within the ranges published by the Colombian Technical Standard (NTC 5093). During the maturation phase, the lulo fruits can increase in size (Jaime-Guerrero *et al*., 2022), acquiring a circular or oval shape (Obregón-La Rosa *et al*., 2021). In the current research, the lulo fruits grew more in width than in length, showing a more oval shape, thus, showing significant differences for AD while not for LD.

As for the color parameters, the L*, a*, b*, and C* coordinates showed the same tendency to increase values as the ripening stage advanced, explaining the greater presence of red and yellow colors in the ripest fruits, and the opposite for the h coordinate. For the MI2 and MI3 classification, no significant differences were found between the groups by ripening stage in L*, b* and c*, in contrast to the ICONTEC classification. During the ripening period of lulo fruits, changes in fruit hue occur with variations from green to yellow-orange due to chlorophyll degradation and synthesis of other pigments (Wills *et al.,* 1998; Burbano Valdivieso & Daza, 2012) that are generally present in the fruit epidermis (Mejía *et al*., 2012). During the ripening period the different stages are best discriminated by hue and variation from green to red (a*) rather than blue to yellow (b*) chroma or

fruit luminosity. The L* coordinate increased as fruit maturity advanced; however, the L* coordinate values showed a decrease in the group of higher maturity, with values lower than those obtained in this research (Mejía *et al*., 2012). The values of a* and b* were higher than those obtained by Gancel *et al*. (2008), similar to values for coordinate a*, and lower than values for coordinate b* as reported by Mejía *et al*. (2012). The increase in C* values responded to a greater vividness of color as the fruits ripened. The h-coordinate decreased significantly ($P<0.05$) with increasing fruit maturity stages. Mejía *et al*. (2012) and Gancel *et al*. (2008) report higher values in h and lower values in C* than those obtained in this research.

The highest percentage of reflectance in the visible spectrum was found at 600 nm, regardless of the ripening stage. These spectra can be related to the different compounds present in the fruits. For example, in apples, reflectance percentage between 425 and 480 nm was the maximum absorption point for carotenoids, 550 nm for anthocyanins, and between 550 nm and 705 nm reflectance for the chlorophyll content (Merzlyak *et al*., 2013). The AUC increased with the maturity stage.

In the physicochemical characterization, pH increased with increasing fruit maturity. In the MI3 clusters, there were no significant differences between B1 and B2 groups. The pH values were lower than those obtained by Mejía *et al*. (2012), Morillo-Coronado *et al*. (2019) and Duarte Alvarado *et al*. (2021) and higher than those by González Loaiza *et al*. (2014). Although the study by González Loaiza *et al*. (2014) reports an increase in pH with increasing maturity stage, Casierra-Posada *et al*. (2004) indicate that the pH value of lulo juice should not be taken as a parameter to determine fruit maturity because it is very similar and ranges from 2.9 to 3.2 from the 1st to the 7th d of harvest. TSS increased with ripening as is generally the case, regardless of the variety of lulo used (Casierra-Posada *et al*., 2004).

TA showed opposite behavior to pH and TSS: acidity decreased in the most mature lulo fruits. Both the studies of Casierra-Posada *et al*. (2004) and González Loaiza *et al*. (2014) report a decrease in acidity as fruits mature, similar to that obtained in this study. In the MI3 classification, TA showed significant differences ($P<0.05$) for group B2, but not in groups A and B1. According to the Colombian Technical Standard NTC 5093, the maximum TA content (expressed as citric acid) in lulo fruit juice, regardless of the fruit maturity stage, should be 3.23%; however, the values obtained were somewhat higher for lulo fruits belonging to groups A and B1. The reduction of TA as well as TSS content can be used as a standard criterion to detect fruit ripening. The MI (TSS/TA) is a good indicator of fruit maturity as it increases significantly during ripening (Ochoa-Vargas *et al*., 2016).

The ICONTEC classification is based on appearance parameters. Color variables are related to MI, because, during ripening color is one of the characteristics with the most significant transformations due to the degradation of green color (chlorophyll) that is associated with the synthesis of yellow (carotenoids) and red-purple (anthocyanins) pigments (Wills *et al*., 1998). However, the differences in various parameters between groups, especially pH, TA, TSS, and MI, show that the ICONTEC classification does not distinguish well between the different stages of maturity. Although the fruits used in this research belong to three groups (groups 3, 4, and 5 according to the Colombian Technical Standard NTC 5093), the results obtained do not justify their classification in three groups but in two.

In the MI3 classification, in general, the parameters (external physical and physicochemical) did not show clear significant differences between the three groups by maturity stage, added to the low percentage (33.33%) in prediction, questioning the need for a third group.

Mejía *et al*. (2012), who conducted a physicochemical characterization of lulo fruits of the Castilla variety at the 6 ripening stages established by the Colombian Technical Standard NTC 5093, already questioned the segmentation into 6 groups, concluding that by measuring color parameters, only three ripening stages are defined: green (corresponding to groups 0, 1 and 2 of the standard), pinton (corresponding to groups 3 and 4) and mature (5) that would support the hypothesis that only two ripening groups can be distinguished when working with color groups 3, 4 and 5 defined by ICONTEC.

In this research, when working with imported lulo fruits, the fruit sample was in a limited range of maturity grades, so it would be convenient to extend the study with a sample that includes sufficient fruit of all maturity stages.

Conclusions

Among the genetic diversity of lulo (varieties, hybrids, etc.), the fruits of the current research were of a medium size, the exterior of the fruit showed a tendency to color red and yellow, TSS content was in the medium range, and acidity and pH were in the medium-high range. The nondestructive

parameters that best discriminated the different groups by maturity stage were W, AD, W/LD.

The ICONTEC classification based on appearance parameters did not respond to different ripening stages. The three groups (Color 3, 4, and 5) classified by ICONTEC were equivalent to 2 stages of maturity. In the classifications based on MI, with 2 groups (MI2), the external physical and physicochemical parameters did distinguish the different groups by ripening stage. In comparison, the classification with 3 groups (MI3), failed to differentiate group B1 from group A or B2. With the equations obtained, the maturity stage of the lulo fruits can be predicted in 75% of the cases only by measuring the weight of the fruits and their longitudinal and axial diameters.

Even though it would be convenient to extend the current research with a larger number of samples, it was possible to classify lulo fruits in an objective way with a limited number of non-destructive parameters that constitutes a very useful tool for an optimal harvest date for these fruits for export, fresh consumption, or use as raw material for the food industry and other purposes.

Acknowledgments

The study was financed by the internal funds of the Universidad Pública de Navarra (UPNA, Spain) for the promotion of research groups.

Conflict of interest statement

The authors declare that there is no conflict of interests regarding the publication of this article.

Author´s contributions

SMGB carried out the research activities, SMGB and MRMA designed the experiment, formal analysis, wrote the article and reviewed the manuscript. All authors have read and approved the final version of the manuscript.

Literature cited

Acosta, O., Pérez, A. M., & Vaillant, F. (2009). Chemical characterization, antioxidant properties, and volatile constituents of naranjilla (*Solanum quitoense* Lam.) cultivated in Costa Rica. *Archivos Latinoamericanos de Nutrición*, *59*(1), 88–94.

Almanza-Merchán, P. J., Velandia D, J. D., & Tovar, Y. P. (2016). Propiedades fisicoquímicas durante el crecimiento y desarrollo en dos variedades de frutos de lulo (*Solanum quitoense* Lam.). *Revista Colombiana de Ciencias Hortícolas, 10*(2), 222–231. https://doi.org/10.17584/rcch.2016v10i2.5065

Altendorf, S. (2017). *Global prospects for mayor tropical fruit. Short-term outlook, challenges and opportunities in a vibrant global marketplace. Food outlook November 2017* (pp. 69–81). Food and Agriculture Organization. https://www.fao.org/fileadmin/templates/est/COMM_MARKETS_MONITORING/Tropical_Fruits/Documents/Tropical_Fruits_Special_Feature.pdf

Altendorf, S. (2018). *Minor tropical fruits (Mainstreaming a niche market). Food Outlook 2018* (pp. 67–74). Food and Agriculture Organization. https://www.fao.org/fileadmin/templates/est/COMM_MARKETS_MONITORING/Tropical_Fruits/Documents/Minor_Tropical_Fruits_FoodOutlook_1_2018.pdf

Andrade-Cuvi, M. J., Moreno-Guerrero, C., Guijarro-Fuertes, M., & Concellón, A. (2015). Caracterización de la naranjilla (*Solanum quitoense*) común en tres estados de madurez. *Revista Iberoamericana de Tecnología Postcosecha*, *16*(2), 215–221.

Angón-Galván, P., Santos-Sánchez, N. F., & Hernández, C. G. (2006). Índices para la determinación de las condiciones óptimas de maduración de un fruto. *Temas de Ciencia y Tecnología*, *10*(30), 3–8.

AOAC-Association of Official Analytical Chemists. (2005a). *Official methods of analysis* (*AOAC 945.10)*. http://www.eoma.aoac.org/methods/result.asp?string=b

AOAC-Association of Official Analytical Chemists. (2005b). *Official methods of analysis* (*AOAC 932.21)*. http://www.eoma.aoac.org/methods/result.asp?string=b

Bernal, J. A., & Díaz, C. A. (2006). Materiales locales y mejorados de tomate de árbol, mora y lulo sembrados por los agricultores y cultivares disponibles para su evaluación en Colombia (Boletín divulgativo N° 7). Corporación Colombiana de Investigación Agropecuaria. https://repository.agrosavia.co/handle/20.500.12324/1225

Burbano Valdivieso, F. A., & Daza, J. (2012, October 16–18). *Image analysis application to determine variations in shape, size and color of biological structures: Determination of changes in size and color of the fruit of Solanum sp. in the process of maturation* [Conference presentation abstract]. 5th International Conference on Biomedical Engineering and Informatics. https://doi.org/10.1109/BMEI.2012.6512945

Casierra-Posada, F., García, E. J., & Lüdders, P. (2004). Determinación del punto óptimo de cosecha en el lulo (*Solanum quitoense* Lam. var. quitoense y septentrionale). *Agronomía Colombiana*, *22*(1), 32–39. https://revistas.unal.edu.co/index.php/agrocol/article/view/17765

Duarte Alvarado, D. E., Lagos Burbano, T. C., Vallejo Cabrera, F. A., & Lagos Santander, L. K. (2021). Evaluación agronómica de introducciones de lulo *Solanum quitoense* Lamarck. *Acta Agronómica, 70*(1), 66–72. https://doi.org/10.15446/acag.v70n1.84150

Emery, K. J., & Webster, M. A. (2019). Individual differences and their implications for color perception. *Current Opinion in Behavioral Sciences, 30,* 28–33. https://doi.org/10.1016/j.cobeha.2019.05.002

FAO (Food and Agriculture Organization of the United Nations). (2020). *Las principales frutas tropicales. Análisis del mercado de 2018*. https://www.fao.org/publications/card/es/c/CA5692ES/

FAO (Food and Agriculture Organization of the United Nations). (2022). *Major tropical fruits: Preliminary results 2021*. https://www.fao.org/3/cb9412en/cb9412en.pdf

Forero, N. M., Gutiérrez, S., Sandoval, R. L., Camacho, J. H., & Meneses, M. A. (2014). Evaluación poscosecha de las características

del lulo (*Solanum quitoense*) cubierto con hoja de plátano. *Temas Agrarios, 19*(1), 73–85. https://doi.org/10.21897/rta.v19i1.726

Forero, D. P., Masatani, C., Fujimoto, Y., Coy-Barrera, E., Peterson, D. G., & Osorio, C. (2016). Spermidine derivatives in lulo (*Solanum quitoense* Lam.) fruit: sensory (taste) versus biofunctional (ACE-inhibition) properties. *Journal of Agricultural and Food Chemistry, 64*(26), 5375–5383. https://doi.org/10.1021/acs.jafc.6b01631

Gancel, A. L., Alter, P., Dhuique-Mayer, C., Ruales, J., & Vaillant, F. (2008). Identifying carotenoids and phenolic compounds in naranjilla (*Solanum quitoense* Lam. var. Puyo hybrid), an Andean fruit. *Journal of Agricultural and Food Chemistry, 56*(24), 11890–11899. https://doi.org/10.1021/jf801515p

González Loaiza, D. I., Ordoñez Santos, L. E., Vanegas Mahecha, P., & Vásquez Amariles, H. D. (2014). Cambios en las propiedades fisicoquímicas de frutos de lulo (*Solanum quitoense* Lam.) cosechados en tres grados de madurez. *Acta Agronómica, 63*(1), 11–17. https://doi.org/10.15446/acag.v63n1.31717

Hinestroza-Córdoba, L. I., Duarte Serna, S., Seguí, L., Barrera, C., & Betoret, N. (2020). Characterization of powdered lulo (*Solanum quitoense*) bagasse as a functional food ingredient. *Foods, 9*(6), Article 723. https://doi.org/10.3390/foods9060723

ICONTEC (Instituto Colombiano de Normas Técnicas y Certificación). (2002*). Frutas frescas. Lulo de Castilla. Especificaciones del empaque (NTC 5093).* https://tienda.icontec.org/gp-frutas-frescas-lulo-de-castilla-especificaciones-del-empaque-ntc5094-2002.html

Jaime-Guerrero, M., Álvarez-Herrera, J. G., & Fischer, G. (2022). Aspectos de la fisiología y el cultivo del lulo (*Solanum quitoense* LAM.) en Colombia: Una revisión. *Revista de Investigación Agraria y Ambiental, 13*(1), 131–148. https://doi.org/10.22490/21456453.4641

Jeong, E., & Jeong, I. (2021). Individual differences in colour perception: The role of low-saturated and complementary colours in ambiguous images. *i-Perception, 12*(6), 1–19. https://doi.org/10.1177/20416695211055767

Lobo Arias, M., Medina Cano, C. I., Delgado Paz, O. A., & Bermeo Giraldo, A. (2007). Variabilidad morfológica de la colección colombiana de lulo (*Solanum quitoense* Lam.) y especies relacionadas de la sección Lasiocarpa. *Revista Facultad Nacional de Agronomía Medellín*, *60*(2), 3939–3964.

Matusiak, M. (2015). Digieye application in cotton colour measurement. *Autex Research Journal*, *15*(2), 77–86. https://doi.org/10.2478/aut-2014-0036

Mejía, C. M., Gaviria, D., Duque, A. L., Rengifo, L., Aguilar, E., & Alegrías, A. H. (2012). Physicochemical characterization of the lulo (*Solanum quitoense* Lam.) Castilla variety in six ripening stages. *Vitae, Revista de la Facultad de Química Farmacéutica, 19*(2), 157–165.

Merzlyak, M. N., Solovchenko, A. E., & Gitelson, A. A. (2013). Reflectance spectral features and non-destructive estimation of chlorophyll, carotenoid and anthocyanin content in apple fruit. *Postharvest Biology and Technology, 27*(2), 197–211. https://doi.org/10.1016/S0925-5214(02)00066-2

Molano-Díaz, J. M., Reyes-Medina, A. J., & Álvarez-Herrera, J. G. (2022). The 1-methylcyclopropene and postharvest storage temperature of lulo fruits (*Solanum quitoense* Lam.). *Biotecnología en el Sector Agropecuario y Agroindustrial, 20*(2), 60–75.

Morillo Coronado, A. C., Rodríguez Fagua, A. D., & Morillo Coronado, Y. (2019). Caracterización morfológica de lulo (*Solanum quitoense* Lam.) en el municipio de Pachavita, Boyacá. *Acta Biológica Colombiana, 24*(2), 291–298. http://doi.org/10.15446/abc.v24n2.75832

Obregón-La Rosa, A. J., Arias-Arroyo, G. C., López-Belchi, M. D., Bracamonte-Romero, M., & Arones Limaymanta, A. (2021). Compuestos nutricionales y bioactivos de *Solanum quitoense* Lam (Quito quito), fruta nativa de los Andes con alto potencial de nutrientes. *Tecnología Química, 41*(1), 92–108.

Ochoa-Vargas, L. M., Balaguera-López, H. E., Ardila-Roa, G., Pinzón-Sandoval, E. H., & Álvarez-Herrera, J. G. (2016). Crecimiento y desarrollo del fruto de lulo (*Solanum quitoense* Lam.) en el municipio de San Antonio del Tequendama (Colombia*). Ciencia y Tecnología Agropecuaria*, *17*(3), 347–359. http://doi.org/10.21930/rcta.vol17_num3_art:512

Ramírez, F., Kallarackal, J., & Davenport, T. L. (2018). Lulo (*Solanum quitoense* Lam.) reproductive physiology: A review. *Scientia Horticulturae, 238*, 163–176. https://doi.org/10.1016/j.scienta.2018.04.046

Ramírez, F. (2021). Notes about Lulo (*Solanum quitoense* Lam.): an important South American underutilized plant. *Genetic Resources and Crop Evolution*, *68*, 93–100. https://doi.org/10.1007/s10722-020-01059-3

UNE-Norma española. (1997). *Zumos de frutas y hortalizas. Determinación de la acidez valorable* (Asociación Española de Normalización-12147). https://tienda.aenor.com/norma-une-en-12147-1997-n0010762

Wills, R. B. H., McGlasson, W. B., Graham, D., & Joyce, D. C. (1998). Structure and composition. In R. B. H. Wills, W. B. McGlasson, D. Graham, & D. C. Joyce (Eds.), *Postharvest: An introduction to the physiology and handling of fruit, vegetables and ornamentals* (pp. 15–27). CAB International.

A predictive model for the determination of cadmium concentration in cocoa beans using laser-induced plasma spectroscopy

Modelo predictivo para la determinación de la concentración de cadmio en granos de cacao mediante espectroscopia de plasma inducido por láser

Sandra Liliana Herrera Celis[1], Jáder Enrique Guerrero Bermúdez[2*], Enrique Mejía-Ospino[1], and Rafael Cabanzo Hernández[1]

ABSTRACT

This study proposes a predictive model to determine the concentration of cadmium (Cd) in cocoa beans based on laser-induced breakdown spectroscopy (LIBS) and partial least squares regression (PLSR-1 or PLS-1). The multivariate calibration model was developed using 46 cocoa bean samples, with Cd concentrations up to 1 mg kg^{-1}. The increase of the LIBS signal in the Cd emission lines was evident when the cocoa bean sample was subjected to a solid-liquid-solid transformation (SLST). The range error ratio (RER) was 7.92, which allowed it to be classified as a screening model. Monte Carlo cross-validation was used, with 60% of samples for calibration and the remaining for testing. The standard error of cross-validation (SECV) and standard error of calibration (SEC) were 0.12 mg kg^{-1} and 0.05 mg kg^{-1}, respectively. The proposed procedure is framed within the alternatives for the chemical analysis of cocoa.

Key words: inorganic contaminants, heavy metals, partial least square regression, atomic spectroscopy.

RESUMEN

Este estudio propone un modelo para predecir la concentración de cadmio (Cd) en granos de cacao basado en espectroscopía de plasma inducido por láser (LIBS) y regresión por mínimos cuadrados parciales (PLSR-1 o PLS-1). El modelo de calibración fue desarrollado a partir de 46 muestras de granos de cacao con concentración no mayor a 1 mg kg^{-1}. El incremento en la señal LIBS fue evidente cuando la muestra de grano de cacao fue sometida a una transformación sólido-líquido-sólido (SLST). La razón del rango de error (RER) es 7.92, lo que permite determinar que el modelo es de tamizaje. Se utilizó la estrategia de validación cruzada Montecarlo con el 60% de las muestras para calibración y las restantes para prueba. El error estándar de validación cruzada (SECV) y de calibración (SEC) fue 0.12 mg kg^{-1} y 0.05 mg kg^{-1}, respectivamente. El procedimiento propuesto se ubica en el marco de las alternativas de inspección y análisis químico del cacao.

Palabras clave: contaminantes inorgánicos**,** metales pesados, regresión por mínimos cuadrados parciales, espectroscopía atómica.

Introduction

Cocoa *(Theobroma cacao* L.) and its derivatives can be considered commodities with health benefits due to their high content of polyphenols and antioxidants (Oliveira *et al*., 2021). Nevertheless, cocoa has been identified as an important source of cadmium (Cd), which is a transition metal without biological function and of recognized toxicity in humans that affects the kidneys and calcium absorption in bones (Järup & Akesson, 2009; Satarug, 2018).

Cadmium is released naturally in soils through the weathering of rocks, where it is usually found in concentrations of less than 0.2 mg kg^{-1} (Gramlich *et al*., 2017). However, anthropogenic activities such as mining, agrochemical industry (fertilizers, pesticides), in addition to its considerable mobility in soil, significantly increase its content. Cadmium absorption by cocoa plants occurs through the roots and is conducted through its vascular system to finally reside in the leaves and fruits (Checa *et al*., 2019; Vanderschueren *et al*., 2020).

The raw material for the cocoa industry comes mainly from Africa, Central and South America. For the latter, numerous studies have shown that cocoa beans (nibs and shells) have relatively high concentrations of cadmium (Bertoldi *et al*., 2016; Argüello *et al*., 2019; Rodríguez Albarrcín *et al*., 2019; Bravo *et al*., 2021). In the Americas, Colombia has the potential as a bean exporter with increasing production. In the period 2020-2021, production reached 70205 t

Received for publication: September 22, 2022. Accepted for publication: November 30, 2022 Doi: 10.15446/agron.colomb.v40n3.104911

[1] Laboratorio de Espectroscopia Atómica y Molecular (LEAM), Centro de Materiales y Nanociencias (CMN), Universidad Industrial de Santander, Parque Tecnológico Guatiguará, Piedecuesta, Santander (Colombia).
[2] Grupo de Óptica y Tratamiento de Señales, Universidad Industrial de Santander, Bucaramanga, Santander (Colombia).
* Corresponding author: jader@uis.edu.co

of dry beans, corresponding to its highest historical record (Fedecacao, 2021). Around 95% of exported beans were categorized as Fine Flavour Cocoa (FFC). FFC is a market category established by the International Cocoa Organization (ICCO) that recognizes sensory attributes such as flowery, fruity, caramelly, and nutty (Escobar *et al*., 2020; Escobar *et al*., 2021).

In general, atomic emission/absorption spectral techniques allow for the quantitative determination of Cd concentrations in cocoa beans, among them: inductively coupled plasma mass spectrometry (ICP-MS), inductively coupled plasma optical emission spectrometry (ICP-OES), graphite furnace atomic absorption spectrometry (GF-AAS), and flame atomic absorption spectrometry (FAAS). These methods for the assessment of Cd concentrations in cocoa are characterized by their robustness and limit of detection (LOD). In ICP-OES, for example, we found LODs near 0.043 mg kg^{-1} (Rodríguez *et al*., 2022). However, the large number of supplies, as well as the generation of environmentally aggressive waste, lead to a search for analysis strategies that minimize these factors. By contrast, laser-induced breakdown spectroscopy (LIBS) has become a useful technique for food analysis that is relatively simple and with a minimum production of polluting waste.

LIBS is suitable for the detection of cadmium in agricultural materials and food (Menegatti *et al*., 2019; Nicolodelli *et al*., 2019; Senesi *et al*., 2019). Chemometrics and LIBS have been proposed for the determination of Cd in fruits and vegetables (Yao *et al*., 2017; Shen *et al*., 2018). Zhao *et al*. (2019) determine Cd in lettuce leaves using enhanced LIBS by adding silver nanoparticles (NELIBS); the enhanced signal of the 214.4 nm line allows prediction of Cd concentrations less than 60 μg kg^{-1} (Zhao *et al*., 2019). Yang *et al*. (2019) proposes a simple and low-cost pre-treatment method for rice grain samples, called solid-liquid-solid transformation that improves the signal to noise ratio for Cd lines in LIBS spectra, obtaining detection limits near 2.8 μg kg^{-1}. Very recently, univariate and multivariate calibration methods, such as partial least squares regression (PLSR), least squares support vector machines (LS-SVM), and extreme learning machines (ELM) in combination with LIBS were proposed for quantitative analysis of Cd in the rice roots (Wang *et al*., 2021).

Previous studies on the determination of Cd in cocoa beans using ICP-OES were developed by Chavez *et al*. (2015) and Oliveira *et al*. (2021). Gramlich *et al*. (2017) study cadmium uptake in soils and cocoa beans by FASS. Also, in Colombia, the organs of cocoa plants and soil are analysed by ICP-MS for the determination of heavy metals, with emphasis on Cd (Aguirre-Forero *et al*., 2020).

In this research, a predictive model was proposed to determine Cd concentration in cocoa beans of Colombian origin, based on LIBS, FAAS (as a reference technique) combined with PLSR-1 (partial least squares regression). This took advantage of the agility to generate LIBS spectra that together with the Cd concentrations determined by FAAS and the chemometric procedures allowed the construction of the model and a reduction in the time of analysis with respect to conventional spectral methodologies. If the procedure proposed in this study is compared with the FAAS technique, the time required to obtain LIBS data is estimated as 1 h (including SLST transformation). In contrast, FAAS requires digestion processes that typically take more than 48 h.

Materials and methods

Samples of cocoa beans of Colombian origin that were dried and ground were collected for one year from different laboratories. Prior to calibration, all samples were homogenized using a mortar.

Determination of cadmium concentration by FAAS: reference method

Sample treatment

Initially 65 samples of cocoa beans of Colombian origin were treated for analysis of the concentration of cadmium by FAAS. The cocoa beans were obtained from different plantations, but the precise geographic location is unknown.

Prior to microwave oven assisted digestion (MWAD), 0.5 g of cocoa beans was immersed in 8 ml of HNO_3 (MERCK, 65%), for 48 h, using teflon vessels (adapted from Oliveira *et al*. (2021)). After this period, 2 ml of H_2O_2 (30%) was added. Samples were introduced into the microwave digestion system (Multiwave GO Anton Paar, GmbH), according to the following procedure: (a) starting from room temperature to reach 80°C in 5 min, remaining at that temperature for 5 min; (b) from 80°C to 150°C for 5 min and staying at that temperature for 5 min; (c) from 150°C to 180°C for 3 min and remaining at that temperature for 25 min. The teflon vessels were allowed to cool to room temperature and carefully opened. The digestion product was transferred to a 25 ml balloon and filled with HNO_3 (0.5%). The washing of the glass and teflon material was carried according to AOAC Official (Jorhem & Engman, 2000).

Atomic absorption analysis

The standard solution was obtained by dissolving 1 g of Cd powder (Cadmium EMSURE® Merck KGaA, Darmstadt, Germany, particle size 0.3-1.6 mm) in 21 ml of HNO_3, in a 1:1 ratio (v/v) and then filled to 1 L with deionised water. From this standard solution a calibration curve was constructed with six Cd concentrations: 0.02, 0.5, 1, 1.5, 2, and 3 mg kg^{-1}.

The analysis was performed on a FAAS spectrometer (Thermo Electron Corporation, USA). The wavelength of the radiation emitted by the Cd hollow cathode lamp was 228.8 nm (current 4 mA). The flame was an air/acetylene oxidising flame with a flow rate of 1.2 L min^{-1} and a flame height of 7 mm. Slit width was 0.5 mm. Each concentration was determined by triplicate and its average value (± standard deviation) is shown in Table 1.

TABLE 1. Cadmium concentrations (mean±standard deviation (SD)) determined by FAAS in 46 samples of dry cocoa beans. In the calibration of the predictive model, only concentrations below 1 mg kg^{-1} were considered (negative concentrations that resulted from the FAAS curve were discarded).

Sample	Cd concentration Mean±SD (mg kg^{-1})	Sample	Cd concentration Mean±SD (mg kg^{-1})
M01	0.29±0.01	M24	0.02±0.01
M02	0.84±0.06	M25	0.05±0.01
M03	0.72±0.04	M26	0.05±0.01
M04	0.32±0.01	M27	0.02±0.01
M05	0.23±0.03	M28	0.02±0.01
M06	0.61±0.04	M29	0.30±0.01
M07	0.96±0.10	M30	0.03±0.01
M08	0.54±0.01	M31	0.03±0.01
M09	0.61±0.03	M32	0.29±0.01
M10	0.19±0.01	M33	0.05±0.02
M11	0.32±0.01	M34	0.05±0.01
M12	0.22±0.01	M35	0.03±0.01
M13	0.17±0.04	M36	0.08±0.02
M14	0.17±0.04	M37	0.02±0.01
M15	0.17±0.01	M38	0.02±0.01
M16	0.17±0.01	M39	0.0058±0.0015
M17	0.16±0.01	M40	0.07±0.01
M18	0.13±0.01	M41	0.21±0.01
M19	0.17±0.01	M42	0.15±0.02
M20	0.29±0.46	M43	0.16±0.01
M21	0.06±0.01	M44	0.28±0.02
M22	0.06±0.03	M45	0.96±0.01
M23	0.03±0.01	M46	0.06±0.01

Detection of cadmium in cocoa beans by LIBS

Determination of cadmium in pellets

In LIBS, the most common process for the analysis of samples is the formation of pellets after its homogenization (Sezer *et al*., 2017; Yang *et al*., 2018; Senesi *et al*., 2019). Pellets were produced from 500 mg of cocoa beans, previously macerated, by applying 2 t cm^{-2} of pressure for 2 min using a hydraulic press (Carver Inc., USA). However, it was only possible to determine Cd in pellets previously contaminated with a high concentration (>15 mg kg^{-1}) of this element. To detect Cd in samples with lower concentrations, it was necessary to implement the SLS transformation, proposed by Yang *et al*. (2019) that is described in the next section. SLST is a commonly used procedure for the quantification of heavy metals in food samples. In cocoa beans, Cd is bound in the chemical forms with other elements (among others: $CdCl_2$, $CdOH^+$, $CdCl_3^-$ and organic ones). At low concentrations of Cd, it is difficult to extract it by laser. For this reason, the addition of 0.1 N HCl allows the release of Cd^{+2} and the formation of soluble salts with the Cl^- ion (Yang *et al*., 2019).

Solid-Liquid-Solid Transformation (SLST)

To 1 g of macerated cocoa beans, 14 ml of 0.1 N HCl solution was added. The solution was submitted to an ultrasonic bath for 15 min. From the supernatant, 200 µl were taken, deposited on a glass sample holder, and allowed to dry at a temperature of 70°C. In this way, a layer of the material was obtained; the process was repeated to a total of five layers (Yang *et al*., 2019).

The experimental parameters were as follow: added volume of 0.1 N HCl solution (10, 12, 14, and 16 ml), and the following ultrasonic bath times using a Branson ultrasonic cleaner 1510, Japan of 5, 10, 15, and 20 min were studied according to the criterion of maximising the area under the spectral curve of the (concatenated) array of the 214.44 nm and 226.50 nm emission lines of the LIBS spectra. Unlike the volume of solution added and the ultrasonic time, the number of layers did not exhibit a maximum (the area under emission line). On the contrary, from the second layer, it grew monotonically as the number of layers increased. Given that more layers mean longer sample preparation time, five layers resulted in a good compromise between sample preparation time and signal intensity.

The emission line of Cd 214.44 nm, Figure 1A-C depicted the behaviour of these experimental parameters. Similar characteristics followed for the Cd 226.50 nm emission line. Table 2 shows the experimental parameters used for the SLS transformation.

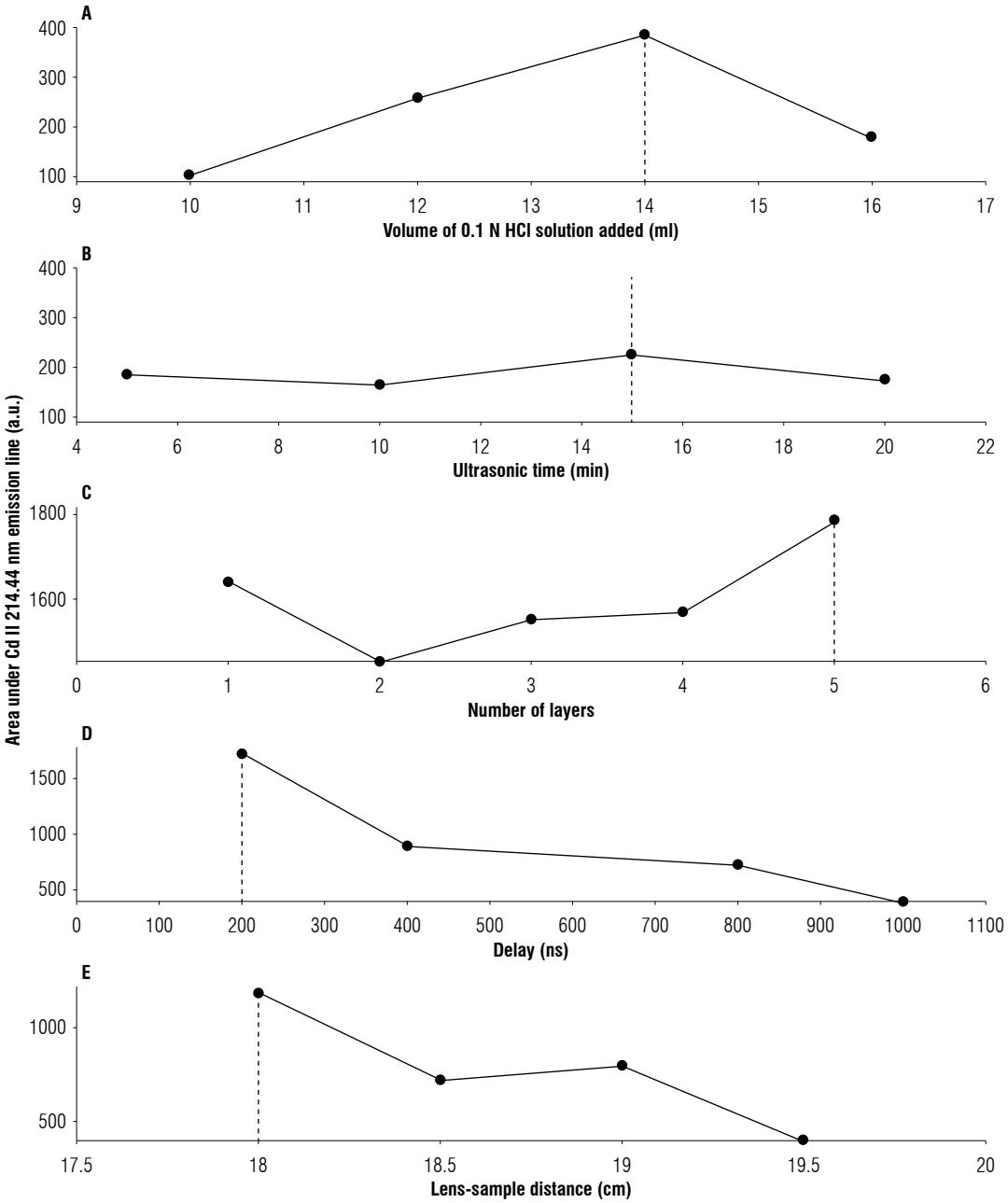

FIGURE 1. Exploration of experimental and instrumental parameters used in the solid-liquid-solid transformation (SLST) and LIBS setup: area under emission lines (214.44 nm) in arbitrary unit (a.u.) vs. (A) Volume of HCl 0.1 N solution added, (B) ultrasonic time, (C) number of layers, (D) delay, and (E) lens-sample distance.

TABLE 2. Result of the optimization of the parameters of the solid-liquid-solid transformation.

SLST-Parameter	Value
Volume of 0.1N HCl solution added	14 ml
Ultrasonic time	15 min
Number of layers	5

Optimization of instrumental parameters for LIBS

LIBS spectra were recorded using a Q-switched Nd:Yag laser (Q-smart, Quantel, Inc., USA) operating at 1064 nm. Adopting the same optimization criterion as in the SLST, we proceeded to set the LIBS instrumental parameters, namely, the delay and lens-sample distance. For a five-layer sample, delays of 200, 400, 800, and 1000 ns were tested with a lens-sample distance of 19.5 cm and 100 shots. Keeping the delay and number of shots constant (200 ns and 100 shots, respectively), the lens-sample distance was varied in the range 18 cm to 19.5 cm. Finally, the number of laser shots on the sample was between 10 and 200, at delay (200 ns) and lens-sample distance (19.5 cm). To

ensure that each laser impact covered a different region on the sample, the glass sample holder was supported on a turntable (with stepper motor). The selected parameters were as follow: a delay of 200 ns, integration time of 5 µs, lens-sample distance of 18 cm and number of shots of 200, pulse duration 5 ns, a repetition rate 10 Hz. As the number of shots increased so did the area under the emission line; however, the sample size limited this number to 200. The laser energy was 150 mJ/pulse. The behaviour of the area under the emission line 214.44 nm against the delay time and the sample lens distance is shown in Figure 1 D-E.

The plasma emission was focused through a quartz lens (focal length, 50 mm) and collected with a quartz optical fiber and introduced into a 0.5 m Czerny-Turner spectrograph (Shamrock 500i, Andor Technology, USA). A two thousand and four hundred grooves/mm diffraction grating (spectral resolution 0.075 nm, dispersion 0.83 nm mm^{-1}, and blazed 250 nm) was used to disperse the emission spectrum that was projected on the image plane of the spectrograph and recorded on an intensified charge-coupled device (ICCD) detector with an array of 1024 × 256 pixels (iStar DH720, Andor Technology, USA). The characteristics of the LIBS spectra acquisition setup are shown in Table 3.

TABLE 3. Characteristics of the LIBS spectra acquisition setup.

Instrumental parameter for LIBS	Value
Laser wavelength	1064 nm
Delay time	200 ns
Number of laser shots	200
Lens-sample distance	18 cm
Laser energy/pulse	150 mJ
Integration time	5 µs
Pulse duration	5 ns
Repetition rate	10 Hz

Figure 2 shows the LIBS signal of cocoa bean sample 21 (0.06±0.01 mg kg^{-1}) before and after SLS transformation. The increase of the signal in the Cd II emission line 214.44 nm is evident.

PLSR model development

PLSR-1 is a well-known chemometric technique for the implementation of predictive models (Otto, 2007). It is characterized by its simplicity and the possibility of obtaining good performance without over-fitting. In developing a prediction model, a compromise must be maintained between the number of latent variables (predictors) and the degrees of freedom (ASTM E1655-05, 2012).

In a PLS-1 predictive model, the relationship between the predictors **x**, and the estimated response, ŷ, is established according to Equation 1:

$$\hat{y} = b\boldsymbol{x} \quad (1)$$

where ŷ corresponds to an estimated concentration of Cd in cocoa beans; *b* is the vector of coefficients of the regression in the partial least squares sense (including the independent term); and **x** is a vector consisting of 33 intensity values (concatenated, with baseline correction and normalised by the area under the spectral curve) of the emission lines 214.44 nm and 226.50 nm. The concatenated array is formed by uniformly sampling over 17 and 16 points the intervals [214.3, 214.7] and [226.4, 226.7] (Fig. 3). Although in FAAS the 228.88 nm emission line is the reference for the measurements, it was not considered for the development of the predictive model due to interference with the iron emission lines.

The multivariate calibration was performed with Monte Carlo cross-validation (MCCV) to ascertain the complexity

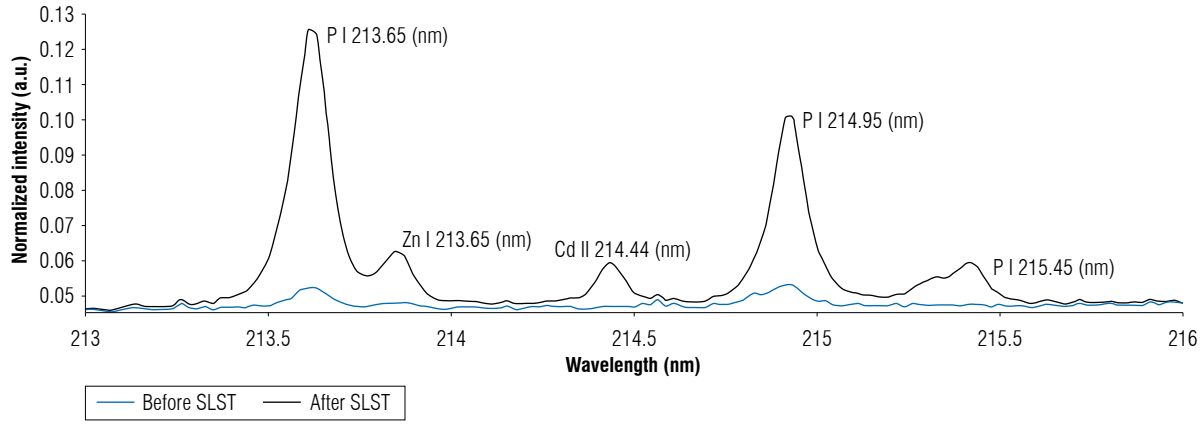

FIGURE 2. The increase of the LIBS signal in the Cd II 214.44 nm spectral line is evident when the cocoa bean sample 21 (0.06±0.01 mg kg^{-1}) is subjected to a solid-liquid-solid transformation (SLST). Normalized intensity in arbitrary unit (a.u.).

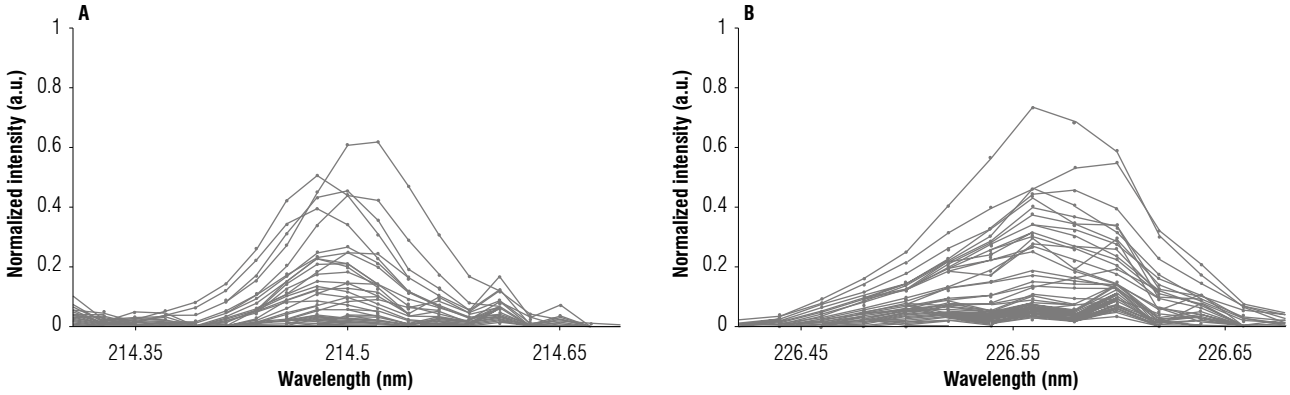

FIGURE 3. LIBS signal normalized by the area under the spectral curve of the Cd II 214.44 nm (A) and Cd II 226.50 nm (B) emission lines. Thirty-three (33) equally spaced points are concatenated to form an array that constitutes the input signal in the predictive model. Normalized intensity in arbitrary unit (a.u.).

of the model, *i.e.*, the number of latent variables (LVs) of the PLS model (Xu & Liang, 2001). This cross-validation strategy requires splitting the samples into two sets, one with n_C samples for training (testing or calibration), and the other with n_{CV} for validation. In all cases, the training set contained the samples with the highest and lowest Cd concentration values. Therefore, the regression model is only valid for interpolating values in that range.

The criteria used to define the number of LVs were the following: the square root of the standard error of calibration (SEC) and cross-validation (SECV), defined according to Equations 2 and 3:

$$SEC = \sqrt{\frac{1}{d_C}\sum_{i=1}^{n_C}(\hat{y}_i - y_i)^2} \quad (2)$$

$$SECV = \sqrt{\frac{1}{d_{CV}}\sum_{i=1}^{n_{CV}}(\hat{y}_i - y_i)^2} \quad (3)$$

where $d_x = n_x-(k+1)$ (with x, c or cv for calibration or cross-validation samples, respectively) corresponds to the degrees of freedom, and k is the number of latent variables (LVs). In Equations 2 and 3, $\hat{y}i$ is the estimated value of Cd concentration corresponding to the *i-th* sample with a measured value *yi*. Another criterion used to determine the number of LVs was the correlation between two successive $\overline{b}$-vectors (the $\overline{b}$-vectors are the average of the b-vectors resulting from each partition, according to Equation 1) (Andrade-Garda, 2009).

Other figures of merit, which allowed us to evaluate the performance of the calibration model developed were as follows: the F-test with degrees of freedom, (k–1) (numerator) and (n_C–k) (denominator) given by Equation 4:

$$F(k-1, n_C-k) = \frac{\sum_{i=1}^{n_C}(\hat{y}_i-\bar{y})^2/(k-1)}{\sum_{i=1}^{n_C}(\hat{y}_i-y_i)^2/(n_C-k)} \quad (4)$$

where $\overline{y}$ is the average of the Cd concentrations used in the calibration group.

The range error ratio, RER, defined according to Equation 5, was calculated as follows:

$$RER = \frac{|y_{MAX}-y_{MIN}|}{SECV} \quad (5)$$

with y_{MAX} and y_{MIN} being the maximum and minimum values of Cd concentration in cocoa beans (range for cross-validation sample set), respectively, determined by FAAS.

The confidence limit at a level of 95% for the performance of the model was calculated as $\hat{y}_i \pm t.SEC.\sqrt{(1 + h_{ii})}$, where t is the student's t value for d_C degrees of freedom. For each training sample, with an estimated value $\hat{y}_i$, h_{ii}, is a scalar taken in order from the main diagonal of the matrix $T \times T'$, where scores T are the coordinates of the sample in the principal components space (ASTM E1655-05, 2012). Finally, as usual, the coefficients of determination for both the set of calibration, R_C^2 and cross-validation R_{CV}^2 are reported.

Results and discussion

The limit of detection (LOD) for FAAS analysis resulted in 0.056 mg kg^{-1}. This figure of merit was calculated according to the expression: $LOD=C_{blank}+3\,\sigma$, where C_{blank} corresponds to an average concentration of ten blanks with σ =0.0019 mg kg^{-1} (standard deviation). Except for the addition of cocoa, the blanks were subjected to the treatment previously described in the sample treatment section. A recovery percentage of 98% was obtained, which means that the sample treatment process and the analytical measurement is acceptable. From the initial set of 65 samples, those whose FAAS analysis resulted in a negative concentration were

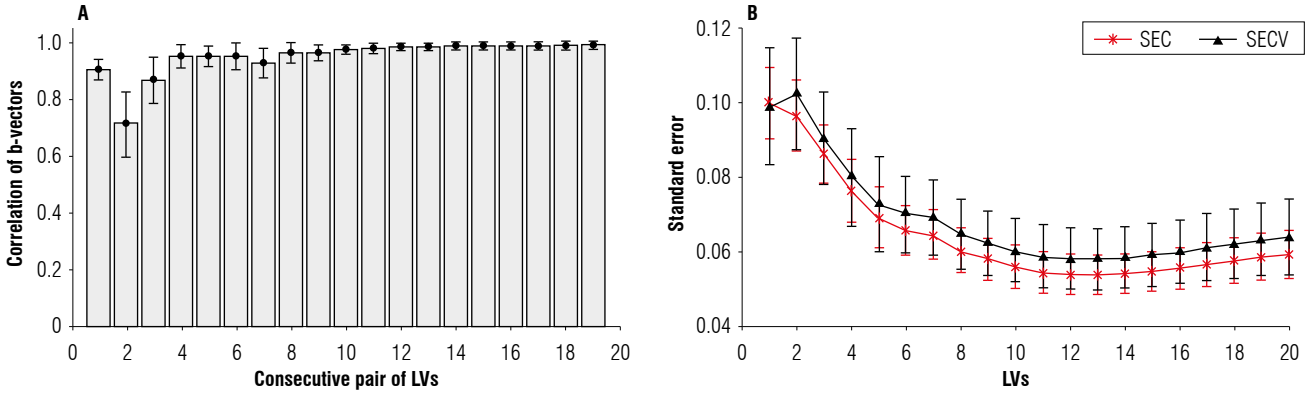

FIGURE 4. Criteria for selecting the dimension (number of latent variables, LVs) of the calibration model. A) corresponds to the correlation of two consecutive $\overline{b}$-vectors; B) the standard error of calibration (SEC) and standard error of cross-validation (SECV) characteristic versus the number of LVs. In A) and B), vertical bars indicate the standard deviation from the average of 1000 partitions.

discarded (negative value means, in this case, Cd concentration below of limit of detection). In addition, due to the small number of samples with concentrations above 1 mg kg^{-1}, the predictive model was limited to this value, taking 46 samples for its development.

The concentration of Cd in cocoa beans using LIBS and FAAS was carried out by applying PLS-1 implemented *on* Matlab R2019b (MathWorks, Inc.) using the statistically inspired modification of the partial least-square (SIMPLS) algorithm (De Jong, 1993; Otto, 2007; Faber & Ferré, 2008). A total of 1000 partitions generated the same number of models for each of the first 20 LVs. Each partition consisted of 60% of the samples for training (28 samples) and the remaining 40% for validation (18 samples). Usually, the number of LVs in the model is selected according to a minimum in SECV (Fig. 4B) that is suggested in this case to be between 12 and 13 LVs.

To respect the degrees of freedom of the calibration mode, this quantity of LVs requires a larger number of samples than those available. For this reason, we use the criterion given by the correlation of two consecutive $\overline{b}$ vectors. In Figure 4A, typical oscillations in this correlation are observed up to the eighth latent variable. Beyond this number of LVs, the correlation tends to remain constant, indicating that there is scarce new information about the model. Based on this behaviour, we selected eight LVs for the construction of the predictive model. The uncertainty reported (vertical bars) were the standard deviations, for each metric, from the 1000 partitions using $\overline{b}$-vectors.

A moderately optimistic model could be proposed by selecting a partition with SECV greater than (or equal to) SEC, and with the smallest distance to the line of identity in the SECV-SEC plane (Fig. 5). It is an empirical fact that when SECV and SEC are calculated for different partitions, using $\overline{b}$-vector in Equation 1, a set of points distributed over an arc segment is obtained. In the SECV-SEC space, moderately optimistic models are located close to the identity line (Niño *et al.*, 2019). Thus, taking the partition closest to this line, the performance metrics of the proposed model are calculated.

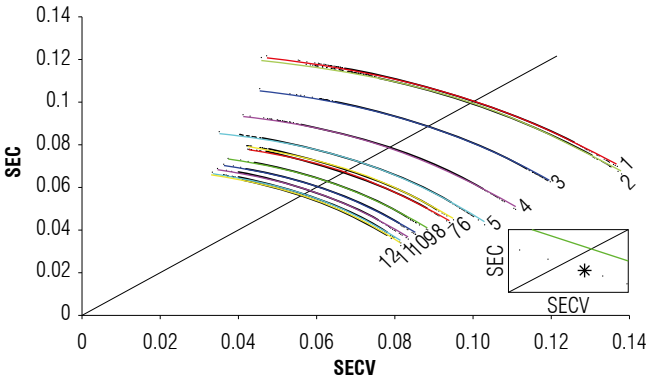

FIGURE 5. In the standard error of cross-validation (SECV)-standard error of calibration (SEC) plane, averages over 1000 partitions are placed on arc segments. For the number of latent variables defined, a partition is selected that satisfies the condition SECV is greater than or equal to SEC. With this partition, the performance metrics for the predictive model are estimated.

For the selected partition, in the eighth LV, the SEC has a value of 0.05±0.0066 mg kg^{-1} with the SECV 0.12±0.0092 mg kg^{-1}. Similarly, the coefficient of determination for calibration and cross-validation samples, R_C^2 and R_{CV}^2 are 0.97±0.0093 and 0.79±0.0042.

The F_{Cal} (calculated F) was 99.23, which must be compared with the F_{Tab}(0.95,7,20), (tabulated F, with a confidence

margin of 95%, N_C=28 and k=8). Since $F_{Cal} > F_{Tab}$=3.01, we can argue that the model appropriately fits the data. On the other hand, the selected partition has a *RER* of 7.92± 2.92, therefore the proposed model can be considered for screening. The performance metrics for the proposed model are summarised in Table 4.

TABLE 4. Parameters describing the performance of the proposed calibration model.

Parameter	Value
Cd concentration range	[0.01-1] mg kg^{-1}
LVs	8
R^2_C	0.97±0.0093
R^2_{CV}	0.79±0.0042
RER	7.92±2.92
SEC	0.05±0.0066 mg kg^{-1}
SECV	0.12±0.0092 mg kg^{-1}
F_{Cal}	99.23
F_{Tab} (0.95,7,20)	3.01
β1 (*p-value*)	0.50
β2 (*p-value*)	0.34

LVs, latent variables; R^2_C and R^2_{CV} are the coefficient of determination for calibration and cross-validation; range error ratio (RER); SEC, standard error of calibration; SECV, standard error of cross-validation; F_{Cal} and F_{Tab} are the F-test statistic values, calculated and tabulated, respectively; p-values for linear (β1) and quadratic (β2) coefficient distributions.

Figure 6 depicts the performance of the proposed calibration model. Note that a small fraction of the samples falls outside the 95% confidence bands (dashed lines). For more details, this information (including residuals, written in brackets) is shown in Table 5. The correlation shows that the model responds to the performance indicators explained in the previous paragraph, following the procedure suggested for the evaluation of trends in residuals of multivariate calibration models by permutation test (Filgueiras *et al.*, 2014). A total of 50.000 permutations allows us to obtain distributions of the linear (β1) and quadratic (β2) coefficients, with *p-values* (β1=0.50 and β2=0.34) greater than 0.05, indicating the absence of linear and quadratic trends, or equivalently, a random behaviour of the residuals with respect to the reference values. Finally, Figure 7 shows the histogram of the residuals for both calibration and cross-validation samples, note that the peak is close to zero.

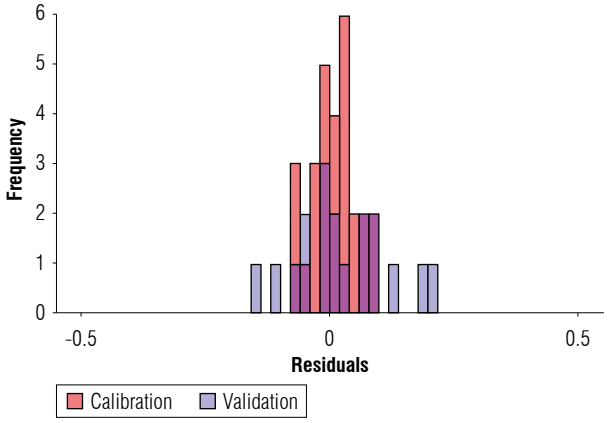

FIGURE 7. Histogram of the residuals for the selected partition. The maximum of the distribution is close to zero.

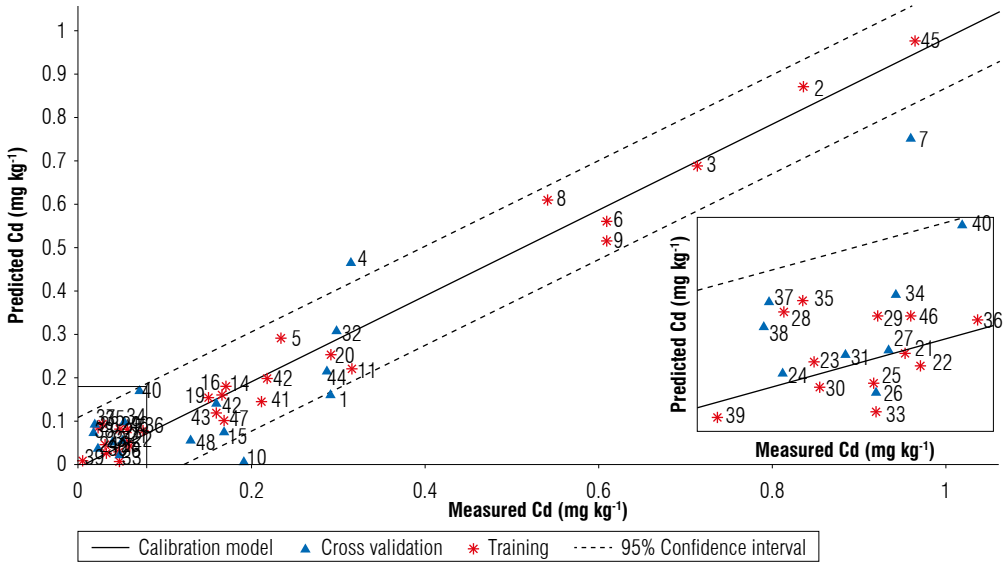

FIGURE 6. Correlation of measured values of Cd concentrations and values predicted by the PLSR-1 model. Dashed lines constitute the 95% confidence band. Samples with measured concentrations close to 0.1 mg kg^{-1} are presented in the box.

TABLE 5. Predicted cadmium concentrations by LIBS in 46 samples of cocoa beans. In parentheses, the residual corresponding to each value predicted by the model.

Sample	Cd Concentration (mg kg^{-1})	Sample	Cd Concentration (mg kg^{-1})
M01	0.19(0.129)	M24	0.02(-0.002)
M02	0.87(-0.034)	M25	0.01(0.031)
M03	0.68(0.0249)	M26	0.009(0.039)
M04	0.46(-0.153)	M27	0.05(0.003)
M05	0.29(-0.058)	M28	0.08(-0.063)
M06	0.56(0.047)	M29	0.08(-0.035)
M07	0.75(0.206)	M30	0.014(0.019)
M08	0.61(-0.069)	M31	0.04(-0.004)
M09	0.52(0.088)	M32	0.31(-0.008)
M10	0.0083(0.183)	M33	-0.01(0.059)
M11	0.22(0.094)	M34	0.10(-0.049)
M12	0.20(0.018)	M35	0.09(-0.069)
M13	0.08(0.096)	M36	0.079(-0.004)
M14	0.18(-0.011)	M37	0.09(-0.078)
M15	0.07(0.096)	M38	0.0716(-0.054)
M16	0.16(0.006)	M39	-0.0164(0.022)
M17	0.10(0.065)	M40	0.17(-0.100)
M18	0.05(0.076)	M41	0.14(0.065)
M19	0.15(-0.003)	M42	0.14(0.018)
M20	0.25(0.039)	M43	0.12(0.037)
M21	0.04(0.009)	M44	0.21(0.074)
M22	0.03(0.025)	M45	0.97(-0.012)
M23	0.039(-0.007)	M46	0.08(-0.026)

Conclusions

In this research, a PLS-1 predictive model was developed to determine the concentration of Cd in cocoa beans from a LIBS spectra. The performance metrics (RER) allow classifying the model as suitable for screening, mainly in the range of 0.2 to 1 mg kg^{-1}. The Monte Carlo cross-validation strategy allowed the selection of a sample partition that yielded a model with adequate correlation, a linear behaviour, which was evident from the diagnostic figures of merit (R^2, residuals and standard errors) and inference tests (F-test). Moreover, it was possible to implement the SLS transformation for the analysis of cocoa beans using LIBS, which significantly improved the signal-to-noise ratio of the spectrum allowing the development of this predictive model with relative experimental simplicity and few chemical reagents, reducing the time compared to other methodologies. The enhancement factor in the predicted concentrations, before and after SLS transformation, was estimated to be around two orders.

Acknowledgments

This research was financially supported by the Vicerrectoría de Investigación y Extensión - Universidad Industrial de Santander, Colombia (VIE-UIS), Internal Project: code 2812.

Conflict of interest statement

The authors declare that there is no conflict of interests regarding the publication of this article.

Author's contributions

RCH conceptualized and devised the methodology. SLHC collected data and contributed to the methodology and formal analysis. JEGB and EMO carried out the formal analysis. All authors contributed to the writing and reviewing of the final version of the manuscript.

Literature cited

Aguirre-Forero, S. E., Piraneque-Gambasica, N. V., & Vásquez-Polo, J. R. (2020). Heavy metals content in soils and cocoa tissues in Magdalena department Colombia: emphasis in cadmium. *Entramado*, *16*(2), 298–310. https://doi.org/10.18041/1900-3803/entramado.2.6753

Andrade-Garda, J. M. (2009). *Basic chemometric techniques in atomic spectroscopy*. RSC.

Argüello, D., Chavez, E., Lauryssen, F., Vanderschueren, R., Smolders, E., & Montalvo, D. (2019). Soil properties and agronomic factors affecting cadmium concentrations in cacao beans: A nationwide survey in Ecuador. *Science of the Total Environment*, *649*, 120–127. https://doi.org/10.1016/j.scitotenv.2018.08.292

ASTM E1655-05. (2012). *Standard practices for infrared multivariate quantitative analysis*. ASTM International. https://doi.org/10.1520/E1655-17

Bertoldi, D., Barbero, A., Camin, F., Caligiani, A., & Larcher, R. (2016). Multielemental fingerprinting and geographic traceability of *Theobroma cacao* beans and cocoa products. *Food Control*, *65*, 46–53. https://doi.org/10.1016/j.foodcont.2016.01.013

Bravo, D., Leon-Moreno, C., Martínez, C. A., Varón-Ramírez, V. M., Araujo-Carrillo, G. A., Vargas, R., Quiroga-Mateus, R., Zamora, A., & Gutierrez Rodríguez, E. A. (2021). The first national survey of cadmium in cacao farm soil in Colombia. *Agronomy*, *11*(4), Article 761. https://doi.org/10.3390/agronomy11040761

Chavez, E., He, Z. L., Stoffella, P. J., Mylavarapu, R. S., Li, Y. C., Moyano, B., & Baligar, V. C. (2015). Concentration of cadmium in cacao beans and its relationship with soil cadmium in southern Ecuador. *Science of the Total Environment*, *533*, 205–214. https://doi.org/10.1016/j.scitotenv.2015.06.106

Checa, K., Gamarra, M., Soto, J., Ipanaqué, W., & La Rosa, G. (2019). Preliminary study of the relation between the content of cadmium and the hyperspectral signature of organic cocoa beans. *Proceedings of the Conference on Electrical, Electronics Engineering, Information and Communication*

Technologies (CHILECON), 1–7. https://doi.org/10.1109/CHILECON47746.2019.8987991

De Jong, S. (1993). SIMPLS: An alternative approach to partial least-squares regression. *Chemometric and Intelligent Laboratory Systems*, *18*(3), 251–263. https://doi.org/10.1016/0169-7439(93)85002-X

Escobar, S., Santander, M., Useche, P., Contreras, C., & Rodríguez, J. (2020). Aligning strategic objectives with research and development activities in a soft commodity sector: A technological plan for Colombian cocoa producers. *Agriculture*, *10*(5), Article 141. https://doi.org/10.3390/agriculture10050141

Escobar, S., Santander, M., Zuluaga, M., Chacón, I., Rodríguez, J., & Vaillant, F. (2021). Fine cocoa beans production: Tracking aroma precursors through a comprehensive analysis of flavor attributes formation. *Food Chemistry*, *365,* Article 130627. https://doi.org/10.1016/j.foodchem.2021.130627

Faber, N. M., & Ferré, F. J. (2008). On the numerical stability of two widely used PLS algorithms. *Journal of Chemometrics*, *22*(2), 101–105. https://doi.org/10.1002/cem.1112

Fedecacao. (2021). *Año cacaotero 2020-2021, el de mayor producción de cacao en la historia de Colombia*. News. https://www.fedecacao.com.co/post/año-cacaotero-2020-2021-el-de-mayor-producción-de-cacao-en-la-historia-de-colombia

Filgueiras, P. R., Alves, J. C. L., Sad, C. M. S., Castro, E. V. R., Dias, J. C. M., & Poppi, R. J. (2014). Evaluation of trends in residuals of multivariate calibration models by permutation test. *Chemometrics and Intelligent Laboratory Systems*, *133*, 33–41. https://doi.org/10.1016/j.chemolab.2014.02.002

Gramlich, A., Tandy, S., Andres, C., Chincheros Paniagua, J., Armengot, L., Schneider, M., & Schulin, R. (2017). Cadmium uptake by cocoa trees in agroforestry and monoculture systems under conventional and organic management. *Science of the Total Environment*, *580*, 677–686. https://doi.org/10.1016/j.scitotenv.2016.12.014

Järup, L., & Åkesson, A. (2009). Current status of cadmium as an environmental health problem. *Toxicology and Applied Pharmacology*, *238*(3), 201–208. https://doi.org/10.1016/j.taap.2009.04.020

Jorhem, L., & Engman, J. (2000). Determination of lead, cadmium, zinc, copper, and iron in foods by atomic absorption spectrometry after microwave digestion: NMKL1 collaborative study. *Journal of AOAC International*, *83*(5), 1189–1203.

Menegatti, C. R., Nicolodelli, G., Senesi, G. S., da Silva, O. A., Filho, H. J. I., Villas-Boas, P. R., Marangoni, B. S., & Milori, D. M. B. P. (2019). Evaluation of LIBS under controlled atmosphere to quantify cadmium at low concentration in landfill leachates. *Applied Physics B*, *125*, Article 74. https://doi.org/10.1007/s00340-019-7189-9

Nicolodelli, G., Cabral, J., Menegatti, C. R., Marangoni, B., & Senesi, G. S. (2019). Recent advances and future trends in LIBS applications to agricultural materials and their food derivatives: An overview of developments in the last decade (2010–2019). Part I. Soils and fertilizers. *TrAC - Trends in Analytical Chemistry*, *115*, 70–82. https://doi.org/10.1016/j.trac.2019.03.032

Niño, A. R., Ramírez, C. X., Hernández, R. C., Picón, H., Guerrero, J. E., & Mejía-Ospino, E. (2019). FTIR-ATR predictive model for determination of asphaltene solubility class index (ASCI) based on partial least-squares regression (PLS-R). *Energy and Fuels*, *33*(12), 12213–12218. https://doi.org/10.1021/acs.energyfuels.9b02829

Oliveira, A. P. F., Milani, R. F., Efraim, P., Morgano, M. A., & Tfouni, S. A. V. (2021). Cd and Pb in cocoa beans: Occurrence and effects of chocolate processing. *Food Control*, *119*, Article 107455. https://doi.org/10.1016/j.foodcont.2020.107455

Otto, M. (2007). *Chemometrics: Statistics and computer application in analytical chemistry* (2nd ed.). Weinheim, Wiley-VCH.

Rodríguez Albarracín, H. S., Darghan Contreras, A. E., & Henao, M. C. (2019). Spatial regression modeling of soils with high cadmium content in a cocoa producing area of Central Colombia. *Geoderma Regional*, *16*, Article e00214. https://doi.org/10.1016/j.geodrs.2019.e00214

Rodríguez Giraldo, Y., Rodríguez Sánchez, S., Torres, L. G., Montenegro, A. C., & Pichimata, M. A. (2022). Development of validation methods to determine cadmium in cocoa almond from the beans by ICP-MS and ICP-OES. *Talanta Open, 5*, Article 100078. https://doi.org/10.1016/j.talo.2021.100078

Satarug, S. (2018). Dietary cadmium intake and its effects on kidneys. *Toxics, 6*(1), Article 15. https://doi.org/10.3390/toxics6010015

Senesi, G. S., Cabral, J., Menegatti, C. R., Marangoni, B., & Nicolodelli, G. (2019). Recent advances and future trends in LIBS applications to agricultural materials and their food derivatives: An overview of developments in the last decade (2010–2019). Part II. Crop plants and their food derivatives. *TrAC - Trends in Analytical Chemistry*, *118*, 453–469. https://doi.org/10.1016/j.trac.2019.05.052

Sezer, B., Bilge, G., & Boyaci, I. H. (2017). Capabilities and limitations of LIBS in food analysis. *TrAC - Trends in Analytical Chemistry*, *97*, 345–353. https://doi.org/10.1016/j.trac.2017.10.003

Shen, T., Kong, W., Liu, F., Chen, Z., Yao, J., Wang, W., Peng, J., Chen, H., & He, Y. (2018). Rapid determination of cadmium contamination in lettuce using laser-induced breakdown spectroscopy. *Molecules*, *23*(11), Article 2930. https://doi.org/10.3390/molecules23112930

Vanderschueren, R., De Mesmaeker, V., Mounicou, S., Isaure, M. P., Doelsch, E., Montalvo, D., Delcour, J. A., Chavez, E., & Smolders, E. (2020). The impact of fermentation on the distribution of cadmium in cacao beans. *Food Research International*, *127*, Article 108743. https://doi.org/10.1016/j.foodres.2019.108743

Wang, W., Kong, W., Shen, T., Man, Z., Zhu, W., He, Y., & Liu, F. (2021). Quantitative analysis of cadmium in rice roots based on LIBS and chemometrics methods. *Environmental Sciences Europe*, *33*(1), Article 37. https://doi.org/10.1186/s12302-021-00480-4

Xu, Q. S., & Liang, Y. Z. (2001). Monte Carlo cross validation. *Chemometrics and Intelligent Laboratory Systems*, *56*(1), 1–11. https://doi.org/10.1016/S0169-7439(00)00122-2

Yang, P., Zhou, R., Zhang, W., Yi, R., Tang, S., Guo, L., Hao, Z., Li, X., Lu, Y., & Zeng, X. (2019). High-sensitivity determination of cadmium and lead in rice using laser-induced breakdown spectroscopy. *Food Chemistry*, *272*, 323–328. https://doi.org/10.1016/j.foodchem.2018.07.214

Yang, P., Zhu, Y., Yang, X., Li, J., Tang, S., Hao, Z., Guo, L., Li, X., Zeng, X., & Lu, Y. (2018). Evaluation of sample preparation

methods for rice geographic origin classification using laser-induced breakdown spectroscopy. *Journal of Cereal Science*, *80*, 111–118. https://doi.org/10.1016/j.jcs.2018.01.007

Yao, M., Yang, H., Huang, L., Chen, T., Rao, G., & Liu, M. (2017). Detection of heavy metal Cd in polluted fresh leafy vegetables by laser-induced breakdown spectroscopy. *Applied Optics*, *56*(14), 4070–4075. https://doi.org/10.1364/ao.56.004070

Zhao, X., Zhao, C., Du, X., & Dong, D. (2019). Detecting and mapping harmful chemicals in fruit and vegetables using nanoparticle-enhanced laser-induced breakdown spectroscopy. *Scientific Reports*, *9*(1), Article 906. https://doi.org/10.1038/s41598-018-37556-w

SCIENTIFIC NOTE

Warming reduces the root density and wheat colonization by arbuscular mycorrhizal fungi in the Yaqui Valley, Mexico

El calentamiento reduce la densidad de raíces y la colonización de hongos micorrízicos arbusculares en trigo en el Valle del Yaqui, México

Ofelda Peñuelas-Rubio[1], Leandris Argentel-Martínez[2*], José Aurelio Leyva Ponce[1], Julio César García-Urías[1], Jaime Garatuza-Payán[2], Enrico Yepez[2], Mirza Hasanuzzaman[3], and Jorge González Aguilera[4]

ABSTRACT

Some studies on the impact of climate changes on wheat have been carried out, but few have explained the possible variations in root morphology and associated microbial diversity. The present study aimed to evaluate the effect of canopy temperature increases of 2°C in wheat during three experimental crop cycles on the initial and final root density and the presence of symbiotic association with arbuscular mycorrhizal fungi (AMF) under field conditions. The warming treatment resulted in the highest percentage of roots (51%) at a greater depth than the control. The warming caused a 38% decrease in the presence of AMF and a 20% decrease in the number of spores per kilogram of soil. The warming treatment generated stress intensities of 18 and 17% in the amount of spore per kilogram of soil and percentage of colonization, respectively.

Key words: climate change, soil fungi, rhizosphere, *Triticum durum* Desf.

RESUMEN

Se han realizado algunos estudios sobre el impacto del cambio climático en el trigo, pero pocos han explicado las posibles variaciones en la morfología de las raíces y la diversidad microbiana asociada. El presente estudio tuvo como objetivo evaluar el efecto del aumento de 2°C en la temperatura del dosel en trigo durante tres ciclos experimentales de cultivo, sobre la densidad de raíces inicial y final, y la presencia en asociación simbiótica con hongos micorrízicos arbusculares (HMA) en condiciones de campo. El tratamiento térmico mostró el mayor porcentaje de raíces (51%) a mayor profundidad que el control. El calentamiento provocó una disminución del 38% en la presencia de HMA y una disminución del 20% en la cantidad de esporas por kilogramo de suelo. El tratamiento térmico generó intensidades de estrés de 18 y 17% en la cantidad de esporas por kilogramo de suelo y en el porcentaje de colonización, respectivamente.

Palabras clave: cambio climático, hongos del suelo, rizosfera, *Triticum durum* Desf.

Introduction

The IPCC (Intergovernmental Panel on Climate Change) reports for the Northwest of Mexico indicates significant thermal variations with temperature increases between 2°C and 4°C for the next 20 years (IPCC, 2014). In this regard, the national and international scientific community state that some crops will show variations from 10% to 30% in their physiological and agronomic performance (Giménez *et al*., 2021; Sadeghi *et al*., 2022). The Yaqui Valley is one of the Mexican northwestern regions with significant temperature increases, and wheat (*Triticum durum* Desf.) is one of the most negatively affected crops (Garatuza-Payán *et al*., 2018).

Some studies of climate change impact on wheat have explained the effects of temperature increase on morphological, physiological, biochemical, molecular, and agronomical indicators (Argentel-Martínez, Arredondo *et al*., 2019; Asseng *et al*., 2019; Liu, 2019; Impa *et al*., 2021). Some other studies are based on parameterized models, using controlled and semi-controlled experimental approaches (Asseng *et al*., 2015; Ahmed *et al*., 2017; Chenu *et al*., 2017; Zhao *et al*., 2019), but few studies have explained the possible variations of root morphology and the associated microbial diversity under climate change scenarios. In this context, the associated microbial diversity contributes significantly to mineral nutrition by increasing the availability of some nutrients, mainly nitrogen, phosphorus,

Received for publication: May 26, 2022. Accepted for publication: September 22, 2022 Doi: 10.15446/agron.colomb.v40n3.102857

[1] Tecnológico Nacional de México, Instituto Tecnológico del Valle del Yaqui, Bácum (Mexico).
[2] Instituto Tecnológico de Sonora, Ciudad Obregón (Mexico).
[3] Department of Agronomy, Sher-e-Bangla Agricultural University (SAU), Dhaka (Bangladesh).
[4] Department of Crop Science, Federal University of Mato Grosso do Sul, Chapadão do Sul (Brazil).
* Corresponding author: largentel.martinez@itvy.edu.mx

and also, the maintenance of humidity in the rhizosphere (Begum *et al*., 2019).

In the Yaqui Valley, the region with the highest wheat production in Mexico, with more than 41% of the national production (Argentel-Martínez, Arredondo *et al*., 2019), some studies explored the relationship between climate change and microbial diversity (Parra-Cota *et al*., 2018; Ingraffia *et al*., 2019) but none reported the arbuscular mycorrhizal fungi (AMF) effects on wheat crop and their relationship with climate change. Hence, wheat production vulnerability predicted for the next ten years in the Yaqui Valley due to climate change scenarios (Garatuza-Payán *et al*., 2018) could be exacerbated if beneficial microorganism diversity decreases in the region, where the contents of soil organic matter are very low (Parra-Cota *et al*., 2018).

For this reason, the present study aimed to evaluate the effect of canopy temperature increase of 2°C on the final root density and the colonization percentage and diversity of the symbiotic association AMF-wheat under field conditions in the Yaqui Valley, Sonora, Mexico.

Materials and methods

Experimental area and treatments

This experiment was carried out during three crop cycles (2016-17, 2017-18, 2018-19) in order to evaluate the effect of a canopy temperature increase of 2°C on agronomic performance of wheat under field conditions (30°27'50.83" N, 60°73'93.24" E) in the Instituto Tecnológico de Sonora, México (Garatuza-Payán *et al*., 2018; Argentel-Martinez, Garatuza-Payán *et al*., 2019). Five adjacent plots with increased temperature in relation to the ambient canopy temperature were established with a randomized design during the 2016-17, 2017-18, and 2018-19 crop cycles, using the crystalline wheat variety CIRNO C2008. Treatments consisted in increasing canopy temperature by 2°C (warming treatment) above the ambient temperature (control treatment). At the end of the experiment, arbuscular mycorrhizal fungi (AMF) colonization was evaluated.

The soil in the experimental area was classified as compacted vertisol (González *et al*., 2003). The national classification of this soil correlates with Halic Haplusterts according to the soil genetic classification methodology developed by Soil Taxonomy (Bockheim *et al*., 2014), which also correlates with the classification proposed by World Reference Base (Mosleh *et al*., 2017).

For higher experimental accuracy, a soil chemical analysis was carried out in the Edaphology Laboratory of the Technological Institute of Sonora (Tab. 1) following the Official Mexican Norm (NOM-021-RECNAT, 2000), which specifies fertility, salinity, and classification of soils. The main chemical feature was the electrical conductivity (EC) value of 1.96 dS m^{-1}, which classified this soil as saline (Nell & Van Huyssteen, 2014). The soil organic matter content (OM) was low, suggesting a decrease in microbial diversity (Ding *et al*., 2014).

Temperature manipulation and control

A temperature increase of 2°C in the crop canopy was applied 15 d after seedling emergence in all crop cycles using six thermal radiators per plot (FTE-1000 model, 1000W, 240 V, 245 mm long x 60 mm wide, Mor Electric Company Heating Association Inc. Comstock Park, MI, USA (Kimball, 2015). The radiators formed a regular hexagon which effectively increased canopy temperature with respect to the adjacent plot at ambient temperature; this was based on an electronic integrative and degradative algorithm that simulates a climate change scenario for the Yaqui Valley for the next 20 years (Kimbal, 2015).

The temperature was controlled using infrared temperature sensors (IRTS Apogee Instruments Inc., Logan, UT, USA) installed on both the control and warming plots (five plots, respectively) with an inclination degree of 45° with respect to the soil surface, covering a circle of $r = 1.5$ m at the center of the plots. Warming was done at a height of 1.20 m of the canopy and started 15 d after the seedling emergence until the harvest (Garatuza-Payán *et al*., 2018).

Soil preparation, seed sowing, and agronomic management

Soil preparation was carried out by the traditional method in the three experimental crop cycles, following the specifications of the technical instructions for wheat in southern

TABLE 1. Agrochemical characteristics of the soil used for the experiment.

pH	OM[1] (%)	EC (dS m^{-1})	Cations (meq L^{-1})				Anions (meq L^{-1})			
			K^+	Na^+	Ca^{2+}	Mg^{2+}	SO_4^{2-}	CO_3^{2-}	HCO_3^-	Cl^-
7.1	0.7	1.96	1.13	8.7	7.8	5.23	4.59	0.85	3.34	5.7

[1] OM: soil organic matter content, EC: electrical conductivity. Methodologies based on NOM-021-RECNAT-2000.

Sonora (Figueroa-López *et al*., 2010), in order to achieve a soil granular structure.

The sowing was carried out on December 7th; 8th and 16th of 2016, 2017, and 2018, respectively, with a URBON-GH sowing machine at a depth of 8 cm, with a towing capacity of six furrows with three rows each, regulated to a density of 170 kg ha^{-1}.

Prior to sowing, bottom fertilization was carried out to a standard of 250 kg ha^{-1} of urea + 50 kg ha^{-1} of mono-ammonium phosphate fertilizer (MAP, 11-52-00). The fertilizer was incorporated during the furrow conformation.

The second and third nitrogen fertilizations were applied immediately before the first and second irrigations at a dose of 50 kg ha^{-1} of urea during tillering and booting phenological phases, respectively. All irrigations were applied at an average depth of 14 cm and at an average irrigation interval of 25 d, when the soil had approximately 75% of field capacity.

Initial and final root density measurements

Four soil rhizosphere samples were extracted from each plot at soil depths of 0-20 cm, 20-40 cm, and 40-60 cm in both treatments at leaf growth phenological phase (30 d after emergence) and during grain ripening (kernel hard). Subsequently, the soil was separated from the roots with water; the roots were cut at the base of the stem and the root volume was measured by volumetry with a glass measuring cylinder that contained an initial volume of 50 ml of water (Tennant, 1975).

Spore quantification and mycorrhizal colonization

During the ripening phenological phase, three samples of plants and rhizosphere soil were taken from each repetition of treatment to quantify the number of AMF spores present on roots and determine the percentage of mycorrhizal colonization. Three replicates of 20 g of soil from each soil sample were processed by the wet sieving technique (Gerderman & Nicolson, 1963) and sucrose gradient (Walker *et al*., 1982) to obtain and quantify the AMF spores. Only viable spores were considered in the quantification, discarding broken, damaged and/or parasitized spores. The root material was washed with distilled water and the thinnest root samples were cut into fragments of 4 cm in length. Later they were stained by the Trypan blue method (Phillips & Hayman, 1970).

The stained roots were mounted in a gridded Petri dish (1 x 1 cm) to perform colonization quantification under the stereoscope (4X) using the intercepts method (McGonigle *et al*., 1990). Counts were performed in duplicate. The presence of any fungal structure (arbuscules, vesicles, or hyphae) in the interior of the roots was considered an indicator of colonization (Sangabriel-Conde *et al*., 2014).

Statistical analysis

After verifying the fulfillment of the theoretical assumptions of normality and variance homogeneity (Komolgorov, 1933) of each evaluated variable (the initial and final root densities and the number of spores by kg of soil), the means, standard deviation, and standard error were calculated. The crop cycles were taken as repetitions due to the similarity of the data. The means were compared following a hypothesis test for continuous quantitative variables, using the theoretical distribution of t-Student for $P<0.01$. Warming stress intensity (WSI) was determined for both variables evaluated following the formula proposed by Fernández (1993): WSI = 1-(variable under warming/variable under control). Subsequently, the variables were compared using a t-Student hypothesis test. For all analyses, the statistical program STATISTICA version for Windows (StatSoft, 2014) was used.

Results

The presented data in each treatment are the result of the average of the three crop cycles due to the absence of significant differences ($P= 0.08322$). The highest root density (51%) was concentrated at a depth of 0-20 cm in the control treatment; however, at this depth, in the warming treatment, the root density was only 27%. In contrast, warming grouped the major root percentage (52%) at a depth of 20-40 cm. The present result indicates that the imposed warming, although intended to create a canopy warming (Kimball, 2015), caused a greater root penetration, which perhaps could contribute to increased mineral uptake available at deeper strata (Tab. 2). On the other hand, at a depth of 40-60 cm, only 16 and 15% of the total volume of roots was found for the control and warming treatments, respectively.

Root growth is critical for crops to use soil water under water-limited conditions. A study conducted by Oussible *et al*. (1992) to investigate the effect of available soil water on root and shoot growth under deficit irrigation in a semiarid environment demonstrated the relationship between root density and leaf area. In the present study, the increase in the deep root system under warming was a morphological mechanism activated to avoid water stress. This mechanism helps to increase water and mineral uptake during adaptation to water stress due to warming conditions (Chen *et al*., 2019).

TABLE 2. Initial and final root density at different soil depths (0-20; 20-40; 40-60 cm) under warming and control treatments [(t value): calculated t value; df: degrees of freedom; p: error probability].

Treatments	Root density (cm cm^{-3})			
	Initial (leaf development)	Final (ripening)		
	0-20	0-20	20-40	40-60
Control	0.03 ± 0.001	0.51 ± 0.02	0.30 ± 0.01	0.16 ± 0.001
Warming	0.03 ± 003	0.27 ± 0.001	0.52 ± 0.002	0.14 ± 0.003
t- value	-0.1739	42.9995	65.6780	19.0548
df	22	22	22	22
p	0.8634	0.0000	0.0000	0.0000

There are many factors that contribute to regulating AMF colonization, such as root density, root exudates, and the availability of nutrients in the rhizosphere (Smith and Read, 2008). In this study, the decrease in root density in the warming treatment was determined according to the obtained AFM colonization percentage.

Arbuscular mycorrhizal fungi colonization and the number of spores in soil

There was a highly significant difference (P=0.0002) in the percentage of AMF colonization in the roots of the crop because of the imposed warming (Fig. 1), with a reduction of 16.7% in the warming treatment with respect to the control treatment. The colonization percentage obtained in the control treatment agrees with Ingraffia *et al*. (2019), who found approximately 29-30% colonization in wheat.

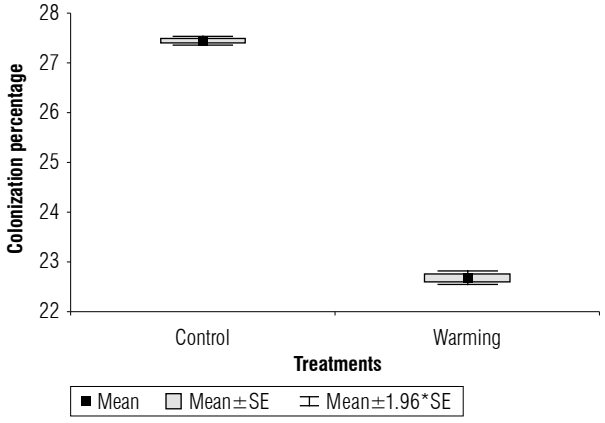

FIGURE 1. Colonization percentage of AMF in wheat under warming and control treatments. SE: standard error of the mean.

This result indicates the adverse effect of temperature increase, as is predicted for Yaqui Valley, in the reduction of fungal diversity and a significant reduction in the colonization percentage. According to Schalamuk *et al*. (2006), changes in soil management can result in crop species without AMF or without certain AMF species because they: (i) cannot tolerate new soil conditions; (ii) are not able to infect the host plant under these conditions; or (iii) are not able to compete with other species of AMF fungi that have become dominant due to new growth conditions (Sieverding, 1991). These results confirm the result obtained in our study (Fig. 1) by reducing the presence of AMF spores by the applied treatment.

The number of spores per 1 kg of soil also decreased by 38.5% (P=0.00031) because of the warming imposed (Fig. 2); the standard deviation of the control treatment was higher, but this variability did not negate the significant differences found.

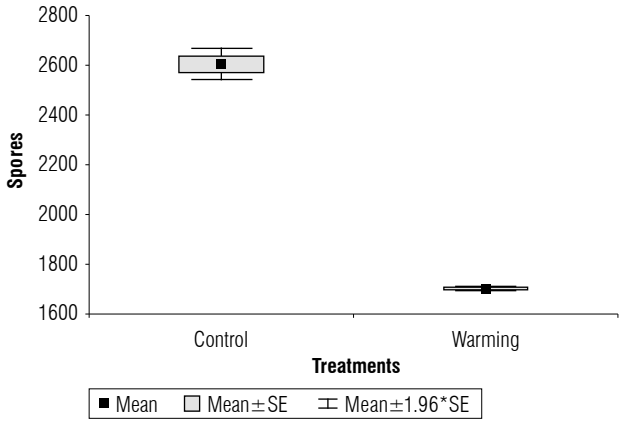

FIGURE 2. Number of spores per kg of soil in the wheat roots under warming and control treatments. SE: standard error of the mean.

Warming stress intensity for AMF colonization and the number of spores in soil

When analyzing the intensity of stress in the evaluated variables, greater (18%) sensitivity was found in the percentage of colonization, with highly significant differences with respect to the number of spores per 1 kg of soil (Fig. 3).

Stress intensity is a calculated parameter that indicates the severity of stressful conditions on biological variables

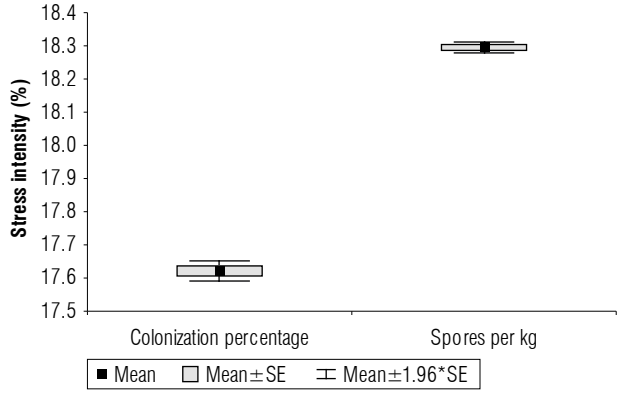

FIGURE 3. Stress intensity for colonization percentage and the number of spores per kg of soil. SE: standard error of the mean.

(mainly root length and plant height) and measures tolerance to some stressful conditions. The present study demonstrated that AMF spores can prevail in the soil, but due to the warming effect, their symbiosis capacity and diversity decrease. This result could affect the availability of some mineral nutrients and water for plant development, reducing agronomic performance of wheat under warming conditions.

Conclusions

Greater root density in the warming treatment was found at greater depths (20-40 cm) than in the control treatment. This response constitutes a morphological tolerance mechanism for heat stress in the variety used in the experiment. Warming caused a 38% decrease in the presence of arbuscular mycorrhizal fungi on wheat roots. The imposed warming generated stress intensities of 18 and 17% in the number of spores per kg of soil and colonization percentage, respectively.

Acknowledgments

We are grateful to the National Technological Institute of Mexico TecNM) and Consejo Estatal de Ciencia y Tecnología – Sonora, Grant No. 20190430 for their support.

Conflict of interest statement

The authors declare that there are no conflicts of interests regarding the publication of this article.

Author's contributions

OPR conducted the research process, specifically performing the experiments; JALP collected data and conducted the experiment under field conditions and was in charge of writing and software management; JCGU contributed to writing and software collection; LAM developed experimental and farming methodology; JGP provided materials and financial resources; JGA provided computing resources; EAY contributed to analysis tools and visualization; MH reviewed the final edition and style. All authors have read and approved the final version of the manuscript.

Literature cited

Ahmed, M., Claudio, S.O., Nelson, R., & Higgins S. (2017). Ensembles modeling approach to study climate change impacts on wheat. In EGU General Assembly Conference [Abstracts]. Munich: European Geosciences Union. 19, 340.

Argentel-Martínez, L., Arredondo, T., Yépez, E. A., & Garatuza-Payán, J. (2019). Effects of experimental warming on peroxidase, nitrate reductase and glutamine synthetase activities in wheat. *Agronomy Research*, *17*(1), 22–32. https://doi.org/10.15159/AR.19.003

Argentel-Martínez, L., Garatuza-Payán, J., Yépez, E. A., Arredondo, T., & de los Santos-Villalobos, S. (2019). Water regime and osmotic adjustment under warming conditions on wheat in the Yaqui Valley, Mexico. *PeerJ*, *7*, Article e7029. https://doi.org/10.7717/peerj.7029

Asseng, S., Ewert, F., Martre, P., Rötter, R. P., Lobell, D. B., Cammarano, D., Kimball, B. A, Ottman, M. J., Wall, G. W., White, J. W., Reynolds, M. P., Alderman, Prasad, P. V. V., Aggarwal, P. K., Anothai, J., Basso, B., Biernath, C., Challinor, A. J., De Sanctis, G., …, & Zhu, Y. (2015). Rising temperatures reduce global wheat production. *Nature Climate Change*, *5*(2), 143–147. https://doi.org/10.1038/NCLIMATE2470

Asseng, S., Martre, P., Maiorano, A., Rötter, R. P., O'Leary, G. J., Fitzgerald, G. J., Girousse, C., Motzo, R., Giunta, F., Ali Babar, M., Reynolds, M. P., Kheir, A. M. S, Thorburn, P. J., Waha, K., Ruane, A. C., Aggarwal, P. K., Ahmed, M., Balkovic, J., Basso, B., …, & Ewert, F. (2019). Climate change impact and adaptation for wheat protein. *Global Change Biology*, *25*(1), 155–173. https://doi.org/10.1111/gcb.14481

Begum, N., Qin, C., Ahanger, M. A., Raza, S., Khan, M. I., Ashraf, M., Ahmed, N., & Zhang, L. (2019). Role of arbuscular mycorrhizal fungi in plant growth regulation: implications in abiotic stress tolerance. *Frontiers in Plant Science*, *10*, Article 1068. https://doi.org/10.3389/fpls.2019.01068

Bockheim, J. G., Gennadiyev, A. N., Hartemink, A. E., & Brevik, E. C. (2014). Soil-forming factors and soil taxonomy. *Geoderma*, *226*, 231–237. https://doi.org/10.1016/j.geoderma.2014.02.016

Chen, R., Huang, J. W., Chen, Z. K., Xu, Y., Liu, J., & Ge, Y. H. (2019). Effect of root density of wheat and okra on hydraulic properties of an unsaturated compacted loam. *European Journal of Soil Science*, *70*(3), 493–506. https://doi.org/10.1111/ejss.12766

Chenu, K., Porter, J. R., Martre, P., Basso, B., Chapman, S. C., Ewert, F., Bindi, M., & Asseng, S. (2017). Contribution of crop models to adaptation in wheat. *Trends in Plant Science*, *22*(6), 472–490. https://doi.org/10.1016/j.tplants.2017.02.003

Ding, G. C., Radl, V., Schloter-Hai, B., Jechalke, S., Heuer, H., Smalla, K., & Schloter, M. (2014). Dynamics of soil bacterial communities in response to repeated application of manure containing sulfadiazine. *PLoS ONE*, *9*(3), Article e92958. https://doi.org/10.1371/journal.pone.0092958

Fernández, G. C. J. (1993). Effective selection criteria for assessing plant tolerance. In C. G. Kuo (Ed.), *Adaptation of food crops to temperature and water stress. International Symposium on Adaptation of Food Crops to Temperature and Water Stress* (pp. 257–270), 13–18 August 1992. Publication number 93–410. Taiwan: Asian Vegetable Research and Development Center.

Figueroa-López, P., Félix-Fuentes, J. L., Fuentes-Dávila, G., Vallenzuela-Herrera, V., Chávez-Villalba, G., & Mendoza-Lugo, J. A. (2010). CIRNO C2008, una nueva variedad de trigo cristalino con alto potencial de rendimiento para Sonora. *Revista Mexicana de Ciencias Agrícolas*, *1*(5), 739–744.

Garatuza-Payán, J., Argentel-Martinez, L., Yépez, E. A., & Arredondo, T. (2018). Initial response of phenology and yield components of wheat (*Triticum durum* L., CIRNO C2008) under experimental warming field conditions in the Yaqui Valley. *PeerJ*, *6*, Article e5064. https://doi.org/10.7717/peerj.5064

Gerdemann, J. W., & Nicolson, T. H. (1963). Spores of mycorrhizal Endogone species extracted from soil by wet sieving and decanting. *Transactions of the British Mycological Society*, *46*(2), 235–244. https://doi.org/10.1016/S0007-1536(63)80079-0

González, R., Canales, A., & Marin, L. E. (2003). Salinización de suelos y acuíferos: el caso del Valle del Yaqui, Sonora, México. *Revista Contacto Ecológico. H. Ayuntamiento de Cajeme*, *5*, 19–23.

Giménez, V. D., Miralles, D. J., García, G. A., & Serrago, R. A. (2021). Can crop management reduce the negative effects of warm nights on wheat yield? *Field Crops Research, 261*, Article 108010. https://doi.org/10.1016/j.fcr.2020.108010

Ingraffia, R., Amato, G., Frenda, A. S., & Giambalvo, D. (2019). Impacts of arbuscular mycorrhizal fungi on nutrient uptake, N_2 fixation, N transfer, and growth in a wheat/faba bean intercropping system. *PLoS ONE*, *14*(3), Article e0213672. https://doi.org/10.1371/journal.pone.0213672

IPCC. (2014). *Climate Change (2014): synthesis report. Intergovernmental Panel on Climate Change*. In R. K. Pachauri, & L. A. Meyer (Eds.), Contribution of working groups I, II and III to the fifth assessment report of the Intergovernmental Panel on Climate Change. Geneve: IPCC, 151.

Impa, S. M., Raju, B., Hein, N. T., Sandhu, J., Prasad, P. V., Walia, H., & Jagadish, S. K. (2021). High night temperature effects on wheat and rice: Current status and way forward. *Plant, Cell & Environment, 44*(7), 2049–2065. https://doi.org/10.1111/pce.14028

Kimball, B. A. (2015). Using canopy resistance for infrared heater control when warming open-field plots. *Agronomy Journal*, *107*(3), 1105–1112. https://doi.org/10.2134/agronj14.0418

Kolmogorov, A. T. (1933). *Basic concepts of probability theory*. Berlin: Julius Springer.

Liu, B., Martre, P., Ewert, F., Porter, J. R., Challinor, A. J., Müller, C., Ruane, A. C., Waha, K, Thorburn, P. J., Aggarwal, P. K., Ahmed, M., Balkovič, J., Basso, B., Biernath, C., Bindi, M., Cammarano, D., De Sanctis, G., Dumont, B., Espadafor, … & Asseng, S. (2019). Global wheat production with 1.5 and 2.0 °C above preindustrial warming. *Global Change Biology*, *25*(4), 1428–1444. https://doi.org/10.1111/gcb.14542

McGonigle, T. P., Miller, M. H., Evans, D. G., Fairchild, G. L., & Swan, J. A. (1990). A new method which gives an objective measure of colonization of roots by vesicular-arbuscular mycorrhizal fungi. *New Phytologist*, *115*(3), 495–501. https://doi.org/10.1111/j.1469-8137.1990.tb00476.x

Mosleh, Z., Salehi, M. H., Jafari, A., & Borujeni, I. E. (2017). Comparison of capability of digitizing methods to predict soil classification according to the soil taxonomy and world reference base for soil resources. *Majallah-i āb va Khāk*, *30*(4), 1180–1191. https://doi.org/10.22067/jsw.v30i4.47091

Nell, J. P., & van Huyssteen, C. W. (2014). Soil classification groups to quantify primary salinity, sodicity and alkalinity in South African soils. *South African Journal of Plant and Soil*, *31*(3), 117–125. https://doi.org/10.1080/02571862.2014.921941

NOM-021-RECNAT-2000. (2002). Norma Oficial Mexicana que establece las especificaciones de fertilizada, salinidad y clasificación de suelos. Estudios, muestreos y análisis. http://www.ordenjuridico.gob.mx/Documentos/Federal/wo69255.pdf

Oussible, M. R. K. C., Crookston, R. K., & Larson, W. E. (1992). Subsurface compaction reduces the root and shoot growth and grain yield of wheat. *Agronomy Journal*, *84*(1), 34–38. https://doi.org/10.2134/agronj1992.00021962008400010008x

Parra-Cota, F. I., Coronel-Acosta, C. B., Amézquita-Avilés, C. F., Santos-Villalobos, S., & Escalante-Martínez, D. I. (2018). Diversidad metabólica de microorganismos edáficos asociados al cultivo de maíz en el Valle del Yaqui, Sonora. *Revista Mexicana de Ciencias Agrícolas*, *9*(2), 431–442. https://doi.org/10.29312/remexca.v9i2.1083

Phillips, J. M., & Hayman. D. S. (1970). Improved procedures for clearing roots and staining parasitic and vesicular-arbuscular mycorrhizal fungi for rapid assessment of infection. *Transactions of the British Mycologycal Society*, *55*(1), 158–161. https://doi.org/10.1016/S0007-1536(70)80110-3

Sadeghi, H., Mohamadi, H., Shamsipour, A., Zarei, K., & Karimi, M. (2022). Spatial relations between climatic variables and wheat yield in Iran. *Geography and Development, 20*(68), 150–173. https://doi.org/10.22111/J10.22111.2022.7008

Sangabriel-Conde, W., Negrete-Yankelevich, S., Maldonado-Mendoza, I. E., & Trejo-Aguilar, D. (2014). Native maize landraces from Los Tuxtlas, Mexico show varying mycorrhizal dependency for P uptake. *Biology Fertility Soils*, *50*(2), 405–414. https://doi.org/10.1007/s00374-013-0847-x

Schalamuk, S., Velazquez, S., Chidichimo, H., & Cabello, M. (2006). Fungal spore diversity of arbuscular mycorrhizal fungi associated with spring wheat: effects of tillage. *Mycologia*, *98*(1), 16–22. https://doi.org/10.1080/15572536.2006.11832708

Sieverding, E. (1991). *Vesicular-arbuscular mycorrhiza management in tropical agrosystems*. Deutsche Gesellschaft für Technische Zusammenarbeit, GTZ No. 224. Eschborn.

Smith, S. E., & Read, D. (2008). The symbionts forming arbuscular mycorrhizas. In S. E. Smith, & D. Read (Eds.), *Mycorrhizal symbiosis* (3rd. ed., pp. 13–41). Academic Press.

StatSoft, Inc. (2014). *Statistica* (*data analysis software system*), Version 12. http://www.statsoft.com

Tennant, D. (1975). A test of a modified line intersect method of estimating root length. *Journal of Ecology*, *63*(3), 995–1001. https://doi.org/10.2307/2258617

Walker, C., Mize, C. W., & McNabb Jr., H. S. (1982). Populations of endogonaceous fungi at two locations in central Iowa. *Canadian Journal of Botany*, *60*(12), 2518–2529. https://doi.org/10.1139/b82-305

Zhao, C., Liu, B., Xiao, L., Hoogenboom, G., Boote, K. J., Kassie, B. T., Pavan, W., Shelia, V., Kim, K. S., Hernandez-Ochoa, I. M., Wallach, D., Porter, C. H., Stockle, C. O., Zhu, Y., & Asseng, S. (2019). A SIMPLE crop model. *European Journal of Agronomy*, *104*, 97–106. https://doi.org/10.1016/j.eja.2019.01.009

SCIENTIFIC NOTE

Population density of aphids in chrysanthemums grown under photoselective screens

Densidad poblacional de áfidos en crisantemos cultivados bajo pantallas fotoselectivas

Caio Henrique Binda de Assis[1], Ronilda Lana Aguiar[1], Anderson Mathias Holtz[1], Evandro Chaves de Oliveira[1], Julielson Oliveira Ataide[2]*, João Marcos Louzada[1], and Robson Prucoli Posse[1]

ABSTRACT

The chrysanthemum is one of the main ornamental species in the world. It has great relevance in the market. Aphids are the main pests that affect the chrysanthemum crop and cause various types of damage to this plant. The objective of this study was to evaluate the influence of different cropping systems using photoselective screens on the population density of aphids in cut chrysanthemum. The study was carried out in an experimental area of the Federal Institute of Espírito Santo – Campus Itapina (Brazil) in a randomized complete block design, according to the split-plot scheme over time. The experiment was established in 3 blocks of 12 m in length with plots of 3 m containing different photoselective screens (red, silver, and black) and the control treatment (open field). Repeated evaluations at different times were done at 0, 15, 30, 45, and 60 d. Data were checked for normality and homoscedasticity and submitted to the Tukey's test ($P<0.05$) and a non-parametric method of smoothing a dispersion graph with local weight (LOESS regression). Regardless of the color of the photoselective screen, there was a lower incidence of aphids compared to the open field treatment in the chrysanthemum culture with an average reduction of 84%. For the different sampling times, the Tukey test did not show significant differences between the means of aphid incidence in the evaluated period. Black, red, and silver photoselective screens promoted significant reductions in aphid populations in chrysanthemums of the variety *Zembla* in the environmental conditions of southeastern Brazil.

Key words: cut flowers, mechanical barrier, behavioral changes.

RESUMEN

El crisantemo es una de las principales especies ornamentales en el mundo con gran relevancia en el mercado. Los áfidos son la principal plaga que afecta al crisantemo, causando diferentes daños. El objetivo del presente trabajo fue evaluar la influencia de diferentes sistemas de cultivo bajo diferentes pantallas fotoselectivas sobre la densidad poblacional de áfidos en crisantemo. El estudio se realizó en un área experimental del Instituto Federal de Espírito Santo – Campus Itapina (Brasil); se empleó un diseño en bloques completamente al azar, con un arreglo de parcelas divididas a través del tiempo. El experimento se estableció en 3 bloques de 12 m de largo, con parcelas de 3 m de largo que contenían las diferentes pantallas fotoselectivas (roja, plateada y negra) y el tratamiento testigo (campo abierto). Las evaluaciones repetidas en el tiempo fueron a los 0, 15, 30, 45 y 60 d. Los datos fueron verificados por normalidad y homocedasticidad y sometidos a la prueba de Tukey ($P<0.05$) y un método no paramétrico de suavizado de un gráfico de dispersión con peso local (regresión LOESS). Independientemente del color de la pantalla fotoselectiva, hubo una menor incidencia de áfidos en comparación con el tratamiento de campo abierto en el cultivo de crisantemo, con una reducción promedio del 84%. Para las diferentes fechas de muestreo, la prueba de Tukey no mostró diferencias significativas entre medias de incidencia de áfidos durante el período evaluado. Las pantallas fotoselectivas negras, rojas y plateadas promovieron reducciones significativas en las poblaciones de áfidos en crisantemos de la variedad *Zembla* en las condiciones ambientales del sureste de Brasil.

Palabras clave: flores de corte, barrera mecánica, cambios de comportamiento.

Introduction

Chrysanthemum, *Chrysanthemum morifolium* Ramat., stands out as one of the main ornamental species in the world with great relevance in the cut flowers and potted plants market (Bhargavi *et al*., 2018). It is a common plant in the northern hemisphere, mainly Asia and Europe, and is one of the main flower species commercialized in countries like India, Colombia, and Brazil (Dhiman *et al*., 2018; Zandonadi *et al*., 2018; Parrado-Moreno *et al*., 2019; Sreedhar *et al*., 2020).

In Brazil, commercial floriculture has greatly expanded and become more competitive in recent years, proving to

Received for publication: July 16, 2022. Accepted for publication: October 28, 2022 Doi: 10.15446/agron.colomb.v40n3.103742

[1] Instituto Federal de Educação, Ciência e Tecnologia do Espírito Santo, ES (Brazil).
[2] Universidade Federal do Espírito Santo, ES (Brazil).
* Corresponding author: julielsonoliveira@hotmail.com

be a very promising commercial sector (Souza *et al*., 2020). Currently, the ornamental chain in the country has 8,000 producers of flowers and plants that together produce more than 2,500 species, including the chrysanthemum, which is among the main species cultivated for cut flowers and potted plants (Instituto Brasileiro de Floricultura, 2021).

Ease of cultivation, high return, great beauty and durability of inflorescences and especially great diversity are characteristics that contribute to the great worldwide popularity of chrysanthemums and make them suitable for various purposes, including interior and exterior decorations of houses, use in exhibitions, and production of garlands and bouquets (Heidemann & Barbosa, 2017; Dhiman *et al*., 2018; Thakur *et al*., 2018). However, the crop is affected by several factors, especially pest attacks, such as aphids, caterpillars, mites, white flies, and thrips (Saicharan *et al*., 2019).

Aphids are considered the most common pests that infest the crop with several species recorded such as *Macrosiphoniella sanborni* Gillette, *Myzus persicae* Sulzer, *Acyrthosiphon pisum* Harris, and *Aphis gossypii* Glover (Ali, 2017). These are small, sap-sucking insects that affect several plant species and can cause a wide range of damage, including weakening and yellowing, sprout deformation, honeydew secretion and consequent fungal development, and virus transmission that cause diseases (Singh & Singh, 2016).

Biotic factors, such as natural enemies and interspecific and intraspecific interactions, and abiotic factors, such as climatic conditions, presence of insecticides, and use of anti-insect and photoselective screens affect population dynamics and insect behavior (Nyamukondiwa *et al*., 2013).

Photoselective screens are tools that are being increasingly used in agricultural and ornamental crops. These screens function as a physical barrier for pests and act by modifying the spectrum and scattering light, a condition that directly influences pest behavior (Shahak *et al*., 2008). In addition, photoselective screens also impact the morphology and physiology of plants, promoting beneficial actions in the development and productivity of crops (Abbasnia *et al*., 2019; Bastías *et al*., 2021).

Researchers around the world have evaluated the influence of photoselective screens on populations of various pest species (Ngelenzi *et al*., 2019; Candian *et al*., 2020). However, in Brazil, studies with photoselective screens are focused on their impact on plants (Almeida *et al*., 2021; Sales *et al*., 2021). There is a gap in relation to the influence of these screens on agricultural pests in the conditions found in Brazil.

In this context, it is urgent to understand the impact of using photo-selective screens on pest populations and to assess their potential for use in ornamental crops under environmental conditions in Brazil. The objective of this study was to evaluate the influence of photoselective screens on the population density of aphids in the cut chrysanthemum variety *Zembla*.

Materials and methods

The study was carried out in the experimental area of the Federal Institute of Espírito Santo – Campus Itapina, located in the district of Itapina in Colatina – ES (Brazil). The region has a tropical climate according to the Köppen classification, characterized by seasonal rainfall and high temperatures (Köppen, 1936; Peel *et al*., 2007). The soil of the experimental area is classified as Dystrophic Red-Yellow Latosol (Santos *et al*., 2018).

Before installing the experiment, two simple samples were collected at a depth of 0 to 20 cm from each bed with a probe-type auger. The samples were homogenized in a clean container to form a composite sample, from which a sample was taken for chemical analysis at the Laboratory of Soil Analysis of IFES - Campus Itapina. This information was used to make fertilization recommendations for the cultivation of the variety *Zembla* chrysanthemum (white). The variety of chrysanthemum *Zembla* (white), acquired from the company Terra Viva located in the municipality of Holambra, São Paulo, was used in the experiment.

The experiment was conducted during the winter, between the months of July and September 2019 (July 24 to September 24). Maximum and minimum air temperature and relative air humidity were obtained from an automatic station of the National Institute of Meteorology (INMET), located in Marilândia - ES, 45 km away from the study (Fig. 1).

The experiment was conducted in a randomized block design, according to a split-plot scheme over time. The primary factor (plots) consisted of 4 different cropping systems: red, silver, and black photoselective shading screens and field conditions (control); and the secondary factor consisted of repeated evaluations over time (0, 15, 30, 45, and 60 d).

We established 3 blocks that consisted of beds 12 m long by 1.20 m wide and 7 planting lines covered by a 2.10 m

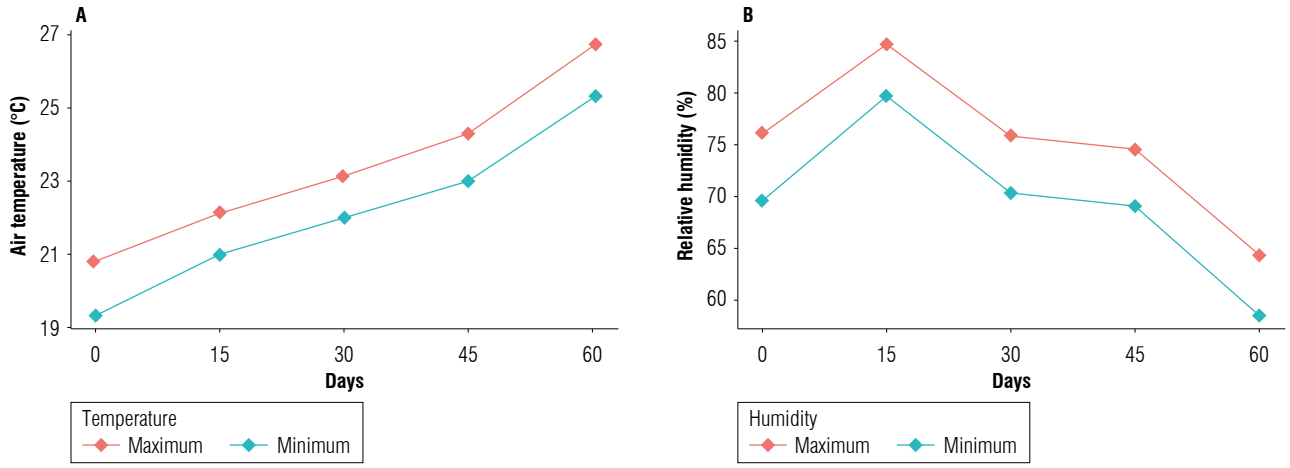

FIGURE 1. Maximum and minimum air temperature and relative air humidity during the experimental period (July 24 to September 24, 2019). INMET automatic station, Marilândia – ES (Brazil), 2019.

high cultivation tunnel (except for the areas related to the control treatment). These were established with a rotating hoe. The plots referring to the different treatments were 3 m long and consisted of 28 plants with a spacing of 15 x 15 cm between them. During the vegetative period, luminous supplementation was performed, supplied by 25 W lamps for 4 h until the plants reached a commercial stem height of 70 cm. Plants were irrigated using a micro sprinkler system. All screens used offered 35% shading.

The infestation of aphids on chrysanthemum plants was natural. To monitor the incidence and population density of this pest, one yellow checkered adhesive trap (10 x 19.5 cm) was used per plot, placed at a height of 10 cm from the plants. Each plot of the block received a trap distributed equidistantly and the evaluations for counting the aphids were carried out every two weeks.

Data were checked for normality and homoscedasticity and submitted to the Tukey's test ($P<0.05$) to compare treatment means. As for the time factor, the non-parametric method of smoothing a scatterplot with local weight (LOESS regression) was applied that estimates curves and surfaces through reference-free smoothing of an explicit mathematical model.

The data violated the assumption of normality and homogeneity of variance; and it was necessary to apply a logarithmic transformation (in base 10), mainly to stabilize the variance between treatments. Due to the fact that the data contains a lot of zeros, the formulation z=log (x + 1) was used, where x represents the original data and z the transformed values. After processing the analyses, the data were returned to the original scale.

Results and discussion

From the analysis of variance, there was no significant interaction between the crop systems under photoselective screens and the evaluation period for the population density of chrysanthemum aphids. For this reason, the factors were analyzed independently (Figs. 2-3).

For the different cropping systems under photoselective screens (F=13.11, $P<0.01$), the results of the Tukey test at the 5% significance level showed that the mean incidence of aphids in the control or field treatment (47.3) differed statistically from the mean values of the other treatments. The data were as follow: 10.7 (black color screen), 7.27 (red color screen) and 5.4 (silver color screen) (Fig. 2).

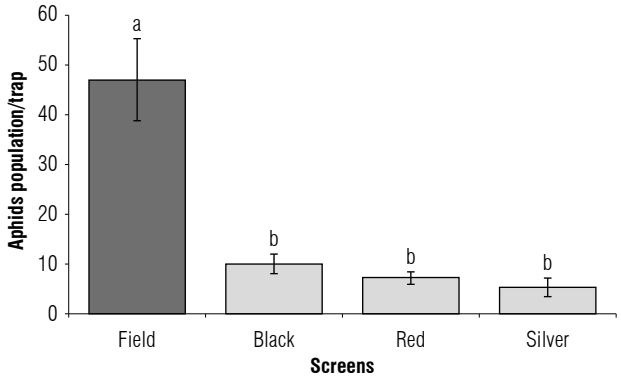

FIGURE 2. Effects of photoselective screens on aphid populations in a crop of *Chrysanthemum morifolium* variety *Zembla*. IFES, Colatina-ES (Brazil), 2019. Means followed by the same letter do not differ from each other by the Tukey test at 5% significance. Bars represent the standard error. Results obtained from the transformation of data into log10 and are presented in its original form.

Therefore, regardless of the color of the screen used, the cultivation of chrysanthemum under photoselective screens promoted a lower incidence of aphids compared to the open field treatment.

The adoption of cultivation techniques aimed at protecting plants and soil has been widely used in agriculture to improve production, yield, and product quality (Shahak, 2014). Photoselective screens or nets have been employed with the aim of protecting plants from adverse conditions such as excessive solar radiation, drought, wind and hail, in addition to their use in protecting against insect attack (Shahak *et al*., 2008; Silva *et al*., 2013; Shahak, 2014).

Although photoselective screens have holes large enough for pests such as aphids, thrips, and whiteflies to pass freely, several studies have demonstrated different responses of these insects to these screens (Shahak *et al*., 2004; Ben-Yakir *et al*., 2008; Shahak, 2014).

Chromatic additives and dispersive and reflective elements added to the composition of photoselective screens allow them to act as spectral modifiers and light disperses (Shahak *et al*., 2008). The fraction of light that passes through the screen holes remains unchanged in terms of its quality, while the light that reaches the wires has its spectrum modified and dispersed (Shahak *et al*., 2004).

Red photoselective screens absorb light in ultraviolet, blue, and green wavelengths of solar radiation and enrich the red and far-red spectral region. Gray screens absorb ultra violet, blue, green, yellow, far red, and infrared radiation and are not good light dispersants, while black ones only act on the amount of light, not altering its quality (Shahak, 2008).

They act as a mechanical barrier for insects as a plastic structure that is placed around the plants, preventing them from reaching the crops and consequently causing direct damage and virus transmission. They also act on the behavior of the aphids, since the perception of ultraviolet light is fundamental for insects for initial flight stimulation, in the location of hosts, in the dispersion within the cultures and in the orientation during the flight, all modified by the photoselective screens (Kigathi & Poehling, 2012). However, as highlighted previously, black screens do not modify the quality of light; and their action is limited to a physical barrier, a condition that may be associated with a higher incidence of aphids in them, although it does not differ statistically from the others (Fig. 2).

Insect vision is promoted by the presence of photoreceptors present in their ocelli and compound eyes. These have ocular photoreceptors capable of recognizing the spectrum of electromagnetic energy in the bandwidth of the ultraviolet (200-400 nm), visible or photosynthetically active radiation (400-700 nm), and far red light (700-800 nm). However, for spectral discrimination to occur, a minimum of two types of photoreceptors located in different parts of compound eyes is necessary (Diaz & Fereres, 2007). Thus, when artificial modifications are made to UV photons, as in the case of photoselective screens, the recognition of the host plant by herbivorous insects is compromised; and, consequently, there is a change in its orientation (Gulidov & Poehling, 2013).

Modifications in pest populational dynamics by using photoselective screens agree with results obtained by Ngelenzi *et al*. (2019) who observed reductions in aphid and whitefly populations in bean (*Phaseolus vulgaris* L.) plants grown under photoselective screens compared to open field treatment. Similarly, Candian *et al*. (2020) obtain significant reductions in the populations of *Halyomorpha halys* Stal and *Drosophila suzukii* Matsumura in apple plants (*Malus domestica* Borkh.) cultivated under photoselective screens.

As for the different epochs, the analysis of variance did not show a significant difference between the averages of aphid incidence in the period evaluated (F=0.8798, P=0.48) (Fig. 3).

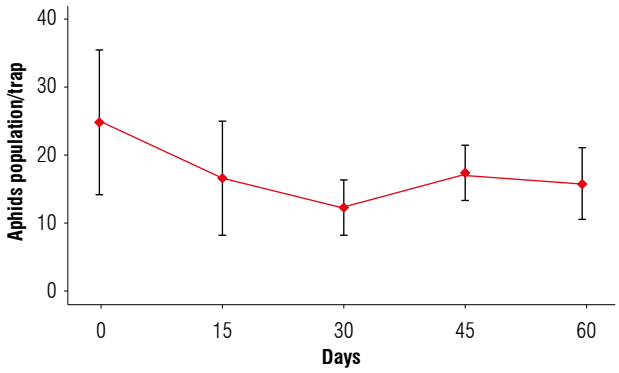

FIGURE 3. Populational fluctuation of aphids in *Chrysanthemum morifolium* variety *Zembla* cultivated between the months of July and September, 2019. IFES, Colatina-ES (Brazil). Bars represent the standard error. Results were obtained from the transformation of data into log10 and presented in its original form.

The local regression method (LOESS) was used to adjust the data considering the variation between epochs within the different levels of the crop system. It is possible to notice that the photoselective screens showed practically the same behavior around a constant value with mild oscillations where both curves remained within the confidence limits

(Fig. 4). However, the effect of different epochs in the control level (field) stood out; the data showed a well-defined non-linear trend. So, it was possible to establish a cubic polynomial model with an R^2=99.7% (Fig. 5).

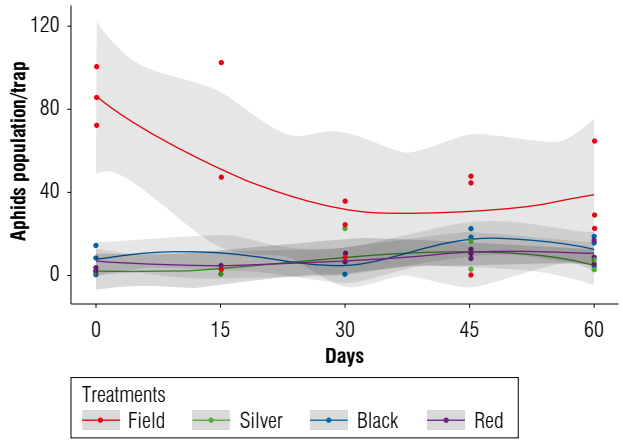

FIGURE 4. Overview of LOESS regression analysis across all treatments, disregarding screen effects over time (d). IFES, Colatina-ES (Brazil), 2019.

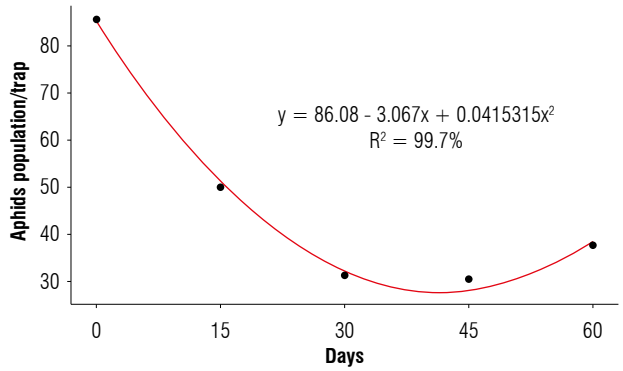

FIGURE 5. LOESS regression curve between the number of aphids and time (d) in open field treatment. IFES, Colatina-ES (Brazil), 2019.

Conclusion

Black, red, and silver photoselective screens promote significant reductions in aphid populations in chrysanthemums of the variety *Zembla* in the environmental conditions of southeastern Brazil.

Acknowledgments

The authors express their gratitude to the Conselho Nacional de Desenvolvimento Científico e Tecnológico (CNPq) (Brazil) for the scholarship and Instituto Federal of Espírito Santo for the support.

Conflict of interest statement

The authors declare that there is no conflict of interests regarding the publication of this article.

Author's contributions

CHBA carried out the experiments; RLA, AMH, ECO, and JOA carried out the laboratory and protected cultivation experiment, collected the data; JML, JOA, and RPP carried out the data analysis and writing. All authors reviewed the final version of the manuscript.

Literature cited

Abbasnia, S. K. Z., Sedaghathoor, S., Padasht Dahkaei, M. N., & Hashemabadi, D. (2019). The effect of light variations by photoselective shade nets on pigments, antioxidant capacity, and growth of two ornamental plant species: Marigold (*Calendula officinalis* L.) and violet (*Viola tricolor*). *Cogent Food & Agriculture, 5*(1), Article 1650415. https://doi.org/10.1080/23311932.2019.1650415

Ali, H. B. (2017). Seasonal population abundance of the chrysanthemum aphids (Homoptera, Aphididae) in the middle of Iraq with pictorial key to species. *Bulletin of the Iraq Natural History Museum*, *14*(4), 315–328. https://doi.org/10.26842/binhm.7.2017.14.4.0315

Almeida, J. M., Calaboni, C., & Rodrigues, P. H. V. (2021). Pigments in flower stems of lisianthus under different photoselective shade nets. *Ornamental Horticulture, 27*(4), 535–543. https://doi.org/10.1590/2447-536X.v27i4.2389

Bastías, R. M., Losciale, P., Chieco, C., & Corelli-Grappadelli, L. (2021). Red and blue netting alters leaf morphological and physiological characteristics in apple trees. *Plants*, *10*(1), 127. https://doi.org/10.3390/plants10010127

Ben-Yakir, D., Hadar, M. D., Offir, Y., Chen, M., & Tregerman, M. (2008). Protecting crops from pests using OptiNet® screens and ChromatiNet® shading nets. *Acta Horticulturae*, *770*, 205–212. https://doi.org/10.17660/ActaHortic.2008.770.24

Bhargavi, S., Hemla, B. N., Chandrashekar, S., Ganapathi, M., & Kantharaj, Y. (2018). Efficacy of bio-stimulants on morphology, flowering and yield of chrysanthemum (*Dendranthema grandiflora*) cv Kolar local under fan and pad greenhouse. *International Journal of Chemical Studies*, *6*(5), 1831–1833.

Candian, V., Pansa, M. G., Santoro, K., Spadaro, D., Tavella, L., & Tedeschi, R. (2020). Photoselective exclusion netting in apple orchards: effectiveness against pests and impact on beneficial arthropods, fungal diseases and fruit quality. *Pest Management Science*, *76*(1), 179–187. https://doi.org/10.1002/ps.5491

Dhiman, S. R., Gupta, Y. C., Thakur, P.; Kashyap, B., Sharma, M., & Sharma, K. (2018). Effect of different black-out materials on off-season pot mum production of chrysanthemum (*Dendranthema grandiflora*). *Indian Journal of Agricultural Sciences*, *88*(4), 601–605.

Diaz, B. M., & Fereres, A. (2007). Ultraviolet-blocking materials as a physical barrier to control insect pests and plant pathogens in protected crops. *Pest Technology*, *1*(2), 85–95.

Gulidov, S., & Poehling, H. M. (2013). Control of aphids and whiteflies on brussels sprouts by means of UV-absorbing plastic films. *Journal of Plant Diseases and Protection*, *120*(3), 122–130. https://doi.org/10.1007/BF03356463

Heidemann, J. C., & Barbosa, J. G. (2017). Production and quality of three varieties of chrysanthemum grown in pots with different

NPK rates. *Ornamental Horticulture*, *23*(4), 426–431. https://doi.org/10.14295/oh.v23i4.1020

Instituto Brasileiro de Floricultura. (2021, November 5). O mercado de flores no Brasil. https://www.ibraflor.com.br/numeros-setor

Kigathi, R., & Poehling, H. M. (2012). UV-absorbing films and nets affect the dispersal of western flower thrips, *Frankliniella occidentalis* (Thysanoptera: Thripidae). *Journal of Applied Entomology*, *136*(10), 761–771. https://doi.org/10.1111/j.1439-0418.2012.01707.x

Köppen, W. (1936). Das geographische System der Klimate. In W. Köppen, & R. Geiger (Eds.), *Handbuch der Klimatologie*. Gebruder Borntrager. http://koeppen-geiger.vu-wien.ac.at/pdf/Koppen_1936.pdf

Ngelenzi, M. J., Otieno, O. J., & Mwanarusi, S. (2019). Improving water use efficiency and insect pest exclusion on French bean (*Phaseolus vulgaris* L.) using different colored agronet covers. *Journal of Agricultural Science*, *11*(3), 159–171. https://doi.org/10.5539/jas.v11n3p159

Nyamukondiwa, C., Weldon, C. W., Chown, S. L., le Roux, P. C., & Terblanche, J. S. (2013). Thermal biology, population fluctuations and implications of temperature extremes for the management of two globally significant insect pests. *Journal of Insect Physiology*, *59*(12), 1199–1211. https://doi.org/10.1016/j.jinsphys.2013.09.004

Parrado Moreno, C. A., Hernández Ricardo, R. E., Velásquez Arredondo, H. I., Lopera Castro, S. H., & Hasenstab, C. (2019). An environmental evaluation of the cut-flower supply chain (*Dendranthema grandiflora*) through a life cycle assessment. *Revista EIA*, *16*(31), 27–42. https://doi.org/10.24050/reia.v16i31.747

Peel, M. C., Finlayson, B. L., & McMahon, T. A. (2007). Updated world map of the Köppen-Geiger climate classification. *Hydrology and Earth System Sciences*, *11*(5), 1633–1644. https://doi.org/10.5194/hess-11-1633-2007

Saicharan, M., Anitha, V., Sridevi, D., & Kameshwari, L. (2019). A brief review on chrysanthemum aphid: *Macrosiphoniella sanbornii* (Gillette) and its management. *International Journal of Current Microbiology and Applied Sciences*, *8*(4), 278–283. https://doi.org/10.20546/ijcmas.2019.804.031

Sales, R. A., Oliveira, E. C., Buzatto, E., Almeida, R. F., Lima, M. J. A., Berili, S. S., Aguiar, R. L., Lovo, M., Posse, R. P., Santos, J. C., Quartezani, W. Z., Salles, R. A., Siman, F., S., & Siman, F. C. (2021). Photo-selective shading screens as a cover for production of purple lettuce. *Scientific Reports*, *11*(1), Article 14972. https://doi.org/10.1038/s41598-021-94437-5

Santos, H. G., Jacomine, P. K. T., Anjos, L. H. C., Oliveira, V. A., Lumbreras, J. F., Coelho, M. R., Almeida, J. A., Filho, J. C. A., Oliveira, J. B., Cunha, T. J. F. (2018). *Sistema brasileiro de classificação de solos* (5th ed.). EMBRAPA. https://www.embrapa.br/solos/busca-de-publicacoes/-/publicacao/1094003/sistema-brasileiro-de-classificacao-de-solos

Shahak, Y. (2008). Photo-selective netting for improved performance of horticultural crops. A review of ornamental and vegetable studies carried out in Israel. *Acta Horticulturae*, *770*, 161–168. https://doi.org/10.17660/ActaHortic.2008.770.18

Shahak, Y., Gal, E., Offir, Y., & Ben-Yakir, D. (2008). Photoselective shade netting integrated with greenhouse technologies for improved performance of vegetable and ornamental crops. *Acta Horticulturae, 797*, 75–80. https://doi.org/10.17660/ActaHortic.2008.797.8

Shahak, Y., Gussakovsky, E. E., Gal, E., & Ganelevin, R. (2004). ColorNets: Crop protection and light-quality manipulation in one technology. *Acta Horticulturae*, *659*, 143–151. https://doi.org/10.17660/ActaHortic.2004.659.17

Shahak, Y. (2014). Photoselective netting: An overview of the concept, research and development and practical implementation in agriculture. *Acta Horticulturae*, *1015*, 155–162. https://doi.org/10.17660/ActaHortic.2014.1015.17

Silva, C. R., Vasconcelos, C. S., Silva, V. J., Sousa, L. B., & Sanches, M. C. (2013). Crescimento de mudas de tomateiro com diferentes telas de sombreamento. *Bioscience Journal*, *29*(S1), 1415–1420.

Singh, R., & Singh, G. (2016). Aphids and their biocontrol. In Omkar (Ed.), *Ecofriendly pest management for food security* (pp. 63–108). Academic Press. https://doi.org/10.1016/B978-0-12-803265-7.00003-8

Souza, J. N. C., Diniz, J. W. M., Silva, F. A. O. & Almeida, N. D. R. (2020). Economic overview of ornamental flowers and plants in Brazil. *Scientific Electronic Archives*, *13*(5), 96–102. https://doi.org/10.36560/1352020943

Sreedhar, M., Vasudha, A., & Syed khudus. (2020). Insect-pests complex studies on chrysanthemum in Pantnagar region. *Journal of Entomology and Zoology Studies*, *8*(2), 1644–1646.

Thakur, N., Nair, S. A., Kumar, R., Bharathi, T. U., Dhananjaya, M. V., & Venugopalan, R. (2018). Evaluation of chrysanthemum (*Dendranthema grandiflora* Tzvelev) for desirable horticultural traits. *International Journal of Current Microbiology and Applied Sciences*, *7*(8), 565–574. https://doi.org/10.20546/ijcmas.2018.708.062

Zandonadi, A. S., Maia, C., Barbosa, J. G., Finger, F. L., & Grossi, J. A. S. (2018). Influence of long days on the production of cut chrysanthemum cultivars. *Horticultura Brasileira*, *36*(1), 33–39. https://doi.org/10.1590/S0102-053620180106

SCIENTIFIC NOTE

Mineral nutrient content of soil and roots of *Solanum paniculatum* L.

Contenido de nutrientes minerales del suelo y raíces de *Solanum paniculatum* L.

Clécio Souza Ramos[1]* and Jonh Aldson Bezerra Tenório[1]

ABSTRACT

Solanum paniculatum L., a species endemic to tropical America and used in folk medicine in the treatment of anemia, hepatic and digestive disorders, has been widely studied. However, to date, no previous studies on correlations between the contents of mineral nutrients in plant roots with their contents in soil have been reported. The aim of this study was to determine the main mineral nutrients found in *S. paniculatum* roots and the soil in their natural habitat. It was observed that *S. paniculatum* roots grow in soils rich in calcium and had a positive correlation in the concentration of Ca with Fe, Na and K and a negative correlation with Zn and Mg. The results contribute to the knowledge of mineral nutrients in *S. paniculatum* as well as to its cultivation.

Key words: Solanaceae, jurubeba, phytotherapy, oxisols.

RESUMEN

Solanum paniculatum L., una especie endémica de América tropical y usada en la medicina popular en el tratamiento de la anemia, trastornos hepáticos y digestivos, ha sido ampliamente estudiada. Sin embargo, hasta la fecha, no se han reportado estudios previos sobre las correlaciones entre los contenidos de nutrientes minerales de las raíces de las plantas con sus contenidos en el suelo. El objetivo de este estudio fue determinar los principales nutrientes minerales que se encuentran en las raíces de *S. paniculatum* y el suelo en su hábitat natural. Se observó que las raíces de *S. paniculatum* crecieron en suelos ricos en calcio y con una correlación positiva en la concentración de Ca con Fe, Na y K así como una correlación negativa con Zn y Mg. Los resultados contribuyen al conocimiento de los nutrientes minerales en *S. paniculatum* así como a su cultivo.

Palabras clave: Solanaceae, jurubeba, fitoterapia, oxisoles.

Introduction

Soil's ability to provide mineral nutrients to plants depends on its physical, chemical, and biological characteristics and their interactions (Ma *et al*., 2022). Attention to the quality of soil has grown and its rational management has increased its productive capacity and guaranteed the quality of the product resulting from the uniformity of planting (Brown *et al*., 2022; Bulut, 2022). The amount of secondary metabolites found in plant species directly relates to soil properties, and their characterization is of fundamental importance to maintain production quality and avoid significant chemical variations of natural products derived from plants (Diomande *et al*., 2015).

Solanum paniculatum L. (Solanaceae) is a widely studied plant; it grows in the tropical Americas and is used for culinary purposes and in folk medicine (Vieira *et al*., 2010; Saqueti *et al*., 2022). *S. paniculatum* is common in almost all of Brazil, where this plant is known as "jurubeba", with fructification throughout the year, abounding in bare lands, roadsides, and degraded pastures (Macedo-Costa *et al*., 2017). Given its medicinal, antidiarrheal, anti-inflammatory, antimicrobial, anti-ulcer, antioxidant, and antitumor properties (Tenório *et al*., 2016; Souza *et al*., 2019), it has been recognized as a phytotherapy medicine by the Brazilian Pharmacopoeia, and the chemistry of *S. paniculatum* fruit and leaf has been well studied (Endringer *et al*., 2010; Gazolla *et al*., 2019). Previous chemical studies of various parts of *S. paniculatum* including roots, fruits and leaves have revealed the presence of steroidal alkaloids, steroidal glycoalkaloids, steroidal saponins, terpenes, and phenylpropanoids (Vieira Júnior *et al*., 2015; Valerino-Díaz *et al*., 2018).

Although the plant has been widely exploited for therapeutic and food purposes, the studies of mineral nutrients in *S. paniculatum* have been neglected. There are many studies on nutrients and soil fertility with other *Solanum* species such as the well-known vegetables tomato (*S. lycopersicum*), potato (*S. tuberosum*), eggplant (*S. melongena*) and bitter tomato (*S. aethiopicum*) (Han *et al*., 2021; Can *et al*., 2022). Thus, this study was directed towards the determination of the main mineral nutrients in the roots of *S. paniculatum* and searched to establish a correlation

Received for publication: April 4, 2022. Accepted for publication: November 4, 2022 Doi: 10.15446/agron.colomb.v40n3.101989

[1] Department of Chemistry, Federal Rural University of Pernambuco, Brazil.
* Corresponding author: clecio.ramos@ufrpe.br

between the contents of mineral nutrients in the roots and in the surrounding soil.

Materials and methods

Plant collection and preparation

Roots from adult *S. paniculatum* L. plants ($n = 5$) separated by a minimum distance of 3 m were randomly collected in an Atlantic Forest fragment located in the city of Camaragibe, in the state of Pernambuco in Northeastern Brazil (7°58'36" S and 34°58'51" W, tropical monsoon climate, according to the Köppen criteria). An annual average maximum temperature of 29.1°C, average annual relative humidity of 83.9%, and average precipitation of 92.1 mm were recorded for the collection site of roots and soils where there is low precipitation in summer and high precipitation in winter. On the day of collection, a temperature of 30.2°C, relative humidity of 74.5%, and precipitation of 7.2 mm were recorded for the collection site. The species was identified by the Instituto Agronômico de Pernambuco - IPA and one accession was deposited in the Herbário Dárdano de Andrade Lima with number 88503 and registered at National System of Genetic Heritage Management and Associated Traditional Knowledge platform under reference number A1096D6. The roots were washed with deionized water and dried on paper towels and then in a circulating air oven for a period of 72 h at a temperature of 40°C. The oven-dried roots were crushed and sieved with a 10-mesh sieve.

Soil sampling

Soil samples ($n = 5$) were collected simultaneously with the roots at a depth of 0-20 cm in the area around the roots of *S. paniculatum* and classified as latosols according to Brazilian Soil Classification System (Santos *et al*., 2018) and typically classified as oxisols (USDA soil taxonomy). Soil samples were air dried, ground and put through a 2 mm mesh before being analyzed. A temperature of 30°C, mean precipitation of 67.2 mm, mean relative air humidity of 74.5% and mean atmospheric pressure of 1012.1 mbar were registered on the day of soil collection (Pernambuco Water and Climate Agency (Agência Pernambucana de Águas e Clima, n.d.) and Brazilian National Institute of Meteorology (Instituto Nacional de Meteorologia do Brasil, n.d.)).

Soil analysis

Soil pH was determined potentiometrically (Bel Engineering PHS3BW, Brazil) in a 1:2.5 soil:deionized water suspension after 1 h of contact, with suspension agitation before reading (Beretta *et al*., 2014). Exchangeable calcium and magnesium were determined by complexometric titration with EDTA (0.0125 mol L^{-1}) using as extractor KCl (1 mol L^{-1}) in a proportion 1:10 solution:extractor, while exchangeable aluminum (Al_{KCl}) was determined by acidity titration with NaOH (0.025 mol L^{-1}) using the same extractor KCl (Shelke & Sheikh, 2020). Exchangeable potassium and sodium were carried out in a double acid solution of HCl (0.05 mol L^{-1}) + H_2SO_4 (0.0125 mol L^{-1}) and determined by flame photometry for potassium (Benfer, BFC 150, Brazil) and by colorimetry for phosphorus (Agilent, 8453 United States), with soil mixed with a solution in a proportion: 1:10 (Brondizio & Moran, 2009). Extractive acidity was measured using the calcium acetate method. A solution of calcium acetate (0.5 M) was used for extraction, buffered to a pH 7.0 in a proportion 1:20 and titrated with a dilute solution of NaOH 0.025 mol L^{-1} (Brondizio & Moran, 2009). The sum of bases (SB) was calculated in cmol kg^{-1} according to the following expression: SB = Ca^{2+} + Mg^{2+} + K^{+} + Na^{+} (Martins *et al*., 2011) while cation exchange capacity (CEC) was calculated in cmol kg^{-1} (pH 7.0) using the expression: CEC = SB + H^{+} + Al^{3+} (Briedis *et al*., 2012). Base saturation (V, %) was determined according to the following expression: V, % = (SB/CEC) x 100, while aluminum (m, %) saturation and sodium (S_{Na}) saturation were calculated according to the following expressions: m = 100 × Al^{3+}/SB + Al^{3+} and S_{Na} =100 × Na CEC, respectively.

Root nutrient analysis

The concentrations of total cadmium, copper, iron, potassium, manganese, sodium, zinc, magnesium, and calcium in the root samples were determined using an atomic absorption spectrophotometer (Varian AA240FS, Mulgrave, Australia) operated under the following parameters: wavelengths for Cd (228.8 nm), Cu (324.7 nm), Fe (248.3 nm), K (769.9 nm), Mn (279.5 nm), Na (589.6 nm), Zn (213.9 nm), Mg (285.2 nm), and Ca (422.7 nm); fuel/oxidizer ratio (2/15.3); lamp current 5 mA; air/acetylene and acetylene/nitrous flame; slit width 0.2 nm; acetylene flow rate 2.0 L min^{-1}; air flow rate 13.5 L min^{-1}; nebulizer flow rate 4.0 mL min^{-1}; and flow time 5 s.

Statistical analysis

Results were expressed as the mean ± standard deviation (SD) and one-way analysis of variance (ANOVA). The Shapiro-Wilk normality test and Pearson's correlation were used to establish relationships among studied parameters. Statistical significance was considered at $P<0.05$ and <0.01. The software BioEstat 5.3 was used to statistical analysis.

Results and discussion

The soil had an acidic pH of 4.6, with high Ca^{2+} content, medium Mg^{2+} content, low K^{+}, Na^{+} and P contents (Tab. 1) (Santos *et al*., 2021).

TABLE 1. Results for soil fertility analysis.

Parameters	Unit	Values
pH		4.6 ± 0.03
P	mg kg^{-1}	5.0 ± 0.26
Ca	$cmol_c\ dm^{-3}$	0.91 ± 01
Mg		0.61 ± 01
K		0.04 ± 0.0
Na		0.06 ± 0.0
SB		1.62 ± 0.01
H		3.40 ± 0.05
Al		0.45 ± 0.04
CEC		5.47 ± 0.04
V	%	29.61 ± 0.50
m		21.74 ± 0.22
S_{Na}		1.10 ± 0.02

SB – sum of bases, V - base saturation, m – aluminum saturation, S_{na} - sodium saturation. Values expressed with mean ± standard deviation.

The values of V, SB, and S_{Na} were low, while the m and CEC values were medium, classifying the soil as poor (Luz *et al*., 2002). In acidic soils, the incorporation of nitrogen can be inhibited due to a reduction in the rate of conversion of ammonium to nitrate. This explains studies reporting high levels of phenolic compounds (Tenório *et al*., 2016) accumulated in plants growing in this type of soil. In general, the effects of mineral nutrients on the levels of shikimic acid derivatives, especially derivatives of cinnamic acid, hydrolysable and condensed tannins, are well documented; deficiencies in nitrogen, phosphorus, sulfur, and potassium generally result in higher concentrations of these metabolites in plants (Gobbo-Neto & Lopes, 2007; Kumar & Goel, 2019). Aran *et al*. (2014) demonstrated that the addition of lime to soil influenced the height and stem diameter of *S. paniculatum*, with an increase of 32.63% and 21.16%, respectively, in relation to the treatment without lime. These results were attributed to an increase in soil pH when OH^{-} and CO_3^{2-} ions interact with the H^{+} and Al^{3+} ions retained in the soil colloids and neutralize them. In turn, this provides increased solubility of Ca^{2+} and Mg^{2+} ions in soil, greater mineralization of soil organic matter and, consequently, increased availability of nutrients for plants, thus, favoring their growth and development.

The analysis of the mineral content in the roots of *S. paniculatum* found a greater concentration of calcium, representing 92.84% of the analyzed mineral nutrients (Tab. 2), which can be attributed to the calcium carbonate precipitation process on root surfaces (Canakci *et al*., 2015).

TABLE 2. Content of mineral nutrients in *S. paniculatum* roots.

Element	Concentration (mg 100 g^{-1})	Percentage from sum of elements analyzed
Ca	7452.00 ± 0.58	92.84
Na	73.25 ± 0.04	0.91
Zn	46.60 ± 0.15	0.58
Fe	227.00 ± 0.47	2.82
K	227.24 ± 0.23	2.83
Mg	2.00 ± 0.10	0.03
Mn	0.37 ± 0.02	0.004
Cd	*nd	-
Cu	nd	-

*Not detected. Values expressed with mean ± standard deviation.

Calcium is important for plants as a constituent of cell walls and membranes, contributing to the structure of cells and the upholding of physical barriers against pathogens (Waraich *et al*., 2012; Thor, 2019). When there is a calcium deficiency, cell membranes begin to disintegrate, cell compartmentation is disrupted, and the binding of Ca with pectin in the cell wall is affected, resulting in cell decomposition (White & Broadley, 2003).

A correlation analysis of the mineral nutrient contents in the roots of *S. paniculatum* was performed (Tab. 3).

The Pearson's correlation between the contents of mineral nutrients revealed a positive correlation between Ca, Na, Fe and K, and between Fe and Mn, which might indicate that as the plant absorbs a mineral nutrient it carries another one (Lira *et al.,* 2021).

Negative correlations were observed between Zn and Ca, Na, Fe, K, Mn as well as between Mg and Na, K and Ca. Thus, the cultivation of *S. paniculatum* should avoid soils rich in zinc, which in high concentrations may interfere with the concentration of Ca, Na, Fe, K and Mn by the species (Treter *et al*., 2021), which can affect the development of the plants. The same effect is explained for Mg, which, apparently, hinders the absorption of Na, K and Ca for the species under study.

A study carried out by Emerenciano *et al*. (2013), using Pearson's correlation analysis, observed that the extent to which *Azadirachta indica* absorbs Fe, Cu, Zn and K

TABLE 3. Pearson's correlation coefficients found between the contents of mineral elements in the roots of *S. paniculatum*.

	Ca	Na	Zn	Fe	K	Mg	Mn
Ca	1.00	-	-	-	-	-	-
Na	0.93	1.00	-	-	-	-	-
Zn	-0.59	-0.84	1.00	-	-	-	-
Fe	0.72	0.92	-0.98	1.00	-	-	-
K	1.00	0.93	-0.59	0.72	1.00	-	-
Mg	-0.79	-0.51	-0.04	-0.14	-0.79	1.00	-
Mn	0.08	0.43	-0.85	0.74	0.08	0.56	1.00

All correlation is coefficients at the $P<0.05$ and <0.01.

determines the synergistic effect of absorption of other mineral nutrients. For the metals K, Ca and Mg, negative correlations were observed, indicating that when a fertilizer rich in potassium is added, there is a reduction in the concentration of Ca and Mg. Iron accounted for 2.82% of the mineral nutrients; in plants, iron is an essential nutrient required for various cellular processes such as respiration, chlorophyll biosynthesis, and electron transport in photosynthesis. Considering that calcium was the major nutrient found in the *S. paniculatum* roots as well as in the surrounding soil, a Pearson correlation analysis between the calcium present in the soil and the mineral nutrients absorbed by the roots was performed (Tab. 4).

TABLE 4. Pearson's correlation coefficient for soil calcium and root nutrient minerals.

Contents of mineral nutrients in roots	Content of calcium in soil
Ca	0.98
Na	0.98
Zn	- 0.73
Fe	0.84
K	0.98
Mg	- 0.65
Mn	0.26

All correlation is coefficients at the $P<0.01$.

The results corroborated the hypothesis of a correlation between the contents of mineral nutrients in the roots, where there is a negative correlation between the Ca and Mg (r = - 0.65). This confirms competition between calcium and magnesium, with a preference for calcium by the plants. During the absorption by roots, nutrients as Ca, Mg, and K can be strongly antagonistic, and Mg is the least taken up nutrient (Farhat *et al*., 2016). In sunflower plants grown under insufficient Mg supply, an increase in Ca and K absorption was observed, indicating competition between these nutrients (Lasa *et al*., 2000). Magnesium uptake increased also during the Ca stress periods reflecting the antagonism between Ca and Mg (Taylor & Locascio, 2004). A negative correlation between the Ca^{2+} concentration in soil and the Zn concentration in roots (r = –0.73) can be associated with high calcium content in the soil, as previously reported for rice seedlings, where zinc absorption was reduced by about 90% with the addition of calcium and magnesium (Sadana & Takka, 1983). Furthermore, the positive correlation between the soil Ca^{2+} contents and the contents of Na, Fe, K, Ca in the *S. paniculatum* roots was confirmed, where in the case of calcium, there could be a simultaneous absorption with these other minerals.

Conclusion

S. paniculatum L. were found abundant in calcium-rich soils, with their roots showing a positive correlation for calcium contents with iron, sodium, potassium and a negative correlation with calcium, magnesium, and zinc. The results contribute to studies of *S. paniculatum* cultures aiming at the production of herbal medicines and food products, as the growth and development of plants depend on the mineral nutrients absorbed by roots from the soil.

Acknowledgments

The authors thank the Provost of Research and Graduate of the Federal Rural University of Pernambuco (Brazil) for financial support. JABT thanks Coordenação de Aperfeiçoamento de Pessoal de Nível Superior for providing a scholarship.

Conflict of interest statement

The authors declare that there is no conflict of interests regarding the publication of this article.

Author's contributions

JABT carried out the field and laboratory experiments. CSR contributed to the data analysis and wrote the article. All authors reviewed the final version of the manuscript.

Literature cited

Agência Pernambucana de Águas e Clima. (n.d.). *Meteorologia* (database). https://www.apac.pe.gov.br/#tabs

Aran, H. D. V., Vieira, C. M., Heredia-Zárate, N. A., Gonçalves, W. V., & Lima, V. T. (2014). Desenvolvimento inicial de jurubeba (*Solanum paniculatum* L.) em substratos contendo resíduos orgânicos e calcários. *Cadernos de Agroecologia*, *9*(4), 1–11.

Beretta, A., Bassahum, D., & Musselli, R. (2014). ¿Medir el pH del suelo en la mezcla suelo: agua en reposo o agitando? *Agrociencia Uruguay*, *18*(2), 90–94.

Briedis, C., Sá, J. C. D. M., Caires, E. F., Navarro, J. F., Inagaki, T. M., & Ferreira, A. O. (2012). Carbono do solo e atributos de fertilidade em resposta à calagem superficial em plantio direto. *Pesquisa Agropecuária Brasileira*, *47*(7), 1007–1014. https://doi.org/10.1590/S0100-204X2012000700018

Brondizio, E. S., & Moran, E. F. (2009). *LBA-ECO LC-09 soil composition and structure in the Brazilian Amazon: 1992-1995* (Data set). Oak Ridge National Laboratory-Distributed Active Archive Center, Oak Ridge, Tennessee, USA. https://doi.org/10.3334/ORNLDAAC/938

Brown, P. H., Zhao, F.-J., & Dobermann, A. (2022). What is a plant nutrient? Changing definitions to advance science and innovation in plant nutrition. *Plant and Soil*, *476*(1), 11–23. https://doi.org/10.1007/s11104-021-05171-w

Bulut, S. (2022). Mineral content of some bread wheat cultivars. *Cereal Research Communications, 2022*. https://doi.org/10.1007/s42976-021-00235-0

Can, H., Ozyigit, I. I., Can, M., Hocaoglu-Ozyigit, A., & Yalcin, I. E. (2022). Multidimensional scaling of the mineral nutrient status and health risk assessment of commonly consumed fruity vegetables marketed in Kyrgyzstan. *Biological Trace Element Research*, *200*(4), 1902–1916. https://doi.org/10.1007/s12011-021-02759-2

Canakci, H., Sidik, W., & Kilic, I. H. (2015). Effect of bacterial calcium carbonate precipitation on compressibility and shear strength of organic soil. *Soils and Foundations*, *55*(5), 1211–1221. https://doi.org/10.1016/j.sandf.2015.09.020

Diomande, L. B., Akotto, O. F., Kanko, C., Tia, V. E., & Yao-Kouame, A. (2015). Occurrence and chemical composition of essential oil from *Lippia multiflora* M. (Verbenaceae) leaves as affected by soil carbon, nitrogen and phosphorus contents in the centre Côte d'Ivoire. *International Journal of Agricultural Policy and Research*, *3*(1), 44–52. https://doi.org/10.15739/IJAPR.025

Emerenciano, D. P., Cruz, Â. M. F., Pereira, J. D. S., Moura, M. F. V., & Maciel, M. A. M. (2013). Determinação da propriedade antioxidante e teores de minerais presentes nas folhas de *Azadirachta indica* A. Juss. *Fitos*, *8*(2), 147–156. https://doi.org/10.5935/1808-9569.20130001

Endringer, D. C., Valadares, Y. M., Campana, P. R. P., Campos, J. J., Guimarães, K. G., Pezzuto, J. M., & Braga, F. C. (2010). Evaluation of Brazilian plants on cancer chemoprevention targets *in vitro*. *Phytotherapy Research*, *24*(6), 928–933. https://doi.org/10.1002/ptr.3050

Farhat, N., Elkhouni, A., Zorrig, W., Smaoui, A., Abdelly, C., & Rabhi, M. (2016). Effects of magnesium deficiency on photosynthesis and carbohydrate partitioning. *Acta Physiologiae Plantarum*, *38*(6), Article 145. https://doi.org/10.1007/s11738-016-2165-z

Gazolla, M. C., Marques, L. M. M., Silva, M. G., Araújo, M. T. M. F., Mendes, R. L., Almeida, J. R. G. S., Vessecchi, R., & Lopes, N. P. (2019). Characterization of 3-aminospirostane alkaloids from roots of *Solanum paniculatum* L. with hepatoprotective activity. *Rapid Communications in Mass Spectrometry*, *34*(S3), Article e8705. https://doi.org/10.1002/rcm.8705

Gobbo-Neto, L., & Lopes, N. P. (2007). Plantas medicinais: fatores de influência no conteúdo de metabólitos secundários. *Química Nova*, *30*(2), 374–381. https://doi.org/10.1590/S0100-40422007000200026

Han, M., Opoku, K. N., Bissah, N. A. B., & Su, T. (2021). *Solanum aethiopicum*: the nutrient-rich vegetable crop with great economic, genetic biodiversity and pharmaceutical potential. *Horticulturae*, *7*(6), Article 126. https://doi.org/10.3390/horticulturae7060126

Instituto Nacional de Meteorologia do Brasil. (n.d.). *Dados meteorológicos* (database). https://portal.inmet.gov.br/#

Kumar, N., & Goel, N. (2019). Phenolic acids: natural versatile molecules with promising therapeutic applications. *Biotechnology Reports*, *24*, Article e00370. https://doi.org/10.1016/j.btre.2019.e00370

Lasa, B., Frechilla, S., Aleu, M., González-Moro, B., Lamsfus, C., & Aparicio-Tejo, P. M. (2000). Effects of low and high levels of magnesium on the response of sunflower plants grown with ammonium and nitrate. *Plant and Soil*, *225*(1), 167–174. https://doi.org/10.1023/A:1026568329860

Lira, A. L. F., Silva, K. A., Rodrigues, M. S., Souza, C. G. P., Moreira, F. B. R., & Lima, A. M. N. (2021). Spatial correlation between soil and leaf macronutrients in semiarid Brazilian mango (*Mangifera indica* L.) fields. *Revista Brasileira de Fruticultura*, *43*(4). https://doi.org/10.1590/0100-29452021149

Luz, M. J. S., Ferreira, G. B., Bezerra, J. R. C. (2002). Adubação e correção do solo: procedimentos a serem adotados em função dos resultados da análise do solo. *Circular Técnica*, *63*, 31 (Serie). Embrapa Algodão (CNPA).

Ma, H., Shurigin, V., Jabborova, D., dela Cruz, J. A., dela Cruz, T. E., Wirth, S., Bellingrath-Kimura, S. D., & Egamberdieva, D. (2022). The integrated effect of microbial inoculants and biochar types on soil biological properties, and plant growth of lettuce (*Lactuca sativa* L.). *Plants*, *11*(3), Article 423. https://doi.org/10.3390/plants11030423

Macedo-Costa, M. R., Sette-de-Souza, P. H., Carneiro, S. E. R., Fernandes, J. M., Langassner, S. M. Z., Pereira, M. S. V., & Lima, K. C. (2017). *Solanum paniculatum* Linn: a potential antimicrobial agent against oral microorganisms. *African Journal of Microbiology Research*, *11*(48), 1688–1692.

Martins, A. L. S., Moura, E. G., & Camacho-Tamayo, J. H. (2011). Evaluation of corn production parameters and their spatial relationship with chemical attributes of the soil. *Agronomía Colombiana*, *29*(1), 99–106. https://revistas.unal.edu.co/index.php/agrocol/article/view/28640

Sadana, U. S., & Takkar, P. N. (1983). Effect of calcium and magnesium on ^{65}zinc absorption and translocation in rice seedlings. *Journal of Plant Nutrition*, *6*(8), 705–715. https://doi.org/10.1080/01904168309363137

Santos, G. P., Pereira, W. E., Lima, R. L. S., Brito Neto, J. F., Dias, B. D. O., & Dias, T. J. (2021). Soil fertility and yield of 'Paluma' guava fertilized with phosphorus, cattle manure, and boron. *Revista Brasileira de Engenharia Agrícola e Ambiental*, *25*(4), 228–234. https://doi.org/10.1590/1807-1929/agriambi.v25n4p228-234

Santos, H. G., Jacomine, P. K. T., Anjos, L. H. C., Oliveira, V. A., Lumbreras, J. F., Coelho, M. R., Almeida, J. A., Araujo Filho, J. C., Oliveira, J. B., & Cunha, T. J. F. (2018). *Sistema brasileiro de classificação de solos* (5th. ed.), Embrapa.

Saqueti, B. H. F., Alves, E. S., Castro, M. C., Ponhozi, I. B., Silva, J. M., Visentainer, J. V., & Santos, O. O. (2022). Influence of drying and roasting on chemical composition, lipid profile and antioxidant activity of jurubeba (*Solanum paniculatum* L.). *Journal of Food Measurement and Characterization*, *16*, 2749–2759. https://doi.org/10.1007/s11694-022-01370-w

Shelke, M. E., & Sheikh, R. R. (2020). Relative study for the determination of calcium and magnesium in milk samples by using complexometric EDTA titration and FAAS. *International Journal of Chemical and Physical Sciences*, *9*(2), 1–3. https://doi.org/10.30731/ijcps.9.2.2020.1-3

Souza, G. R., De-Oliveira, A. C. A. X., Soares, V., Chagas, L. F., Barbi, N. S., Paumgartten, F. J. R., & Silva, A. J. R. (2019). Chemical profile, liver protective effects and analgesic properties of a *Solanum paniculatum* leaf extract. *Biomedicine & Pharmacotherapy, 110*, 129–138. https://doi.org/10.1016/j.biopha.2018.11.036

Taylor, M. D., & Locascio, S. J. (2004). Blossom-end rot: a calcium deficiency. *Journal of Plant Nutrition*, *27*(1), 123–139. https://doi.org/10.1081/PLN-120027551

Tenório, J. A. B., Monte, D. S., Silva, T. M. G., Silva, T. G., & Ramos, C. S. (2016). *Solanum paniculatum* root extract reduces diarrhea in rats. *Revista Brasileira de Farmacognosia*, *26*(3), 375–378. https://doi.org/10.1016/j.bjp.2016.02.003

Thor, K. (2019). Calcium – nutrient and messenger. *Frontiers in Plant Science, 10*, Article 440. https://doi.org/10.3389/fpls.2019.00440

Treter, R. J., Carvalho, I. R., Hutra, D. J., Loro, M. V., Cavinatto, M., Lautenchleger, F., & Sfalcin, I. C. (2022). Symptoms and interrelationships of macro and micronutrients available for soybean. *Agronomy Science and Biotechnology*, *8*, 1–15. https://doi.org/10.33158/ASB.r150.v8.2022

Valerino-Díaz, A. B., Gamiotea-Turro, D., Zanatta, A. C., Vilegas, W., Martins, C. H. G., Silva, T. S., Rastrelli, L., & Santos, L. C. (2018). New polyhydroxylated steroidal saponins from *Solanum paniculatum* L. leaf alcohol tincture with antibacterial activity against oral pathogens. *Journal of Agricultural and Food Chemistry*, *66*(33), 8703–8713. https://doi.org/10.1021/acs.jafc.8b01262

Vieira Júnior, G. M., Rocha, C. Q., Rodrigues, T. S., Hiruma-Lima, C. A., & Vilegas, W. (2015). New steroidal saponins and anti-ulcer activity from *Solanum paniculatum* L. *Food Chemistry*, *186*, 160–167. https://doi.org/10.1016/j.foodchem.2014.08.005

Vieira, P. M., Santos, S. C., & Chen-Chen, L. (2010). Assessment of mutagenicity and cytotoxicity of *Solanum paniculatum* L. extracts using *in vivo* micronucleus test in mice. *Brazilian Journal of Biology*, *70*(3), 601–606. https://doi.org/10.1590/S1519-69842010000300017

Waraich, E. A., Ahmad, R., Halim, A., & Aziz, T. (2012). Alleviation of temperature stress by nutrient management in crop plants: a review. *Journal of Soil Science and Plant Nutrition*, *12*(2), 221–244. https://doi.org/10.4067/S0718-95162012000200003

White, P. J., & Broadley, M. R. (2003). Calcium in plants. *Annals of Botany*, *92*(4), 487–511. https://doi.org/10.1093/aob/mcg164

Editorial policy

Agronomía Colombiana is a scientific and technical publication of the agricultural sector, edited by the Faculty of Agricultural Sciences of Universidad Nacional de Colombia - Bogota campus. It is directed to agricultural science researchers, extension workers and to all professionals involved in science development and technological applications for the benefit of agricultural producers and their activity.

Issued as a triannual publication, this journal is intended to transfer research results in different areas of Agronomy in the tropics and subtropics. Original unpublished papers are, therefore, accepted in the following areas: plant physiology, crop nutrition and fertilization, genetics and plant breeding, entomology, phytopathology, integrated crop protection, agroecology, weed science, environmental management, geomatics, soil science, water and irrigation, agroclimatology and climate change, post-harvest and agricultural industrialization, rural and agricultural entrepreneurial development, agrarian economy, and agricultural marketing.

The authors of the manuscripts submitted to *Agronomía Colombiana* must be aware of and avoid scientific misconduct (code of conduct by Committee on Publication Ethics, COPE) related to: scientific fraud in all or part of the data of the study and data falsification and manipulation; dishonesty due to fictitious authorship or gifting or exchange of co-authorship, duplicate publications, partial or complete, in different journals and self-plagiarism by reusing portions of previous writings; citation omission, citation copying without consultation and excessive self-citation, among others. The authors have the following rights: fair and impartial evaluation of articles done in a reasonable amount of time, correspondence taken seriously and requests for changes and corrections respected, manuscripts subject to review by the peer reviewers, and articles remained unaltered.

Agronomía Colombiana uses a double-blind peer review process anticipated by the previous quick preliminary review. The manuscripts must be submitted according to the rules established in the instructions to authors. If the articles fulfill the minimum criteria established for the preliminary review in terms of language and scope, these are sent to three or more expert reviewers in the specific area of knowledge to obtain two or three evaluations; two of the experts are external to the Universidad Nacional de Colombia, and the third one belongs to the research and teaching staff of the Universidad Nacional de Colombia. When the manuscript obtains two approval evaluations, the manuscript can be considered for publication by the editors; if two of the reviewers consider that the scientific level of the manuscript is not acceptable for publication, the manuscript will be rejected. Once the peer-review process is completed, the manuscript is sent back to the author(s) who must introduce the suggested corrections and answer all the questions obtained from the reviewers or the Editor. Finally, the Editor-in-Chief or the Editorial Committee reserves the right to accept or reject the submitted manuscripts.

For additional information, correspondence, subscriptions and journal swap, you may contact Universidad Nacional de Colombia, Facultad de Ciencias Agrarias, Journal *Agronomía Colombiana*, Bogota campus; P.O. Box 14490, Bogota-Colombia; phone numbers: (571) 316 5355 / 316 5000 extension 10265; e-mail: agrocol_fabog@unal.edu.co; the digital version of the journal is available at http://www.scielo.org.co and http://www.revistas.unal.edu.co/index.php/agrocol

Instructions to authors

The manuscripts submitted for publication to the Editorial Committee must be unpublished. In consequence, those that have been previously published in other journals, technical or scientific publications will be rejected. Contributions to the study and the submitted manuscript and any conflict of interest must be declared by the authors in the sections created for these purposes.

To submit manuscripts, the authors must be registered in our platform (https://revistas.unal.edu.co/index.php/

agrocol/about/submissions#onlineSubmissions) and follow the submission instructions. Corresponding authors will be required to use their ORCID Id when submitting a manuscript. After manuscript submission, papers will be screened for plagiarism using a specialized software. In case of finding a significant level of duplication, the manuscript will be rejected.

At the preliminary review stage, two aspects, English grammar and scope, will be assessed in order to ensure the minimum requirements of any manuscript to be peer-reviewed. If the manuscript is rejected during the preliminary review because of the English grammar aspect, authors are encouraged to edit their manuscript for language using professional services and submit the manuscript again. When the reason for preliminary reject is a mismatch of the scope between the manuscript and the journal interests, resubmission should be avoided.

Agronomía Colombiana accepts the following three types of original articles:

- **Scientific and technological research papers**: Those documents presenting detailed original research results. The most generally applied structure has four main parts: introduction, materials and methods, results and discussion, and conclusions.
- **Review articles**: Published only at the invitation of the Editor-in-Chief and with the approval of the Editorial Committee of *Agronomía Colombiana*. The review article should present an unbiased summary of the current understanding of a topic considered as a priority by the Editorial or Scientific Committee of *Agronomía Colombiana*.
- **Scientific notes**: Brief document introducing original preliminary or partial results of a scientific or technical research, which usually needs immediate publication.

Format and organization of the text

Research article length should not exceed 5,200 words, whereas scientific notes should have no more than 4,000 words. As review articles contain a large amount of detailed information, their length may be greater than research articles but should not exceed 8,000 words, or 10,000 words including the list of references. For review articles, the list of references (Literature cited section) should include at least 50 references. Tables and figures, that is to say, diagrams, drawings, schematic and flow diagrams, pictures, and maps should be consecutively numbered (Table 1 ...Table n; Figure 1... Figure n, etc.).

Texts and tables should be prepared using the MS Word® processor. Manuscripts including tables as embedded images will not be published. All text should be double-spaced including table headers, figure captions and cited literature. All pages must be numbered consecutively. Line numbering on each page is mandatory. Tables and diagrams of frequency (bar and circular diagrams) should be included in the mentioned Word file as well as in their original MS-Excel® or other graphic formats but maintaining a high resolution. Other figures, including photographs and drawings should be submitted in digital JPG (or JPEG) compression format, with a minimum resolution of 300 dpi.

As a general rule, tables and figures should only be submitted in black and white, except for those intended for the cover page of the Journal or for those cases in which it is absolutely necessary to present them in color (at the judgment and discretion of the Editor).

Languages, units, and style

The journal's official language is English. Regarding measurement units, the metric system (SI) should be consistently used through the manuscript, unless the need is seen to apply any specific units that are of frequent use by the scientific community. Multiplication followed by negative superscript (e.g., kg ha^{-1}) can only be used with SI units. The slash (/) is a mathematical operation symbol that indicates "divided by". Anyway, in sciences it is used as a substitute for the word "per", and it is used to indicate rates. Use the slash to connect SI to non-SI units (e.g., 10°C/h or 10 L/pot).

Decimal fractions should be separated by a point (.), not a comma (,).

All abbreviations should be explained in full length when first mentioned in the manuscript.

With regards to the tenses, the most commonly used ones are the past, for the introduction, procedures and results; and the present, for the discussion.

Title and authors

The title in English, as well as its corresponding Spanish translation, shall not exceed 15 words. The scientific names of plants and animals shall be italicized and lowercased, except for the first letter of the genus (and of the species author), which must be uppercased.

The authors (including first and second names) shall be listed in order of their contribution to the research and preparation of the manuscript, in completely justified text format (filling the whole line, or, if necessary, the next

one below) under the translated version of the title. At the bottom of the article's first page, only the name and city location of the employer or supporting institution(s), and the e-mail address of the corresponding author should be included.

Abstract, resumen, and key words

The Abstract should be written in English with Spanish translation for the "Resumen". Both texts should contain brief (no longer than 200 words in a single paragraph) and accurate descriptions of the paper's premise, justification, methods, results and significance. Both language versions shall be mandatorily provided with a list of (maximum six) key words that have not appeared in the title or abstract, and included in the Agrovoc thesaurus by Agris (FAO).

Introduction

The introduction must include the delimitation and current status of the problem, the theoretical or conceptual basis of the research, the literature review on the topic, and the objectives and justification of the research. Common names must be accompanied by the corresponding scientific ones, plus the abbreviation of the species author surname when mentioned for the first time.

Materials and methods

Besides a clear, precise and sequential description of the materials used for the research (plant or animal materials, plus agricultural or laboratory tools), this section illustrates the procedures and protocols followed, and the experimental design chosen for the statistical analysis of the data.

Results and discussion

Results and discussion can be displayed in two different sections or in a single section at the authors' convenience. The results shall be presented in a logical, objective, and sequential order, using text, tables (abbreviated as Tab.) and figures (abbreviated as Fig.). The latter two should be easily understandable and self-explanatory, in spite of having been thoroughly explained in the text. The charts should be two-dimensional and prepared in black and white, resorting to a tone intensity degradation to illustrate variations between columns. Diagram curves must be prepared in black, dashed or continuous lines (- - - - or ———), using the following conventions: ▪, ▲, ◆, ●, □, ◊, ○. The tables should contain a few columns and lines.

Averages should be accompanied by their corresponding Standard Error (SE) values. The discussion shall be complete and exhaustive, emphasizing the highlights and comparing them to the literature data.

This section should briefly and concisely summarize the most important findings of the research.

Conclusion (optional)

A short conclusion section is useful for a long or complex discussion. It should provide readers with a brief summary of the main achievements from the results of the study. It can also contain final remarks and a brief description of future complementary studies that should be addressed.

Acknowledgments

When considered necessary, the authors may acknowledge the researchers or entities that contributed - conceptually, financially or practically - to the research: specialists, commercial organizations, governmental or private entities, and associations of professionals or technicians.

Conflict of interest statement

All manuscripts that are submitted to and published in *Agronomía Colombiana* must be accompanied by a conflict of interest disclosure statement by the authors. Please, include such a statement or declaration at the end of your manuscript, following any acknowledgments and prior to the references, under the heading 'Conflict of interest statement'.

Example: The authors declare that there is no conflict of interest regarding the publication of this article.

Author's contributions

This information is mandatory for *Agronomía Colombiana* from 2020 onwards. In order to describe each of the authors' contribution, please follow the CRediT taxonomy and use the following roles as a guide:

Contributor roles

Conceptualization: AAA formulated the overarching research goals and aims.

Data curation: AAA carried out activities to annotate scrub data and maintain research data for initial use and later re-use.

Formal analysis: AAA applied statistical, mathematical, computational, or other formal techniques to analyze or synthesize study data.

Funding acquisition: AAA obtained the financial support for the project leading to this publication.

Investigation: AAA conducted the research and investigation process, specifically performing the experiments or data/evidence collection.

Methodology: AAA developed or designed the methodology; created the models.

Project administration: AAA managed and coordinated the research activity planning and execution.

Resources: AAA provided the study materials, reagents, laboratory samples, instrumentation, computing resources, or other analysis tools.

Software: AAA implemented the computer code and supporting algorithms/software.

Supervision: AAA oversaw and led the research activity planning and execution.

Validation: AAA verified the overall replication/reproducibility of results/experiments and other research outputs.

Visualization: AAA prepared, created, and/or presented the published work and oversaw its visualization/data presentation.

Writing – original draft: AAA wrote/translated the initial draft.

Writing – review & editing: AAA carried out the critical review, commentary, or revision of the manuscript.

Authors have to keep in mind the CRediT taxonomy is not useful to determine who is eligible as author, but to state the contribution of each author in the study or the article. More information about the CRediT taxonomy is available in: https://casrai.org/credit/

Example: MYD and AFT designed the experiments, AFT carried out the field and laboratory experiments, AFT contributed to the data analysis, MYD and AFT wrote the article. All authors reviewed the manuscript.

Citations and literature cited

The system (author(s), year) will be consistently applied to all citations intended to support affirmations made in the article's text. When the cited reference has three or more authors, the citation shall only mention the name of the first author, accompanied by the Latin expression et al. (which means 'and others'), italicized and followed by a period, and separated from the year by a comma: (García *et al*., 2003). Alternatively, you can leave just the year in parenthesis: García *et al*. (2003). In case of references with only two authors, citations should include both names separated by '&': (García & López, 2012) or García and López (2012). Tables and figures should be cited in parenthesis as follows: (Tab. 1), (Tab. 2), (Tab. 3), etc., or (Fig. 1), (Fig. 2), (Fig. 3), etc. In the text, each table or figure must be referred to using a capital T or F, for example: ...as shown in Table 1, Table 2, Table 3, etc., or in Figure 1, Figure 2, Figure 3, etc.

The complete list of cited references in alphabetical order, according to the authors' surnames, must be included at the end of the article. When the list includes various publications of the same author(s), they shall be listed in chronological order. When they correspond to the same year, they must be differentiated with lower case letters: 2008a, 2008b, etc.

Agronomía Colombiana has adopted the American Psychological Association (APA) standards (https://apastyle.apa.org/about-apa-style) to elaborate the final list of references cited in the text ("Literature cited" section). This standard will be required for new manuscripts received from March 1st, 2020 onwards.

Basic information about the use of APA for the list of references is available here: https://apastyle.apa.org/style-grammar-guidelines/references. In order to illustrate these standards, authors can check some examples about how to create each item of the list of references, keeping in mind the type of publication cited as follows (click on each option to open APA web information):

Journal article

Example: García-Arias, F., Sánchez-Betancourt, E., & Núñez, V. (2018). Fertility recovery of anther-derived haploid cape gooseberry (*Physalis peruviana* L.) plants. *Agronomía Colombiana*, *36*(3), 201–209. https://doi.org/10.15446/agron.colomb.v36n3.73108

Published dissertation or thesis references

Example: Franco, C. V. (2012). *Efecto de la colchicina sobre el número cromosómico, número de cloroplastos y características morfológicas del fruto en ecotipos de uchuva (*Physalis peruviana *L.) Colombia, Kenia y Perú* [Undergraduate thesis, Universidad Francisco de Paula Santander]. UFPS Library. http://alejandria.ufps.edu.co/descargas/tesis/1610259.pdf

Whole book

Example: Suescún, L., Sánchez, E., Gómez, M., García-Arias, F. L., & Núñez Zarantes, V. M. (2011). *Producción de plantas genéticamente puras de uchuva*. Editorial Kimpres Ltda.

Edited book chapter

Example: Ligarreto, G., Lobo, M., & Correa, A. (2005). Recursos genéticos del género *Physalis* en Colombia. In G. Fischer, D. Miranda, W. Piedrahita, & J. Romero. (Eds.), *Avances en cultivo, poscosecha y exportación de la uchuva* Physalis peruviana *L. en Colombia* (pp. 329–338). Universidad Nacional de Colombia.

For other types of references such as technical reports, conference presentations or proceedings, magazine articles or preprints see https://apastyle.apa.org/style-grammar-guidelines/references/examples. Archival documents, letters, collections and unpublished documents can be referenced using some standards users can find here: https://apastyle.apa.org/style-grammar-guidelines/references/archival. In this link (http://shorturl.at/xGIPZ) authors can find a summary of the APA style for references created by Mendeley.

Authors can also consider the use of some APA list of reference generators such as Reference Management (Mendeley, https://www.mendeley.com/reference-management/mendeley-desktop), Scribbr (https://www.scribbr.com/apa-citation-generator/#/) or MyBib (https://www.mybib.com/).

Whenever possible, please provide a valid DOI for each reference in the literature cited.

AUTHOR INDEX OF *AGRONOMÍA COLOMBIANA* VOLUME 40, 2022

Continue

Author name	Article title	Location
Botero Fernández Verónica	Spectral behavior of banana with *Foc* R1 infection: Analysis of Williams and Gros Michel clones	No. 3, pp. 372-382
Botero Ramirez Andrea	Soil, climate, and management practices associated with the prevalence of clubroot in Colombia	No. 2, pp. 228-236
Cabanzo Hernández Rafael	A predictive model for the determination of cadmium concentration in cocoa beans using laser-induced plasma spectroscopy	No. 3, pp. 429-439
Calero Hurtado Alexander	Taxonomic identification and diversity of effective soil microorganisms: towards a better understanding of this microbiome	No. 2, pp. 278-292
Carabeo Annerys	Taxonomic identification and diversity of effective soil microorganisms: towards a better understanding of this microbiome	No. 2, pp. 278-292
Casagrande Cleiton Renato	Combining ability and selection of wheat populations for a tropical environment	No. 2, pp. 174-185
Castañeda Ruiz Rafael Felipe	Abundance of *Beauveria* spp. and *Metarhizium* spp. in maize and banana agroecosystems in central Cuba	No. 1, pp. 141-146
Castellanos Ruiz Kristal	Critical dilution curves for calcium, magnesium, and sulfur in potato (*Solanum tuberosum* L. Group Andigenum) cultivars Diacol Capiro and Pastusa Suprema	No. 2, pp. 198-211
Castricini Ariane	Quality of *Butia capitata* fruits harvested at different maturity stages	No. 1, pp. 69-76
Cayón Salinas Daniel Gerardo	Discriminant analysis for estimating meristematic differentiation point based on morphometric indicators in banana (*Musa* AAA)	No. 3, pp. 354-360
Chagas Edvan Alves	Selection of *Myrciaria dubia* clones under conditions of the savanna/ forest transition of Roraima through multivariate analysis	No. 1, pp. 3-11
Chagas Pollyana Cardoso	Selection of *Myrciaria dubia* clones under conditions of the savanna/ forest transition of Roraima through multivariate analysis	No. 1, pp. 3-11
Chantre Guillermo Rubén	Biological studies of *Puccinia lantanae*, a potential biocontrol agent of "Lippia" (*Phyla nodiflora* var. *minor*)	No. 3, pp. 383-394
Chaparro Giraldo Alejandro	Intellectual property on the design of genetically modified tobacco containing a *phaC* gene for peroxisomal biosynthesis of polyhydroxyalkanoates	No. 3, pp. 323-335
Chaparro Giraldo Alejandro	Equivalence of grain and forage composition in corn hybrid (*Zea mays* L.) from genetically modified off-patent (event TC1507) and non-genetically modified conventional corn	No.2, pp 155-164
Concenço Germani	Dynamics of the weed community during pineapple growth in the Brazilian semi-arid region	No. 1, pp. 109-119
Darghan Contreras Enrique	Economic efficiency of biochar as an amendment for *Acacia mangium* Willd. plantations	No. 1, pp. 120-128
Darghan Contreras Aquiles Enrique	Discriminant analysis for estimating meristematic differentiation point based on morphometric indicators in banana (*Musa* AAA)	No. 3, pp. 354-360
Darghan Enrique	Leaf area prediction models from growth measurements in Andean blueberry (*Vaccinium meridionale* Swartz) in the nursery	No. 3, pp. 361-371
Demicheli Pedro Mendes	Dynamics of the weed community during pineapple growth in the Brazilian semi-arid region	No. 1, pp. 109-119
Díaz Salcedo Raquel Oriana	Design and development of a mixed alcoholic beverage kinetics using asaí (*Euterpe precatoria*) and copoazú (*Theobroma grandiflorum*)	No. 1, pp. 129-140
Erazo Amaya Jorge Zamir	Selection of *Myrciaria dubia* clones under conditions of the savanna/ forest transition of Roraima through multivariate analysis	No. 1, pp. 3-11
Figueiredo Alex	Use of reduced Bokashi doses is similar to NPK fertilization in iceberg lettuce production	No. 2, pp. 293-299
Filgueira Duarte Juan José	Basal rot in carnation (*Dianthus caryophyllus* L.) is caused by *Fusarium verticillioides* (Sacc.) Nirenberg	No. 1, pp. 29-40
Fischer Gerhard	Altitude as a determinant of fruit quality with emphasis on the Andean tropics of Colombia. A review	No. 2, pp. 212-227
Flores Cocas Josué Mauricio	Nitrous oxide flux from soil with *Urochloa brizantha* under nitrogen fertilization in Honduras	No. 3, pp. 403-410
Fonseca Carreño Jorge Armando	Bioherbicidal activity of seed extract of *Campomanesia lineatifolia* on the weed *Sonchus oleraceus* L.	No. 1, pp. 49-57
França Hildegardo Seibert	*Ocimum gratissimum* L.: A natural alternative against fungi associated with bean and maize seeds during storage	No. 3, pp. 395-402
Fregonezi Gustavo Adolfo de Freitas	Use of reduced Bokashi doses is similar to NPK fertilization in iceberg lettuce production	No. 2, pp. 293-299
Garatuza Payán Jaime	Warming reduces the root density and wheat colonization by arbuscular mycorrhizal fungi in the Yaqui Valley, Mexico	No. 3, pp. 440-446
García Celsa	Soil, climate, and management practices associated with the prevalence of clubroot in Colombia	No. 2, pp. 228-236

Continue

Author name	Article title	Location
García Urías Julio César	Warming reduces the root density and wheat colonization by arbuscular mycorrhizal fungi in the Yaqui Valley, Mexico	No. 3, pp. 440-446
García Vivas Yuly Samanta	Nitrous oxide flux from soil with *Urochloa brizantha* under nitrogen fertilization in Honduras	No. 3, pp. 403-410
Gil Zuleiqui	Taxonomic identification and diversity of effective soil microorganisms: towards a better understanding of this microbiome	No. 2, pp. 278-292
Giovanelli Bruno Flaibam	Growth, development, and chlorophyll indexes of glyphosate and glufosinate-tolerant maize under herbicide application	No. 1, pp. 41-48
Gómez Sánchez Manuel Iván	Critical dilution curves for calcium, magnesium, and sulfur in potato (*Solanum tuberosum* L. Group Andigenum) cultivars Diacol Capiro and Pastusa Suprema	No. 2, pp. 198-211
Gómez-Caro Sandra	*Fusarium* species that cause corn stalk rot in the Ubaté valley of Cundinamarca, Colombia	No. 2, pp. 237-248
Góngora Botero Carmenza Esther	Plant growth and phosphorus uptake of coffee seedlings through mycorrhizal inoculation	No. 1, pp. 77-84
González Aguilera Jorge	Warming reduces the root density and wheat colonization by arbuscular mycorrhizal fungi in the Yaqui Valley, Mexico	No. 3, pp. 440-446
González Bonilla Sofía Marcela	Characterization and classification of lulo (*Solanum quitoense* Lam.) fruits by ripening stage using partial least squares discriminant analysis (PLS-DA)	No. 3, pp. 419-428
González Osorio Hernán	Plant growth and phosphorus uptake of coffee seedlings through mycorrhizal inoculation	No. 1, pp. 77-84
Grigio Maria Luiza	Selection of *Myrciaria dubia* clones under conditions of the savanna/ forest transition of Roraima through multivariate analysis	No. 1, pp. 3-11
Grijalva Verdugo Claudia	Total polyphenolic, antioxidants, and cytotoxic activity of infusions from soursop (*Annona muricata*) leaves from two Mexican regions	No. 2, pp. 300-310
Guerra Guzmán Dilmer Gabriel	Agronomic evaluation of chonto tomato (*Solanum lycopersicum* Mill.) lines of determinate growth	No. 3, pp. 336-343
Guerrero Bermúdez Jáder Enrique	A predictive model for the determination of cadmium concentration in cocoa beans using laser-induced plasma spectroscopy	No. 3, pp. 429-439
Guillén Huachua Wilfredo Felipe	Genetic variability of yam (*Dioscorea trifida*) genotypes in the Ucayali region, Peru	No. 1, pp. 12-21
Hasanuzzaman Mirza	Warming reduces the root density and wheat colonization by arbuscular mycorrhizal fungi in the Yaqui Valley, Mexico	No. 3, pp. 440-446
Hata Fernando Teruhiko	Use of reduced Bokashi doses is similar to NPK fertilization in iceberg lettuce production	No. 2, pp. 293-299
Heiba Hany Elsayed	Genetic improvement of faba bean (*Vicia faba* L.) genotypes selected for resistance to chocolate spot disease	No. 2, pp. 186-197
Heidari Hassan	Dual-purpose production of forage and seeds in maize by detopping and defoliation	No. 2, pp. 270-277
Henao Toro Martha Cecilia	Selection of the minimum indicator set for agricultural sustainability assessments at the plot scale	No. 1, pp. 98-108
Henderson Deborah	Taxonomic identification and diversity of effective soil microorganisms: towards a better understanding of this microbiome	No. 2, pp. 278-292
Hernández Gómez María Soledad	Design and development of a mixed alcoholic beverage kinetics using asaí (*Euterpe precatoria*) and copoazú (*Theobroma grandiflorum*)	No. 1, pp. 129-140
Herrera Celis Sandra Liliana	A predictive model for the determination of cadmium concentration in cocoa beans using laser-induced plasma spectroscopy	No. 3, pp. 429-439
Holtz Anderson Mathias	Population density of aphids in chrysanthemums grown under photoselective screens	No. 3, pp. 447-452
Hoyos Carvajal Lilliana María	Spectral behavior of banana with *Foc* R1 infection: Analysis of Williams and Gros Michel clones	No. 3, pp. 372-382
Ibrahim Mostafa	Genetic improvement of faba bean (*Vicia faba* L.) genotypes selected for resistance to chocolate spot disease	No. 2, pp. 186-197
Imbachi Quinchua Luis Carlos	Fitting growth curves of coffee plants in the nursery stage of growth: A functional approach	No.3, pp. 344-353
Jaime Guerrero Marilcen	La aplicación poscosecha de acibenzolar-S-metil y extractos vegetales afecta las propiedades fisicoquímicas de los frutos de arándano (*Vaccinium corymbosum* L.)	No. 1, pp. 58-68
Jaramillo Padilla Sandra Patricia	Plant growth and phosphorus uptake of coffee seedlings through mycorrhizal inoculation	No. 1, pp. 77-84
Jiménez Janet	Taxonomic identification and diversity of effective soil microorganisms: towards a better understanding of this microbiome	No. 2, pp. 278-292
Karapetyan Astghik	Assessment of physicochemical characteristics of biofertilizers and their role in the rooting capacity of plants	No. 2, pp. 311-315
Komolafe Oluwatosin	Effect of different fertilizers on yield and grain composition of maize in the tropical rainforest zone	No. 3, pp. 411-418

Continue

Author name	Article title	Location
Krenchinski Fabio Henrique	Growth, development, and chlorophyll indexes of glyphosate and glufosinate-tolerant maize under herbicide application	No. 1, pp. 41-48
Lahooni Sahar	Efficiency of herbicides for weed control in chickpea and effect of their residues on wheat growth	No. 2, pp. 249-257
Lana Aguiar Ronilda	Population density of aphids in chrysanthemums grown under photoselective screens	No. 3, pp. 447-452
Lemes Chabeli Abreu	Abundance of *Beauveria* spp. and *Metarhizium* spp. in maize and banana agroecosystems in central Cuba	No. 1, pp. 141-146
León Burgos Andrés Felipe	Fitting growth curves of coffee plants in the nursery stage of growth: A functional approach	No.3, pp. 344-353
Leyva Ponce José Aurelio	Warming reduces the root density and wheat colonization by arbuscular mycorrhizal fungi in the Yaqui Valley, Mexico	No. 3, pp. 440-446
Ligarreto Moreno Gustavo	*Fusarium* species that cause corn stalk rot in the Ubaté valley of Cundinamarca, Colombia	No. 2, pp. 237-248
Lima Danilo Pezzoto de	Use of reduced Bokashi doses is similar to NPK fertilization in iceberg lettuce production	No. 2, pp. 293-299
Lima Gabriel Wolter	Combining ability and selection of wheat populations for a tropical environment	No. 2, pp. 174-185
Lima Juliana Trindade	*Ocimum gratissimum* L.: A natural alternative against fungi associated with bean and maize seeds during storage	No. 3, pp. 395-402
Lizarazo Peña Pedro	Leaf area prediction models from growth measurements in Andean blueberry (*Vaccinium meridionale* Swartz) in the nursery	No. 3, pp. 361-371
López Camilo Andrés	Effect of biochar use as a substrate on granadilla (*Passiflora ligularis* Juss.) growth parameters	No. 1, pp. 22-28
López Pazos Silvio Alejandro	Intellectual property on the design of genetically modified tobacco containing a *phaC* gene for peroxisomal biosynthesis of polyhydroxyalkanoates	No. 3, pp. 323-335
Louzada João Marcos	Population density of aphids in chrysanthemums grown under photoselective screens	No. 3, pp. 447-452
Macías Echeverri Estefania	Spectral behavior of banana with *Foc* R1 infection: Analysis of Williams and Gros Michel clones	No. 3, pp. 372-382
Magnitskiy Stanislav	Leaf area prediction models from growth measurements in Andean blueberry (*Vaccinium meridionale* Swartz) in the nursery	No. 3, pp. 361-371
Mahdy Ehab Mawad Badr	Genetic improvement of faba bean (*Vicia faba* L.) genotypes selected for resistance to chocolate spot disease	No. 2, pp. 186-197
Mahgoub Elsayed	Genetic improvement of faba bean (*Vicia faba* L.) genotypes selected for resistance to chocolate spot disease	No. 2, pp. 186-197
Mahmoud Ahmed	Genetic improvement of faba bean (*Vicia faba* L.) genotypes selected for resistance to chocolate spot disease	No. 2, pp. 186-197
Maia Victor Martins	Dynamics of the weed community during pineapple growth in the Brazilian semi-arid region	No. 1, pp. 109-119
Maldonado Archila Germán	*Fusarium* species that cause corn stalk rot in the Ubaté valley of Cundinamarca, Colombia	No. 2, pp. 237-248
Maranhão Camila Maida de Albuquerque	Quality of *Butia capitata* fruits harvested at different maturity stages	No. 1, pp. 69-76
Marín Ortiz Juan Carlos	Spectral behavior of banana with *Foc* R1 infection: Analysis of Williams and Gros Michel clones	No. 3, pp. 372-382
Marín Arroyo María Remedios	Characterization and classification of lulo (*Solanum quitoense* Lam.) fruits by ripening stage using partial least squares discriminant analysis (PLS-DA)	No. 3, pp. 419-428
Martineli Maristella	Quality of *Butia capitata* fruits harvested at different maturity stages	No. 1, pp. 69-76
Martínez Acosta Ana María	Discriminant analysis for estimating meristematic differentiation point based on morphometric indicators in banana (*Musa* AAA)	No. 3, pp. 354-360
Martínez Cárdenas Claudia Andrea	Bioherbicidal activity of seed extract of *Campomanesia lineatifolia* on the weed *Sonchus oleraceus* L.	No. 1, pp. 49-57
Mejía Ospino Enrique	A predictive model for the determination of cadmium concentration in cocoa beans using laser-induced plasma spectroscopy	No. 3, pp. 429-439
Mezzomo Henrique Caletti	Combining ability and selection of wheat populations for a tropical environment	No. 2, pp. 174-185
Molina Villarreal Angie	The oil palm cadastre in Colombia	No. 2, pp. 258-269
Monroy Ingrid Elizabeth	Basal rot in carnation (*Dianthus caryophyllus* L.) is caused by *Fusarium verticillioides* (Sacc.) Nirenberg	No. 1, pp. 29-40
Monsalve Camacho Oscar Iván	Selection of the minimum indicator set for agricultural sustainability assessments at the plot scale	No. 1, pp. 98-108
Montoya Anaya Diana	Total polyphenolic, antioxidants, and cytotoxic activity of infusions from soursop (*Annona muricata*) leaves from two Mexican regions	No. 2, pp. 300-310

Continue

Author name	Article title	Location
Moreno Fonseca Liz Patricia	Leaf area prediction models from growth measurements in Andean blueberry (*Vaccinium meridionale* Swartz) in the nursery	No. 3, pp. 361-371
Mousavi Sayed Karim	Efficiency of herbicides for weed control in chickpea and effect of their residues on wheat growth	No. 2, pp. 249-257
Nardino Maicon	Combining ability and selection of wheat populations for a tropical environment	No. 2, pp. 174-185
Neto João Luiz Lopes Monteiro	Selection of *Myrciaria dubia* clones under conditions of the savanna/ forest transition of Roraima through multivariate analysis	No. 1, pp. 3-11
Núñez Colin Carlos Alberto	Total polyphenolic, antioxidants, and cytotoxic activity of infusions from soursop (*Annona muricata*) leaves from two Mexican regions	No. 2, pp. 300-310
Ñústez López Carlos Eduardo	Control of N-$NH4^+$ and K^+ leaching in potato using a carrageenan hydrogel	No. 1, pp. 85-97
Oliveira Evandro Chaves de	Population density of aphids in chrysanthemums grown under photoselective screens	No. 3, pp. 447-452
Ortiz Grisales Sanín	Agronomic evaluation of chonto tomato (*Solanum lycopersicum* Mill.) lines of determinate growth	No. 3, pp. 336-343
Osorio Walter	Plant growth and phosphorus uptake of coffee seedlings through mycorrhizal inoculation	No. 1, pp. 77-84
Padilla Huertas Fabián Leonardo	Soil, climate, and management practices associated with the prevalence of clubroot in Colombia	No. 2, pp. 228-236
Paiz Gutiérrez Noé Humberto	Nitrous oxide flux from soil with *Urochloa brizantha* under nitrogen fertilization in Honduras	No. 3, pp. 403-410
Parra Coronado Alfonso	Altitude as a determinant of fruit quality with emphasis on the Andean tropics of Colombia. A review	No. 2, pp. 212-227
Peñuelas Rubio Ofelda	Warming reduces the root density and wheat colonization by arbuscular mycorrhizal fungi in the Yaqui Valley, Mexico	No. 3, pp. 440-446
Pereira Loranny Danielle	Quality of *Butia capitata* fruits harvested at different maturity stages	No. 1, pp. 69-76
Pereira Vinicius Gabriel Caneppele	Growth, development, and chlorophyll indexes of glyphosate and glufosinate-tolerant maize under herbicide application	No. 1, pp. 41-48
Portal Orelvis	Abundance of *Beauveria* spp. and *Metarhizium* spp. in maize and banana agroecosystems in central Cuba	No. 1, pp. 141-146
Portela Diana Daniela	Intellectual property on the design of genetically modified tobacco containing a *phaC* gene for peroxisomal biosynthesis of polyhydroxyalkanoates	No. 3, pp. 323-335
Posse Robson Prucoli	Population density of aphids in chrysanthemums grown under photoselective screens	No. 3, pp. 447-452
Puentes Montealegre Nicolás	Control of N-$NH4^+$ and K^+ leaching in potato using a carrageenan hydrogel	No. 1, pp. 85-97
Puentes Escobar Tatiana Camila	Effect of biochar use as a substrate on granadilla (*Passiflora ligularis* Juss.) growth parameters	No. 1, pp. 22-28
Quinche Carol Yineth	Basal rot in carnation (*Dianthus caryophyllus* L.) is caused by *Fusarium verticillioides* (Sacc.) Nirenberg	No. 1, pp. 29-40
Quintero Mendoza Willian	Design and development of a mixed alcoholic beverage kinetics using asaí (*Euterpe precatoria*) and copoazú (*Theobroma grandiflorum*)	No. 1, pp. 129-140
Ramírez Carlos	Fitting growth curves of coffee plants in the nursery stage of growth: A functional approach	No.3, pp. 344-353
Ramos Clécio Souza	Mineral nutrient content of soil and roots of *Solanum paniculatum* L.	No. 3, pp. 453-458
Ramos Yordanys	Abundance of *Beauveria* spp. and *Metarhizium* spp. in maize and banana agroecosystems in central Cuba	No. 1, pp. 141-146
Rendón Sáenz José Raúl	Fitting growth curves of coffee plants in the nursery stage of growth: A functional approach	No.3, pp. 344-353
Resende Juliano Tadeu Vilela de	Use of reduced Bokashi doses is similar to NPK fertilization in iceberg lettuce production	No. 2, pp. 293-299
Reyes Moreno Giovanni	Economic efficiency of biochar as an amendment for *Acacia mangium* Willd. plantations	No. 1, pp. 120-128
Rincón Romero Victor Orlando	The oil palm cadastre in Colombia	No. 2, pp. 258-269
Rincón Sandoval Cindy Melissa	Basal rot in carnation (*Dianthus caryophyllus* L.) is caused by *Fusarium verticillioides* (Sacc.) Nirenberg	No. 1, pp. 29-40
Rodríguez Molano Luis Ernesto	Critical dilution curves for calcium, magnesium, and sulfur in potato (*Solanum tuberosum* L. Group Andigenum) cultivars Diacol Capiro and Pastusa Suprema	No. 2, pp. 198-211
Rodríguez Carlosama Adalberto	Effect of biochar use as a substrate on granadilla (*Passiflora ligularis* Juss.) growth parameters	No. 1, pp. 22-28
Rodríguez Carrillo María Guadalupe	Total polyphenolic, antioxidants, and cytotoxic activity of infusions from soursop (*Annona muricata*) leaves from two Mexican regions	No. 2, pp. 300-310
Rodríguez Núñez Jesús Rubén	Total polyphenolic, antioxidants, and cytotoxic activity of infusions from soursop (*Annona muricata*) leaves from two Mexican regions	No. 2, pp. 300-310

Continue

Author name	Article title	Location
Rozo Gladys	Control of N-$NH4^+$ and K^+ leaching in potato using a carrageenan hydrogel	No. 1, pp. 85-97
Ruiz Berrío Hernán David	La aplicación poscosecha de acibenzolar-S-metil y extractos vegetales afecta las propiedades fisicoquímicas de los frutos de arándano (*Vaccinium corymbosum* L.)	No. 1, pp. 58-68
Sabeti Payman	Efficiency of herbicides for weed control in chickpea and effect of their residues on wheat growth	No. 2, pp. 249-257
Sakazaki Roberto Tadashi	Selection of *Myrciaria dubia* clones under conditions of the savanna/ forest transition of Roraima through multivariate analysis	No. 1, pp. 3-11
Salazar Villareal Fredy Antonio	Agronomic evaluation of chonto tomato (*Solanum lycopersicum* Mill.) lines of determinate growth	No. 3, pp. 336-343
Salazar Villareal Myrian Del Carmen	Agronomic evaluation of chonto tomato (*Solanum lycopersicum* Mill.) lines of determinate growth	No. 3, pp. 336-343
Santamaría Vanegas Johanna	Control of N-$NH4^+$ and K^+ leaching in potato using a carrageenan hydrogel	No. 1, pp. 85-97
Santos João Rafael Prudêncio dos	Dynamics of the weed community during pineapple growth in the Brazilian semi-arid region	No. 1, pp. 109-119
Santos Julia Lavínia Oliveira	Quality of *Butia capitata* fruits harvested at different maturity stages	No. 1, pp. 69-76
Sarmiento Felipe	Intellectual property on the design of genetically modified tobacco containing a *phaC* gene for peroxisomal biosynthesis of polyhydroxyalkanoates	No. 3, pp. 323-335
Silva André Felipe Moreira	Growth, development, and chlorophyll indexes of glyphosate and glufosinate-tolerant maize under herbicide application	No. 1, pp. 41-48
Silva Bruno Soares da	Dynamics of the weed community during pineapple growth in the Brazilian semi-arid region	No. 1, pp. 109-119
Silva Caique Machado	Combining ability and selection of wheat populations for a tropical environment	No. 2, pp. 174-185
Siqueira Raphael Henrique da Silva	Selection of *Myrciaria dubia* clones under conditions of the savanna/ forest transition of Roraima through multivariate analysis	No. 1, pp. 3-11
Sosa Alejandro Joaquín	Biological studies of *Puccinia lantanae*, a potential biocontrol agent of "Lippia" (*Phyla nodiflora* var. *minor*)	No. 3, pp. 383-394
Sosa Rodrigues Breno Augusto	Nitrous oxide flux from soil with *Urochloa brizantha* under nitrogen fertilization in Honduras	No. 3, pp. 403-410
Soto Johana Carolina	Basal rot in carnation (*Dianthus caryophyllus* L.) is caused by *Fusarium verticillioides* (Sacc.) Nirenberg	No. 1, pp. 29-40
Souza Antonio Fernando de	*Ocimum gratissimum* L.: A natural alternative against fungi associated with bean and maize seeds during storage	No. 3, pp. 395-402
Suárez Rodríguez Hernan Darío	Equivalence of grain and forage composition in corn hybrid (*Zea mays* L.) from genetically modified off-patent (event TC1507) and non-genetically modified conventional corn	No.2, pp 155-164
Tahmasebi Iraj	Efficiency of herbicides for weed control in chickpea and effect of their residues on wheat growth	No. 2, pp. 249-257
Tenório Jonh Aldson Bezerra	Mineral nutrient content of soil and roots of *Solanum paniculatum* L.	No. 3, pp. 453-458
Tibocha Ardila Yuli Stephani	Application of the BLUPe predictor in the selection of potential soybean varieties for Orinoquia	No. 2, pp. 165-173
Tobar López Diego	Nitrous oxide flux from soil with *Urochloa brizantha* under nitrogen fertilization in Honduras	No. 3, pp. 403-410
Torres León Jorge Luis	The oil palm cadastre in Colombia	No. 2, pp. 258-269
Traversa Guadalupe	Biological studies of *Puccinia lantanae*, a potential biocontrol agent of "Lippia" (*Phyla nodiflora* var. *minor*)	No. 3, pp. 383-394
Tuisima Coral Lady Laura	Genetic variability of yam (*Dioscorea trifida*) genotypes in the Ucayali region, Peru	No. 1, pp. 12-21
Unigarro Muñoz Carlos Andrés	Fitting growth curves of coffee plants in the nursery stage of growth: A functional approach	No.3, pp. 344-353
Valencia Ramírez Rubén Alfredo	Application of the BLUPe predictor in the selection of potential soybean varieties for Orinoquia	No. 2, pp. 165-173
Vallecillo Godoy Alexis Josué	Agronomic evaluation of chonto tomato (*Solanum lycopersicum* Mill.) lines of determinate growth	No. 3, pp. 336-343
Vallejo Cabrera Franco Alirio	Agronomic evaluation of chonto tomato (*Solanum lycopersicum* Mill.) lines of determinate growth	No. 3, pp. 336-343
Vásquez Martínez Mariam	Leaf area prediction models from growth measurements in Andean blueberry (*Vaccinium meridionale* Swartz) in the nursery	No. 3, pp. 361-371
Ventura Maurício Ursi	Use of reduced Bokashi doses is similar to NPK fertilization in iceberg lettuce production	No. 2, pp. 293-299
Victoria Filho Ricardo	Growth, development, and chlorophyll indexes of glyphosate and glufosinate-tolerant maize under herbicide application	No. 1, pp. 41-48
Villamil Bolaños Fabián	Intellectual property on the design of genetically modified tobacco containing a *phaC* gene for peroxisomal biosynthesis of polyhydroxyalkanoates	No. 3, pp. 323-335
Villareal Fuentes Juan Manuel	Total polyphenolic, antioxidants, and cytotoxic activity of infusions from soursop (*Annona muricata*) leaves from two Mexican regions	No. 2, pp. 300-310

Continue

Author name	Article title	Location
Wanderley Christina da Silva	Use of reduced Bokashi doses is similar to NPK fertilization in iceberg lettuce production	No. 2, pp. 293-299
Wobeto Katle Samaya	Growth, development, and chlorophyll indexes of glyphosate and glufosinate-tolerant maize under herbicide application	No. 1, pp. 41-48
Yepez Enrico	Warming reduces the root density and wheat colonization by arbuscular mycorrhizal fungi in the Yaqui Valley, Mexico	No. 3, pp. 440-446
Zabala Quimbayo Andrea	The oil palm cadastre in Colombia	No. 2, pp. 258-269
Zapata Henao Sebastián	Spectral behavior of banana with *Foc* R1 infection: Analysis of Williams and Gros Michel clones	No. 3, pp. 372-382
Zborowski Luiz Guilherme Carvalho	Selection of *Myrciaria dubia* clones under conditions of the savanna/ forest transition of Roraima through multivariate analysis	No. 1, pp. 3-11
Zelaya Méndez Elsa Gabriela	Nitrous oxide flux from soil with *Urochloa brizantha* under nitrogen fertilization in Honduras	No. 3, pp. 403-410

AGRONOMIA COLOMBIANA

VOLUME XL, No. 3 SEPTEMBER-DECEMBER 2022 ISSN (print): 0120-9965 / ISSN (online): 2357-3732

AGRONOMIA COLOMBIANA

P.O. Box 14490, Bogotá-Colombia

(571) 316 5355 / (571) 316 5000 ext. 10265

E-mail: agrocol_fabog@unal.edu.co

http://www.revistas.unal.edu.co/index.php/agrocol

http://www.scielo.org.co